2012-03-08

Follicular Dendritic Cells, Human Immunodeficency Virus Type 1, and Alpha 1 Antitrypsin

Xueyuan Zhou
Brigham Young University - Provo

Follicular Dendritic Cells, Human Immunodeficiency Virus Type-1, and Alpha-1-Antitrypsin

Xueyuan Zhou

A dissertation submitted to the faculty of
Brigham Young University
in partial fulfillment of the requirements for the degree of

Doctor of Philosophy

Gregory F. Burton, Chair
Allen R. Buskirk
Barry M. Willardson
David M. Belnap
Keith A. Crandall

Department of Chemistry and Biochemistry

Brigham Young University

April 2012

ABSTRACT

Follicular Dendritic Cells, Human Immunodeficiency Virus Type 1, and Alpha-1-Antitrypsin

Xueyuan Zhou
Department of Chemistry and Biochemistry, BYU
Doctor of Philosophy

HIV/AIDS is raging and causing millions of deaths around the world. The major challenge in treating HIV/AIDS is the establishment of HIV reservoirs where the viruse escapes both drug and immune system attempts at eradication. Throughout the course of HIV/AIDS, productive HIV infection occurs primarily in the lymphoid follicles or germinal centers (GC) surrounding follicular dendritic cells (FDC). In the GCs, FDCs trap and maintain infectious HIV for years and provide these infectious viruses to the host cells. FDCs also attract B and T cells into the GCs and increase the ability of CD4+ T cells to be infected. Additionally, FDCs also mediate the increase of HIV replication in HIV-infected CD4+ T cells. Recently, several clinical cases and *in vitro* studies suggest that alpha-1-antitrypsin (AAT) might inhibit HIV infection and replication. Therefore, I hypothesized that AAT inhibited both the infection and replication of HIV in primary CD4+ T cells. I also postulated that AAT inhibited the FDC-mediated contributions that potentiate HIV infection and replication. To test whether AAT inhibited HIV infection in lymphocytes, CD4+ T cells were pretreated with AAT and then incubated with HIV to detect HIV infection. To exam whether AAT inhibited HIV replication, infected CD4+ T cells were cultured with AAT to detect the replication of HIV. To determine whether AAT blocked the FDC-mediated contributions to HIV pathogenesis, activated or resting FDCs were treated with AAT to detect the trapping and maintenance of HIV. The results suggested that AAT inhibited HIV entry into CD4+ T cells by directly interacting with gp41 and thereby inhibiting the interaction between HIV and CD4+ T cells. AAT also inhibited HIV replication in infected CD4+ T cells. Further study revealed that AAT interacted with low-density lipoprotein-receptor related protein to mediate the internalization of AAT through a clathrin-dependent endocytic process in CD4+ T cells. Subsequently, internalized AAT was transported from the endosome to the lysosome and then released into the cytosol. In the cytosol, AAT directly interacted with IκBα to block its polyubiquitinylation at lysine residue 48, which resulted in the accumulation of phosphorylated/ubiqutinylated IκBα in the cytosol. In turn, the dissociation of IκBα from NF-κB was blocked, which thereby inhibited the nuclear translocation and activation of NF-κB. Additionally, AAT also down-regulated FDC-CD32 and FDC-CD21 expression, which are regulated by NF-κB, thereby inhibiting the trapping and maintenance of HIV on FDCs. Hence, AAT not only suppresses HIV replication, but also blocks HIV replication in CD4+ T cells. Moreover, AAT also inhibits the activation of FDCs thereby affecting the trapping and maintenance of HIV.

Keywords: HIV replication, HIV infection, HIV reservoir, Tummor necrosis factor α, IκBα, Type II Fc gamma receptor, Type II complement receptor

ACKNOWLEDGEMENTS

I thank Dr. Gregory F. Burton for his excellent mentoring during my time in his laboratory. I also thank the other members of my graduate committee, Drs. Allen R. Buskirk, Barry M. Willardson, David M. Belnap, and Keith A. Crandall, for their time, patience, and critical analysis of my work. I would especially like to thank Drs. Karen J. Merrell and John T. Prince, and Ryan Taylor for their technical advice. I am also grateful to colleagues in the Burton laboratory, past and present; they have assisted and guided my research and it has been a pleasure to work with them.

I thank my family for their unconditional love. This work represents a significant sacrifice on their behalf as well. Finally, I thank every person and organization, who has helped me, who is helping me, and who will help me.

TABLE OF CONTENTS

LIST OF FIGURES

INTRODUCTION

Human immunodeficiency virus (HIV) type 1 infection results in the development of the severe immunodeficiency, acquired immunodeficiency syndrome (AIDS) (1). Since it was discovered in the early 1980s, HIV/AIDS has raged throughout the world (2, 3). This disease currently infects over 30 million individuals and causes more than two million deaths per year in men, women, and children (4). Although HIV/AIDS has been intensely studied since its discovery, there are still many aspects of its pathogenesis that remain unclear. A major obstacle in treating HIV/AIDS disease is the establishment of sanctuary sites or "reservoirs" where HIV escapes both drug and immune system attempts at eradication (5). Follicular dendritic cells (FDCs) are one of the largest HIV reservoirs in humans and the one about which the least is known (6, 7). Recently, a clinical case study suggested that alpha-1-antitrypsin (AAT) deficiency is associated with accelerated HIV/AIDS progression, suggesting that AAT might be an endogenous inhibitor of HIV/AIDS (8-11). The focus of this dissertation is to characterize the molecular mechanism(s) of AAT inhibition of FDC-mediated HIV infection, replication, trapping and maintenance of infectivity. A better understanding of the molecular mechanism of the inhibitory effect of AAT on HIV/AIDS might provide better therapies and intervention strategies for the treatment of this disease.

HIV: HIV is a complex lentivirus that infects mammalian cells that express CD4 receptors and chemokine co-receptors (C-C chemokine receptor type 5 (CCR5) or C-X-C chemokine receptor type 4 (CXCR4)) (12). In its life cycle, HIV has two principal stages: infection and replication. When HIV infection occurs, the glycoprotein gp120 on HIV interacts with CD4 receptors on the host cell to form a gp120/CD4 complex (13, 14). Subsequently, the newly formed complex undergoes a structural conformational change to expose the chemokine

binding domains of viral gp120, which allows them to interact with target chemokine receptors (CCR5 or CXCR4) on the host cell (15-19). The interactions between viral gp120 and the host cell's CD4 receptors and chemokine receptors (CCR5 or CXCR4) promote the more stable two-pronged attachment (gp120/CD4 and gp120/CCR5 or gp120/CXCR4) and prepare the N-terminal fusion peptide of viral gp41 to penetrate the plasma membrane of the host cell (20-25). After penetrating the plasma membrane of the host cell, the two repeat sequences of viral gp41 interact with each other, causing the collapse of the extracellular portion of viral gp41. This interaction brings the viral membrane and the cellular plasma membrane into close enough proximity to allow the fusion of the membranes and the release of the HIV capsid, which contains reverse transcriptase, integrase, ribonuclease, and protease, into the host cell (26-30). In the host cell, newly internalized viral reverse transcriptase liberates the single-stranded (+ polarity) viral RNA and copies it into complementary DNA molecules (cDNA) (31). Subsequently, the viral DNA is transported into the host cell's nucleus. In the nucleus, HIV integrase mediates the integration of viral DNA into the host genome where it resides for the lifespan of the host cell (32).

HIV replication begins with the transcription and translation of viral genes, which leads to the production of progeny virus. Occasionally, rather than being actively expressed, integrated HIV DNA remains dormant (i.e., in the latent stage) in the infected cells (33). HIV viral gene expression is tightly controlled by the activation of cellular transcription factors, including Nuclear Factor kappa B (NF-κB), Specificity Protein 1 (SP1), Activator Protein 2 (AP2), and the Nuclear Factor of Activated T-cells (NFAT). These factors are associated with the activation of the host cell and can bind to specific DNA binding sites within the long terminal repeat (LTR) of the viral genome to control its activity (34). Thus, when infected cells become activated, they

induce the activation of transcription factors, which in turn bind to DNA binding sites within the LTR of the viral genome and mediate the transcription of HIV genes resulting in their translation into viral proteins (35-37).

FDCs and HIV: FDCs are unique cells that are usually found in the follicles of secondary lymphoid tissues (38). FDCs can trap antigens in immune complex form and maintain the antigens for years through the interaction between antibody-antigen immune complex and type II Fc gamma receptor (FcgammaRII, CD32) (39, 40). Unlike normal dendritic cells that internalize, process, and present antigen to T lymphocytes, FDCs do not internalize trapped antigens, process nor present them to T cells (41). Recent reports demonstrate that FDCs exist both inactive and activated states (42). Further studies reveal that FDCs can be activated through the CD32 signaling pathway or the Toll-like receptor 4 (TLR4) signaling pathway (43, 44). The activation of FDCs results in a number of changes including the increased expression of CD32, intercellular adhesion molecule 1 (ICAM-1), vascular cell adhesion molecule-1 (VCAM-1), B-cell-activating factor (BAFF), type II complement receptor (CR2, CD21), CD21-ligand, C4-binding protein (C4BP), tumor necrosis factor α (TNF*α),* interleukin-6 (IL-6), and interleukin-7 (IL-7) (45-49). These factors or mediators contribute to the germinal center (GC) response, memory B cells, and antibody generation (50).

In HIV/AIDS patients, HIV infection and replication usually occur in secondary lymphoid tissues and the major ongoing infection sites are in and around the GCs where FDCs reside (6, 7, 51, a nd 52). These observations indicate that the GC environment with FDCs is highly suitable for HIV transmission and replication. Further studies reveal that FDCs trap and retain HIV for years and serve as a major HIV reservoir that protects the virus from destruction in the GCs (53-55). These reservoirs are the most significant treatment obstacles in HIV/AIDS

and provide a continuing source of infectious virus to perpetuate disease. Usually, FDCs are confined to the follicles of secondary lymphoid tissues where they trap and retain numerous antigens, including highly infectious HIV particles (5-7, 38, 41, 51, and 52). These antigens are trapped in the form of immune complexes comprised of specific antibody and/or complement components through FDC-CD32 and/or CD21 (45, 46, 54-56). In addition to providing infectious HIV to T cells, FDCs also up-regulate CXCR4 on CD4+ T cells, thereby increasing the ability of CD4+ T cells to become infected (57). Immediately adjacent to FDCs with trapped HIV are GC B cells which are not infected with virus, and GC T cells and macrophages, which are main infection targets of HIV (52). HIV-bearing FDCs also produce C-X-C motif chemokine 13 (CXCL13) to attract B and T cells to migrate into the GCs likely increasing the ability of CD4+ T cells to be infected (57, 58). Moreover, FDCs also provide signals to activate infected CD4+ T cells to produce more HIV (47). The importance of FDCs reservoir for HIV/AIDS and its contributions to HIV/AIDS pathogenesis are confirmed by the finding that virus replication persists around FDCs throughout the course of the disease (45, 46). These events combined lead to virus spread and diversification (59, 60).

Although FDCs trap and maintain HIV in the GCs, the molecular mechanism still remains controversial. Some reports show that FDCs trap HIV through the interaction between FDC-CD32 and HIV immune complexes, composed of virus and HIV-specific antibody, or between FDC-CD21 and HIV immune complexes/complement proteins (38, 55, and 61-64). Other studies reveal that FDCs trap HIV particles without the presence of HIV antibody and complement proteins (56, 65-67). However, only FDC-CD32 or FDC-CD21-trapped HIV appears to maintain its infectivity (6, 7, and 41). After HIV enters the GCs, FDCs trap and retain large amounts of virus on their surface using FDC-CD32 and/or FDC-CD21 (5, 45, 46, and 55).

Meanwhile, the expression of FDC-CD32 is related to the activation of FDCs. FDC activation also leads to increased production of TNFα, IL-6, and IL-7, which are important for HIV transmission (45-49). Therefore, the activation of FDCs is an essential event for the trapping and maintenance of HIV on FDCs and HIV transmission.

AAT and HIV: AAT is a naturally occurring serine protease inhibitor (serpin) found in human blood that is produced in the liver and has a half-life of about four days in circulation (68, 69). Clinically, AAT is used to treat chronic obstructive pulmonary diseases, which exists in patients deficient of AAT and therefore have unlimited neutrophil elastase activity that leads to pulmonary tissue damage (70). AAT can also facilitate islet cell mass regeneration in diabetes and promote immune tolerance in allograft transplantation of pancreatic tissue (71, 72). Additionally, the production of endogenous pro-inflammatory cytokines is also inhibited by AAT treatment in whole blood (73).

In blood, HIV-1 cannot be propagated without diluting the blood and activating the lymphocytes (11, 74). HIV infection is also rarely contracted by the oral route. This apparent immunity to infection via oral exposure is thought to result from the presence of natural and salivary secretory leukocyte protease inhibitor (SLPI) (75-79). In infected patients, HIV proliferation occurs principally in lymph nodes, where the concentration of specific serum constituents (putative inhibitors including AAT) is reduced (45). These observations suggest that there are potent endogenous HIV inhibitors in the blood and saliva, which might block HIV infection and replication. Logical candidates of endogenous HIV inhibitors include the serine protease inhibitors found in the saliva and blood. Among these serine proteases inhibitors, AAT is the most abundant circulating factor and many studies suggest that AAT inhibits HIV replication and infection (8, 9, 80-87). Clinical studies examining the active and inactive AAT

levels in asymptomatic and symptomatic HIV-infected subjects reveal that asymptomatic HIV positive individuals have higher levels of inactivated AAT than symptomatic individuals (59). In one reported case, an individual with AAT-deficiency experienced a more rapid decline in CD4+ T cell numbers (10). Importantly, it has been reported that AAT down-regulates HIV replication by inhibiting NF-κB activation in interleukin-18-stimulated HIV-infected primary monocytes cells and in HIV-infected neoplastic cell lines (11, 88). However, the molecular mechanism of AAT inhibiting NF-κB activation and HIV replication remains unclear. Moreover, a recent study also reveals that the 20-amino-acid C'-terminal fragment of AAT suppresses HIV infection by interacting with gp41 and interfering with the entry of HIV into host cells (9). However, it is unknown whether full-length AAT also blocks HIV infection.

Although there is evidence showing that AAT inhibits HIV infection and replication, the molecular mechanism for these activities remains to be elucidated. In this work, I seek to determine whether intact AAT inhibits HIV infection and replication in primary CD4+ T cells. I also investigate the molecular mechanism of the inhibitory effect of full-length AAT on HIV infection and replication. Because AAT blocks HIV replication from HIV-infected CD4+ T cells by inhibiting the activation of NF-κB that is essential for FDC activation and HIV trapping and maintenance, I also investigated whether AAT inhibited FDC activation, which likely plays an important role in HIV trapping and maintenance and HIV/AIDS pathogenesis. An increase in the understanding of the inhibitory effect of AAT on HIV/AIDS pathogenesis may provide important new tools and potential treatments to this disease.

MATERIALS AND METHODS

Recombinant HIV generation

Human embryonic kideney 293T cells (293T cells) were cultured in DMEM containing HEPES (20 mM), nonessential amino acid (1%), L-glutamine (2 mM), 10% heat-inactivated and defined FBS (GIBCO/Invitrogen), and gentamicin (50 μg/mL; Life Technologies) and then transfected with pLET-LAI (encoding the envelope of the recombinant HIV) and LTR vectors (encoding the core of the recombinant HIV, including a wild type, NF-κB I binding site mutation, NF-κB II binding site mutation, NF-κB I and II binding site mutations, SP-1 binding site mutation, AP-2 binding site mutation, and NF-IL6 binding site mutation vectors; these vectors were generously provided by Vincente Planelles and Alberto Bosque in University of Utah, Salt Lake City, UT) using Lipofectamine™ 2000 (Invitrogen) as directed. Briefly, one day before transfection, 293T cells (5×10^5 cells/mL, 500 μL per well) were plated in a 6-well cell culture plate with antibiotics-free DMEM. Before transfection, pLET-LAI (3 μg) and LTR vector (3 μg) were mixed in 50 μL of Opti-MEM®I Reduced Serum Medium (Invitrogen) and Lipofectamine™ 2000 (10 μL) was also diluted into 50 μL of Opti-MEM® I Reduced Serum Medium. After 5 minutes incubation, prepared vectors were mixed with prepared Lipofectamine™ 2000 and incubated for 20 minutes at room temperature. Next, the mixture was added to the cells and incubated for 6 hours at 37 ºC. After 6 hours incubation, the culture medium was changed to normal DMEM with 10% FBS and antibiotics and incubated for 6 days to collect the supernatant fluid to confirm the production of recombinant HIV by detecting HIV p24 as described below.

HIV virus preparation

HIV-1_{IIIB} stock was prepared by propagating HIV-1_{IIIB} in neoplastic H9 cells. Virus was harvested at the time when p24 and/or reverse transcriptase production reached a peak. The virus was pooled, filtered through a 0.45-μm membrane, and stored in aliquots in liquid nitrogen until used. Our HIV-1_{IIIB} preparations typically contained 1 μg/mL of p24 and 1×10^6 cpm reverse transcriptase activity. Unless otherwise noted, virus infections were performed using HIV-1_{IIIB}. However, where indicated, the 91US054 (X4) or 92US714 (R5) HIV-1 primary isolates (NIH AIDS Research and Reference Reagent Program) were used after propagation in mitogen-stimulated peripheral blood mononuclear cells (PBMC) as described below. HIV-1_{Bal} was prepared by propagating HIV-1_{Bal} in mitogen-stimulated CD4+ T cells or macrophages as described below. Primary virus stocks contained 140 to 200 ng/mL p24 and $3 \sim 4.5 \times 10^5$ cpm reverse transcriptase activity.

Cell line culture and HIV infection

Jurkat, SupT1, or Hut78 T cells were propagated in complete tissue culture medium (CM) consisting of RPMI 1640 with HEPES (20 mM), nonessential amino acid (1%), L-glutamine (2 mM), 10% heat-inactivated and defined FBS (GIBCO/Invitrogen), and gentamicin (50 μg/mL; Life Technologies). For HIV infection, these cells were centrifuged and the culture medium was removed. Next, the cells were resuspended in HIV stock (1 mL) and incubated at 37 ºC for 2 hours. After HIV infection, unbound virus was removed by washing with phosphate buffered saline (PBS) and the infected cells were cultured in CM under the conditions described in each experiment.

CD4+ T cell isolation and infection

CD4+ T cells were prepared from whole blood obtained from healthy, HIV-negative donors. The blood was applied to Ficoll-Paque-Plus (GE Healthcare) and centrifuged as directed to obtain PBMCs. Next, CD4+ T cells were isolated from PBMCs using negative selection via a CD4+ T cell isolation Kit II (Miltenyi Biotech) as directed. Isolated CD4+ T cells were activated by phytohemagglutinin (PHA; 5 μg/mL; Sigma) for 3 days in CM. Next, CD4+ T cells were incubated in CM containing interlukin-2 (IL-2) (20 U/mL; NIH AIDS Reference and Reagent Program; Hoffmann-La Roche, Inc.) for 2 hours at 37 ºC. For infection, CD4+ T cells were centrifuged and the culture medium was removed. Subsequentially, these cells were re-suspended in HIV stock (1 mL) and incubated at 37 ºC for 2 hours. After HIV infection, unbound virus was removed by washing with PBS and infected CD4+ T cells were cultured in CM with 20% FBS and IL-2 (20 U/mL) under the conditions described in each experiment.

Macrophage isolation and infection

Macrophages were prepared from whole blood obtained from healthy, HIV-negative donors. PBMCs were prepared as directed above. Macrophages were then isolated from the PBMCs by culturing the PBMCs in CM with 20% FBS and 10% human serum (Gemini Bio-products) for 7 days. Afterwards, the attached macrophages were collected using a cell scrapper and incubated in CM with 20% FBS. For infection, the culture medium was removed and the macrophages were incubated with HIV stock (1 mL) at 37 ºC for 2 hours. After HIV infection, unbound virus was removed by washing with PBS and the infected macrophages were cultured in CM with 20% FBS under the conditions described in each experiment.

FDC isolation and supernatant fluid collection

FDCs were isolated from human tonsils as described (47, 88). Briefly, the tonsils were cut into small pieces and digested with an enzyme cocktail containing Blendzyme (Roche Applied Science) and DNaseI (Sigma). Resulting single cells were washed twice in PBS. Next, the cells were resuspended in 5 mL CM and goat IgG (Chrompure, Jackson ImmunoResearch) was added. After 1-hour incubation on ice to minimize non-specific binding of IgG to FcR, the cells were treated with mouse IgM, anti-human FDC mAb, HJ2 (kindly provided by Dr. M. Nahm, University of Alabama at Birmingham) and incubated on ice overnight. Subsequently, the cells were added to pre-formed continuous Percoll gradients (GE Healthcare, 50%) and then centrifuged. The low-density cell fraction (1.050-1.060 g/mL) was collected, washed with PBS to remove Percoll, and resuspended in CM. The cells were next treated with FITC-conjugated goat anti-mouse IgM (Jackson Immuno research). After incubation and washing, the FDCs were isolated by flow cytometry (FACS). Isolated FDCs were cultured in CM with 10% FBS. The cell-free FDC-supernatant fluid was collected after 6 days incubation.

Quantitative real time PCR assay

To detect HIV viral RNA production, the cell-free supernatant fluid from the culture system was collected and HIV viral RNA was isolated using a QIAamp viral RNA mini Kit (QIAamp, USA) as directed. The isolated viral RNA was reverse-transcripted into cDNA using random primer (Invitrogen) and SuperScript III reverse transcriptase (Invitrogen) as directed. The synthesized cDNA was used as template for quantitative real time PCR (qPCR, TaqMan) with the primers and probe for HIV Reverse-transcriptase (forward primer (nt 3696 in HXB2): 5'-TGGGTACCAGCACACAAAGG-3', reverse primer (nt 3850): 5'-ATCACTAGCCATTGCTCTCCAAT-3', probe: ATTGGAGGAAATGAAC-MBG (FAM

labeled)) with TaqMan Universal PCR Master Mix (Applied Biosystems) as directed. PCR conditions were as follows: 50 ºC × 2 minutes (1 ×), 95 ºC × 10 minutes (1 ×); followed by 60 cycles of: 95 ºC × 15 seconds, 60 ºC × 1 minutes in an ABI 7500 thermocycler (Applied Biosystems). A standard curve was prepared using known concentrations (i.e., copy numbers) of ACH-2 DNA to determine the number of copies of viral RNA present in the cultures. The primers were used at 900 nM and the probe at 250 nM.

To detect HIV infection efficiency, the cells (5×10^5 cells/sample) were washed three times with cold PBS and then resuspended in 1 mL DNA-STAT 60 (Tel-Test, TX) to extract the DNA. Next, 0.2 mL chloroform was added and the sample was vortexed for 15 seconds. The sample was then centrifuged at 12,000 × g for 15 minutes at 4 ºC. Following the centrifugation, the aqueous phase containing the DNA was collected and an equal volume of cold isopropanol was added. The mixture was incubated for 5 minutes at room temperature. Afterwards, the mixture was centrifuged at 12,000 × g for 10 minutes at 4 ºC to precipitate the DNA. One volume of 75% ethanol was added to the DNA pellet followed by brief vortexing and subsequent centrifuged at 7,500 × g for 5 minutes at 4 ºC. The fluid was decanted and the remaining DNA pellet was dried and then resuspended in 1 mM EDTA (pH 7). The DNA was used as template for qPCR using the primers and probe for GAPDH (Applied Biosystem; VIC-TAMRA-labeled; Lot. NO.: 4310884E-1003044; worked as endogenous control) and HIV reverse-transcriptase described above with TaqMan Universal PCR Master Mix. PCR conditions were the same as that described above.

To detect the HIV viral RNA in the cytosol or on the cell membrane, the cells were infected or cultured with HIV as indicated in each experiment and then collected to isolate total RNA using RNA-STAT60 (Tel-Test, TX) according to the manufacturer's protocol, except that

following precipitation of the RNA with isopropanol, the centrifugation time was increased to 45 minutes to fully precipitate the total RNA. The resulting RNA preparation was treated with DNase I (DNA-*free*; Ambion, Inc.) to remove contaminating DNA. Purifed RNA was reverse-transcripted into cDNA using random primer and SuperScript III reverse transcriptase as directed. Subsequently, the cDNA was used as template for qPCR using the primers and probe for GAPDH (endogenous control) and HIV reverse-transcriptase described above with TaqMan Universal PCR Master Mix. PCR conditions were the same as that described above.

To detect HIV integration, the cells were washed three times with cold PBS. The DNA was extracted following the protocol described above. Subsequently, the isolated DNA was used as template for quantitative real time Alu-PCR with the following primers and probe for HIV and human genome (forward primer: 5'-TCTGGCTAACTAGGGAACCCA-3', reverse primer: 5'-CTGACTAAAAGGGTCTGAGG-3', probe: 5'-FAM-TTAAGCCTCAATAAAGCTTGCCTTGAGTGC-3') as directed. Meanwhile, GAPDH was also detected using the same DNA as template as endogenous control. PCR conditions were the same as that described above.

To detect the mRNA expression of specific proteins, the total RNA was isolated from the cells using RNA-STAT60 (Tel-Test, TX) following the protocol described above. The isolated RNA was reverse-transcripted into cDNA using oligo(dT) (Invitrogen) and SuperScript III reverse transcriptase as directed. Subsequently, the cDNA was used as template for qPCR with the following primers and probe for TNFα (Applied Biosystem; FAM-labeled; Lot. NO.: Hs00174128_m1), CD32 (Applied Biosystem; FAM-labeled; Lot. NO.: Hs00269610_m1), CD21 (Applied Biosystem; FAM-labeled; Lot. NO.: Hs00153398_m1), CXCL13 (Applied Biosystem; FAM-labeled; Lot. NO.: Hs00922245_m1), CXCR5 (Applied Biosystem; FAM-

labeled; Lot. NO.: Hs00540527_m1), and GAPDH with TaqMan Universal PCR Master Mix. PCR conditions were the same as that described above.

Enzyme-linked immunosorbent assay (ELISA)

To detect HIV p24 production, the cell-free tissue culture supernatant was collected and the production of p24 was detected using an HIV-1 p24 antigen ELISA kit (ZeptoMetrix Corporation, USA) following the directions provided. Briefly, viral particles were lysed with lysis buffer and then they were added to a washed plate coated with an antibody towards the HIV p24 antigen. After incubating for 2 hours at 37 ºC, the plate was washed and the HIV-1 p24 detector antibody was added followed by incubation at 37 ºC for 1 hour. Afterwards, the plate was washed and the secondary horse radish peroxidase (HRP)-conjugated antibody was added. After incubating for 30 minutes at 37 ºC, the plate was washed and the substrate was added and allowed to react for 30 minutes after which the reaction was stopped. The absorbance at 450 nm was detected on an ELISA reader.

To detect HIV p24 in the cytosol or on the cell membrane, cells were infected or cultured with HIV as indicated in each experiment and then the cells were collected to isolate whole cell protein. The whole cell protein was extracted by suspending the cell pellet in RIPA lysis buffer (50 mM Tris-HCl (pH7.4), 1% CHAPS, 250 mM NaCl, 0.5% Triton X-100, 1% Igepal CA-630, 1 mM DTT, 1 mM Na_3VO_4, 1 mM NaF, 1 mM PMSF, 4 mM EDTA, protease inhibitor cocktail (Roche, USA)) and vortexing for 60 sesconds. The mixture was then incubated on ice for 45 minutes and homogenized with a small gauge needle by drawing 3 times. After homogenizing, the mixture was centrifuged at 14,000 × g for 10 minutes at 4 ºC to collect the supernatant (the whole cell protein). HIV p24 was detected by HIV-1 p24 antigen ELISA kit (ZeptoMetrix

Corporation, USA) following the protocol described above using the extracted proteins (containing HIV proteins).

To detect TNFα production, the cell-free supernatant fluid from the cultured cells was collected and the quantity of TNFα produced was detected using the RayBio® Human TNF-alpha ELISA Kit (RayBiotech, Inc.) following the directions provided with the kit. Briefly, the cell-free supernatant fluid was collected from the culture and added to the washed plate coated with an antibody against human TNFα. After incubating for 2.5 hours at room temperature, the plate was washed and a biotinylated detector antibody was added and incubated at room temperature for 1 hour. Subsequently, the plate was washed and HRP-conjugated strepavidin was added. After incubating for 45 minutes at room temperature, unbound HRP-strepavidin was removed and TMB substrate was added to react for 30 minutes at room temperature. The reaction was stopped and the absorbance at 450 nm was detected on an ELISA reader.

To detect CXCL13 production, the cell-free supernatant was collected and the quantity of CXCL13 produced was detected by the Quantikine® Human CXCL13/BLC/BCA-1 Immunoassay kit (R&D system) following the directions provided with the kit. Briefly, the cell-free supernatant fluid from the culture system was collected and added to the washed plate coated with an antibody against human CXCL13/BLC/BCA-1. After incubating for 2 hours at room temperate, the plate was washed and a HRP-conjugated detector antibody was added and incubated at room temperature for 2 hours. The plate was next washed and the substrate was added to react for 30 minutes at room temperature. The reaction was stopped and the absorbance at 450 nm was detected on an ELISA reader.

Protein isolation

To extract the cytosolic and nuclear proteins, the cells (10^7 cells/sample) were collected and washed three times with ice cold PBS. 150 μL Buffer A (10 mM Tris-HCl (pH7.4), 1.5 mM $MgCl_2$, 10 mM KCl, 2 mM DTT, 0.1% Triton X-100, 2.5 mM NaH_2PO_4, 1 mM Na_3VO_4, 1 mM NaF, 1 mM PMSF, protease and phosphatase inhibitor cocktail) was added to the cell pellet and inverted gently. The mixture was incubated on ice for 15 minutes and centrifuged at 250 × g for 5 minutes at 4 °C to discard the supernatant. Next, 100μ L buffer A was added to the cell pellet again and re-suspended with a syringe with a small gauge needle by drawing up and down 5 times. The mixture was centrifuged at 8,000 × g for 20 minutes at 4 ºC and the supernatant was cytosolic protein. To extract the nuclear protein, the pellet after cytosolic protein extraction was re-suspended in 80 μL Buffer B (20 mM Tris-HCl (pH7.4), 1.5 mM $MgCl_2$, 420 mM KCl, 0.2 mM EDTA, 2 mM DTT, 1% Igepal CA-630, 25%(V/V) glycerol, 2.5 mM NaH_2PO_4, 1 mM Na_3VO_4, 1 mM NaF, 1 mM PMSF, protease and phosphatase inhibitor cocktail). The nuclei were disrupted with a new syringe with a small gauge needle by drawing 5 times. The mixture was agitated gently at 4 ºC for 50 minutes and centrifuged at 16,000 × g for 5 minutes. The supernatant was nuclear protein.

To extract the whole cell proteins, the cells were collected and washed three times with ice cold PBS. 150 μL RIPA lysis buffer was added to the cell pellet to extract the whole cell proteins following the protocol described above. To extract the whole viral proteins, HIV was washed and concentrated by centrifuging at 60,000 × g for 2 hours. RIPA lysis buffer was added to the viral pellet to extract the whole viral proteins following the protocol for whole cell protein isolation.

Western blot assay

The whole viral proteins, whole cell proteins, nuclear proteins, or cytosolic proteins were mixed with 4 × loading buffer (250mM Tris-HCl (pH8.8), 4% (W/V) SDS, 4% (V/V) beta-metcaptoethanol, 40% (V/V) glycerol, 0.01% (W/V) bromophenol blue) and incubated at room temperature. After the 20-minute inubation, the mixture was incubated at 100 ºC for 5 minutes. The proteins were separated by SDS-PAGE and transferred to Hybond-C or Hybond-P membrane (Amershan Life Science). After blocking in TBS with 5% non-fat milk for 2 hours at room temperature, the membrane was incubated with the primary antibody (rabbit anti-human p105/p50 (Abcam), rabbit anti-human p65 (Abcam), rabbit anti-human IκBα (Abcam), rabbit anti-human phosphorylated IκBα (S32 and S36) (Abcam), rabbit anti-human GAPDH (Abcam), rabbit anti-human β-actin (Abcam), rabbit anti-human ubiquitin (Pierce), goat anti-human A1AT (Bethyl), rabbit anti-human IKK alpha (Abcam), rabbit anti-human proteasome 19S S4 (Abcam), rabbit anti-human proteasome 20S alpha and beta (Abcam), mouse anti-human clathrin (Abcam), rabbit anti-human cullin 1 (Abcam), rabbit anti-human β-TRCP2 (Abcam), rabbit anti-human Skp1 (Abcam), rabbit anti-human E1 ubiquitin activating enzyme (Abcam), rabbit anti-human ubiquitin (lys-48 specific) (Millipore), rabbit anti-human ubiquitin (lys-63 specific) (Millipore), mouse anti-human low density LRP (Abcam), rat anti-human LAMP1 (Abcam), rat anti-human LAMP 2 (Abcam), mouse anti-human CD120a polyclonal antibody (TNFR1, Beckman Coulter), rabbit anti-human Rab 4 (Abcam), rabbit anti-human Rab 5 enzyme (Abcam), rabbit anti-human UbcH5 (Abcam), goat anti-human gp120 (Abcam), goat anti-human gp41 (Abcam), mouse anti-human CD4 (Immunotech), mouse anti-human CCR5 (Pharmingem), mouse anti-human CXCR4 (B&D), mouse anti-human TLR4 (Abcam), mouse anti-human CD32 (Immunotech), mouse anti-human CD21 (Immunotech), mouse anti-human CXCR5 (R&D), rabbit anti-human p50

polyclonal antibody (Millipore), rabbit anti-human p65 polyclonal antibody (Millipore), rabbit anti-human β-actin polyclonal antibody (Upstate), or rabbit anti-human phosphorylated c-Jun (Ser73) polyclonal antibody (Millipore-Upstate)) in TBS with 5% non-fat milk for 2 hours at room temperature. Next, the membrane was washed three times in TBS with 0.1% Tween-20 and 5% non-fat milk. After washing, the membrane was incubated with the HRP-linked secondary antibody (donkey anti-rabbit IgG-HRP (Jackson), mouse anti-rat IgG-HRP (Jackson), donkey anti-goat IgG-HRP (Jackson) or rat anti-mouse IgG-HRP (Jackson)) in TBS with 5% non-fat milk. Lastly, the membrane was washed in TBS with 0.1% Tween-20 and 5% non-fat milk and then developed using an ECL Advance Western Blotting Detection Kit (GE Healthcare). Semiquantitation was performed with a phosphorimager.

Immunoprecipitation and IKK Protein Kinase Activity Assays

The whole cell proteins were extracted by treating cells with 200 μL IκB kinase (IKK) CE buffer (10 mM HEPES-KOH, pH 7.4, 250 mM NaCl, 1 mM EDTA, 0.5% Igepal CA-630, 0.2% Tween 20, 2 mM dithiothreitol, 1 mM PMSF, 20 mM β-glycerophosphate, 10 mM NaF, 0.1 mM Na_3VO_4 and protease inhibitor cocktail). Equal amounts of cytosolic extracts were incubated with 1 μg of IKKα antibody (Abcam) for 2 hours at 4 °C and then incubated with protein A/G-conjugated agarose beads for 1 hour at 4 °C. After the beads were washed twice with IKK CE buffer and once with Kinase Buffer (20 mM HEPES, pH 7.4, 100 mM NaCl, 10 mM $MgCl_2$, 2 mM dithiothreitol, 1 mM PMSF, 20 mM beta-glycerophosphate, 10 mM NaF, 0.1 mM Na_3VO_4), purified IKK was incubated with 20 μL Kinase Buffer containing 20 μM ATP and 0.5 μg of bacterially expressed NF-κB inhibitor α subunit (IκBα) (Santa Cruz Biotechnology) substrate at 37 °C for 30 minutes. The reaction mixture was separated by SDS-PAGE and IκBα or phosphorylates IκBα was detected by Western blotting.

NF-κB DNA binding activity assay

The DNA binding activity of NF-κB was detected using an NF-κB Family Transcription Factor Assay Kit (Chemicon international) following the provided directions. Briefly, the nuclear or cytosolic protein was added to the plate coated with the κB binding sequence (5'-GGGACTTTCC-3') and incubated for 1 hour at room temperature. After washing three times, the primary antibody (rabbit anti-human p65 or p50) was added and incubated for 1 hour at room temperature. Next, the plate was washed three times and incubated with sthe econdary antibody (anti-rabbit IgG-HRP) for 30 minutes at room temperature. After washing three times, the substance was added and incubated for 30 minutes to stop the reaction. The absorbance at 450 nm was detected.

Immunoprecipitation assay

The whole viral proteins, whole cell proteins, nuclear proteins, or cytosolic proteins (1 mg, 1 mg/mL) were mixed with protein A/G agarose beads (100 μL) and incubated for 1 hour at 4 ºC. The beads were next centrifuged to collect the supernatant fluid without non-specific binding proteins. Afterwards, a specific antibody was added to the supernatant fluid and incubated at 4 ºC for 2 hours. Next, protein A/G beads (100 μL) were added and the mixture was incubated for 1 hour at 4 ºC. The mixture was centrifuged to collect the beads. The beads were then washed three times with lysis buffer. 4 × loading buffer was added to the beads and boiled for 10 minutes. Subsequently, the mixture was centrifuged for 5 minutes at 3,000 × g at 4 ºC. The supernatant fluid was collected for SDS-PAGE and detected by Western blotting.

Pulse-Chase Assay for the half-life of IκBα or ubquitinylated IκBα at K48 or K63

HIV-infected cells (2×10^6 cells/sample) were incubated in the presence or absence of AAT or stimulus for 24 hours. The cells were collected and washed 2 times with 3 mL methionine-free RPMI 1640 medium supplemented with 10% dialyzed FBS. Methionine-free RPMI 1640 medium supplemented with 10% dialyzed FBS (2 mL) was added to the cells and incubated for 1 hour. The cells were next collected and treated with 1 mL of 200 μCi/mL ^{35}S-labeled methionine supplemented methionine-free RPMI 1640 medium with 10% dialyzed FBS. The cells were incubated for another 10 minutes and the radioactive medium was removed. The cells were washed three times with 3 mL of 4 mM methionine supplemented methionine-free RPMI 1640 medium with 10% dialyzed FBS and then cultured in 2 mL of the same medium for a specific time (as showed in each experiment). After the incubation, the cells were collected and washed three times with ice cold PBS. The whole cell protein was extracted following the protocol described above. The isolated whole cell proteins were mixed with protein A/G agarose beads to carry out immunoprecipitation assay using IκBα antibody, following the protocol described above. Subsequently, the precipitated IκBα was divided into two aliquots. One aliquot was resuspended in 4 × loading buffer and boiled for 10 minutes to separate by SDS-PAGE. The radioactivity (total IκBα) was detected with a phosphorimager. Meanwhile, the other aliquot was resuspended in RIPA lysis buffer and boiled for 10 minutes to release protein A/G beads from the IκBα antibody and the IκBα complex. Next, the mixture was centrifuged to remove the beads. The supernatant fluid containing total IκBα was treated with the site-specific antibody to polyubquitin linked at K48 or K63 at 4 ºC for 2 hours. After incubation, protein A/G beads were added and incubated for 1 hour at 4 ºC and centrifuged to collect the beads. After the beads were washed three times with RIPA lysis buffer, they were resuspended in 4 × loading buffer and

boiled for 10 minutes prior to separation using SDS-PAGE and the radioactivity was detected with a phosphorimager.

Assay of 20S proteasome activity

The activity of the 20S proteasome was detected *in vitro* following the manual (20S proteasome activity assay kit, Chemicon international). Briefly, the cell lysate containing 20S proteasome or immunoprecipitation-purified (anti-19S or anti-20S) 20S preteasome was mixed with the substrate in the kit. After 2 hours incubation at 37 °C, the fluorescence was quantified using a 380/460nm filter set in a fluorometer. Higher fluorescence indicated higher 20S proteasome activity.

Biotinylation or Alexa Fluor® 488 conjugation of AAT

AAT was biotinylated using an EZ-link® sulfo-NHS-LC-Biotinalation kit (Pierce) following the protocol provided. Briefly, Sulfo-NHS-LC-Biotin was added to AAT and then incubated for 2 hours on ice. After incubation, excess Sulfo-NHS-LC-Biotin was washed by passing the mixture through the provided column. The biotinylated AAT was washed off the column and collected to measure the level of biotin incorporation following the protocol provided. In addition, AAT was conjugated with Alexa Fluor® 488 dye following the protocol in the provided manual (Alexa Fluor® 488 protein Labeling Kit, Invitrogen). Briefly, Alexa Fluor® 488 carboxylic acid, TFP ester, bis (triethylammonium salt) was added to AAT and then incubated at room temperature for 1 hour. After incubation, the labeled AAT was separated and collected by size-exclusion chromatography. The level of Alexa Fluor® 488 was detected following the instruction in the manufacturer's provided protocol.

Confocal microscopy

The cells were treated with Alexa Fluor® 488-labeled AAT as shown in each experiment. Non-internalized AAT was removed by washing three times with PBS and then the cells were subjected to fixation using 4% paraformaldehyde in PBS. After fixation, the cells were plated on glass slides and the green fluorescence was detected using an Olympus Confocal Microscope. The image was constructed by overlaying multiple pictures taken at different places in the "Z" axis.

In vitro ubiquitinylation

The cells (5×10^7) were collected and washed three times with ice cold PBS. Lysis buffer (10 mM Tris-HCl (pH7.4), 1.5 mM $MgCl_2$, 10 mM KCl, 2 mM DTT, 0.1% Triton X-100, 2.5 mM NaH_2PO_4, 1 mM Na_3VO_4, 1 mM NaF, 1 mM PMSF, protease inhibitor cocktail) was added to the cell pellet and inverted gently. The mixture was then incubated on ice for 15 minutes and centrifuged at 250 × g for 5 minutes at 4 ºC to discard the supernatant. Next, lysis buffer was added to the cell pellet and resuspended with a syringe with a small gauge needle by drawing 3 times. The mixture was centrifuged at 10,000 × g for 30 minutes at 4 ºC to collect the cytosolic proteins. The cytosolic proteins were incubated with protein A/G agrose beads to pre-clean the cytosolic proteins. After pre-cleaning, the specific antibody (IKKα, E1, UbcH5, Skp1, Cul1, or β-TRCP2 antibody) was added to precipitate the protein complexes (IKK, E1, E2 or E3 complex). Meanwhile, the pre-cleaned cytosolic proteins were treated with a phosphorylated IκBα antibody to remove phosphorylated IκBα. Next, the pre-cleaned cytosolic proteins without phosphorylated IκBα were incubated with an IκBα antibody to precipitate the IκBα complexes. To purify ubiquitin, the pre-cleaned cytosolic proteins were run through a 10KD filter to collect the flow-through. Subsequently, a ubiquitin antibody was added into the flow-through to

precipitate ubiquitin. After obtaining the IKK complex, IκBα, E1 complex, E2 complex, E3 complex, and ubiquitin, 0.5 μg recombinant IκBα (Santa Cruz Biotechnology) or purified IκBα was incubated with the purified IKK complex in Kinase Buffer containing 20 μM ATP at 30 °C for 30 minutes to phosphoylate IκBα *in vitro*. Subsequently, the purified E1, E2, E3, and ubiquitin were added to the mixture. Meanwhile, 10 mM ATP/50 μM $ZnCl_2$/2 mM DTT were also added to ubiquitinylate IκBα *in vitro* in the presence or absence of AAT. The phosphorylation and ubiqitinylation of IκBα were detected by Western blotting.

RNAi

Cells were incubated in CM with 10% FBS. One day before transfection, the cells were grown in the medium without antibiotics. Specific or control siRNA was diluted into Opti-MEM® I reduced serum medium without serum and mixed gently. DNA-Lipofectamine 2000 was also diluted into Opti-MEM® I reduced serum medium without serum and mixed gently. After 5 minutes incubation at room temperature, the diluted siRNA and DNA-Lipofectamine 2000 were combined and incubated for 20 minutes at room temperature. Subsequently, the mixture was added to the cells and mixed gently. After 6 hours incubation at 37 °C, the medium was removed and normal CM with serum and antibiotics was applied. The transfected cells were incubated for protein expression assay.

Cellular membrane receptor identification

Cells were washed with cold PBS and incubated with AAT for 1 hour at 4 ºC. Excess AAT was washed off and 3mM dithiobis succinimidylpropionate (DSP, Thermo Scientific) was added and incubated for 30 minutes to stabilize the interaction between AAT and cellular membrane proteins. Next, the reaction was stopped by treating with 10-20 mM Tris buffer and

the membrane proteins were extracted with a membrane protein extraction kit (BioVision) following the provided protocol. The isolated membrane proteins were incubated with the AAT antibody to precipitate the proteins interacting with AAT. The precipitated proteins were separated by SDS-PAGE and the specific protein bands were cut and digested with the sequencing grade modified trypsin (Promega). The digested peptides were identified by peptide mass fingerprinting assay using the high performance liquid chromatography-mass spectrometry system (HPLC-MS) (QSTAR or Orbitrap) as described below.

Viral membrane receptor interaction identification

HIV was washed and concentrated by centrifuging at 60,000 × g for 2 hours at 4 ºC. Concentrated virus particles were then incubated with AAT for 1 hour at 4 ºC and DSP was added and incubated for 30 minutes to stabilize the interaction between AAT and viral membrane proteins. Next, the reaction was stopped by treating with Tris buffer and the viral proteins were extracted following the whole viral protein extraction protocol described above. The isolated viral proteins were incubated with the AAT antibody to precipitate the proteins interacting with AAT. Subsequently, the precipitated proteins were separated by SDS-PAGE and the specific protein bands were cut and digested with the sequencing grade modified trypsin (Promega). The digested peptides were identified by peptide mass fingerprinting assay using the HPLC-MS system (QSTAR or Orbitrap) as described below.

In-gel digestion for peptide mass fingerprinting assay

The proteins were separated by SDS-PAGE and the appropriate bands were cut for peptide mass fingerprinting assay. Briefly, the gel bands were washed with 50% acetonitrile and 50 mM ammonium bicarbonate and then dried in a steriled hood. Next, the dried gel bands were

reduced with DTT (75 mM) and alkylated with iodoacetamide (0.3 M) in 100 mM ammonium bicarbonate. The gel bands were then digested with Promega sequencing Grade Modified Trypsin for 8 hours and the digestion reaction was stopped by formic acid. The digested gel bands were sonicated for 20 minutes and pulse-centrifuged to collect the digested peptides. Subsequently, the digested peptides were analyzed on the HPLC-MS system (Applied Biosystem API QSTAR pulsar I LC/MS system or Thermo scientific LTQ XL Orbitrap LC/MS system). The protein was identified by searching the specific mass spectrum in the Mascot database.

In-gel filter-aided sample preparation (FASP) or FASP for peptide mass fingerprinting assay

The proteins were separated by SDS-PAGE and the appropriate bands were cut. The collected gel bands were then transferred to a P1000 tip and centrifuged into a tube. Next, the gel pieces were loaded into a P200 tip to be further shredded by centrifugation. The shredded gels were then destained by treating with 50% acetonitrile/4 M urea/ 50 mM Tris buffer (pH8.5) for 25 minutes and transferred into a 30KD filter tube to remove the destaining solution by centrifugation. Next, the shredded gel was treated with 8 M urea/ 100 mM Tris/0.1 M DTT buffer (pH8.5) (to break the disulfide bond) or 8 M urea/100 mM Tris buffer (pH8.5) (to maintain the disulfide bond). After DTT treatment, the gel pieces were treated with 8 M urea/100 mM Tris/50 mM iodoacetamide buffer (pH8.5) (to maintain the disulfide bond, I would skip this step). Next, the gel pieces were incubated with 50mM ammonium bicarbonate and then digested with the Promega sequencing grade modified trypsin for 24 hours. The digestion reaction was stopped by formic acid. The peptides were analyzed on the HPLC-MS system. The proteins were identified by searching the specific mass spectrum in the Mascot database.

Detection of HIV reverse-transcriptase activity

HIV-infected CD4+ T cells (10^6 cells) were collected and washed three times with ice cold PBS. Next, 50 µL lysis buffer (50 mM Tris (pH 7.9), 500 mM NaCl, 1% Triton X-100, 2 mM PMSF, 20% glycerol, 1 mM DTT and protease inhibitor cocktail) was added to the cell pellet and vortexed for 60 seconds. The mixture was then incubated on ice for 45 minutes and homogenized with a small gauge needle by drawing 3 times. After homogenizing, the mixture was centrifuged at 14,000 × g for 10 minutes at 4 °C to collect the supernatant containing HIV reverse transcriptase. Subsequently, the supernatant was treated with DNase I to remove contaminating DNA. The activity of HIV reverse transcriptase was detected using an EnzChek® Reverse Transcriptase Assay Kit (Invitrogen) following the provided directions. Briefly, the poly(A) ribonucleotide template was mixed with the oligo $d(T)_{16}$ primer and incubated at room temperature. After the 1-hour incubation, the mixture was diluted by 200-fold with the RNase-free water and then aliquoted (20 µL/sample). 5 µL samples diluted in dilution buffer (50 mM Tris-HCl, 20% glycerol, 2 mM DTT, pH 7.6) was then added and incubated at 25°C for 60 minutes. At the end of incubation, 2 µL of 200 mM EDTA was added to stop the reaction. Next, the PicoGreen reagent diluted in Tris-EDTA buffer was added to the mixture and incubate for 5 minutes at room temperature. FITC fluorescence (excitation ~480 nm, emission ~520 nm) was then measured and the fluorescence value of the control was subtracted from the sample signals.

Statistical analysis

Analysis of data was performed using Student *t* test. *P* values of ≤ 0.05 were considered significant. Unless specifically stated, the error bars indicate the standard error of the means (SEM).

Studies using human cells/tissues

Studies using blood or tissue-derived cells obtained from humans were reviewed and approved by an appropriate institutional review board.

RESULTS

AAT suppression of HIV infection, HIV replication, and HIV trapping and maintenance on FDCs is difficult to study *in vivo* due to the inherent difficulties in using human beings as manipulable experimental models. To study these complex interactions, *in vitro* models have been developed (5-7, 47, 55-61, 88-90). In this dissertation, cultures of primary human CD4+ T cells and tonsillar FDCs were used as the working models to test whether AAT inhibited HIV infection, HIV replication, and HIV trapping and maintenance on FDCs.

Section I: Transcription factors and HIV replication

In infected cells, HIV replication is tightly regulated by the activation of transcription factors (34). The U3 region of the HIV LTR contains a number of binding sites for cellular transcription factors, including NF-κB (98, 99). Thus, I first investigated which transcription factor(s) was/were most essential for HIV replication. To achieve this goal, I produced recombinant human immunodeficiency virus with mutations at the transcription factor binding sites within the 3'-LTR. This was accomplished by transfecting HEK293T cells with the pLET-LAI vector (coding for the envelope of HIV_{LAI}) and vectors encoding envelope deficient HIV with wild type or mutated LTRs, generously provided by Drs. Vicente Planelles and Alberto Bosque in the Department of Pathology at the University of Utah (**Figure 1A**). Following transfection of HEK293T cells, varying amunt of p24 and viral RNA were observed (**Figures 1B and 1C**). To determine the effect(s) of mutated LTRs on virus integration and virus p24 production as a measure of virus replication, activated primary CD4+ T cells were infected with the recombinant viruses (**Figure 2**). I first sought to determine if the mutated LTRs had any affect on HIV integration, regardless of the presence of FDCs or FDC supernatant that will

increase HIC replication in infected CD4+ T cells (the mechanism will be diusccused below) (**Figures 2A, 3B, ans 3D**). No significant differences were noted in the amount of integrated virus regardless of the type of mutation in the LTR. However, when HIV replication and the production of p24 were assessed, the effects of the various mutations became evident regardless of the presence of FDCs or their supernatant (**Figures 2B, 3A, and 3C**). The most severe decrease in HIV production occurred when virus without an SP-1 binding site was monitored and this was only slightly more impactful than the mutation in both of the NF-kB binding sites ($p < 0.05$). The absence of AP-2, which was found in the middle of the NF-kB sites, was also apparent ($p < 0.05$). Similar virus production was observed with the other mutations. Thus, these data indicated that the transcription factors SP-1, AP-2, and NF-κB played an essential role in HIV replication.

Section II: FDCs and HIV/AIDS pathogenesis

FDCs increased HIV replication by producing TNFα to activate CD4+ T cells through the NF-κB signaling pathway (***This section was copyrighted by the American Society for Microbiology for my paper published on the Journal of Virology (2009, Volume 83, page 150 to page 158, DOI: 10.1128/JVI.01652-08) and I got the permission from the Journal of Virology (License Number: 2860901498845; License date: Mar 02, 2012) to use the materials in my PhD dissertation*****).*** FDCs are one of the major reservoirs of HIV in the human body and they trap and retain HIV in an infectious form for months (5, 7, 55, a nd 61). FDCs also up-regulate the expression of CXCR4 on CD4+ T cells that increases the ability of these cells to be infected by X4-tropic HIV (57). Moreover, FDCs produce the chemokine CXCL13 that attracts both T and B cells into the GCs, where they exist adjacent to FDCs. FDCs also trap HIV and increase the possibility of CD4+ T cells to be infected by this virus (57). There is also evidence

suggesting that FDCs provide signals that trigger infected cells to produce more viruses; however, the molecular mechanism remains unclear (6, 51, and 52). To determine whether FDCs contributed to HIV replication, I co-cultured FDCs with *in vitro* HIV-infected primary CD4+ T lymphocytes and measured the resulting p24 and viral RNA production (**Figure 4**). The results revealed that a significant increase in HIV p24 and viral RNA production was detected when FDCs were cocultured with HIV-1_{IIIB}-infected, PHA- and IL-2- stimulated primary CD4+ T cells ($p < 0.05$), even though these FDCs do not become infected themselves (91, 92). To determine whether the FDC signaling that increased HIV transcription was soluble or membrane bound, infected CD4+ T cells were incubated with FDCs, FDCs separated from CD4+ T cells by a semipermeable membrane (Transwell; 3.0-μm; Corning, NY), or a cell-free supernatant fluid from FDC cultures (6 days incubation) (**Figure 4**). The results indicated that the FDC supernatant fluid and FDCs in the transwells recapitulated the effect of intact FDCs, as measured by both quantitative viral RNA levels (**Figure 4A**) and p24 protein production (**Figure 4B**) ($p < 0.05$).

Because TNFα is known to be a major activator of NF-kB that in turn activates HIV transcription and is also important in the development and maintenance of FDCs (93-97), the supernatant fluid from FDC cultures was examined to determine if soluble TNFα was present. Moreover, TNFα mRNA expression in FDCs was also detected by quantative real time reverse-transcription PCR (qRT-PCR). The tonsillar FDCs expressed and produced TNFα, but this varied from sample to sample with the mean concentration equaling 154 pg/mL (**Figure 5**). I also found that the addition of 167 pg/ml recombinant TNFα to infected CD4+T cells recapitulated the effect of FDCs or their supernatant in viral RNA generation and p24 production (**Figure 6**) ($p < 0.05$). To confirm that FDC-produced TNFα mediated the observed increase in

HIV production, I cultured infected CD4+ T cells in the presence or absence of FDCs, FDC supernatant, recombinant TNFα, or soluble TNF receptor fusion protein (TNFR-Ig) to block endogenously produced TNFα (**Figure 6**). The results demonstrated that the addition of TNFR-Ig completely inhibited the signal present in FDCs or FDC supernatant ($p < 0.05$), confirming the role of FDC-produced TNFα in increasing HIV transcription and virus production. TNFR-Ig was also able to block the signaling from recombinant TNFα ($p < 0.05$). Furthermore, control irrelevant mouse immunoglobulin did not substantively affect the production of p24 or viral RNA (**Figure 6**). Together these results indicated that FDCs secreted TNFα that increased HIV production in *in vitro*-infected CD4+ T cells.

Because TNFα is the quintessential activator of NF-κB (100), I reasoned that FDC-produced TNFα would induce an increased level of activated NF-κB p50 and p65 in the infected CD4+ T cells incubated with FDCs or their supernatant. Therefore, I cultured FDCs and infected T cells as before, isolated the nuclear and cytoplasmic fractions of the infected T cells and monitored the NF-κB components (**Figure 7**). I observed increased nuclear translocation of both p50 and p65 and corresponding decreases of the cytoplasmic concentrations of these NF-κB components. Furthermore, I observed an increase in the DNA binding activity of NF-κB p65 and p50 when the HIV-infected CD4+ T cells were cultured with FDCs, FDC supernatant, or recombinant TNFα (**Figure 8**) ($p < 0.05$). Moreover, TNFR-Ig blocked the increase of nuclear translocation and DNA binding activity of NF-κB p65 and p50 ($p < 0.05$). In contrast, the use of an irrelevant control antibody had no effect upon DNA binding of NF-κB p65 and p50 (**Figure 7 and Figure 8**).

In the cytosol, NF-κB p65 and p50 are bound by their inhibitor, IκBα (100). When TNFα binds to the TNF receptor (TNFR), IκBα kinase (IKK) is activated to phosphorylate IκBα on

serine residues 32 and 36. After phosphorylation, IκBα is ubiquitinylated on residue K21 and K22 and polyubiquitinylated at residue K48 of linked ubiquitin. Next the polyubiquitinylated IκBα at K48 was degraded by the 26S protesome to release NF-κB p65 and p50. Subsequently, free NF-κB p65 and p50 translocates into the nucleus and binds to the DNA binding sites to trigger targeted gene expression (101). The results above demonstrated that FDC-produced TNFα increased the nuclear translocation and DNA binding activity of NF-κB p65 and p50. However, these results could not eliminate the possibility that FDCs also increased the expression of TNFR or IKK in CD4+ T cells to further activate NF-κB. Thus, I investigated whether FDCs interfered with the expression of TNFR and IKK. To achieve this goal, I co-cultured FDCs, FDC supernatant fluid, or recombinant TNFα with CD4+ T cells to detect the expression of TNFR and IKK. The results revealed that FDCs, FDC supernatant fluid, and recombinant TNFα did not obviously alter the overall expression of TNFR and IKK. However, the amount of phosphorylated IKKα in the cells increased dramatically, which suggested that the activation of IKK was up-regulated by the presence of FDCs, FDC supernatant fluid, or recombinant TNFα (**Figure 9A**). To further confirm that FDCs, FDC supernatant fluid and recombinant TNFα increased the activity of IKK, I precipitated the IKK complex using an IKKα-specific antibody and then incubated this IKK complex with recombinant IκBα to detect the phosphorylation of IκBα. The results demonstrated that the activity of the IKK complex was much higher in the CD4+ T cells cultured with FDCs, FDC supernatant fluid, or recombinant TNFα (**Figure 9B**). Therefore, these results suggested that FDC-produced TNFα triggered the activation of IKK and NF-κB without interfering with the overall expression of TNFR and IKK. Subsequently, activated NF-κB mediated the increase of HIV replication in HIV-infected CD4+ T cells.

FDCs trapped and maintained HIV through FDC-CD32 and FDC-CD21. FDCs trap and maintain antigens in the form of immune complexes comprised of specific antibody/antigens and/or complement proteins in the secondary lymphoid tissue (38, 41-44, 67, and 102). Previous studies in our lab have revealed that FDCs maintain HIV and protect these viruses from degradation for many months without being infected (5, 6, 55, and 61). However, the molecular mechanism for this "protection" is unclear yet. To investigate whether AAT inhibited HIV trapping and maintenance on FDCs, I determined how FDCs trapped HIV and maintained its infectious nature. FDCs were co-cultured with HIV-1_{IIIB} in the presence of fresh human serum (to provide complement proteins) and HIV-specific antibody (mouse anti-gp120 antibody; to form immune complexes with HIV). The binding of HIV-1_{IIIB} to FDCs was measured using qPCR and ELISA to detect viral RNA and p24, respectively. The results indicated that FDCs bound the highest quantity of HIV-1_{IIIB} when fresh human serum and HIV antibody were present (~ 5% increase in the presence of human serum, 25% increase in the presence of mouse gp120 antibody, and 36% increase in the presence of both fresh human serum and gp120 antibody) ($p < 0.05$) (**Figures 10A and 10B**). To investigate how long FDCs maintained HIV infectivity, at the end of the incubation, these FDCs were also co-cultured with activated primary CD4+ T cells to determine whether the trapped viruses were still able to transmit infection. The results revealed that FDCs still trapped numerous viruses even after a 6-week incubation (6%, 11%, 16%, 22%, 41%, 52%, and 70% decrease after 1, 2, 3, 4, 5, and 6 weeks incubation, respectively) ($p < 0.05$) (**Figures 10A and 10B**). However, the infectivity of these trapped viruses disappeared after 5-weeks of incubation even in the presence of fresh human serum and HIV antibody. Moreover, the presence of HIV-specific antibody and human serum prolonged the infectivity of the trapped viruses (less than 2 weeks for control group, less than 3 weeks for the group with human serum,

less than 5 weeks for the group with mouse gp120 antibody, and less than 5 weeks for the group with both human serum and mouse gp120 antibody). At the same time point, the viruses from the group with human serum and HIV antibody maintained a higher level of infectivity as indicated by the increased amounts of p24 and viral RNA present after infection ($p < 0.05$) (**Figures 10C and 10D**). These results indicated that FDCs trapped HIV, regardless of the presence of antibody and human serum. However, these trapped HIV viruses could not maintain their infectivity unless they were in the form of immune complexes on FDCs. Even in the form of immune complexes, FDCs could not maintain 100% of the infectivity of trapped HIV. Furthermore, these results also suggested that HIV antibody and complement proteins helped FDCs trap more HIV. Moreover, complement proteins increased the trapping of HIV and contributed to the maintenance of trapped HIV mediated by virus-specific antibody.

Because gp120 loss or shedding from an HIV particle is a contributing factor to the elimination of HIV infectivity (24, 25, 103, and 104), I postulated that the decreasing infectivity of FDC-trapped HIV, regardless of the formation of HIV immune complexes, was related to the shedding of gp120 from gp41 on HIV. Virus propagated in macrophages differs from the same virus produced in CD4 T cells in that gp160 is not cleaved into gp120 and gp41 in the macrophage (S. Gartner, personal communication). Therefore, to test this hypothesis, I propagated HIV-1_{Bal} or HIV-1_{IIIB} in activated primary human CD4+ T cells or macrophages and then characterized the expression of gp120/p41 in these produced viruses. As expected, HIV-1_{Bal} produced from macrophages contained only gp160, whereas HIV-1_{Bal} and HIV-1_{IIIB} produced from CD4+ T cells contained both gp120 and gp41 (**Figure 11**). Because HIV-1_{Bal} produced from macrophages contained only full length gp160 instead of gp120 and gp41 due to the lack of proteolytic cleavage of gp160, the dissociation of gp120 from gp41 that could lead to a loss of

infectivity would not occur in macrophage propagated HIV-1_{Bal}. I then co-cultured FDCs with these viruses and measured the ability of each to maintain their infectivity. The results showed that there was no obvious difference in the pattern of FDC trapping of HIV-1_{IIIB} produced from CD4+ T cells, HIV-1_{Bal} produced from CD4+ T cells, and HIV-1_{Bal} produced from macrophages (**Figure 12A and 12B**). However, FDC-trapped HIV-1_{Bal} produced from macrophages still maintained infectivity after 6 weeks incubation. In contrast, T cell produced virus with non-covalently associated gp120 and gp41 lost its infectivity within 5 weeks when trapped on FDCs (**Figure 12C and 12D**). Moreover, FDCs also trapped HIV-1_{Bal} produced from macrophages and maintained their infectivity after 6 weeks of incubation, even without the presence of HIV antibody (gp120 antibody) and complement proteins (human serum). However, the trapping and maintenance characteristic of HIV-1_{bal} produced from CD4+ T cell was similar with that of HIV-1_{IIIB} (**Figure 13 and Figure 14**). Collectively, these results suggested that the shedding of gp120 from HIV played an important role in the loss of viral infectivity and suggested that FDC-trapping of HIV immune complexes likely decreased gp120 shedding thereby protecting the virus from degradation.

The results above indicated that the presence of HIV-specific antibody and human serum increased virus trapping and maintenance of HIV infectivity on FDCs. Because FDCs trap immune complexes including viruses using CD32 and CD21, the data suggested that FDC-CD32 and FDC-CD21 might play an important role in HIV trapping and maintenance. To clarify whether CD32 and/or CD21 were necessary in this process, FDC-CD21 and/or FDC-CD32 were blocked with specific antibody or knocked-down with specific siRNA and the trapped virus was then characterized (**Figure 16 and Figure 17**). The results indicated that CD32 and CD21 siRNA specifically knocked-down the expression of FDC-CD32 and FDC-CD21 within 3 days

(**Figure 15**). FDCs with CD32 or CD21 siRNA treatment trapped less HIV-1_{IIIB} (about 22% and 9% decrease for CD32 and CD21 siRNA treatment, respectively) ($p < 0.05$). FDCs with both CD32 and CD21 siRNA treatment trapped much less HIV-1_{IIIB} (about 26% decrease) ($p < 0.05$) (**Figure 16A and 16B**). Moreover, FDCs with CD32 or CD21 antibody treatment also trapped less HIV-1_{IIIB} (about 21% and 10% decrease for mouse CD32 and CD21 antibody treatment, respectively) ($p < 0.05$). FDCs with both CD32 and CD21 antibody treatment also trapped much less HIV-1_{IIIB} (about 23% decrease) ($p < 0.05$) (**Figure 17A and 17B**). When we co-cultured these virus-binding FDCs with CD4+ T cells to detect the infectivity of trapped HIV-1_{IIIB}, the results demonstrated that their infectivity decreased sharply after treatment with CD32-specific antibody or siRNA ($p < 0.05$). Furthermore, CD21-specific antibody or siRNA also slightly inhibited the infectivity of the FDC-trapped viruses ($p < 0.05$) (**Figure 16 and Figure 17**). The infectivity of trapped HIV-1_{IIIB} could not be detected within 2 weeks if FDCs were treated with CD32 siRNA. I also could not detect the infectivity within 1 week when FDCs were treated with CD32 and CD21 siRNA simultaneously. Moreover, CD21 siRNA treatment alone also slightly decreased the infectivity ($p < 0.05$) (**Figure 16C and 16D**). At the same time point, the viruses from the group with CD32 and/or CD21 siRNA treatment maintained lower infectivity ($p < 0.05$) (**Figure 16C and 16D**). Additionally, I could not detect the infectivity within 3 weeks if FDCs were treated with anti-CD32. When FDCs were treated with CD32- and CD21- specific antibodies, I also could not detect the infectivity within 2 w eeks. Furthermore, anti-CD21 treatment alone only slightly decreased the infectivity ($p < 0.05$) (**Figure 17C and 17D**). At the same time point, the viruses from the group treated with anti-CD32 and/or anti-CD21 also maintained lower infectivity ($p < 0.05$) (**Figure 17C and 17D**). These results suggested that FDC-CD32 increased the trapping of HIV and played an important role in maintaining the

infectivity of trapped HIV. Moreover, these results suggested that FDC-CD21 might also contribute to this process.

FDCs activation contributed to HIV/AIDS pathogenesis. Recent reports reveal that FDC activation plays a pivotal role in antigen trapping. Moreover, FDC activation also results in increased expression of cell receptors and the production of cytokines that might be helpful for HIV transmission (43, 44). Therefore, I investigated whether FDCs might be activated *in vitro* and whether activated FDCs trapped more HIV and maintained higher infectivity than FDCs with no activation. To achieve the first goal, isolated FDCs were stimulated with lipopolysaccharide (LPS) or HIV immune complexes pre-formed by incubating HIV in the presence of gp120-specific antibody. The results demonstrated that LPS and HIV immune complexes significantly increased the expression of FDC-CD32 ($p < 0.05$), which played an essential role in HIV trapping and maintenance of viral infectivity (**Figure 18A and 18C**). Moreover, FDC-CD21 expression was also up-regulated with the treatment of LPS, which also contributed to HIV trapping and maintenance ($p < 0.05$) (**Figure 18A and 18B**). When these FDCs were treated with anti-CD32 or anti-CD21, the results demonstrated that CD32-specific antibody completely blocked the increased expression of FDC-CD32 that would be expected upon incubation with HIV immune complexes ($p < 0.05$) (**Figure 18**). Furthermore, the results also revealed that LPS significantly increased NF-κB p50 and p65 nuclear translocation and down-regulated the accumulation of phosphorylated IκBα in the cytosol. This increase in activated NF-κB was not blocked by CD32 or CD21 antibody treatment. Moreover, LPS and HIV immune complexes did not alter the overall expression of NF-κB p50 and p65 and Toll like receptor 4 (TLR4) (**Figure 18 and Figure 19**). Additionally, LPS increased TNFα production in FDCs ($p < 0.05$) (**Figure 20**), which played an essential role in mediating HIV replication from

infected CD4+ T cells. LPS also upregulated CXCL13 expression and production in FDCs ($p < 0.05$) (**Figure 21**), which increased the migration ability of CD4+ T cells into the GCs (57, 58). Furthermore, CD21 and CD32 antibody (IgG) did not alter the activation of FDCs. However, if FDCs were treated with IgM immune complexes (formed with Chromepure mouse IgM and rat, IgG antibody directed against mouse IgM), I also detected increased expression of FDC-CD32 ($p < 0.05$), which was similar with the results using HIV immune complex treatment (**Figure 18, Figure 19, and Figure 22**). These results suggested that CD32-mediated FDC activation was a result of CD32 receptor aggregation. To detect whether activated FDCs trapped more HIV and maintained higher infectivity, I co-cultured these stimulated FDCs with HIV-1_{IIIB} to detect the trapping and maintenance of HIV. The results revealed that activated FDCs trapped more HIV-1_{IIIB} and maintained higher infectivity ($p < 0.05$) (**Figure 23**). Thus, these results suggested that FDCs could be activated *in vitro* through the NF-κB signaling pathway, which in turn mediated the increased expression and production of FDC-CD32, FDC-CD21, TNFα, and CXCL13. Furthermore, the CD32 signaling pathway also contributed to FDC-CD32 expression and production while it had no obvious effect on FDC-CD21, TNFα, and CXCL13 expression and production. Moreover, *in vitro* activated FDCs trapped more infectious HIV and maintained the infectivity of these viruses.

Section III: AAT and HIV infection

Recent studies report that the C-terminal fragment of AAT inhibits HIV infection (8, 9, and 105). In this dissertation, I first sought to investigate whether full-length AAT also inhibited HIV infection. Activated primary CD4+ T cells were therefore cultured in the presence or absence of 5 mg/mL AAT for 1 hour and then infected with HIV-1_{IIIB} without removing AAT. After infection, the cells were washed to remove unbound viruses and AAT. Subsequently, the

cells were treated with trypsin to remove un-internalized HIV-1_{IIIB} and then incubated at the same condition as before HIV infection to detect the integration of viral DNA. Because the concentration of AAT at 5 mg/mL occurs in inflammatory subjects and is thus physiologically relevant and AAT at this concentration clearly inhibits HIV replication (68, 69, and 88), I selected this concentration for the remainder of our experiments. The resultant viral DNA integration was monitored using quantitative real time Alu-PCR (**Figure 24**). As expected, CD4+ T cells with AAT pre-treatment had much less viral DNA integrated into the host genome in comparison to untreated CD4+ T cells, regardless of the removal of un-internalized HIV-1_{IIIB} (about 50% lower) ($p < 0.05$) (**Figure 24A**). However, the integration of viral DNA did not change substantively if the activated primary CD4+ T cells were infected first and then co-cultured with AAT (**Figure 24B**). I also tested the effect of AAT on viral DNA integration using primary R5 and X4 isolates of HIV, HIV-$1_{92US714}$ and HIV-$1_{91US054}$, respectively with similar results to those seen with HIV-1_{IIIB} (**Figure 25**). Thus, these results suggested that full length AAT inhibited HIV infection and that the inhibition was not mediated by bl ocking the integration of viral DNA into the host genome.

HIV infection includes the entry of HIV into the host cell, the reverse transcription of HIV viral RNA in the host cell, and the integration of HIV viral DNA into the host genome (14, 15, 20, 24, 25, 29, 31, a nd 32). The results above demonstrated that AAT did not interfere with the integration of HIV DNA into the host genome. Thus, I reasoned that AAT might inhibit HIV entry or viral RNA reverse transcription. To test whether AAT blocked the activity of HIV reverse transcriptase and thereby inhibited viral RNA reverse transcription, activated primary CD4+ T cells were incubated in the presence or absence of AAT and then infected with HIV-1_{IIIB} without removing AAT. After infection, unbound viruses and AAT were removed and the cells

were cultured in the presence or absence of trypsin to remove un-internalized viruses. Following trypsin treatment to remove extracellular virus, the cells were incubated as before. Subsequently, the activity of viral reverse transcriptase in these CD4+ T cells was measured (**Figure 26**). The results showed that the activity of HIV reverse transcriptase in AAT-pretreated CD4+ T cells was much lower than that in the untreated CD4+ T cells (about 50% lower) ($p < 0.05$) (**Figure 26A**). However, in the absence of preincubation with AAT, the activity of the viral reverse transcriptase appeared to be the same regardless of whether or not AAT was added after viral entry (**Figure 26B**). Moreover, AAT also had a si milar effect in the cells infected with the primary isolates HIV-$1_{92US714}$ and HIV-$1_{91US054}$ (**Figure 27**).

Next, I sought to determine whether AAT inhibited HIV entry into CD4+ T cells (**Figure 28**). The results indicated that the amount of non-internalized HIV-1_{IIIB} (i.e., that in the supernatant fluid) was almost identical regardless of the presence or absence of AAT (**Figure 28A and 28B**). In contrast, the entry of HIV-1_{IIIB} into AAT-pretreated CD4+ T cells was decreased by about two-fold, regardless of trypsin treatment ($p < 0.05$) (**Figure 28C and 28D**). Furthermore, AAT also inhibited the entry of primary isolate HIV-$1_{92US714}$ (R5) and HIV-$1_{91US054}$ (X4) into CD4+ T cells, without interfering with the binding of viruses on the cells (**Figure 29 and Figure 30**). Collectively, these results indicated that the inhibitory effect of AAT on HIV infection was associated with the entry of HIV into CD4+ T cells.

I then sought to determine the mechanism of AAT-mediated inhibition of HIV entry into CD4+ T cells. One possible mechanism was that AAT down-regulated the CD4 receptor, the CXCR4 co-receptor, or the CCR5 co-receptor on the target cells to mediate lower amounts of virus internalization into the cells. To test this hypothesis, activated primary CD4+ T cells were treated with AAT and the expression of CD4, CCR5, and CXCR4 was measured by Western

blotting at different time points. The results revealed that AAT had no obvious effect on the expression of CD4, CCR5, and CXCR4 in CD4+ T cells (**Figure 31**). Thus, the inhibitory effect of AAT on HIV entry was not mediated by altering the expression of CD4, CCR5, or CXCR4 receptors on CD4+ T cells. Another possible mechanism was that AAT interacted with CD4, CCR5, or CXCR4 receptors to interfere with the interaction between HIV and the host CD4+ T cells. To test this hypothesis, activated primary CD4+ T cells were incubated with AAT and unbound AAT was removed. Subsequently, the cross-linker, DSP, was added to stabilize the interaction between the host CD4+ T cells and AAT. Cellular membrane proteins interacting with AAT were precipitated using AAT-specific antibody and separated by SDS-PAGE. The specific bands on the gel were identified by peptide mass fingerprinting assay. The results revealed that the AAT antibody-precipitated complex did not contain CD4, CCR5, or CXCR4 (**Figure 32**). Therefore, AAT inhibition of HIV entry was not mediated by interacting with CD4, CXCR4 and CCR5 on the cell membrane to block the interaction between HIV and the host CD4+ T cell. A third possible mechanism of action was that AAT interacted with HIV envelope proteins to inhibit the interaction between virus and the cells. To examine this hypothesis, HIV-1_{IIIB} was incubated with AAT and then DSP was added to stabilize the interaction between HIV and AAT. Viral membrane proteins interacting with AAT were also precipitated using AAT-specific antibody and separated by SDS-PAGE. The specific bands on the gel were identified by peptide mass fingerprinting. The results revealed that the AAT antibody-precipitated complex contained both gp120 and gp41 (**Figure 33**A). When HIV-1_{IIIB} was co-cultured with AAT and DSP was added, gp120 and gp41 were also detected in the AAT antibody-precipitated viral membrane proteins by Western blotting (**Figure 33B**). Furthermore, if HIV-1_{IIIB} was co-cultured with AAT and gp120-specific antibody was added to immunoprecipitate the complex, I also

detected that AAT associated with HIV (**Figure 33C**). Similar results were obtained using the primary isolates HIV-$1_{92US714}$ (R5) and HIV-$1_{91US054}$ (X4) (**Figure 34**). Co-culture of AAT with recombinant gp41 or gp120 followed by immunoprecipitation revealed that AAT only interacted with gp41 directly (**Figure 33D**). Collectively, these results suggested that AAT inhibited HIV entry into CD4+ T cells by interacting with the HIV membrane protein gp41, thereby inhibiting the interaction between the virus and CD4+ cells.

Section IV: AAT and HIV replication (*This section was copyrighted by the American Association of Immunologists, Inc. (Copyright 2011. The American Association of Immunologists, Inc.) for my paper published on the Journal of Immunology (2011, Volume 186 No. 5, page 3148 to page 3155, DOI: 10.4049/jimmunol.1001358) and I got the permission from the Journal of Immunology to use the materials in my PhD dissertation*.)

Recent studies report that AAT inhibits HIV replication (10, 11). The results in section II also demonstrated that FDCs increased HIV-1 replication by producing TNFα that in turn activated the NF-κB signaling pathway thereby inducing HIV transcription and virus production in the infected lymphocytes. Because AAT is reported to decrease HIV replication in infected monocytic cells and PBMCs in a manner that decreased NF-κB activation (83, 88), I postulated that AAT might also inhibit FDC-mediated HIV transcription and virus production. Activated primary CD4+ T cells were therefore infected with HIV-1_{IIIB} *in vitro* and co-cultured with FDC supernatant fluid, which contained TNFα to activate NF-κB. Subsequently, AAT was added to these cultures, and the resultant virus replication was monitored as before. As expected, FDC supernatant fluid increased viral RNA and p24 production in infected T cells ($p < 0.05$) (**Figure 35**). In comparison to untreated T cells, AAT significantly decreased viral RNA and p24 production in these infected CD4+ T cells, regardless of the presence of FDC supernatant fluid (p

< 0.05). I also compared infected T cells co-cultured with intact FDCs or with FDC supernatant fluid and found both FDC preparations equally capable of increasing HIV production. AAT inhibited virus production under both conditions ($p < 0.05$) (**Figure 35**). I also tested the effect of AAT on HIV replication in infected CD4+ T cells using an R5 (92US714) or X4 (91US054) primary isolate of HIV. AAT inhibited HIV replication of the primary isolates regardless of the tropism of the virus isolate, and this effect persisted in the presence or absence of FDC supernatant ($p < 0.05$) (**Figure 36**). These results indicated that AAT inhibited HIV replication using both primary and laboratory-adapted HIV isolates.

Because FDCs and their supernatant fluid increased HIV transcription and virus production by increasing the activation of NF-κB, and AAT is associated with inhibiting NF-κB activation in HIV-infected promonocytic U1 cells (11), I reasoned that AAT might inhibit FDC-mediated HIV replication by blocking the nuclear translocation of NF-κB induced by FDC-TNFα. Because NF-κB activation is the result of the activation of IKK, I first detected the expression and activity of IKK with the treatment of FDC supernatant and AAT. The results demonstrated that FDC supernatant increased the amount of phosphorylated IKKα. Moreover, FDC supernatant also increased IKK activity while it did not interfere with the overall expression of IKKα obviously ($p < 0.05$). The addition of AAT had no obvious effect on IKK expression and activation (**Figure 37**). Meanwhile, I also detected decreased amount of the lower band of p-IKKa in the whole cell protein. The possible explanation for this was that I loaded a slightly different amount of whole proteins because the amount of all p-IKKa and β-actin was lower in whole proteins. Next, CD4+ T cells were infected with HIV and cultured as before with FDC supernatant fluid in the presence or absence of AAT, and the nuclear translocation and DNA binding activity of NF-κB p50 and p65 were detected on whole cell, cytoplasmic, and nuclear

lysates of these cells (**Figure 38**). As expected, the infected T cells cultured with FDC-supernatant demonstrated an increased nuclear translocation and DNA binding activity of NF-κB p50 and p65 while simultaneously showing a decreased cytoplasmic concentration of these components. In the cultures that contained AAT with or without FDC supernatant, decreased nuclear translocation and DNA binding activity of NF-κB p50 and p65 was observed ($p < 0.05$). Meanwhile, I also observed decreased amounts of nuclear NF-κB and increased amounts of cytoplasmic phosphorylated IκBα when AAT was present (**Figure 38**). To determine whether the phosphorylated IκBα remained bound to the NF-κB p50 and p65 complex in the cytoplasm, the infected CD4+ T cells were cultured and lysed as before and subjected to immunoprecipitation using an antibody directed against IκBα (**Figure 39**). These results showed that NF-κB still associated with IκBα if AAT was present. Together, these results suggested that AAT blocked HIV replication by inhibiting NF-κB activation, which was not mediated by inhibiting the phosphorylation of IκBα.

Next, I determined whether AAT blocked NF-κB activation by inhibiting the ubiquitinylation of phosphorylated IκBα by culturing cells as before and subjecting the cell lysates to immunoprecipitation using an ubiquitin-specific antibody (**Figure 39**). The results revealed that AAT treatment did not block the ubiquitinylation of phosphorylated IκBα, which still associated with the NF-κB components p65 and p50. AAT also appeared to induce the accumulation of phospho-ubiquitinylated IκBα, p65, and p50 in the cytosol. These results were consistent with the rapid degradation of phospho-ubiquitinylated IκBα in the absence of AAT. In the cells exposed to FDC supernatant, the presence of AAT also increased the accumulation of IκBα, p50, and p65 in the cytosol. Furthermore, when the ubiquitin-precipitated complexes were probed for ubiquitin, I also detected numerous proteins, indicating that ubiquitination was

ongoing and was not nonspecifically blocked by A AT (**Figure 39**). Collectively, these data suggested that although IκBα was both phosphorylated and ubiquitinated, it did not appear to be degraded normally, thereby resulting in IκBα accumulation in the cytosol along with the NF-κB components p50 and p65.

I further reasoned that if AAT inhibited the degradation of IκBα, its half life should be increased. Therefore, I cultured infected CD4+ T cells with AAT and monitored IκBα decay in a pulse-chase experiment (**Figure 40**). In the cells incubated without AAT, in the presence or absence of FDC supernatant, IκBα was degraded to undetectable levels between 60 and 90 minutes. However, in the presence of AAT, IκBα decay was almost completely blocked, with detectable levels persisting for at least 32 hours. Therefore, AAT appeared to inhibit NF-κB activation in HIV-infected target cells by interfering with IκBα degradation with resultant blockade of the nuclear translocation of the p50/p65 NF-κB heterodimer.

Because AAT appeared to inhibit NF-κB activation by blocking the downstream process of IκBα phosphorylation and ubiquitination, I next sought to determine whether AAT inhibited the enzymatic activity of the 26S proteasome, composed of 20S and 19S subunits, which degrades phosphorylated and ubiquitinylated IκBα (106). Infected CD4+ T cells were again cultured with or without AAT, the cells were lysed, and the proteasome complex was immunoprecipitated using the antibody specific to the 20S subunits or 19S subunits. The enzymatic activity of the 20S proteasome in the cell lysate, immunoprecipitated complex using either 20S subunit-specific antibody or 19S subunit-specific antibody was then measured. The results indicated that there was no significant difference between the cultures with or without AAT treatment (**Figure 41**). Thus, AAT did not appear to inhibit the activity of proteasome.

Conjugation of polyubiquitin to target proteins occurs via linkage to different lysine residues on ubiquitin, and the linkages used can affect the fates of the targeted proteins (107, 108). When the target protein is conjugated via ubiquitin lysine residue 48 (K48), the molecule is targeted for proteasomal degradation, whereas ubiquitin conjugation via lysine residue 63 (K63) does not result in degradation of the protein (109). To determine whether IκBα polyubiquitination occurred via residue K48 or K63, I precipitated the IκBα complex with IκBα antibody in the presence or absence of AAT and performed immunoblotting using ubiquitin linkage-specific antibodies (**Figure 42A**). In the presence of AAT, I saw a shift from conjugation of ubiquitin molecules through residue K48 to linkage with K63 and this intensified between 24 and 72 hours incubation. Concomitantly, an increase in phospho-IκBα was observed, as seen previously. Thus, it appeared that the mechanism of AAT-mediated inhibition of NF-κB nuclear translocation was mediated by altering the polyubiquitination pattern of phospho-IκBα, which resulted in decreased degradation of this NF-κB inhibitor.

To determine if the altered ubiquitination patterns resulted in a prolonged half-life of IκBα observed previously, I performed a pulse-chase experiment with a double immunoprecipitation, first with an IκBα-specific antibody, and then, after releasing IκBα from the beads, antibodies specific for ubiquitin linked via residue K48 or K63 (**Figure 42B**). Consistent with the hypothesis that a prolonged half-life was associated with increased ubiquitin linkage with K63, IκBα with ubiquitin conjugated via K48 was not observed after 120 minutes in the presence of AAT, whereas in the same cultures, K63 ubiquitinated-IκBα persisted for at least 32 hours. Collectively, these data indicated that AAT prolonged the half-life of IκBα by shifting the pattern of IκBα ubiquitination from a predominant K48 linkage to a K63 linkage.

I also examined the ability of AAT to affect NF-κB activation with a variety of stimuli that activate NF-κB in addition to FDC supernatant and with or without HIV infection (**Figure 43**). Although the overall degree of activation varied somewhat between cells activated with different stimuli, AAT consistently decreased the nuclear translocation of p50 and p65 in both the presence and absence of HIV infection. I also precipitated IκBα in the presence and absence of HIV infection to determine whether HIV affected AAT-mediated differential polyubiquitination. Similar band intensities were observed regardless of the presence of HIV, and the kinetics of altered ubiquitination followed the same pattern as seen above (**Figure 43**).

Next, I investigated whether exogenous AAT was internalized by CD4+ T lymphocytes. HIV-infected CD4+ T cells were therefore cultured with AAT or biotin-labeled AAT, after which the cells were harvested and examined for the presence of AAT in the nucleus and cytoplasm. The results demonstrated that AAT was present in each of these cellular compartments. When infected CD4+ T cells were cultured with Alexa Fluor® 488-labeled AAT and then examined for the presence of AAT by confocal microscopy, I also detected the presence of AAT in these cells (**Figure 44**). To ensure that virus detected on the confocal microscope was internalized and not residing on the surface of the cells, I treated them with trypsin to remove non-internalized virus but this did not alter the detection of fluorescent AAT. When I treated uninfected CD4+ T cells with fluorescently-labeled AAT, similar results were also obtained (**Figure 45**). Thus, these results are consistent with AAT internalization in the primary CD4+ T cells.

To further characterize the internalization of AAT and determine if it's associated with components of the NF-κB complex, we performed immunoprecipitation using a specific antibody to AAT or IκBα followed by immunoblotting (**Figure 46**). The results indicated that

AAT formed a complex with phospho-IκBα and the p50/p65 components of NF-κB. Moreover, when IκBα was precipitated, I detected AAT only when it was exogenously added, indicating that there was no detectable endogenous intracellular AAT. Next, I explored the possibility that AAT inhibited proteasomal degradation of IκBα as a mechanism of cytoplasmic retention. As shown in Figure 45, precipitation of the 19S and 20S proteasome subunits failed to detect the presence of AAT or components of the NF-κB complex. When I performed pulse-chase experiments to detect the kinetics of AAT entry and half-life, I found that it could be detected within 30 minutes of treatment and persisted inside the cells for at least 72 hours in Figure 44. Immunoprecipitation of IκBα revealed that the association of IκBα with AAT was detected within 3 hours and remained in association for at least 72 hours. These data were consistent with the entry of exogenous AAT into the cell and its association with the NF-κB-IκBα complex, leading to interference with IκBα proteasomal degradation.

Next, I sought to determine the molecular mechanism of AAT internalization. Because most mammalian cells uptake extracellular particles and proteins through an endocytic process, I also investigated whether AAT internalization was an endocytic process in CD4+ T cells. To test this hypothesis, infected CD4+ T cells were pretreated with a broad-spectrum endocytosis inhibitor, methyl-beta-cyclodextrin, and then examined for AAT internalization. The results showed that methyl-beta-cyclodextrin pretreatment blocked AAT internalization (**Figure 47**). Because the endocytic process is comprised of one of two major categories, clathrin-dependent and clathrin-independent endocytosis (110), I also investigated whether the internalization of AAT was clathrin-dependent or independent. To answer this question, CD4+ T cells were pretreated with a clathrin-depedent endocytosis inhibitor (chlorpromazine) or caveoli-dependent endocytosis inhibitors (filipin and nystatin) after which they were examined for the ability to

internalize AAT. The results demonstrated that chlorpromazine pretreatment completely blocked the internalization of AAT while filipin or nystatin pretreatment had no obvious effect (**Figure 47**). These results suggested that AAT internalization in CD4+ T cells was a clathrin-dependent endocytosis process.

Although CD4+ T cells internalized AAT through an endocytic process, it was unclear whether intracellular or extracellular AAT exerted the inhibitory effect on NF-κB activation and HIV replication. To investigate this, infected CD4+ T cells were pretreated with methyl-beta-cyclodextrin, chlorpromazine, filipin, or nystatin and their effects on the activation of NF-κBp65/p50 were determined in the presence or absence of AAT. I also examined concomitant effects on HIV replication as assessed by HIV p24 and viral RNA (**Figure 48)**. As expected, AAT inhibited NF-κB activation by blocking p65 and p50 nuclear translocation. AAT also suppressed HIV replication ($p < 0.05$). Methyl-beta-cyclodextrin and chlorpromazine pretreatment completely blocked the inhibitory effect of AAT on NF-κB activation and HIV replication ($p < 0.05$) whereas filipin and nystatin pretreatment had no obvious effect. These results suggested that intracellular AAT exerted the inhibitory effect on NF-κB activation and HIV replication.

Usually, endocytic processes are mediated by the interactions between membrane bound receptors and their ligands (111). In ext sought to identify whether AAT interacted with membrane receptors on CD4+ T cells to permit its internalization. To identify the membrane receptors interacting with AAT, infected CD4+ T cells were co-cultured with AAT and the interaction between AAT and potential membrane receptors was stabilized using DSP to extract membrane proteins. Subsequently, AAT-specific antibody was added to immunoprecipitate AAT and any proteins interacting with it. The specific proteins were identified by peptide mass

fingerprinting assay using a LC-MS/MS system. As shown in Figure 32, AAT interacted with several membrane proteins on C D4+ T cells. Among these proteins, low-density lipoprotein (LDL)-receptor-related protein 1 (LRP1) was a promising candidate (112, 113). To identify whether LRP1 played an essential role in AAT internalization, the receptor was "knocked-down" using LRP1 siRNA or blocked with LRP1-specific antibody. The results showed that LRP1 siRNA efficiently blocked LRP expression and completely inhibited AAT internalization. LRP1-specific antibody also blocked AAT internalization (**Figure 49**). Furthermore, the results demonstrated that LRP1 siRNA efficiently eliminated the inhibitory effect of AAT on the nuclear translocation of NF-κB p65 and p50 and the production of HIV ($p < 0.05$) (**Figure 50**). Because AAT internalization in CD4+ T cells was a clathrin-dependent endocytosis process, I next sought to determine whether LRP1 also associated with clathrin to mediate AAT internalization. To test this postulate, LPR1-, AAT-, or clathrin-specific antibodies were added to imunoprecipitate their corresponding proteins and the interactions among these proteins were detected by Western blotting. As expected, the interaction among AAT, LRP1, and clathrin was detected (**Figure 49**). Taken together, these results suggested that LRP1 on CD4+ T cells interacted with AAT and mediated its internalization through a clathrin-dependent, endocytic process.

Usually, receptor-mediated clathrin-dependent endocytosis mediates the uptake of extracellular molecules and transports them from the endosome to the lysosome (111). In the lysosome, internalized molecules are degradated, recycled back to the cell surface, trafficked to the organelles, or released into the cytosol (114-116). To investigate how AAT was transported into the cytosol of CD4+ T cells thereby altering the ubiquitinylation pattern of cytosolic IκBa, I utilized infected CD4+ T cells that were incubated with AAT for 3 hours. After this incubation,

any remaining non-internalized AAT was removed. The cytosolic location of AAT was detected by confocal microscopy. The results demonstrated that AAT was confined to a specific cellular compartment early and then became distributed homogenously in the cytosol (**Figure 51**). When AAT was immunoprecipitated at different time points, the results indicated that AAT associated with LRP1 and the endosomal proteins, Rab4 and Rab 5, during the first several hours. Subsequently, AAT associated with the lysosomal proteins, Lamp1 and Lamp2. After a 6-hour incubation, no interaction was detected between AAT and the lysosome or the endosome but AAT was distributed evenly in the cytosol (**Figure 51**). Thus, these results suggested that internalized AAT might be transported from the endosome to the lysosome and then released or trafficked into the cytosol.

To confirm that AAT was transported from the endosome to the lysosome and then released or trafficked into the cytosol, infected CD4+ T cells were treated with BAPTA-AM or ammonium chloride to block the fusion of the endosome with the lysosome. Subsequently, the transportation of AAT, the nuclear translocation of NF-κB p65 and p50, and the replication of HIV were monitored. The results indicated that the endosome-lysosome fusion inhibitor, BAPTA-AM and ammonium chloride, blocked the homogenous distribution of AAT and confined AAT into a specific cellular compartment (**Figure 52**). As expected, after BAPTA-AM and ammonium chloride treatment, AAT was associated with LRP1 and the endosome proteins, Rab4 and Rab 5, but not the lysosomal proteins, Lamp1 and Lamp2 (**Figure 52**). Moreover, BAPTA-AM and ammonium chloride treatment also blocked the inhibitory effect of AAT on the nuclear translocation of NF-κB p65 and p50 and the replication of HIV ($p < 0.05$) (**Figure 53**). Collectively, these results suggested that LRP1 and clathrin mediated the internalization of AAT

in CD4+ T cells, and that internalized AAT was transported from the endosome to the lysosome and then released or transported into the cytosol, where it could interact with cytosloic IκBα.

Although AAT altered the ubiquitinylation pattern of IκBα to inhibit NF-κB activation and HIV replication, the molecular mechanism remained unclear. I investigated whether the cytosolic AAT and IκBα directly interacted to exert the observed inhibitory effect. Infected CD4+ T cells were cultured with AAT for 24 hours and then AAT or IκBα was immunoprecipitated from the cytosolic proteins. The results demonstrated that AAT associated with the IκBα complex (**Figure 54**). In the cytosol, IκBα usually binds to NF-κB p65 and p50 to block their nuclear translocation (100). Thus, I next determined whether AAT directly interacted with IκBα, p65, or p50. AAT was therefore incubated with recombinant IκBα. Subsequently, AAT- or IκBα-specific antibodies were added to immunoprecipitate their respective target proteins and detect the direct interaction between AAT and IκBα. The results showed that AAT directly interacted with IκBα *in vitro* (**Figure 54**). Meanwhile, I could not detect any direct interaction between AAT and p65 or between AAT and p50 when AAT was incubated with p65 or p50 (**Figure 55**).

In T lymphocytes, IκBα is polyubiquitinated through the activity of an E1 ubiquitin-activating enzyme, the Ubch5 E2 ubiquitin-conjugating enzyme, and the Skp1, Cullin 1 (Cul1), and F-box protein (SCF) β transducin repeat containing protein (β-TrCP2) SCFIκB E3 ligase complex (100, 101, 117, and 118). Next, I sought to determine whether AAT interacted with the E1 ubiquitin-activating enzyme complex, the E2 ubiquitin-conjugating complex, or the SCF E3 ligase complex to alter the polubiquitiylation pattern of IκBα. Infected CD4+ T cells were prepared as before and subjected to immunoprecipitation of the IKK complex, the E1 ubiquitin-activating enzyme complex, or the E2 ubiquitin-conjugating complex (Ubch5) with their

corresponding specific antibodies. I also precipitated the SCF E3 ligase complex with antibody directed against Skp1, Cul1, or β-TrCP2. To obtain IκBα, I first removed phosphorylated IκBα by immunoprecipitation with an antibody against phosphorylated IκBα and then precipitated IκBα with an antibody to IκBα. To collect ubiquitin, I passed the cell lysate through a 10KD filter and immunoprecipitated ubiquitin from the flow-through fraction. Subsequently, I co-cultured AAT with the immunoprecipitated IKK complex, E1 ubiquitin-activating enzyme complex, E2 ubiquitin-conjugating complex, SCF-IκB E3 ligase complex, IκBα, or ubiquitin to detect any potential interactions between them. The results demonstrated that AAT interacted only with the IκBα complex (**Figure 56**). I also incubated recombinant IκBα or immunoprecipitated IκBα with the IKK complex, the E1 ubiquitin-activating enzyme complex, the E2 ubiquitin-conjugating complex, or the E3 ligase complex to detect the *in vitro* phosphorylation and ubiquitinylation of IκBα. In addition, ATP and ubiquitin were added to initiate the reaction in the presence or absence of AAT (**Figure 57A**). The results indicated that AAT had no obvious effect on IκBα phosphorylation. Moreover, AAT did not affect the polyubiquitinylation of phosphorylated IκBα conjugated through residue K63 (**Figure 57B**). However, the presence of AAT blocked the polyubiquitinylation of phosphorylated IκBα conjugated through residue K48 (**Figure 57B and 57C**). Together, these results suggested that cytosolic AAT interacted with phospho-IκBα directly to block its polyubiqutinylation on residue K48.

Section V: AAT, FDC activation, and HIV/AIDS pathogenesis

The results in section II coupled with previous studies in our lab suggested that FDC activation played a pivotal role in HIV/AIDS pathogenesis, affecting HIV trapping and maintenance of infectivity by FDCs, FDC-mediated HIV replication in CD4+ T cells, and CD4+

T cell migration into GCs (42-44, 47, 55, 60, 89). The results in section II also demonstrated that FDC activation could be acheived *in vitro* with specific activators. Moreover, the results in section IV demonstrated that AAT inhibited NF-κB activation in normal and HIV-infected CD4+ T cells by altering the ubiquitinylation pattern of phosphorylated IκBα. Because FDC activation involves the activation of the NF-κB complex (42-44), I postulated that AAT also inhibited FDC activation by suppressing the activation of NF-κB and thereby blocking the contribution of FDCs to HIV pathogenesis. To test this hypothesis, I first investigated whether FDCs internalized AAT as CD4+ T cells did. Just as with T cells, fluorescently labeled AAT appeared to be inside FDCs after incubation (**Figure 58**). Next, I investigated whether AAT blocked NF-κB activation in resting or activated FDCs. E*x vivo* or *in vitro* activated FDCs were treated with AAT and the activation of NF-κB was measured by detecting the nuclear translocation of NF-κB p65 and p50, the accumulation of phosphorylated IκBα in the cytosol, and the ubiquitinylation pattern change of phosphorylated IκBα. The results indicated that AAT treatment or pretreatment of the FDCs inhibited the nuclear translocation of NF-κB p65 and p50. LPS dramatically increased the nuclear translocation of these proteins, which was inhibited by AAT treatment. However, HIV immune complexes (pre-formed by incubating HIV in the presence of gp120-specific antibody) had no obvious effect on the nuclear translocation of NF-κB p65 and p50. Moreover, the presence of CD32- or CD21-specific antibodies did not interfere with the nuclear translocation of NF-κB p65 and p50 in resting or activated FDCs (**Figure 59**). The results showed that AAT treatment or pretreatment dramatically elevated the amounts of phosphorylated IκBα in the cytosol, regardless of the treatment of LPS, HIV immune complexes, anti-CD32, or anti-CD21 (**Figure 60**), consistent with the results in AAT-treated CD4+ T cells. Because AAT inhibited NF-κB activation by altering the ubiquitinylation pattern of IκBα in CD4+ T cells, I also sought

to determine whether the ubiquitinylation pattern of IκBα in FDCs was changed by AAT treatment. Therefore, FDCs or AAT-pretreated FDCs were incubated with AAT, LPS, HIV immune complexes, anti-CD32, or anti-CD21. The results indicated that AAT dramatically increased the amounts of ubiquitinylated IκBα conjugated at K63, regardless of the treatment of LPS, HIV immune complexes, or antibodies to CD32 or CD21. AAT also significantly decreased the amounts of ubiquitinylated IκBα conjugated to K48 (**Figure 61**), which was consistent with the results obtained in AAT-treated CD4+ T cells. The results also demonstrated that the expression of p65, p50, and TLR4 was not affected by the treatment with AAT, LPS, HIV immune complexes, anti-CD32, or anti-CD21 in FDCs or AAT-pretreated FDCs (**Figure 62**). These results suggested that FDCs internalized AAT and that it blocked NF-κB activation by altering the ubiquitinylation pattern of IκBα in FDCs just as we found in primary CD4+ T cells.

Because the results in section II demonstrated that FDC-CD32 played an essential role in HIV trapping and maintenance and that FDC-CD21 also appeared to contribute to this process, I next sought to investigate whether AAT inhibited the expression of FDC-CD32 and FDC-CD21 thereby altering the ability of FDCs to trap and maintain the infectious nature of HIV. To test this hypothesis, the mRNA and protein expression of CD32 and CD21 were detected after no treatment or AAT-pretreatment of FDCs incubated with LPS, HIV immune complexes, anti-CD32, anti-CD21, or AAT. LPS and HIV immune complexes increased FDC-CD32 expression, which could be blocked by AAT treatment. Moreover, LPS also increased FDC-CD21 expression, and this too was suppressed by AAT treatment. Anti-CD32 completely blocked the increased expression of CD32 that was induced by HIV immune complexes ($p < 0.05$) (**Figures 63 – 65**). When these FDCs were incubated with HIV-1_{IIIB} and a gp120-specific antibody and fresh human serum (source of complement proteins) to detect the trapping of HIV, LPS or HIV

immune complex-stimulated FDCs trapped more HIV-1_{IIIB} than control FDCs ($p < 0.05$). AAT treatment or pretreatment decreased the amount of virus trapped on these FDCs ($p < 0.05$). If these FDCs were incubated with HIV-1_{IIIB}, gp120-specific antibody, and fresh human serum in the presence of LPS, HIV immune complexes, or AAT again (under the same condition as used previously), HIV trapping decreased even more ($p < 0.05$). Furthermore, the addition of AAT to the FDCs also inhibited the infectivity of the trapped HIV ($p < 0.05$). This infectivity disappeared within 3 weeks in the presence of AAT (**Figure 66**). Thus, it appeared that AAT could significantly inhibit FDC trapping of HIV and the maintenance of viral infectivity.

The results in section II demonstrated that FDCs increased HIV replication by secreting TNFα, which activated NF-κB in the infected CD4+ T cells. Moreover, previous studies in our lab revealed that FDCs attracted GC T cells by producing CXCL13 (58). Thus, I also investigated whether AAT inhibited the expression and production of TNFα and CXCL13 in FDCs. FDCs or AAT-pretreated FDCs were incubated with LPS, HIV immune complexes (preforemed with a gp120-specific antibody and HIV-1_{IIIB}), anti-CD32, anti-CD21, or AAT. Specific FDC mRNA expression and protein production of TNFα was detected by qPCR and ELISA respectively (**Figures 67 and 68)**. LPS increased TNFα production (**Figure 67**) and TNFα mRNA generation (**Figure 68**), both of which were inhibited by AAT treatment ($p < 0.05$). However, incubation of FDCs with HIV immune complexes slightly increased TNFα expression and production, but this was inhibited by AAT treatment ($p < 0.05$) (**Figure 67 and Figure 68**). The results indicated that LPS up-regulated CXCL13 expression and production, which was blocked by AAT treatment ($p < 0.05$) (**Figure 69**). Thus, it appeared that AAT inhibited FDC activation, which in turn affected this cell's ability to increase HIV replication and mediate T cell migration into GCs.

DISCUSSION

Section I: FDCs and HIV/AIDS pathogenesis

Transcription factors and HIV replication: HIV infection if left untreated typically results in the development of AIDS, which is a major diseaes in the world today (1-3). In its life cycle, HIV has two principal stages: infection and replication. The infection stage includes the entry of virus into the host cell, the reverse transcription of viral RNA, its translocation into the host cell's nucleus, and its integration into the host genome (12, 23, 29-31). The replication stage of the virus life cycle begins with the transcription of viral genes leading to the production of progeny virus. Usually, the replication of HIV is tightly controlled by the activation of cellular transcription factors including NF-κB, SP1, AP2, and NFAT, which bind to specific sites within the LTR of the viral genome thereby controlling virus activity (34).

The results I presented in this dissertation indicated that mutation of HIV SP1 and NF-κB binding sites in the LTR blocked viral replication. Mutation of the AP2 binding sites also inhibited HIV replication. In mammalian cells, AP2 and SP1 are required for cell survival (119-122). NF-κB plays an important role in immune responses, including antibody generation and cytokine production (123). NF-κB activation is also related to the activation of CD4+ T lymphocytes, a major target for HIV infection and replication (124). Thus, NF-κB plays a very important role in HIV replication. It should be noted that the LTR contains additional DNA binding sites for other transcription factors that were not investigated in this thesis. It will be interesting to investigate the role of these additional DNA binding sites for transcription factors to determine their contributions to HIV replication.

FDCs, HIV trapping and maintenance: Although tremendous advances have been made in the treatment of HIV/AIDS, a major obstacle in treatment and eradication is the

existence of HIV reservoirs in the human body where the virus is stored in a protected manner. These reservoirs include latently-infected CD4+ T cells, macrophages and FDCs (7, 125). FDCs form a large reservoir of infectious and genetically diverse HIV that can perpetuate infection (7). These cells are located in the GCs of secondary lymphoid tissues, where they interact intimately with surrounding lymphocytes. In the GCs, FDCs trap and retain large amounts of antigens including HIV particles, and these are maintained in an infectious form for many months (5, 7, 39-41, 51, and 126). In this dissertation, the results indicated that FDCs trapped more HIV when HIV-specific antibody and complement proteins were present, suggesting that both antibody and complement components play an important role in mediating the interactions between HIV particles and FDCs. The presence of HIV antibody allows the viruse to form immune complexes (composed of HIV and gp120 antibody), whose Fc portion interacts with FDC-CD32 to mediate the trapping of HIV on FDCs. Moreover, complement proteins and FDC-CD21 also contribute to this process. Currently, the role of HIV-specific antibody and complement proteins in HIV trapping and maintenance on FDCs is somewhat controversial. Some studies suggest that HIV antibody is essential for HIV trapping and maintenance on FDCs (5, 38, 55, 62-64), while others report that HIV antibody is not necessary (65). These later reports by several groups suggest that complement proteins and their degradation products, particularly C3, appear to be important for virus trapping on FDCs (56, 66, and 67). My results suggest that both HIV immune complexes with and without complement proteins and FDC-CD32 and FDC-CD21 are important for HIV trapping. Importantly, FDCs still maintained the capability to trap HIV when CD32 and CD21 were blocked or knocked-down. Moreover, FDCs also trapped HIV even in the absence of HIV-specific antibody and complement proteins. These observations suggest that HIV trapping on FDCs does not solely depend on the interaction of HIV immune complexes/FDC-CD32 and HIV

immune complexes/complement components/FDC-CD21.These other unknown interactions that contribute to HIV binding on FDCs may be an interesting project to pursue in the future.

In addition to mediating virus binding to FDCs, the interaction of viral immune complexes with FDC-CD32 and FDC-CD21 also plays an important role in maintaining the infectivity of trapped HIV. In the GCs, FDC-CD32 plays an important role in trapping and maintaining antigens (62). A previous study from our lab indicates that HIV immune complexes/FDC-CD32 interactions play an essential role in maintaining the infectivity of HIV as evidenced by the reduction of this ability when FDC-CD32 is blocked (55). My results also confirmed that the presence of HIV-specific antibody contributed to maintain the infectivity of trapped virus and that complement proteins contributed slightly to this process. Moreover, when FDC-CD32 was knocked-down with specific siRNA or was blocked with specific antibody, HIV infectivity disappeared rapidly. In contrast, downregulation of FDC-CD21 with specific siRNA or blocking CD21 with CD21 antibody only slightly decreased the infectivity of trapped virus. Thus, the interaction of HIV immune complexes/FDC-CD32 is required to maintain the infectivity of trapped HIV. Moreover, the interaction of HIV immune complexes/complement proteins/FDC-CD21 contributes to this process. Recent studies reveal that gp120 shedding from HIV is a contributing factor to the loss of HIV infectivity (24, 25, 103, and 104). I found that when FDCs were incubated with HIV-1_{Bal} produced in macrophages (which produce HIV gp160 with gp120 a nd gp41 covelently linked and not further processed), all FDC-trapped viruses maintained their infectivity, regardless of the presence of HIV-specific antibody or complement proteins. In contrast when the same virus was propagated in T cells (which process gp160 so that gp120 and gp41are non-covalently associated), the presence of virus-specific antibody and/or complement proteins was important in FDC-mediated maintenance of virus infectivity. Thus,

gp120 shedding from HIV appears to play an important role in the loss of infectivity of FDC-trapped HIV-1_{IIIB}. The shedding of gp120 is reduced if the viruses are in the form of immune complexes and associated with FDC-CD32. The interaction between HIV immune complexes/complement proteins and FDC-CD21 may stabilize this process and protect the shedding of gp120. I envision that FDCs bind HIV immune complexes on multiple dendritic processes using a number of FDC-CD32 receptors, and that these interactions may physically constrain gp120 shedding from the viral particles. The binding of HIV-specific antibody to antigens (e.g., pg120) present on the surface of viral particles permits the association of HIV particles with FDC-CD32. This association may also inhibit gp120 shedding by creating isolated regions in which the envelope glycoproteins are trapped between interacting dendritic processes of FDCs. In this manner, FDCs would thereby block the release of gp120. Alternatively, it may be that the presence of antibody on the viral envelope coupled with FDCs hinders or prevents the loss of gp120. Previous data from our lab also indicated that when antibody directed to MHC proteins present on the virion surface was present, it maintained viral infectivity as well as antibody directed to gp120. Therefore, the interaction of HIV immune complexes/FDC-CD32 maintains the infectious ability of these viruses and correlates with a reduced shedding of the HIV gp120. Additionally, the interaction between HIV immune complexes/complement proteins and FDC-CD21 may also stabilize this process through an unknown mechanism. Although the interaction of HIV immune complexes/FDC-CD32 and HIV immune complex/complement proteins/FDC-CD21 inhibits gp120 shedding from HIV and maintains virus infectivity, the inhibition is not permanent. In the present thesis, my in vitro results reveal that the infectivity of FDC-trapped HIV-1_{IIIB} disappeared after 5 weeks incubation even in the presence of HIV antibody and complement proteins while almost all FDC-trapped HIV-1_{Bal} viruses still maintain

their infectivity after 6 weeks incubation. This result suggests that the shedding of gp120 from HIV is prolonged but not completely blocked *in vitro* in the presence of HIV antibody and complement components.

FDCs and HIV replication (*This section was copyrighted by the American Society for Microbiology for my paper published on the Journal of Virology (2009, Volume 83, page 150 to page 158, DOI: 10.1128/JVI.01652-08) and I got the permission from the Journal of Virology (License Number: 2860901498845; License date: Mar 02, 2012) to use the materials in my PhD dissertation*): In humans, FDCs serve as a resevior of infectious virus that escapes the effects of neutralizing antibody and contains archived quasispecies that are not found elsewhere (5, 7). In the GCs, FDCs produce CXCL13 that serves as a chemoattractant for GC T and B cells (57). FDCs also provide additional signals that increase the expression of CXCR4 on GC T cells (58). With increased CXCR4 expression, GC T cells are more sensitive to infection by X4-tropic HIV. Moreover, the interactions between FDCs and CD4+ T-cells trigger the generation of two regulators of G-coupled protein signaling, RGS13 and RGS16. In T cells, the expression of these regulators correlates with a decreased migration capability to CXCL12, a signal outside the GCs that may help GC T cells to invade this site (58). This decreased migration capability prolongs the time that CD4+ T cells stay in the GCs adjacent to FDCs, thereby increasing the posibilities of infection by FDC-trapped HIV (58). Moreover, FDCs also increase HIV transcription and virus production in CD4+ T cells. The increased virus transcription and production was mediated by the secretion of TNFα from FDCs, which in turn resulted in the activation of NF-κB.

In my studies, I found that FDCs alone produced enough TNFα to increase HIV replication in HIV-infected CD4+ T cells. Adding a similar quantity of recombinant TNFα to the

cultures of infected T cells recapitulated the effect of FDCs or their supernatant. Moreover, adding this amount of TNFα to the cultures also activated NF-κB in the same manner observed when FDCs or FDC supernatant were present. Thus, TNFα produced in FDCs is sufficient to account for the observed increases in HIV replication. It is also possible that the FDC-TNFα signaling is much more effecient *in situ* than observed in the *in vitro* setting where soluble signal could diffuse throughout the culture medium. The high efficiency of the FDC-TNFα signaling is due to to the physical proximity of FDC with adjacent cells. Furthermoer, the direct physical interaction between FDCs and GC T cells would likely transmit HIV, while providing TNFα-mediated activation signals to facilitate productive infection of the target cells. Thus, the FDC-T-cell network may be even more significant *in vivo* than what we observed *in vitro*.

Additionally, the observation that TNFR-Ig completely blocked the increased HIV replication induced by F DCs or FDC supernatant fluid further confirms that FDC-produced TNFα mediated the increase of virus replication in CD4+ T cells. These observations are highly suggestive and strongly supportive of the concept that FDC signals induce increased HIV transcription *in vivo*. The results are also in agreement with those suggesting that GC T cells from HIV-infected subjects demonstrated a higher frequency of HIV infection than other CD4+ lymphocytes and that these GC T cells produced higher level of viruses than other CD4 T cells (127, 128). Moreover, these results provide a rational explanation for these observations and confirm the potential importance of the GC environment, in large part contributed by FDCs, to HIV/AIDS pathogenesis.

Although it is known that TNFα increases the transcription of HIV, this is the first report indicating that isolated FDCs produce this cytokine to increase HIV transcription and virus production in infected CD4+ lymphocytes. The result that FDCs express and secrete TNFα is in

contrast to the findings of a report that failed to detect TNFα mRNA in cDNA preparations of FDCs (129). The reason for this difference is unknown yet, but it may relate to the differences in isolation and testing procedures as well as the difference of tissue samples. In this thesis, I persistently detected TNFα-specific mRNA in FACS-sorted FDC preparations. The different specimens produced levels of TNFα ranging from a low of 79 to a high of 198 picograms per milliliter and the differences may be related to the local activation status of the tissues from which the FDCs were isolated. Therefore, FDC-produced TNF-α might play an essential role in the persistent hyperimmune activation in HIV-infected individuals.

The FDC-mediated increase of HIV replication may play an important role in HIV/AIDS pathogenesis by ensuring that initial contact of GC T cells with FDC-trapped HIV leads to the establishment of HIV infection followed by virus expression. Furthermore, infected lymphocytes at other sites may migrate into the GCs, where they can be activated by FDC signaling to produce virus expression. Additionally, it may also be interesting to investigate whether circulating, latently infected T cells that are HIV reservoirs and contact with FDCs could be activated to express virus. This hypothesis has not yet been tested, but it appears to be a reasonable consideration due to the observation that TNFα induces latently infected cell lines to express virus (130). Therefore, FDC-produced TNFα mediates the increase of HIV expression that explains persisting virus expression in the GCs surrounding FDCs (45, 46, and 52).

FDC activation and HIV: The phenotype of FDCs in primary and secondary follicles is very different. In secondary follicles, FDCs bear high levels of CD32, ICAM-1, and VCAM-1, which represent the activated state (62, 90, 131-134). In contrast, in primary follicles, FDCs can be found by labeling with anti-CD21, but CD32, ICAM-1, and VCAM-1 levels are low and difficult to detect, representing the resting or inactive state (62, 132, and 133). Activated FDCs

play an essential role in antigen trapping including HIV (42-44, 46-49, and 67). The activation of FDCs builds a microenvironment that is highly conducive to HIV transmission and replication (48-50). Recent studies reveal that LPS from bacterial transmigration and antigen immune complexes can both trigger the activation of FDCs and thereby promote specific antibody production and somatic hypermutation (46, 42-44). In mammalian cells, LPS interacts with TLR4 and subsequently mediates the activation of NF-κB through a calcium-dependent mechanism (100). My results demonstrated that FDCs consistently expressed TLR4, regardless of the stimulation of LPS, which may relate to the state of chronic activation that exists in tonsillar tissues. LPS treatment activated NF-κB by increasing the nuclear translocation of p65 and p50 i n FDCs and thereby up-regulated the expression of FDC-CD32 and FDC-CD21. Furthermore, increased expression of FDC-CD32 and FDC-CD21 trapped more HIV and maintained its infectivity. These results suggest that LPS-mediated FDC activation may play an important role in trapping HIV and maintaining the infectivity of trapped viruses. Moreover, LPS also increased TNFα production from FDCs, which can subsequently activate infected T lymphocytes and increase HIV replication (47). LPS also increased CXCL13 expression in FDCs, which promotes the migration of T lymphocytes into the GCs thereby increasing their ability to contact infectious virus trapped on FDCs (58, 135). Thus, LPS-mediated FDC activation not only participates in the trapping and maintenance of HIV, but creates a microenvironment that is conducive to virus transmission and replication.

CD32 is generally considered to be an inhibitory receptor and is known to reduce the functionality of B cells, mast cells, and conventional dendritic cells (136, 137). However, in tonsillar FDCs, CD32 appears to promote a phenotype associated with FDC accessory cell activity (43, 44). A recent report indicates that IKK2-dependent signals are critical for immune

complex-driven induction of VCAM-1 and ICAM-1 expression in FDCs through the canonical NF-κB pathway. In contrast, p55 TNFR is essential for FDC network formation and maintenance, which is independent of IKK2 (138). However, the results in this thesis indicated that HIV immune complexes increased FDC-CD32 expression without interfering with the activation of the classical NF-κB signaling pathway suggesting that in FDCs, CD32 is not an inhibitory receptor. It should be noted that HIV immune complexes did not alter the expression of FDC-CD21, TNFα, and CXCL13. Thus, it will be interesting to investigate further the molecular mechanism of HIV immune complex-mediated signaling that increases CD32 expression in human FDCs.

Summary: The net result of these FDC contributions to the GC microenvironment is to create an ideal site where infectious virus, susceptible target cells, and activation signals come together, thereby maintaining the disease state. A better understanding of FDC contributions to virus transmission and disease progression will certainly increase our knowledge of HIV pathogenesis and may be helpful in the design of better intervention strategies that specifically target the FDC reservoir of HIV.

Section II: AAT and HIV/AIDS pathogenesis

AAT inhibition of HIV infection: Recent studies have demonstrated that the level of AAT in whole blood may relate to HIV/AIDS pathogenesis. Pre-existing AAT deficiency is believed to be associated with accelerated HIV progression (10, 139). Studies have revealed that AAT potently inhibits HIV replication (8, 11, 80-83). When CD4+ T cells were pretreated with AAT and then infected with HIV, the results demonstrated that CD4+ T cells with AAT pretreatment produced much less virus than the CD4+ T cells without AAT pretreatment,

suggesting that AAT interferes with HIV infection. My testing indicated that AAT inhibited HIV infection by blocking HIV entry into the host CD4+ T cells.

HIV entry into the host cells involves the interaction between HIV gp120/gp41 and host cell CD4/CXCR4 or CCR5 receptors on the cell membrane (12). Some researchers postulate that AAT inhibition of HIV entry is related to the interaction between AAT and cell membrane proteins (105) while others report that the inhibition of HIV entry is related to an interaction between AAT and viral membrane proteins, such as gp41 (9, 140). My results did not provide any information as to whether AAT interacts with cell membrane proteins to inhibit HIV entry. AAT had no obvious effect on CD4, CXCR4 and CCR5 expression in CD4+ T cells. When I precipitated the cell membrane proteins that might interact with AAT, I detected several membrane proteins but surprisely no CD4, CCR5, CXCR4, or other HIV infection-related proteins. When I precipitated HIV associated membrane proteins, I detected a strong interaction between AAT and the HIV glycoprotein gp160 (composed of gp120 and gp41). When pure recombinant gp120 or gp41 was incubated with AAT, AAT only directly interacted with gp41. However, the molecular mechanism whereby AAT interacts with gp41 remains unknown. . The study of J. Münch et. al. demonstrates that VIRIP, a 20-residue C-proximal sub-fragment of AAT, can interact with the fusion peptide domain of gp41, thereby interfering with the entry of HIV into host cells (9, 140). Thus, my data are consistent with the suggestion that AAT may inhibit virus entry by binding to gp41 and blocking its ability to interact with the host cell membrane.

AAT-mediated inhibition of HIV replication (*This section was copyrighted by the American Association of Immunologists, Inc. (Copyright 2011. The American Association of Immunologists, Inc.) for my paper published on the Journal of Immunology (2011, Volume*

186 No. 5, page 3148 to page 3155, DOI: 10.4049/jimmunol.1001358) and I got the permission from the Journal of Immunology to use the materials in my PhD dissertation.): In this study, I reported the ability of AAT to inhibit HIV replication, including that mediated by FDCs. AAT inhibited NF-κB activation, regardless of the presence of FDC supernatant that contains NF-κB activator TNFα (47), by prolonging the half-life of IκBα, which in turn remained bound to cytoplasmic NF-κB. IκBα preservation in the cytoplasm blocked the nuclear translocation of NF-κB and its subsequent activation of HIV transcription. Initially, I was surprised by the observation that AAT decreased nuclear NF-κB while at the same time increasing levels of cytoplasmic phospho-IκBα. I first postulated that AAT inhibited the ubiquitination of phosphorylated IκBα, resulting in the continued association of IκBα with NF-κB thereby blocking the activation of this transcription factor. However, my results indicated that AAT did not block the ubquitinylation of cytoplasmic phospho-IκBα. I then reasoned that AAT blocked the proteolytic activity of the 26S proteasome. To my surprise, when intact immunoprecipitated proteasomes were examined, no AAT-induced depression of the 20S proteolytic activity was measured, suggesting that AAT did not inhibit NF-κB activation by suppressing proteasome function. Furthermore, immunoprecipitation of both the 19S and 20S proteasomal subunits failed to detect AAT association with the proteasome. These data established that AAT blocked IκBα degradation following phosphorylation and ubiquitination but prior to proteasomal degradation.

In humans, the 8.5-KD ubiquitin molecule contains seven lysine residues. Polyubiquitination occurs via an isopeptide linkage between the C-terminal glycine residue of an ubiquitin molecule bound to a target protein and one of seven lysine residues of additional ubiquitin molecules that form a polyubiquitin complex. Conjugation of polyubiquitin to target proteins *via* linkage to different lysine molecules on ubiquitin can lead to different fates of the

targeted proteins (101, 108). Polyubiquitinylation at K48 results in the degradation of the target proteins while polyubiquitinylation at other lysine residues including K63 exerts other cellular functions, including protein-protein interactions, cell signaling, localization within the cell, and functional regulation of proteins (107-109). My findings indicated that AAT induced a shift in the pattern of polyubiquitination of IκBα consisting of a decrease in K48 linkages and a concomitant increase in polyubiquitination using K63 linkages. These data directly correlated with a significantly increased half-life of IκBα and the resulting inhibition of NF-κB activation.

In mammalian cells, extracelluar stimuli including TNF-α induce IKK activation that results in phosphorylation of IκBα on serine residues 32 and 36. Following phosphorylation, IκBα monoubiquitinylation occurs on residue K21 and K22 that is subsequently polyubiquitinylated through the activity of the Skp1, Cullin 1, a nd F-box protein (SCF) β transducin repeat containing protein SCFIκB E3 ligase complex (100, 101). In turn, β-TrCP ubiquitinylates phosphorylated IκBα at specific lysines in the presence of Ub-activating (E1) and -conjugating (Ubch5) enzymes. Usually, the SCFIκB E3 ligase complex mediates the polyubiquitinylation of the target protein using ubiquitin residue K48, which is followed by the proteasomal degradation of the target protein (101, 117, and 118). In this dissertation, when the NF-κB/IκBα complex was precipitated using an antibody specific for IκBα, I detected AAT in the complex. Moreover, AAT directly interacted with recombinant IκBα, not NF-κB (p65 and p50). AAT also did not interact with the E1 complex, the E2 (Ubch5) complex, and the SCF E3 ligase complex (Skp1, Cullin 1 and β-TrCP). When I detected the *in vitro* polyubiquitinylation of phosphorylated IκBα, I found that the presence of AAT totally blocked the polyubiquitinylation of phosphorylated IκBα at K48 while the polyubiquitinylation of phosphorylated IκBα at K63 did not change obviously. These facts suggested that the direct interaction between AAT and

IκBα blocked the polyubiquitinylation of phosphorylated IκBα at K48. However, structural studies are still necessary to clarify the molecular mechanism.

Next, I s ought to determine whether intracellular or extracellular AAT exerts the inhibitory effect on NF-κB activation and HIV replication. In this thesis, I found that the general endocytosis inhibitor, methyl-beta-cyclodextrin, completely blocked AAT internalization in CD4+ T cells. I also found that AAT internalization was blocked after treatment of cells with the clathrin-dependent endocytosis inhibitor, chlorpromazine. Moreover, methyl-beta-cyclodextrin and chlorpromazine treatment of the same cells eliminated the inhibitory effect of AAT on NF-κB activation and HIV replication. Thus, in CD4+ T cells, AAT internalization is a clathrin-dependent endocytic process and only intercellular AAT exerts an inhibitory effect on NF-κB activation and HIV replication. In endothelial cells, intracellular uptake of AAT is also a clathrin-dependent endocytic process (141, 142). However, some reports suggest that AAT internalization is caveoli-dependent due to the identification of AAT in the caveolar fraction of the plasma membrane of endothelial cells (143). My results revealed that the inhibitor of caveoli-mediated endocytosis, filipin or nystatin, did not block AAT internalization in CD4+ T cells, but I did not examine endothelial cells in my research. My functional studies also showed that the caveoli pathway inhibitors did not interfere with the inhibitory effect of AAT on NF-κB activation and HIV replication. Although I cannot rule out the contributions of nonclathrin or noncaveoli-mediated endocytosis to the uptake of AAT, the profound effect of specific inhibitory strategies using chlorpromazine indicated that AAT was primarily internalized *via* clathrin-mediated endocytosis.

Clathrin-dependent endocytosis occurs in almost all mammalian cells and mediates the internalization of numerous essential nutrients and factors including the cholesterol-laden low-

density lipoprotein particles that bind to the LDL receptor, and iron-laden transferrin that binds to the transferrin receptor (144, 145). My results demonstrated that AAT directly interacted with LRP1 on CD4+ T cells. Furthermore, AAT internalization was completely blocked by LRP1 siRNA and LRP1-specific antibody treatment of CD4+ T cells. In turn, the inhibitory effect of AAT on NF-κB activation and HIV replication was completely eliminated by LRP1 siRNA and LRP1 antibody treatment. When I immunoprecipitated AAT, LRP1 or clathrin from the whole cell lysate using an antibody against AAT, LRP1 or clathrin respectiviely, I detected interactions among AAT, LRP1 and clathrin. Previously, reports indicated that a cell surface protein, serpin-enzyme complex (SEC) receptor, recognized and interacted with AAT on the cell membrane (146). The recognition and interaction between AAT and SEC mediated the internalization of AAT in some carcinoma cell lines (147). Here, my results demonstrated that LRP1, one of the SEC receptors, played an essential role in AAT internalization in CD4+ T cells. Moreover, several *in vitro* studies reported that free AAT would be internalized via SEC/LRP-mediated endocytosis only when AAT formed a complex with its target enzymes (112, 113). However, in the present study, I detected AAT internalization without the formation of an AAT-enzyme complex. A possible explanation for the difference was that AAT might interact with target enzymes on the membrane of CD4+ T cells or in the culture medium to form an AAT-enzyme complex. In turn, the complex would interact with LRP1 to mediate its internalization. Another potential explanation was that AAT had no need to form a complex with an enzyme to permit its internalization *in vivo*. Regardless of these possible explanations, it is reasonable to conclude that AAT internalization is predominantly mediated through an LRP1-mediated clathrin-depedent endocytic process.

Receptor-mediated endocytosis *via* clathrin-coated pits is a shared pathway used for the internalization of a variety of ligand-receptor complexes, including LRP1-ligand (111). Although there is still uncertainty about many aspects of the endocytic pathways, the general transportation of internalized protein is from the endosome to the lysosome (116, 148, and 149). The most common fates of these internalized molecules are degradation or recycling back to the cell surface. However, many alternate fates are possible such as trafficking to organelles like the Golgi apparatus or translocation into the cytosol (150, 151). In my research, the results suggested that AAT associated with the endosome early and then translocated into the lysosome. Moreover, treatment of cells with an endosome-lysosome fusion inhibitor blocked the transportation of AAT from the endosome to the lysosome and eliminated the inhibitory effect of intracellular AAT on NF-κB activation and HIV replication. I also detected that AAT escaped from the lysosome and appeared to be distributed evenly throughout the cytosol, although initially this observation surprised me. However, proteins escaping from the lysosome occurs in many mammalian cells (148, 149, 116, 152-156). Thus, it is reasonable to conclude that clathrin and LRP1 meidate AAT internalization and that internalized AAT is transported from the endosome to the lysosome after which it is released into the cytosol, where it can interact with IκBα and alter the polyubiquitinylation pattern of IκBα. Future research could examine the processes involved in AAT entry from the lysosome to the cytosol.

In summary, AAT internalization is a clathrin-dependent LRP1-mediated endocytic process in CD4+ T cells. Once internalized, AAT is transported from the endosome to the lysosome, where it is released into the cytosol and can interact with cytosolic IκBα to block the polyubiquitinylation of phosphorylated IκBα at K48. In turn, the dissociation of IκBα from NF-κB is blocked because IκBα remains bound to p65/p50 thereby "masking" its nuclear

localization signal. These events lead to the inhibition of NF-κB nuclear translocation and activation of HIV production.

AAT inhibition of FDC activation and HIV pathogenesis: In T lymphocytes, AAT dramatically inhibited NF-κB activation as described above. It also impacted the activation of FDCs, which requires NF-κB. My results indicated that AAT affects FDC-NF-κB in a manner identical to that observed in CD4+ T cells. AAT treatment also inhibited CD32 and CD21 expression in FDCs, even in the presence of the FDC activator, LPS, and this effect was associated with decreased virus trapping. AAT also inhibited the trapping of HIV-1_{IIIB} on FDCs if it was present after the FDCs were co-cultured with virus. Additionally, the FDC mediated maintenance of HIV infectivity was inhibited more potently when the untreated or LPS-stimulated FDCs were continually cultured with AAT. Thus, AAT down-regulates FDC-CD32 and FDC-CD21 expression and thereby inhibits the trapping of HIV on these FDCs. The reason for the lower amount of trapped HIV on F DCs with the persisitent presence of AAT in the culture system might be due to the lower level FDC-CD32 and FDC-CD21. Alternatively, AAT itself might interfere with the interactions, among HIV immune complexes, the complement proteins, FDC-CD32, and FDC-CD21, to lower the amount of trapped HIV. Whatever the mechanism might be, AAT efficiently blocks FDC activation and subsequently inhibits HIV trapping and maintenance.

In the GCs, FDCs attract GC T cells by producing CXCL13 (58). Moreover, FDCs also increase HIV replication by secreting TNFα, which in turn activates NF-κB in infected CD4+ T cells. CXCL13 and TNFα expression are related to NF-κB activation (157). When AAT was added to resting or LPS-activated FDCs, the results revealed that the expression of CXCL13 and

TNFα was inhibited. Thus, AAT might also inhibit the contribution of FDCs to HIV transmission and replication in the GCs, but this still needs further study.

Summary: The net result of the inhibitory effects of AAT on H IV infection, HIV replication, and HIV reservoirs is likely to inhibit the pathogenesis of HIV/AIDS. A better knowledge of the molecular mechanism of AAT-mediated effects on inhibiting HIV/AIDS pathogenesis may be helpful to design better intervention strategies for this major world problem.

ABBREVIATIONS

HIV, Human immunodeficiency virus, type I; **AIDS**, acquired immunodeficiency syndrome; **FDC**, Follicular dendritic cell; **AAT**, alpha-1-antitrypsin; **CCR5**, C-C chemokine receptor 5; **CXCR4**, C-X-C chemokine receptor 4; **NF-κB**, nuclear factor κB; **SP1**, specificity protein 1; **AP2**, activator protein 2; **NFAT**, nuclear factor of activated T-cells; **LTR**, long terminal repeat; **CD32** or **FcγRII**: type II Fc gamma receptor; **TLR4**, Toll-like receptor 4; **ICAM-1,** intercellular adhesion molecule 1; **VCAM-1**, vascular cell adhesion molecule-1; **BAFF**, B-cell-activating factor belonging to the TNF family; **CR2** or **CD21**, complement receptor II; **C4BP**, C4-binding protein; **TNF*α***, tumor necrosis factor α; **IL-2**, interleukin-2; **IL-6**, interleukin-6 ; **IL-7**, interleukin-7; **GC**, germinal center; **CXCL13**, C-X-C motif chemokine 13; **CM**, complete tissue culture medium; **PBMC**, peripheral blood mononuclear cells; **PHA**, phytohemagglutinin; **PBS**, phosphate buffered saline; **IgG**, immunoglobulin G; **IgM**, immunoglobulin M; **PCR**, polymerase chain reaction; **qPCR**, quantitative real time PCR; **RT-PCR**, reverse transcriptase PCR; **ELISA**, enzyme-linked immunosorbent assay; **IκB**, NF-κB inhibitor; **IKK**, IκB kinase; **DSP**, dithiobis succinimidylpropionate; **FASP**, filter-aided sample preparation; **TNFR**, TNF receptor; **LPS**, lipopolysaccharide; **LDL**, low density lipoprotein; **LRP**, LDL-receptor-related protein; **SCF**, Skp1, Cullin 1, and F-box β transducin repeat containing protein.

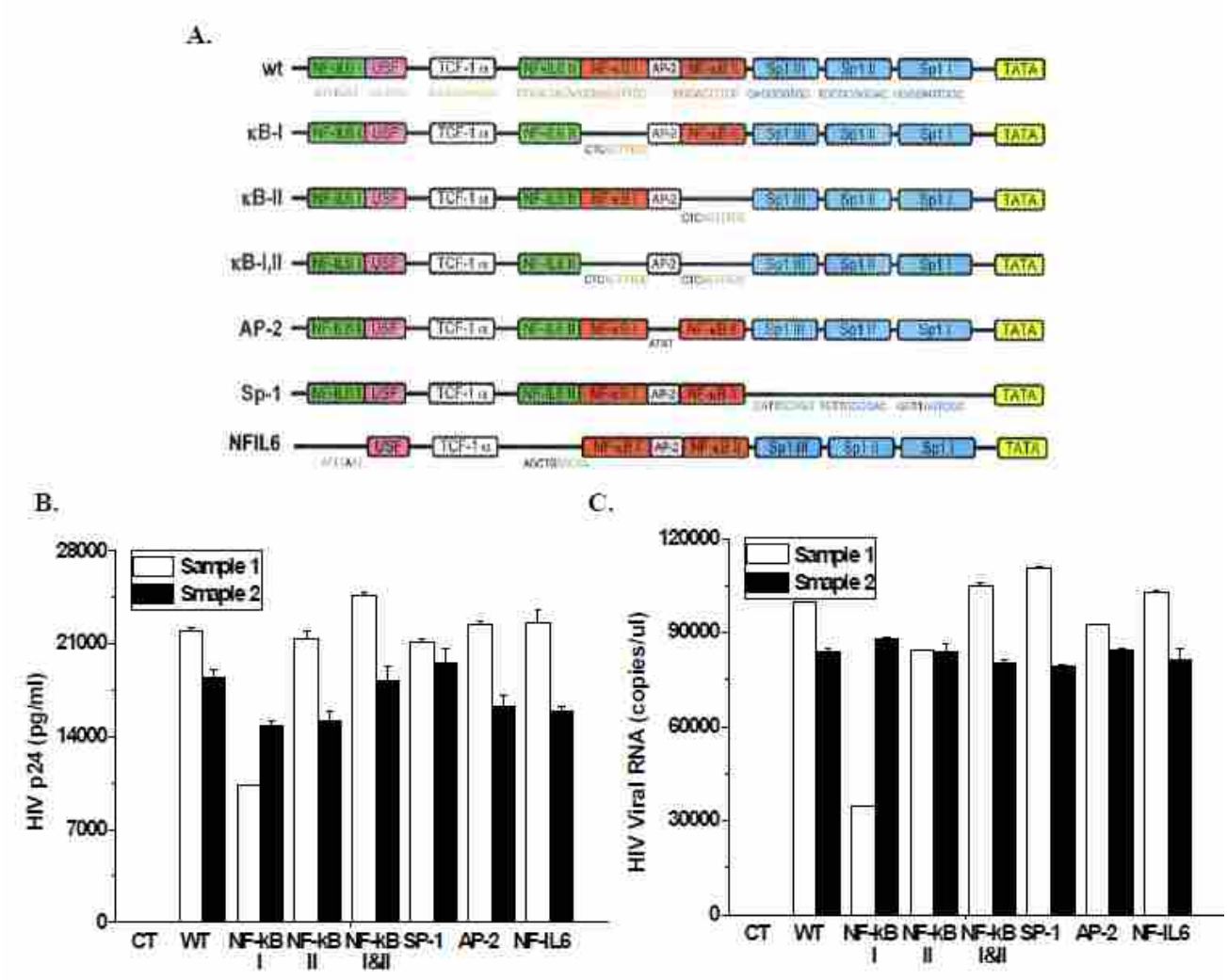

Figure 1. Prodution of recombinant HIV with mutations at the transcription factor binding sites in the 3'-LTR. (A). Mutation map of the LTR vectors generously provided by Drs. V. Planelles and A. Bosque. HEK293T cells (2×10^5 cells/sample in a final volume of 500 μL transfection medium) were co-transfected with the pLET-LAI vector (3 μg) and the vector (3 μg) encoding the wild type or mutated LTR. After 6 days of incubation, recombinant virus particles were collected and monitored for viral protein p24 (B) and viral RNA (C) in the supernatant fluid. CT: HEK293T cells were mock transfected (control); WT: LTR vector without mutation (wild type); NFκB I: LTR vector with NF-κB site I mutation; NFκB II: LTR vector with NF-κB site II mutation; NFκB I&II: LTR vector with NF-κB site I&II mutations; SP1: LTR vector with SP-1 site I, II &III mutated; AP2: LTR vector with AP-2 site mutated; NFIL6: LTR vector with NF-IL6 site I&II mutated. Sample 1 and sample 2 represent virus preparations obtained from independent transfections.

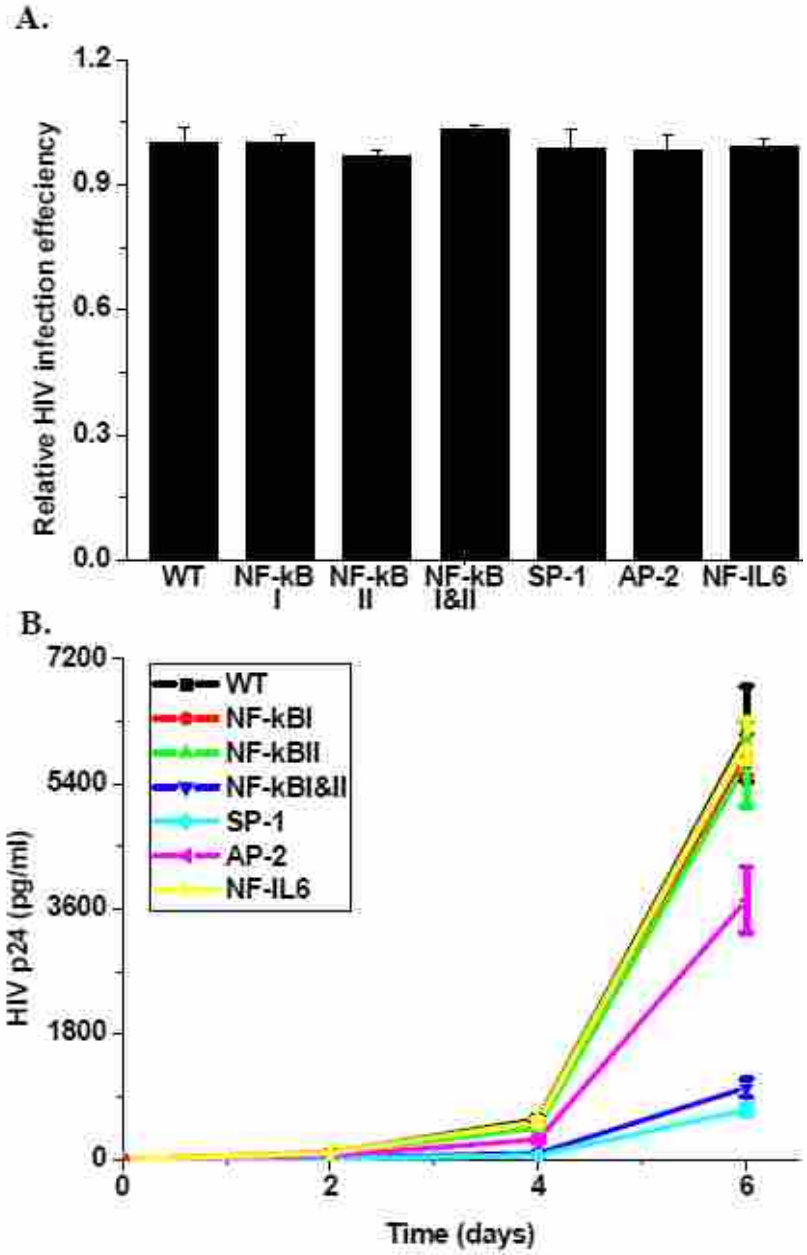

Figure 2. Virus production depended upon the presence of the transcription factors SP-1, NF-kB and AP-2. Recombinant, LTR-mutated HIV was produced in 293T cells using vectors provided by V. Planelles and A. Bosque, University of Utah, Dept. of Pathology. Primary CD4+ T cells (5×10^5 cells/sample in a final volume of 500 µL culture medium) were infected as described in Methods and Materials with wild-type or mutated recombinant virus and assessed for viral integration (A) and virus production (B). Virus integration was measured by quantitative real time Alu-PCR after 20 hours of incubation and normalized to GAPDH whereas virus production was measured at the time intervals indicated. WT: infected with wild type recombinant HIV; NF-κB I: infected with recombinant HIV with NF-κB site I mutation; NF-κB II: infected with recombinant HIV with NF-κB site II mutation; NF-κB I&II: infected with recombinant HIV with NF-κB site I&II mutation; SP-1: infected with recombinant HIV with SP-1 site I, II & III mutation; AP-2: infected with recombinant HIV with AP-2 site mutation; NF-IL6: infected with recombinant HIV with NF-IL6 site I&II mutation.

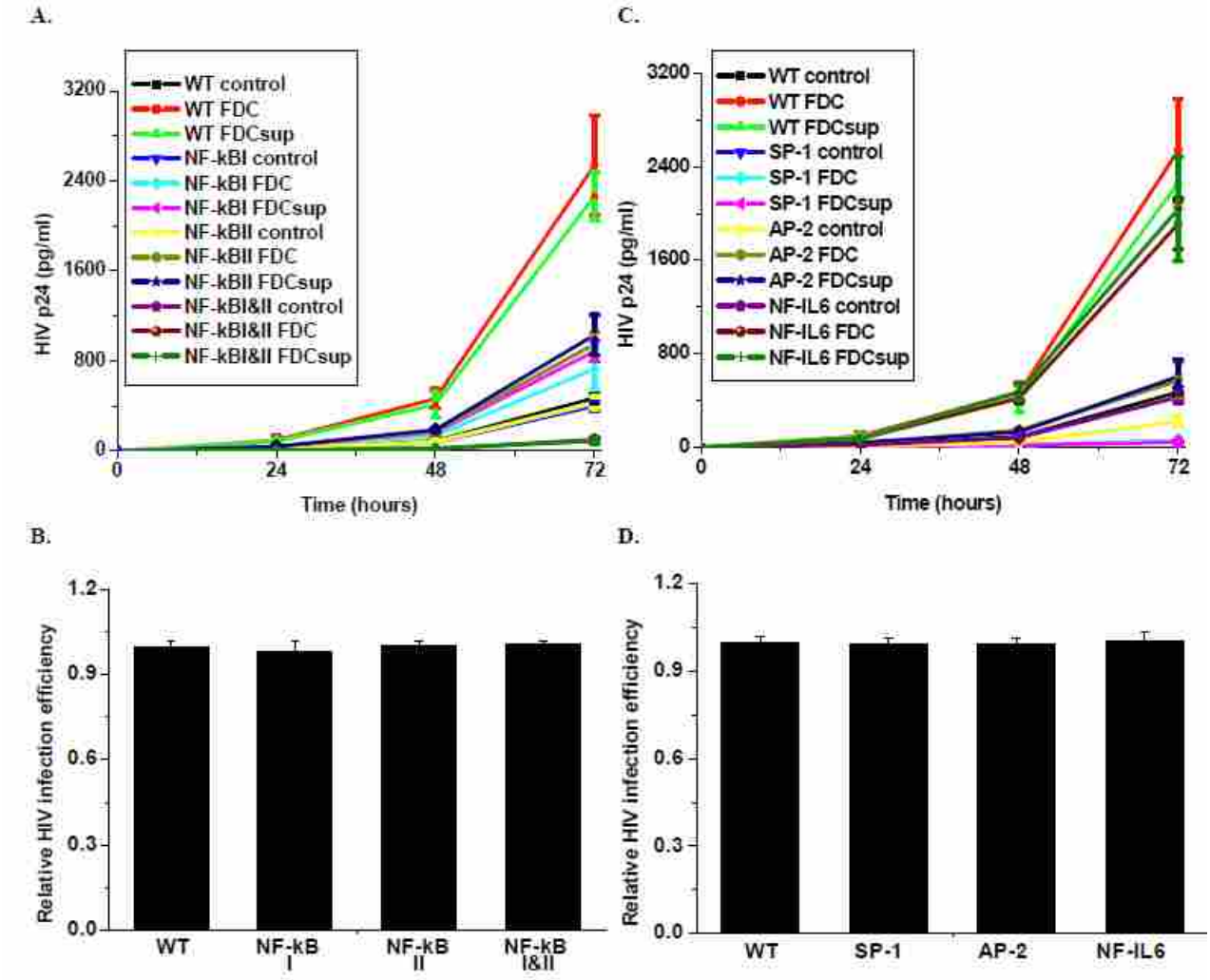

Figure 3. Replication of recombinant HIV in activated primary CD4+ T cells. Activated primary CD4+ T cells were infected as described in figure 2. Subsequently, the infected cells (5×10^5 cells/sample in a final volume of 500 μL culture medium) were incubated for 0, 24, 48, or 72 hours in the presence or absence of FDCs (10 CD4+ T cells to 1 FDC) or FDC supernatant fluid (10% (v/v), FDCsup). At the end of incubation, the supernatant was collected to detect HIV p24 (A and C). The infection efficiency of the recombinant HIV in CD4+ T cells was determined by detecting integrated viral DNA in the cells using Alu-PCR after 20 hours incubation (normalized to GAPDH, B and D). WT: infected with wild type recombinant HIV; NF-κB I: infected with recombinant HIV with NF-κB I binding site mutation; NF-κB II: infected with recombinant HIV with NF-κB II binding site mutation; NF-κB I&II: infected with recombinant HIV with NF-κB I&II binding sites mutation; SP-1: infected with recombinant HIV with SP-1 I, II & III binding sites mutation; AP-2: infected with recombinant HIV with AP-2 binding site mutation; NF-IL6: infected with recombinant HIV with NF-IL6 I&II binding site mutation. Control: CD4+ T cells were incubated in complete medium; FDC: FDCs were co-incubated with CD4+ T cells; FDCsup: CD4+ T cells were incubated with FDC supernatant fluid.

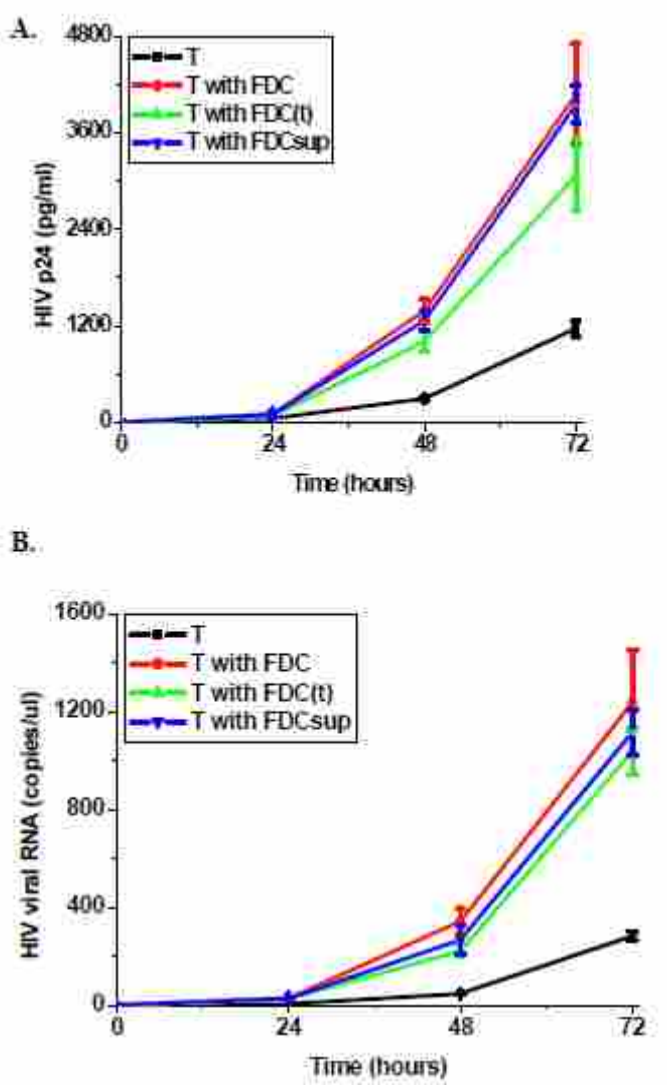

Figure 4. FDCs increased HIV replication in primary CD4+ T cells. Activated primary CD4+ T cells were infected with HIV-1_{IIIB}. After infection, these CD4+ T cells (5×10^5 cells/sample in a final volume of 500 μL culture medium) were cultured with FDC supernatant fluid (10% (v/v), FDCsup) or FDCs (10 CD4+ T cells to 1 FDC) sperated (FDC(t)) by a 3.0-μm Transwell membrane or not (FDC). After 0, 24, 48, or 72-hour incubation, the supernatant fluid was collected to detect p24 (A) and viral RNA (B) production. Part of the figure was published in my previous paper (47).

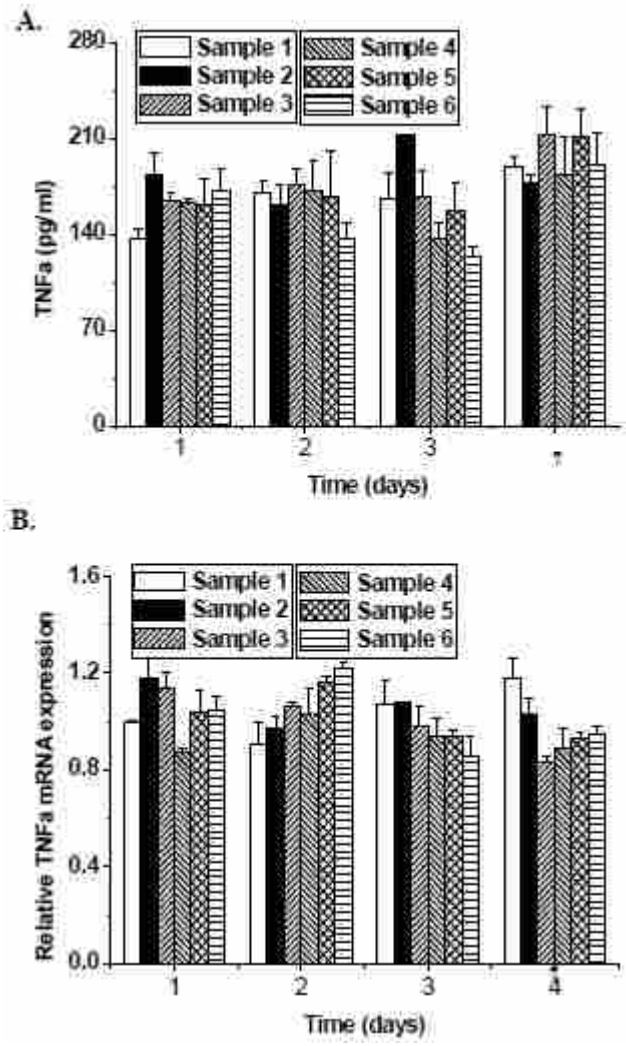

Figure 5. FDCs expressed and secreted TNFα. Isolated tonsillar FDCs (2×10^5 cells/sample in a final volume of 200 μL culture medium) were incubated for 1, 2, 3, or 7 days. Subsequently, the supernatant fluid was collected to detect TNFα production (A). FDCs were collected to isolate total RNA (B). The expression of TNFα mRNA was detected and normalized to endogenous GAPDH. Part of the figure was published in my previous paper (47).

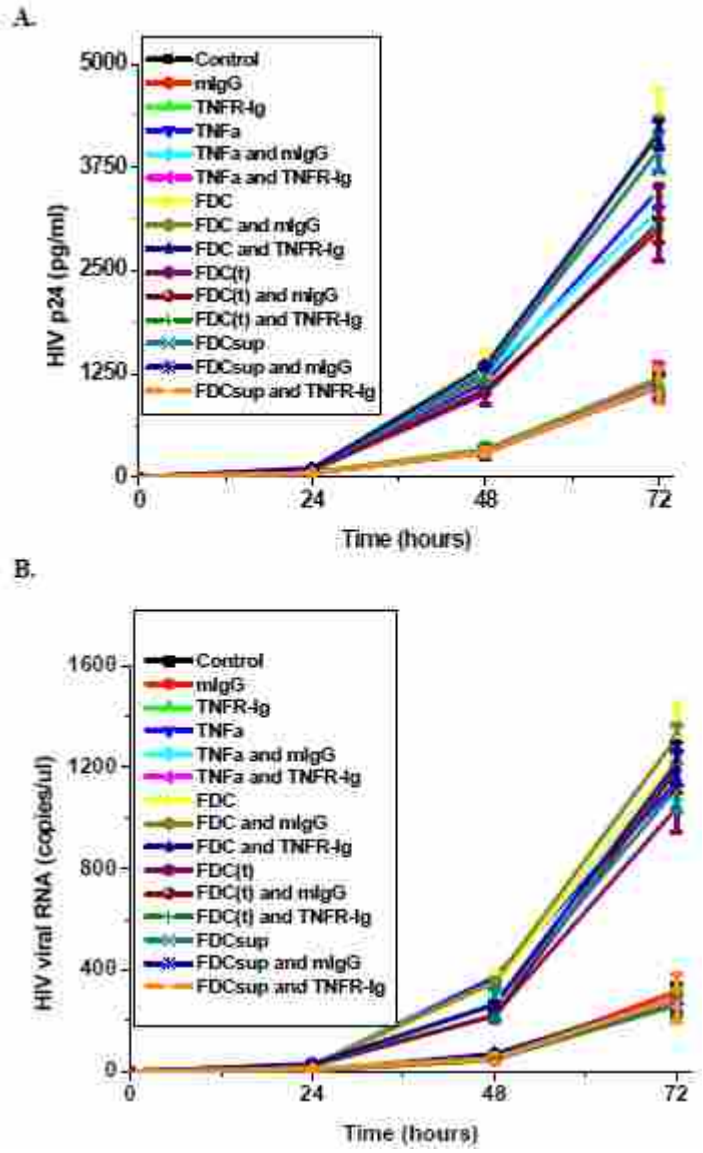

Figure 6. FDC-produced TNFα increased HIV production in HIV-infected CD4+ T cells. Activated primary CD4+ T cells were infected with HIV-1_{IIIB} as before. After infection, the cells (5×10^5 cells/sample in a final volume of 500 µL culture medium) were cultured with 20 µg/mL TNFR-Ig, 20 µg/mL mouse IgG (mIgG, isotope control), 167 pg/mL TNFα, FDC supernatant fluid (FDCsup, 10% (v/v)), or FDCs (10 CD4+ T cells to 1 FDC) separated (FDC(t)) by a 3.0 µm Transwell membrane or not (FDC). After 0, 24, 48, or 72-hour incubation, the supernatant fluid was collected to detect viral RNA (A) and p24 (B) production. Part of the figure was published in my previous paper (47).

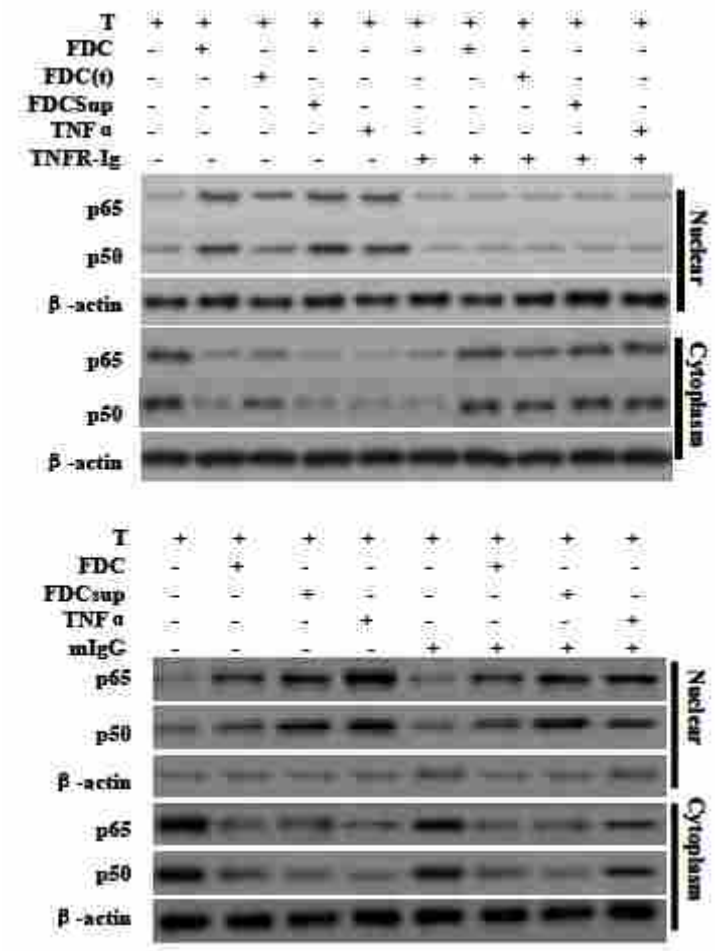

Figure 7. FDCs and FDC supernatant increased the nuclear translocation of p65 and p50 in HIV-infected CD4+ T cells. Activated primary CD4+ T cells were infected with HIV-1_{IIIB} as before. After infection, the cells (10^7 cells/sample in a final volume of 10 mL culture medium) were cultured with 20 μg/mL TNFR-Ig, 20 μg/mL mouse IgG (mIgG, isotope control), 167 pg/mL TNFα, FDC supernatant fluid (FDCsup, 10% (v/v)), or FDCs (10 CD4+ T cells to 1 FDC) separated (FDC(t)) by a 3.0 μm Transwell membrane or not (FDC). After 24 hours incubation, the cytoplasm and nuclear proteins were isolated to detect the nuclear translocation of p65 or p50 by Western blot. Part of the figure was published in my previous paper (47).

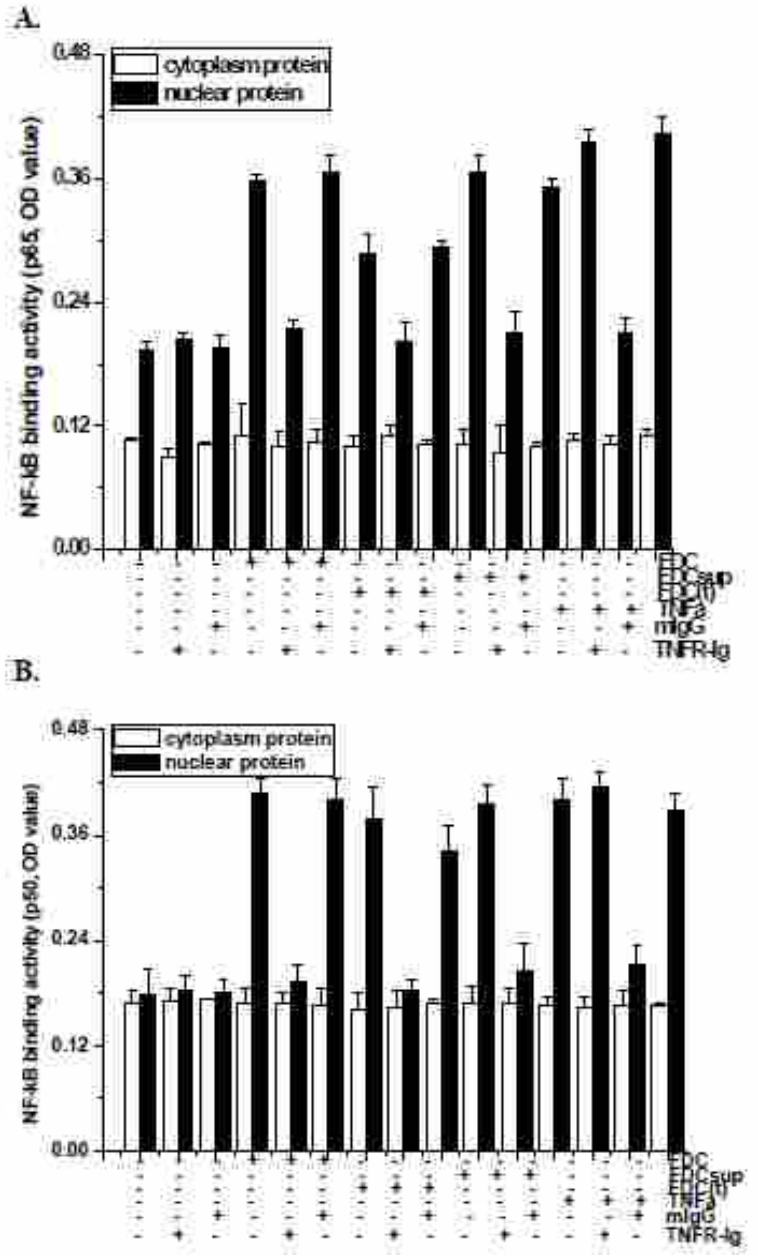

Figure 8. FDCs and FDC supernatant increased the DNA b inding activity of NF-κB in HIV-infected CD4+ T cells. Activated primary CD4+ T cells were infected with HIV-1_{IIIB} as before. After infection, these CD4+ T cells (10^7 cells/sample in a final volume of 10 mL culture medium) were cultured with 20 μg/mL TNFR-Ig, 20 μg/mL mouse IgG (mIgG, isotope control), 167 pg/mL TNFα, FDC supernatant fluid (FDCsup, 10% (v/v)), or FDCs (10 CD4+ T cells to 1 FDC) separated (FDC(t)) by a 3.0 μm Transwell membrane or not (FDC). After 24 hours incubation, the cytoplasm and nuclear proteins were isolated to detect the DNA binding activity of NF-κB p65 (A) or p50 (B).

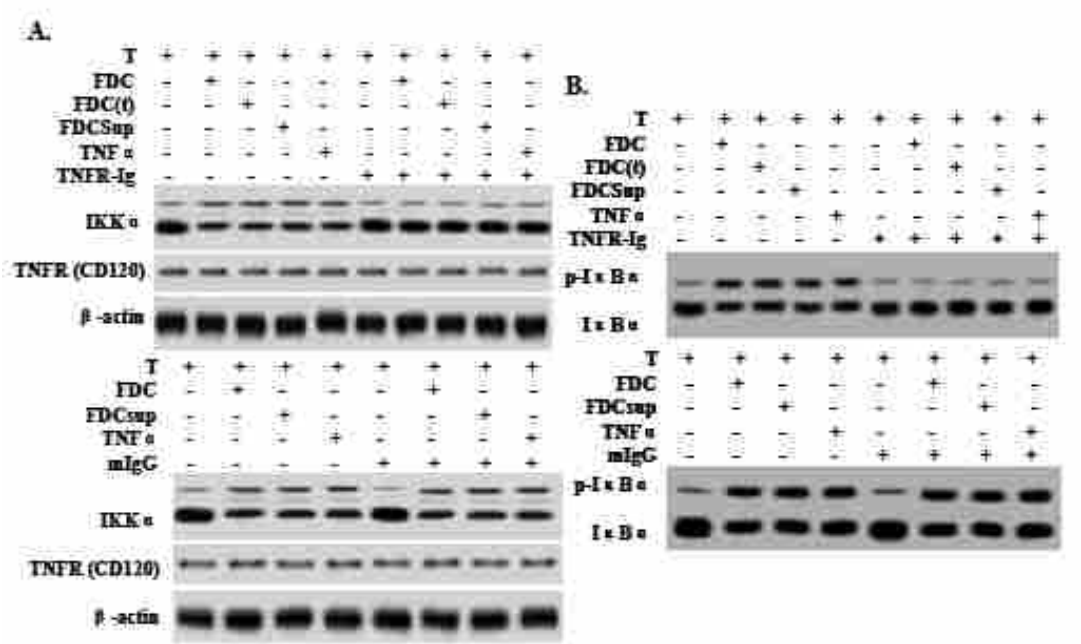

Figure 9. FDCs activated IKK without interfering with the expression of TNFR in HIV-infected CD4+ T cells. Activated primary CD4+ T cells were infected with HIV-1_{IIIB} as before. After infection, the cells (5×10^6 cells/sample in a final volume of 5 mL cultue medium) were cultured with 20 μg/mL TNFR-Ig, 20 μg/mL mouse IgG (mIgG, isotope control), 167 pg/mL TNFα, FDC supernatant fluid (FDCsup, 10% (v/v)), or FDCs (10 CD4+ T cells to 1 FDC) separated (FDC(t)) by a 3.0 μm Transwell membrane or not (FDC). After 24 hours incubation, the whole cell proteins were isolated from the cells to detect the expression of TNFR and IKK (A). Subsequently, IKK complex was precipitated with IKKα antibody and purified IKK complex was incubated with kinase buffer containing ATP and bacterially expressed IκBα as substrate. IκBα or phosphorylated IκBα was detected by Western blotting (B).

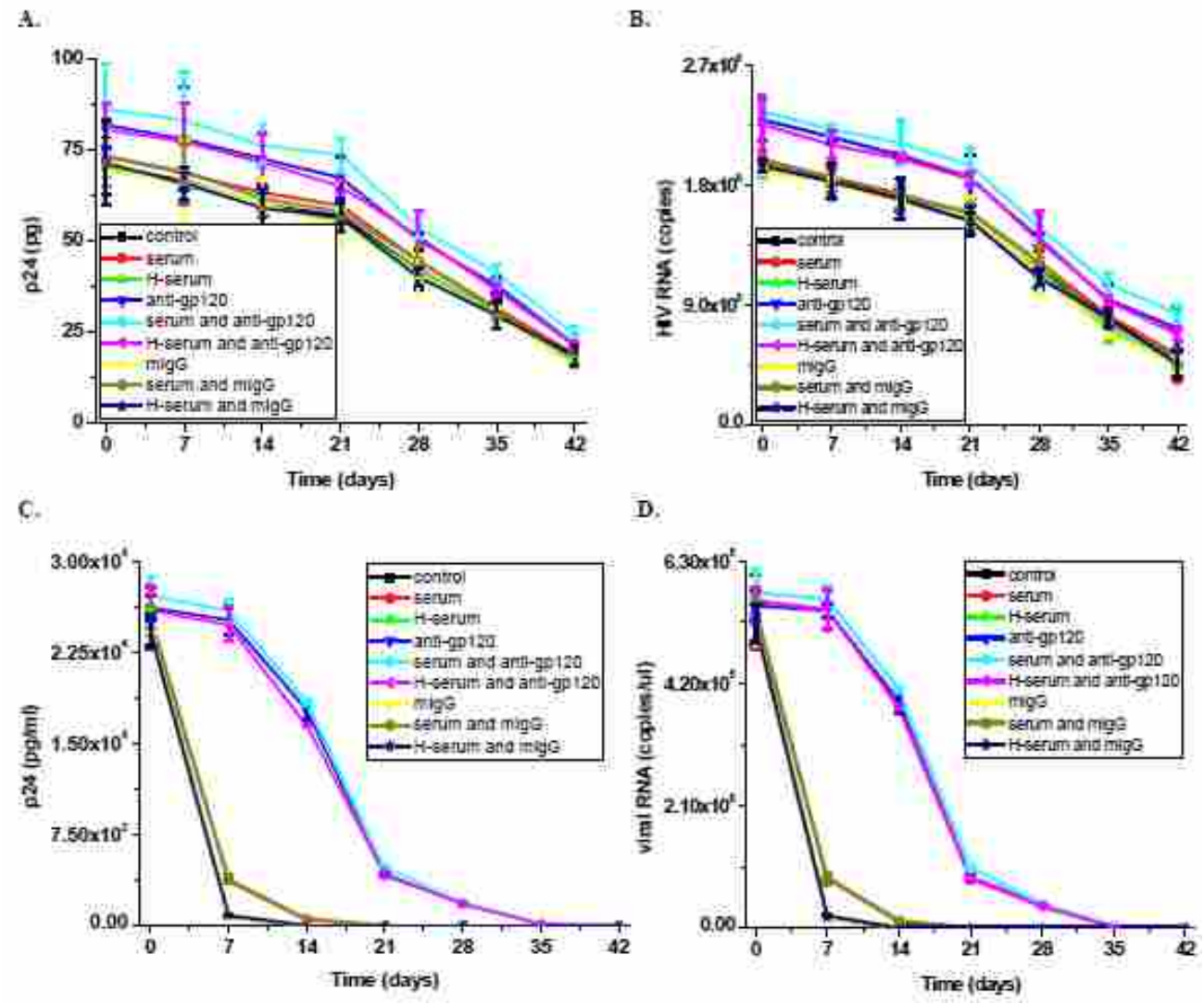

Figure 10. FDCs stabized the trapping and infectivity of HIV-1_{IIIB} in the presence of HIV-specific antibody and complement proteins. Isolated FDCs (10^5 cells/sample in a final volume of 200 µL) were incubated with HIV-1_{IIIB} (50 µL; containing ~ 50 ng of HIV p24) in the presence or absence of human serum (5 µL), heat-denatured human serum (5 µL), gp120 antibody (10 µg), or mouse IgG (isotope control for gp120 antibody; 10 µg) for 2 hours. Subsequently, unbound viruses were removed and FDCs (10^5 cells/mL) were incubated for 0, 7, 14, 21, 28, 35, or 42 days. After incubation, FDCs were divided into two aliquots. One aliquot was lysed to detect cytosolic p24 (A) and viral RNA (B). The other aliquot was incubated with CD4+ T cells (10^6 cells/sample in 4 mL culture medium; 10 CD4+ T cells to 1 FDC) for 7 days to monitor HIV p24 (C) and viral RNA production (D) in the supernatant fluid. Control: FDCs incubated with HIV-1_{IIIB}; serum: FDCs incubated with HIV-1_{IIIB} in the presence of fresh human serum; H-serum: FDCs incubated with HIV-1_{IIIB} in the presence of heat denatured human serum (no complement); anti-gp120: FDCs incubated with HIV-1_{IIIB} in the presence of gp120 antibody; mIgG: FDCs incubated with HIV-1_{IIIB} in the presence of mouse IgG.

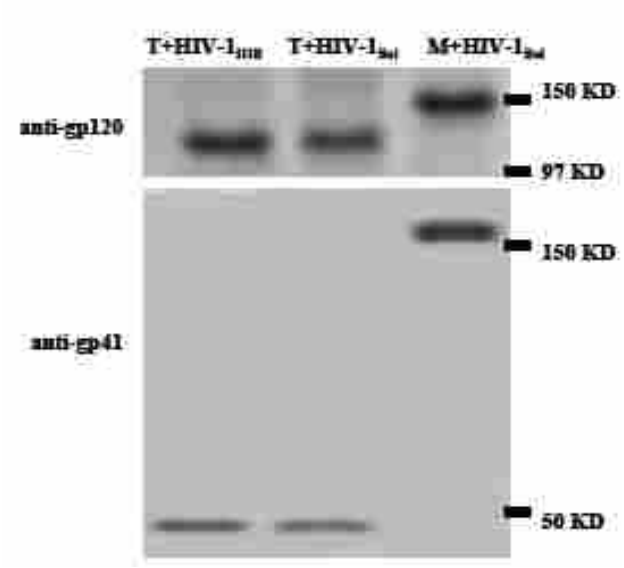

Figure 11. Macrophage produced HIV-1 contained only full length gp160 whereas T cell produced virus contains both distinct gp 120 and gp41. Primary CD4+ T cells (2×10^6 cells/sample) and macrophages (2×10^6 cells/sample) were isolated and infected with HIV-1_{IIIB} or HIV-1_{Bal} for 2 hours. Following infection, the cells were incubated for 2 weeks in 8 mL culture medium. Produced HIV particles were collected and concentrated by centrifuging at 60,000 × g for 2 hours. Viral proteins were extracted and gp120 and gp41 were detected by Western blotting. T+HIV-1_{IIIB}: HIV from HIV-1_{IIIB}-infected CD4+ T cells; T+HIV-1_{Bal}: HIV from HIV-1_{Bal}-infected CD4+ T cells; M+HIV-1_{Bal}: HIV from HIV-1_{Bal}-infected macrophages.

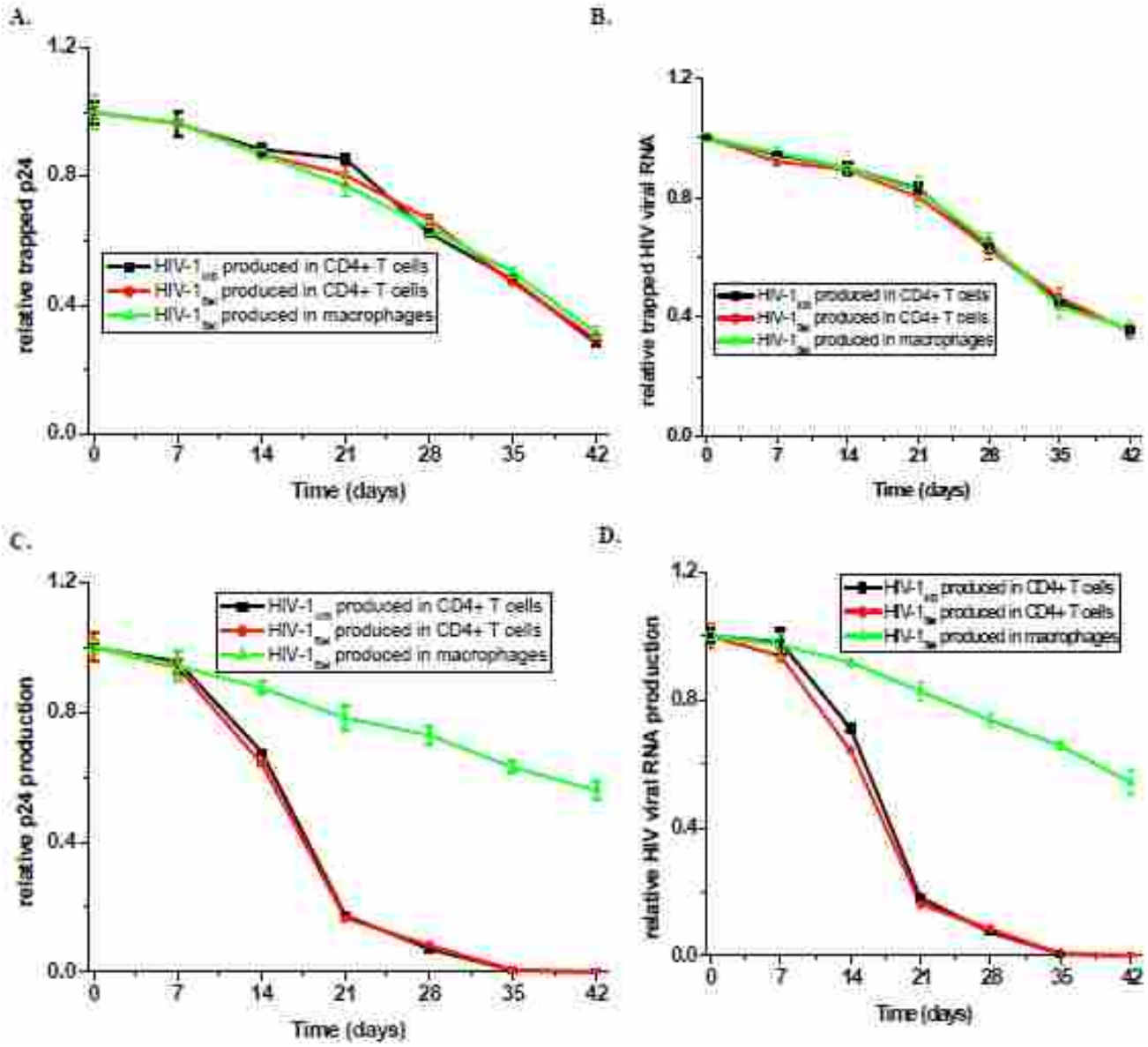

Figure 12. The shedding of gp120 from HIV diminished the infectivity of these viruses and suggested that FDC-trapping minimized this shedding. Isolated FDCs (10^5 cells/sample in a final volume of 200 μL) were incubated with HIV-1_{IIIB} (50 μL) or HIV-1_{Bal} (50 μL) produced in CD4+ T cells or macrophages in the presence of human serum (5 μL) and gp120 antibody (10 μg) for 2 hours. Unbound viruses were removed and these FDCs (10^5 cells/mL) were incubated for 0, 7, 14, 21, 28, 35, or 42 days. After incubation, these FDCs were divided into two aliquots. One aliquot was lysed to detect p24 (A) and viral RNA (B) trapped on FDCs. The other aliquot was incubated with CD4+ T cells (10^6 cells/sample in 4 mL culture medium; 10 CD4+ T cells to 1 FDC) for 7 days to collect the supernatant fluid. HIV p24 (C) and viral RNA production (D) in the supernatant fluid were detected. All samples in each group were normalized to the trapping and infectivity of HIV on FDCs at the time point "0".

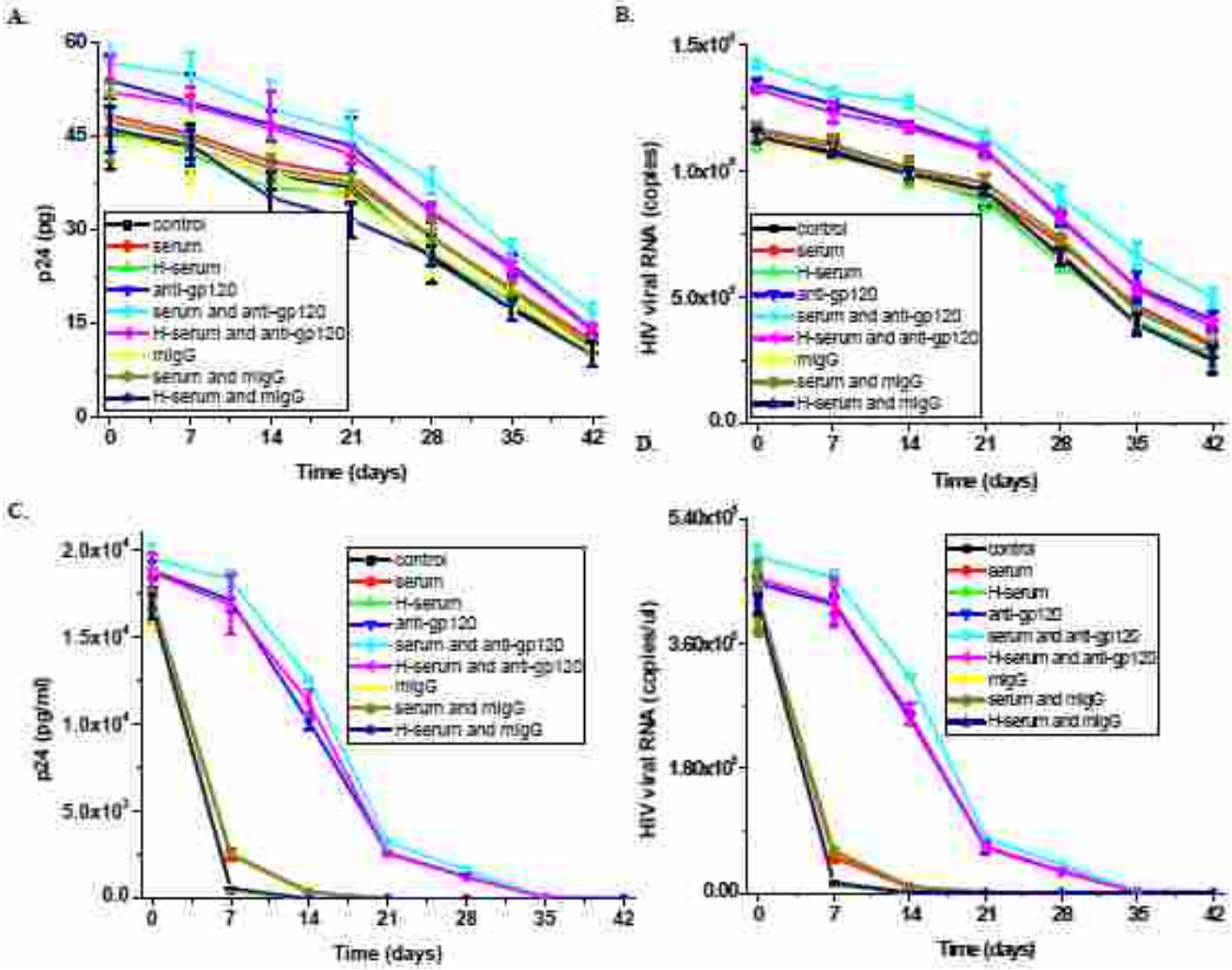

Figure 13. FDC trapping and maintenance of T cell-propagated HIV-1_{Bal} infectivity. Isolated FDCs (10^5 cells/sample in a final volume of 200 μL) were incubated with HIV-1_{Bal} (50 μL) produced in CD4+ T cells in the presence or absence of human serum (5 μL), heat denatured human serum (5 μL), gp120 antibody (10 μg), or mouse IgG (10 μg) for 2 hours. Subsequently, unbound viruses were removed and these FDCs (10^5 cells/mL) were incubated for 0, 7, 14, 21, 28, 35, or 42 days. After incubation, these FDCs were divided into two aliquots. One aliquot was lysed to detect cytosolic p24 (A) and viral RNA (B). The other aliquot was incubated with CD4+ T cells (10^6 cells/sample in 4 mL culture medium; 10 CD4+ T cells to 1 FDC) for 7 days to determine whether the trapped virus maintained its infectious nature. HIV p24 (C) and viral RNA production (D) in the supernatant fluid were detected. Control: FDCs incubated with HIV-1_{Bal}; serum: FDCs incubated with HIV-1_{Bal} in the presence of human serum; H-serum: FDCs incubated with HIV-1_{Bal} in the presence of heat denatured human serum; anti-gp120: FDCs incubated with HIV-1_{Bal} in the presence of gp120 antibody; mIgG: FDCs incubated with HIV-1_{Bal} in the presence of mouse IgG.

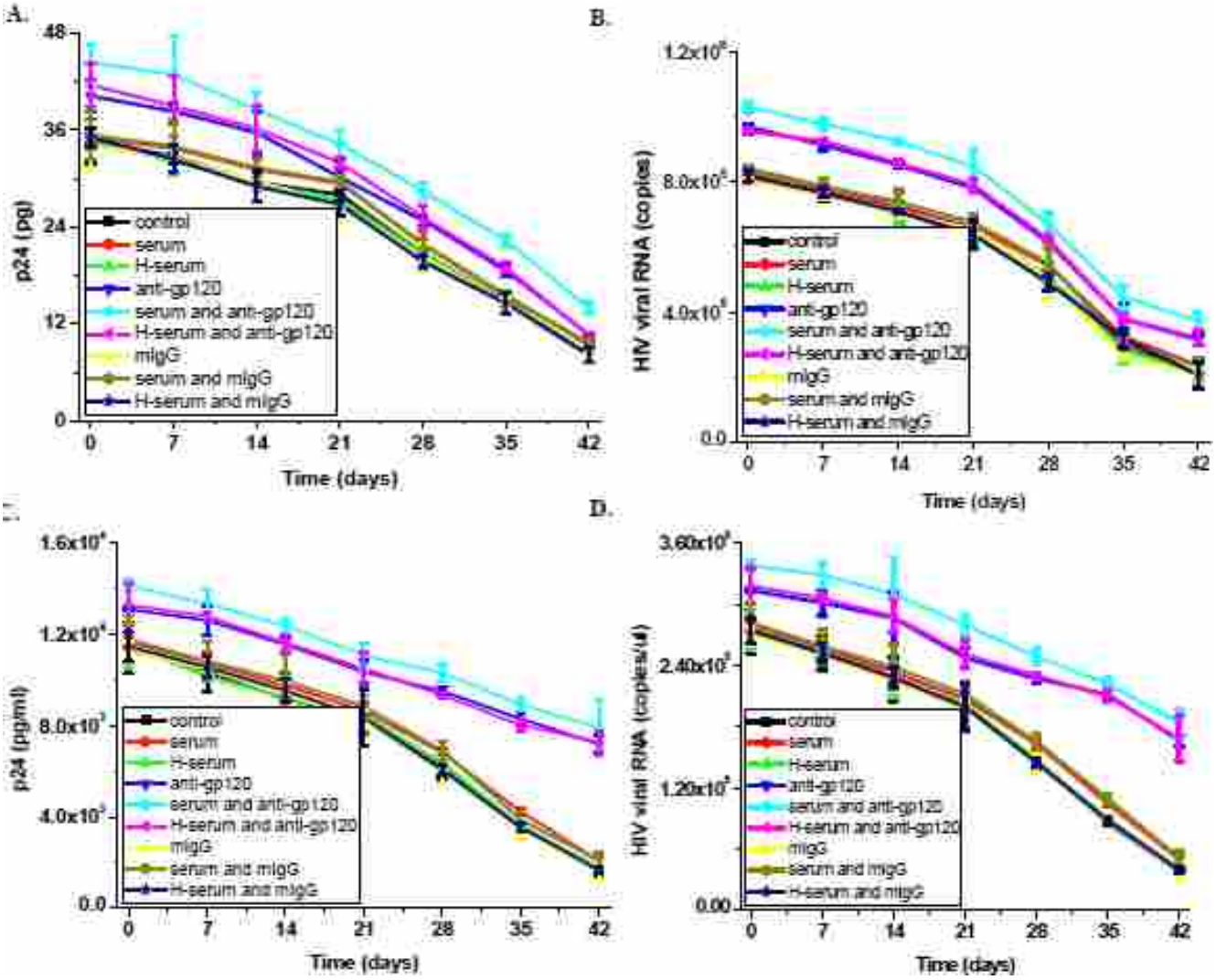

Figure 14. FDC trapping and maintenance of infectivity of macrophage-propagated HIV-1_{Bal}. Isolated FDCs (10^5 cells/sample in a final volume of 200 μL) were incubated with HIV-1_{Bal} (50 μL) produced in macrophages in the presence or absence of human serum (5 μL), heat denatured human serum (5 μL), gp120 antibody (10 μg), or mouse IgG (10 μg) for 2 hours. Subsequently, unbound viruses were removed and these FDCs (10^5 cells/sample) were incubated for 0, 7, 14, 21, 28, 35, or 42 days. After incubation, these FDCs were divided into two aliquots. One aliquot was lysed to detect cytosolic p24 (A) and viral RNA (B). The other aliquot was incubated with CD4+ T cells (10^6 cells/sample in 4 mL culture medium; 10 CD4+ T cells to 1 FDC) for 7 days to collect the supernatant fluid. HIV p24 (C) and viral RNA production (D) in the supernatant fluid were detected. Control: FDCs incubated with HIV-1_{Bal}; serum: FDCs incubated with HIV-1_{Bal} in the presence of human serum; H-serum: FDCs incubated with HIV-1_{Bal} in the presence of heat denatured human serum; anti-gp120: FDCs incubated with HIV-1_{Bal} in the presence of gp120 antibody; mIgG: FDCs incubated with HIV-1_{Bal} in the presence of mouse IgG.

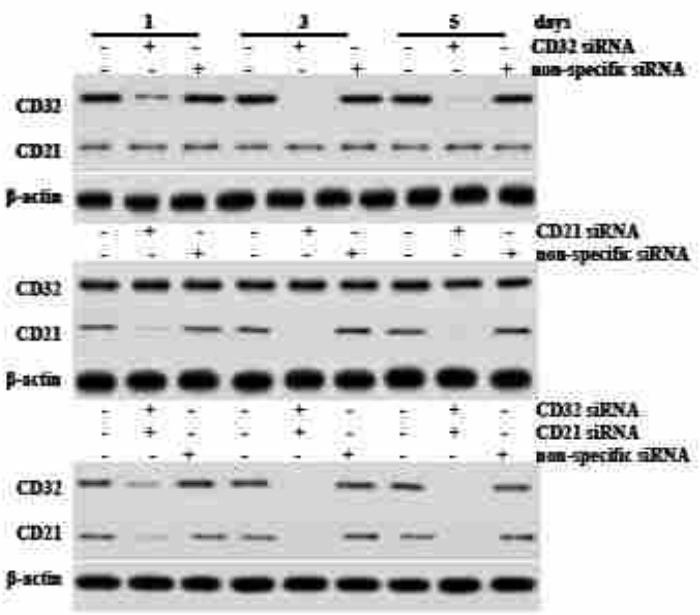

Figure 15. CD32- and CD21-specific siRNA knocked-down FDC-CD32 and FDC-CD21 expression. Isolated tonsillar FDCs (10^6 cells/sample in a final volume of 1 mL culture medium) were treated with CD32 siRNA, CD21 siRNA, or non-specific siRNA for 1, 3, or 5 days. At the end of incubation, CD32 or CD21 expression was detected by Western blotting. β-actin was used as a loading control.

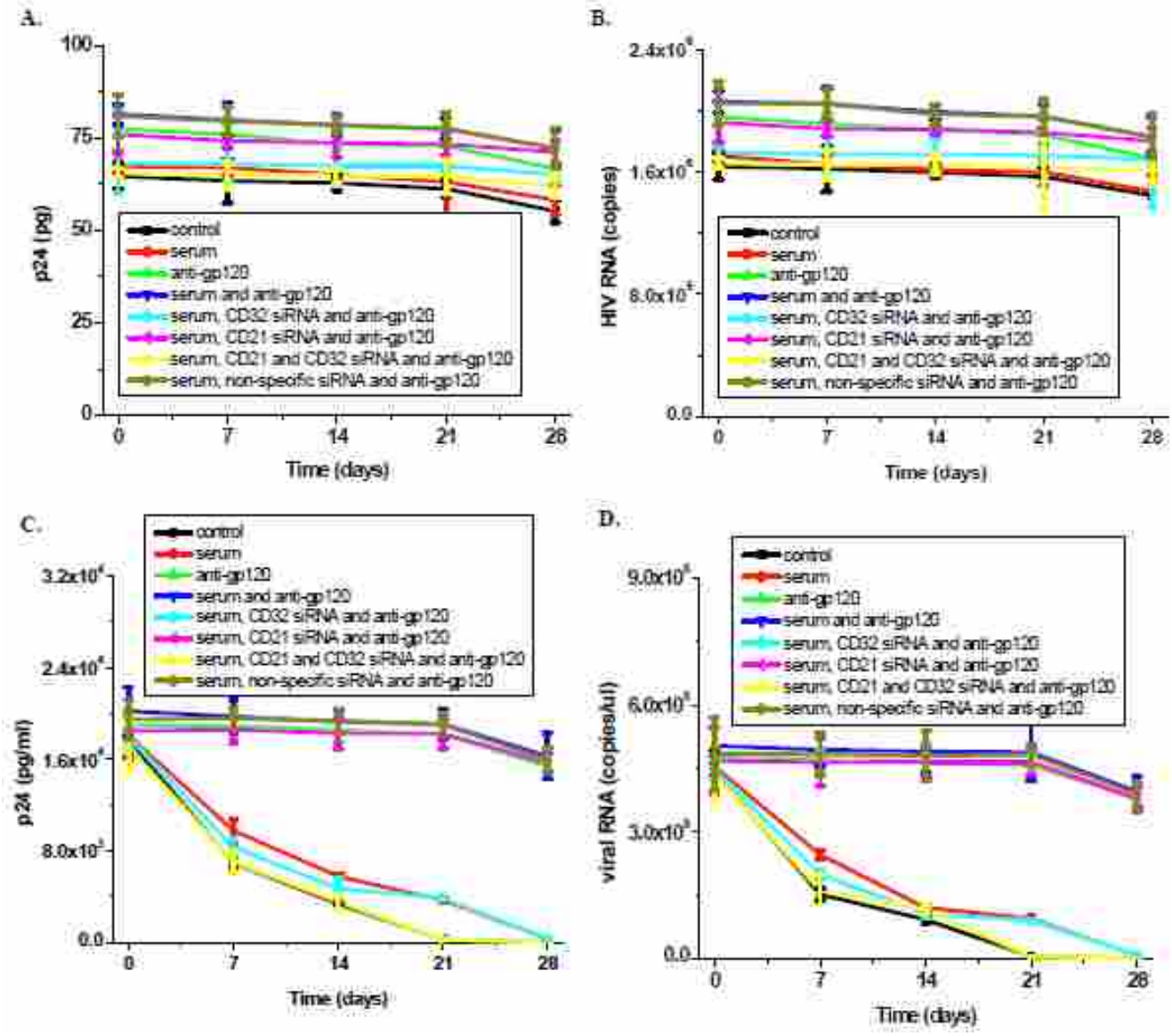

Figure 16. CD32 and CD21 siRNA inhibited the trapping and maintenance of HIV-1_{IIIB} on FDCs. Isolated tonsillar FDCs were treated with CD32 siRNA, CD21 siRNA, or non-specific siRNA for 3 days. Subsequently, these FDCs (10^5 cells/sample in a final volume of 200 μL) were incubated with HIV-1_{IIIB} (50 μL) in the presence or absence of human serum (5 μL) or gp120 antibody (10 μg) for 2 hours. Subsequently, unbound viruses were removed and these FDCs (10^5 cells/mL) were incubated for 0, 7, 14, 21, or 28 days. After incubation, these FDCs were divided into two aliquots. One aliquot was lysed to detect cytosolic p24 (A) and viral RNA (B). The other aliquot was incubated with CD4+ T cells (10^6 cells/sample in 4 mL culture medium; 10 CD4+ T cells to 1 FDC) for 7 days to collect the supernatant fluid. HIV p24 (C) and viral RNA production (D) in the supernatant fluid were detected. Control: FDCs incubated with HIV-1_{IIIB}; serum: FDCs incubated with HIV-1_{IIIB} in the presence of human serum; anti-gp120: FDCs incubated with HIV-1_{IIIB} in the presence of gp120 antibody; CD32 siRNA: FDCs with CD32 siRNA treatment; CD21 siRNA: FDCs withCD21 siRNA treatment; non-specific siRNA: FDCs with non-specific siRNA treatment.

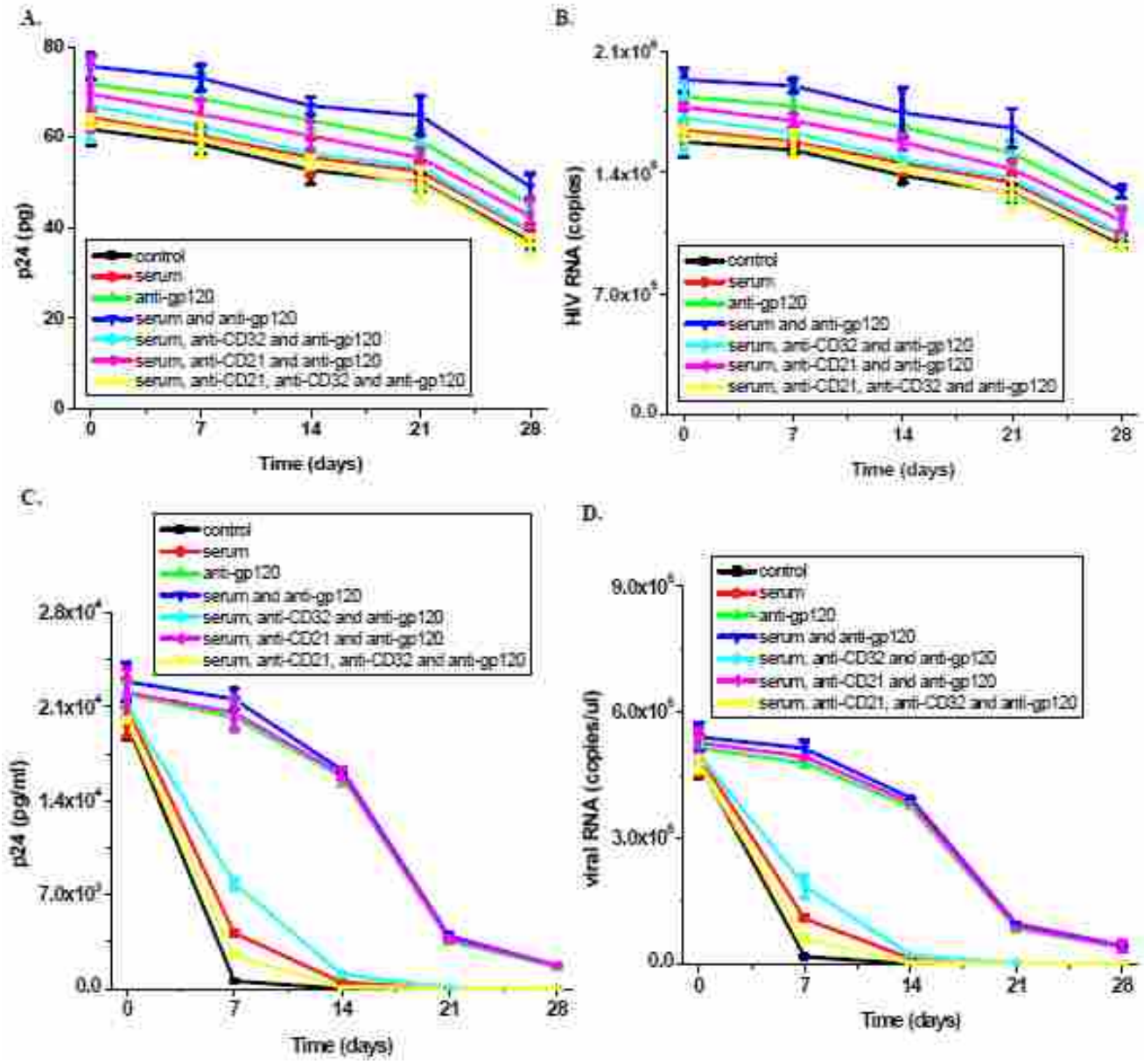

Figure 17. CD32- and CD21-specific antibody inhibited the trapping and maintenance of HIV-1_{IIIB} on FDCs. Isolated FDCs (10^5 cells/sample in a final volume of 200 μL) were incubated with HIV-1_{IIIB} (50 μL) in the presence or absence of human serum (5 μL), gp120 antibody (10 μg), CD32 antibody (10 μg), or CD21 antibody (10 μg) for 2 hours. Unbound viruses were removed and these FDCs (10^5 cells/mL) were incubated for 0, 7, 14, 21, or 28 days. After incubation, these FDCs were divided into two aliquots. One aliquot was lysed to detect cytosolic p24 (A) and viral RNA (B). The other aliquot was incubated with CD4+ T cells (10^6 cells/sample in 4 mL culture medium; 10 CD4+ T cells to 1 FDC) for 7 days to collect the supernatant fluid. HIV p24 (C) and viral RNA production (D) in the supernatant fluid were detected. Control: FDCs incubated with HIV-1_{IIIB}; serum: FDCs incubated with HIV-1_{IIIB} in the presence of human serum; anti-gp120: FDCs incubated with HIV-1_{IIIB} in the presence of gp120 antibody; anti-CD32: FDCs incubated with CD32 antibody; anti-CD21: FDCs incubated with CD21 antibody.

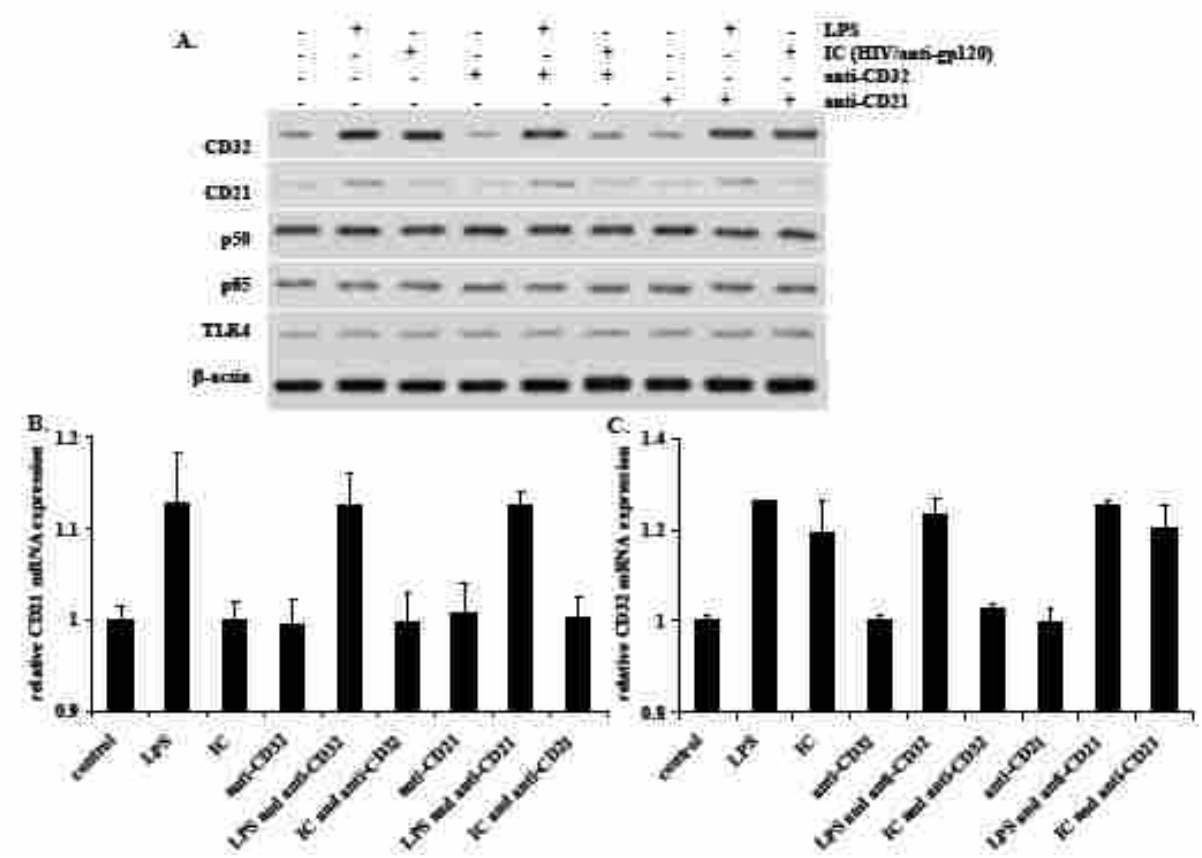

Figure 18. Effect of LPS and HIV immune complex on the expression and production of FDC-CD32 and -CD21. Isolated tonsillar FDCs (10^6 cells/sample in a final volume of 1 mL) were treated with 10 μg/mL LPS, HIV immune complexes (preformed by incubating 50 μL HIV-1_{IIIB} with 10 μg gp120 antibody for 30 minutes), CD32 antibody (10 μg), or CD21 antibody (10 μg) for 1 day. At the end of incubation, the cells were divided into two aliquots. One aliquot was lysed to extract the whole cell proteins. The expression of CD32, CD21, p50, p65, and TLR4 was detected by Western blotting (A). β-actin served as a loading control. The other aliquot was lysed to extract total RNA. The mRNA expression of CD32 and CD21 was detected by qPCR. GAPDH served as an endogenous control (B and C).

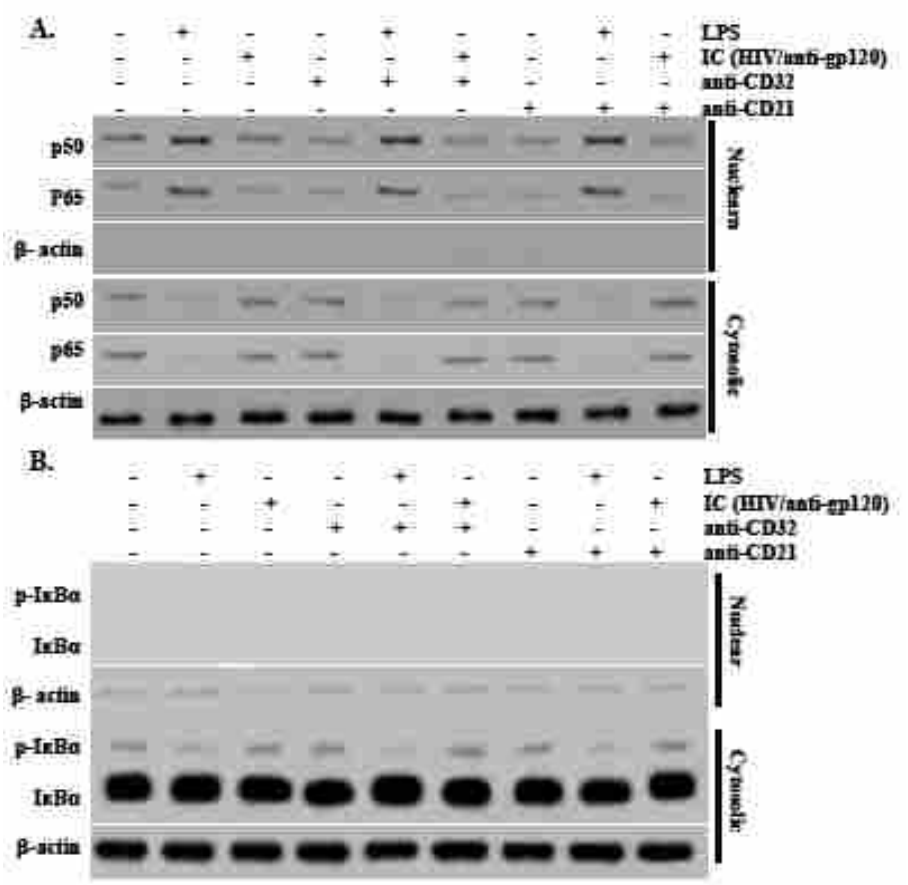

Figure 19. Effects of LPS and HIV immune complexes on NF-κB activation in FDCs. Isolated tonsillar FDCs (4×10^6 cells/sample in a final volume of 4 mL) were treated with 10 μg/mL LPS, HIV immune complexes (preformed by incubating 50 μL HIV-1_{IIIB} with 10 μg gp120 antibody for 30 minutes), CD32 antibody (10 μg), or CD21 antibody (10 μg) for 1 day. At the end of incubation, the nuclear and cytosolic proteins were extracted. The accumulation of p50, p65, phosphorylated IκBα, and IκBα in the cytosol or nucleus was detected by Western blotting (A and B). β-actin served as a loading control.

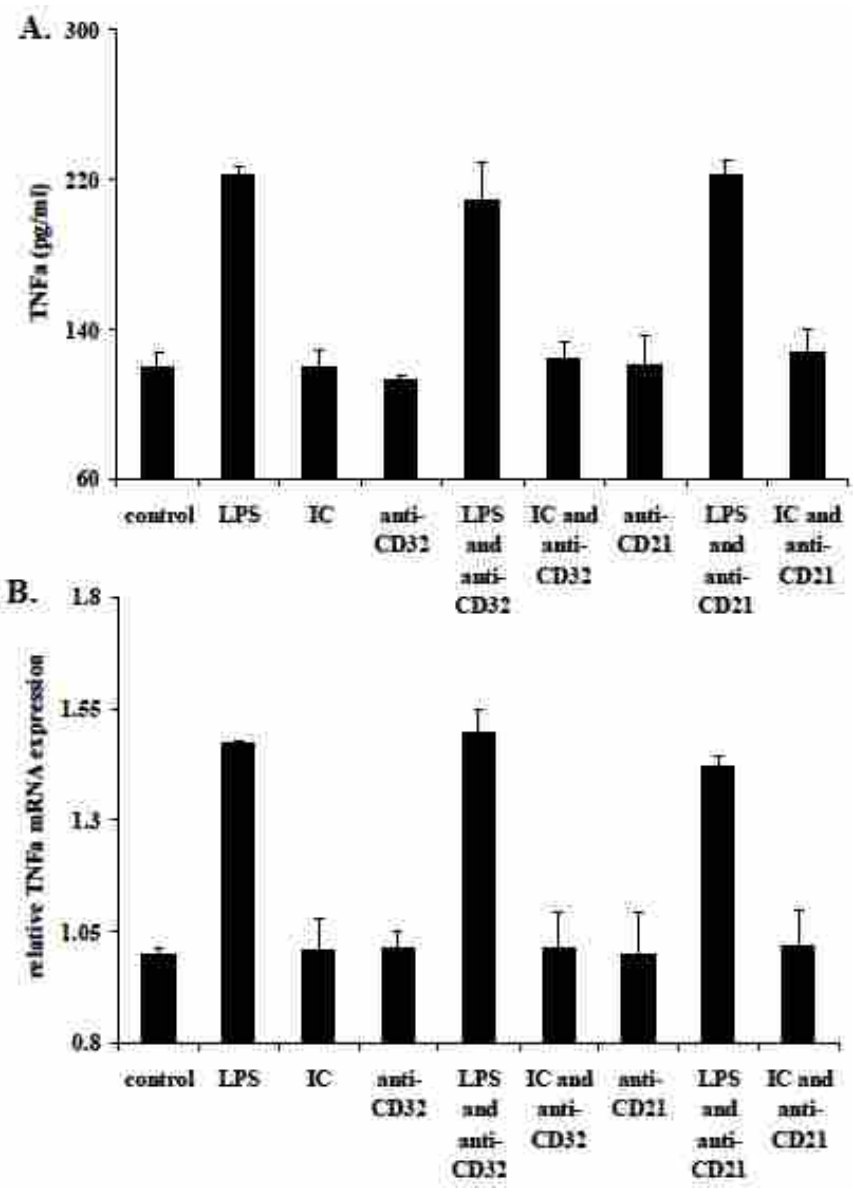

Figure 20. Effect of LPS and HIV immune complex on the expression and production of TNFα in FDCs. Isolated tonsillar FDCs (2×10^5 cells/sample in a final volume of 200 μL) were treated with 10 μg/mL LPS, HIV immune complexes (preformed by incubating 50 μL HIV-1_{IIIB} with 10 μg gp120 antibody for 30 minutes), CD32 antibody (10 μg), or CD21 antibody (10 μg) for 1 day. At the end of incubation, the supernatant fluid was collected to detect the production of TNFα by ELISA(A). The cells were lysed to extract total RNA. The mRNA expression of TNFα was detected by qPCR. GAPDH worked as an endogenous control (B).

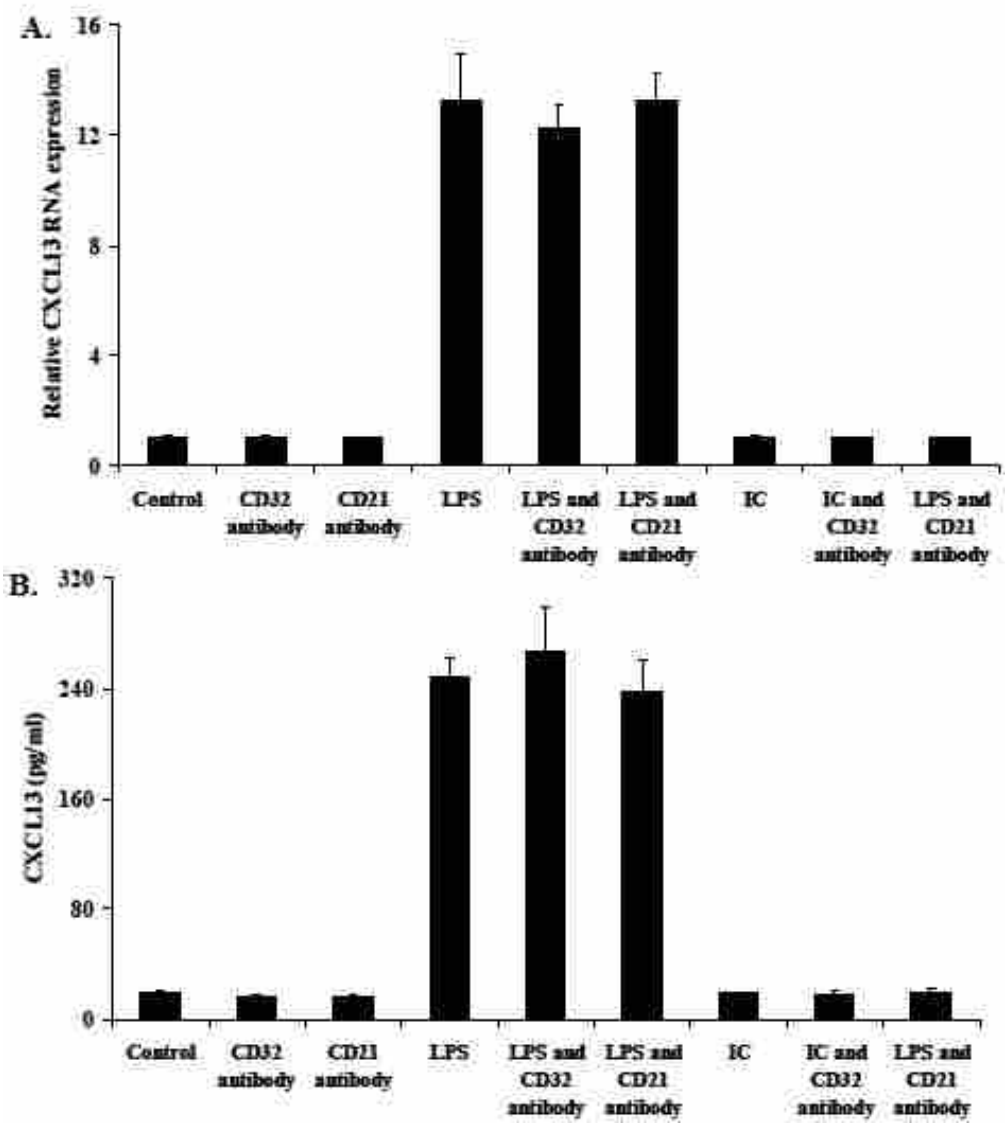

Figure 21. Effect of LPS and HIV immune complex on the expression and production of CXCL13 in FDCs. Isolated tonsillar FDCs (2×10^5 cells/sample in a final volume of 200 μL) were treated with 10 μg/mL LPS, HIV immune complexes (preformed by incubating 50 μL HIV-1_{IIIB} with 10 μg gp120 antibody for 30 minutes), CD32 antibody (10 μg), or CD21 antibody (10 μg) for 1 day. At the end of incubation, the cells were lysed to extract total RNA. The mRNA expression of CXCL13 was detected by qPCR. GAPDH worked as an endogenous control (A). The supernatant fluid was collected to detect the production of CXCL13 by ELISA (B).

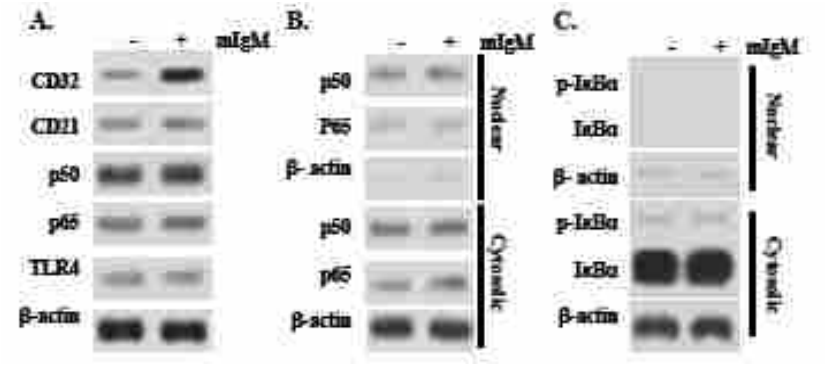

Figure 22. IgM increased CD32 expression without inducing NF-κB activation in FDCs. Isolated FDCs (4 × 10^6 cells/sample in a final volume of 4 mL culture medium) were treated with mouse IgM (preformed by incubating 10 μg rat-anti mouse IgG with 10 μg mouse IgM) for 1 day. At the end of incubation, the whole cell, nuclear, and cytosolic proteins were extracted. The expression of CD32, CD21, p50, p65, and TLR4 was detected by Western blotting (A). The accumulation of p50, p65, phosphorylated IκBα, and IκBα in the cytosol or nucleus was detected by Western blotting (B and C). β-actin worked as a loading control.

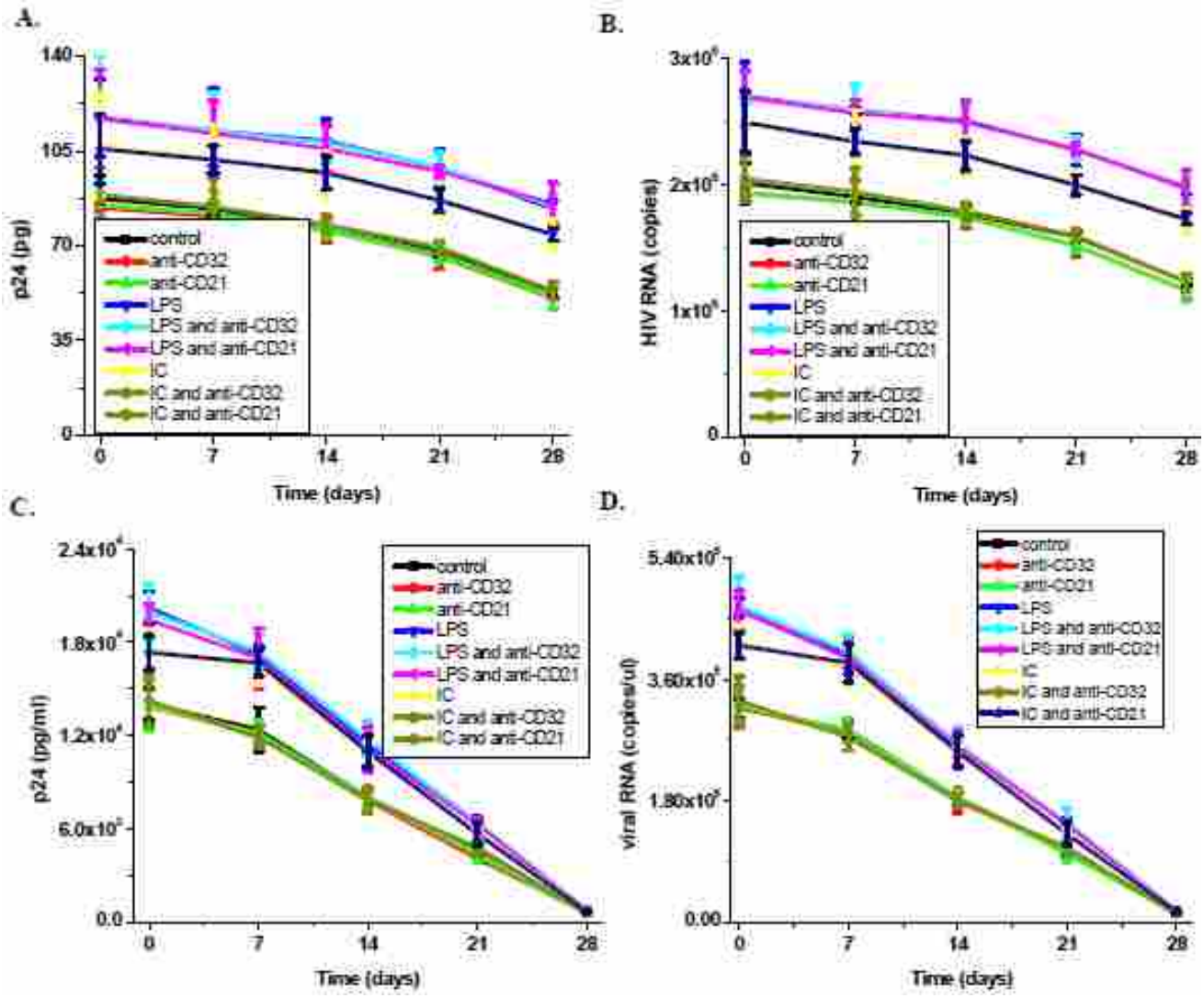

Figure 23. Activated FDCs trapped more HIV and maintained higher infectivity. Isolated FDCs (10^5 cells/sample in a final volume of 200 µL) were incuated in the presence or absence of 10 µg/ml LPS, HIV immune complexes (preformed by incubating 50 µL HIV-1_{IIIB} with 10 µg gp120 antibody for 30 minutes), 10 µg CD21 antibody, or 10 µg CD32 antibody for 1 day. Subsequently, these activated FDCs were washed and incubated with HIV-1_{IIIB} (50 µL), human serum (5 µL), and gp120 antibody (10 µg) for 2 hours. Unbound viruses were then removed. These FDCs (10^5 cells/mL) were incubated for 0, 7, 14, 21, or 28 days. After incubation, FDCs were divided into two aliquots. One aliquot was lysed to detect cytosolic p24 (A) and viral RNA (B). The other aliquot was incubated with CD4+ T cells (10^6 cells/sample in 4 mL culture medium; 10 CD4+ T cells to 1 FDC) for 7 days to collect the supernatant fluid. HIV p24 (C) and viral RNA production (D) in the supernatant fluid were detected. Control: resting FDCs; anti-CD32: FDCs with CD32 antibody treatment; anti-CD21: FDCs with CD21 antibody treatment; LPS: FDCs with LPS treatment; IC: FDCs with HIV immune complex treatment.

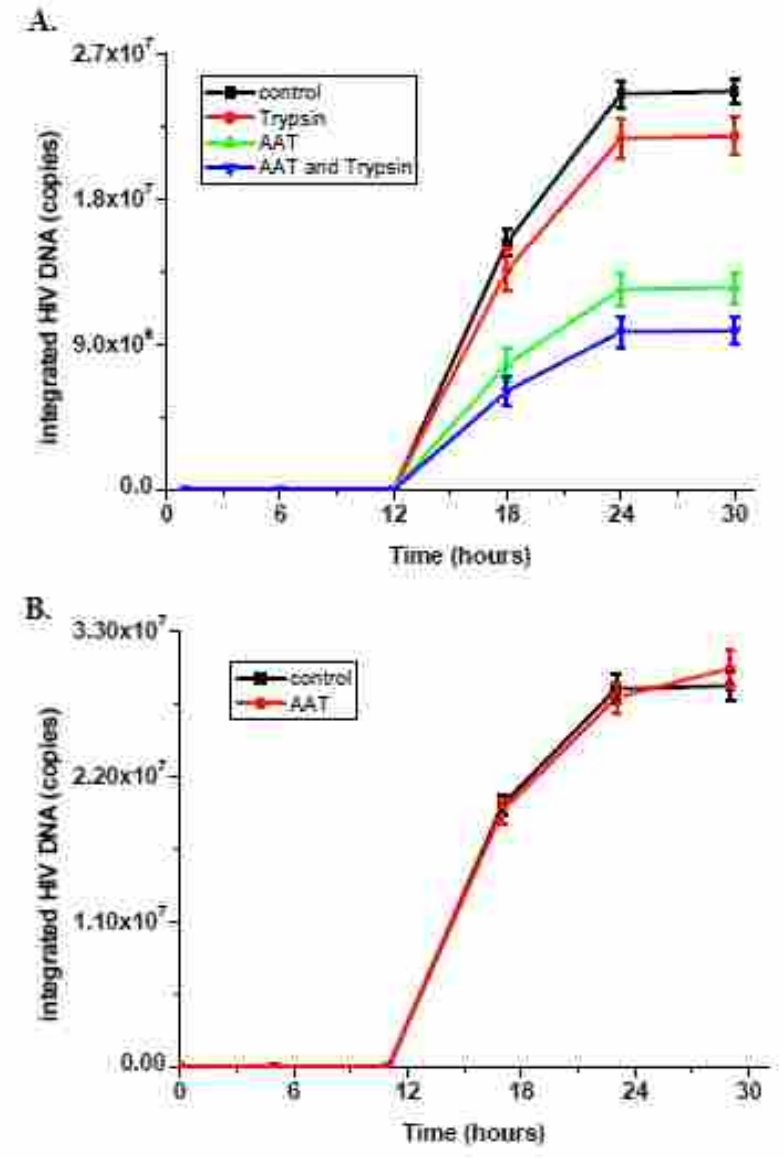

Figure 24. AAT did not interfere with the integration of HIV viral DNA into the host genome. Activated primary CD4+ T cells (10^6 cells/sample in a final volume of 1 mL culture medium) were divided into two aliquots. One aliquot was incubated in the presence or absence of 5 mg/mL AAT for 1 hour. After AAT pretreatment, these cells were infected with HIV-1_{IIIB} (500 µL) without removing AAT. Subsequently, the infected CD4+ T cells were treated with or without trypsin for 10 minutes. After trypsin-treatment, unbound viruses were removed. Next, these cells were incubated for 1, 6, 12, 18, 24, or 30 hours in the presence or absence of AAT (the same condition as before HIV infection) to isolate DNA. The integration of HIV viral DNA into the host genome was detected using quantitative Alu-PCR (A). Meanwhile, the other aliquot was infected with HIV-1_{IIIB} without AAT pretreatment and then incubated for 1 more hour. Next, these cells were incubated in the presence or absence of AAT. After 0, 5, 11, 17, 23, or 29 hours incubation, DNA was extracted to detect the integration of HIV viral DNA into the host genome (B). GAPDH worked as an endogenous control.

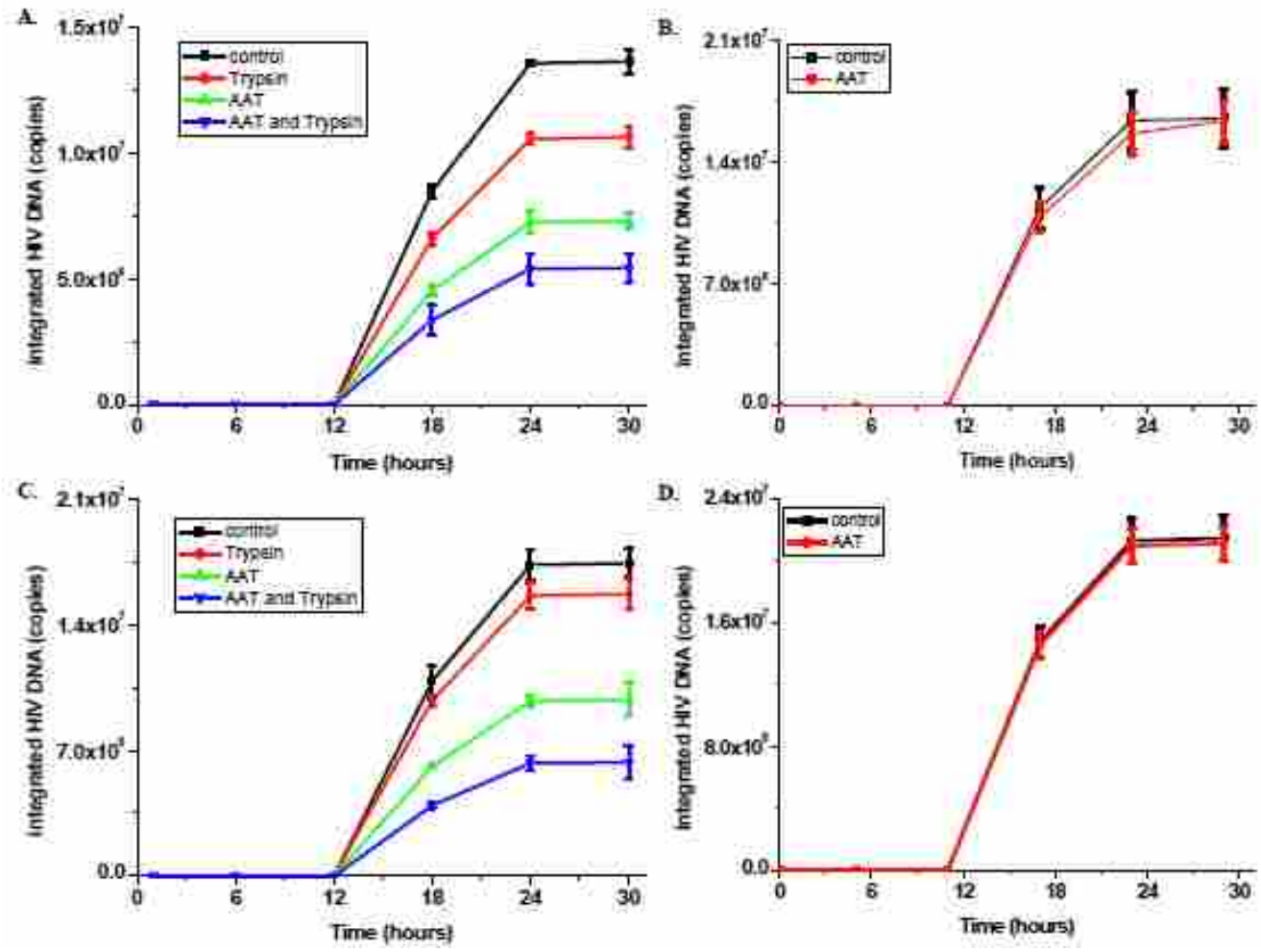

Figure 25. AAT did not interfere with the integration of primary HIV viral DNA into host genome. Activated primary CD4+ T cells (10^6 cells/sample in a final volume of 1 mL culture medium) were divided into two aliquots. One aliquot was incubated in the presence or absence of 5 mg/mL AAT for 1 hour. After AAT pretreatment, these cells were infected with 500 µL primary CXCR4-tropic virus, HIV-$1_{91US054}$ (A), or 500 µL CCR5-tropic virus, HIV-$1_{92US714}$ (C), without removing AAT. Subsequently, infected CD4+ T cells were treated with or without trypsin for 10 minutes. After trypsin-treatment, these cells were washed to remove unbound viruses. Next, these cells were incubated for 1, 6, 12, 18, 24, or 30 hours in the presence or absence of AAT (the same condition as before HIV infection) to isolate DNA. The integration of HIV viral DNA i nto the host genome was detected by quantitative Alu-PCR. Meanwhile, the other aliquot was i nfected with HIV-$1_{91US054}$ (B) or HIV-$1_{92US714}$ (D) without AAT pretreatment and incubated for 1 more hour. Next, the cells were incubated in the presence or absence of AAT. After 0, 5, 11, 17, 23, or 29 hours incubation, DNA was extracted and the integration of HIV viral DNA into the host genome was detected (B and D). GAPDH worked as endogenous control.

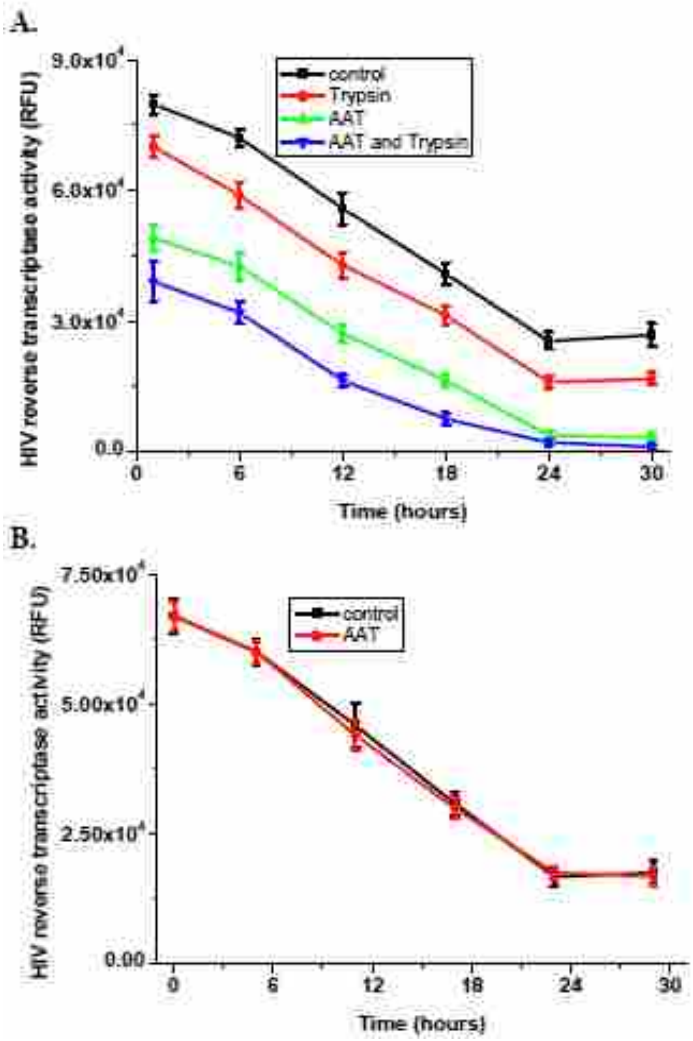

Figure 26. AAT did not inhibit the activity of HIV reverse transcriptase. Activated primary CD4+ T cells (10^6 cells/sample in a final volume of 1 mL culture medium) were divided into two aliquots. One aliquot was pretreated with or without 5 mg/mL AAT for 1 hour. After AAT pretreatment, these cells were infected with HIV-1_{IIIB} (500 μL) without removing AAT. Subsequently, infected CD4+ T cells were treated with or without trypsin for 10 minutes. After trypsin-treatment, these cells were washed to remove unbound viruses. Next, these cells were incubated for 1, 6, 12, 18, 24, or 30 hours in the presence or absenc of AAT (the same condition as before HIV infection) to isolate whole cell and viral proteins. The activity of HIV reverse transcriptase was detected following the protocol described in the Material and Methods section (A). Meanwhile, the other aliquot was infected with HIV-1_{IIIB} without AAT pretreatment and incubated for 1 more hour. Next, the samples were incubated in the presence or absence of AAT. After 0, 5, 11, 17, 23, or 29 hours incubation, the whole cell and viral proteins were extracted and the activity of HIV reverse transcriptase was detected (B).

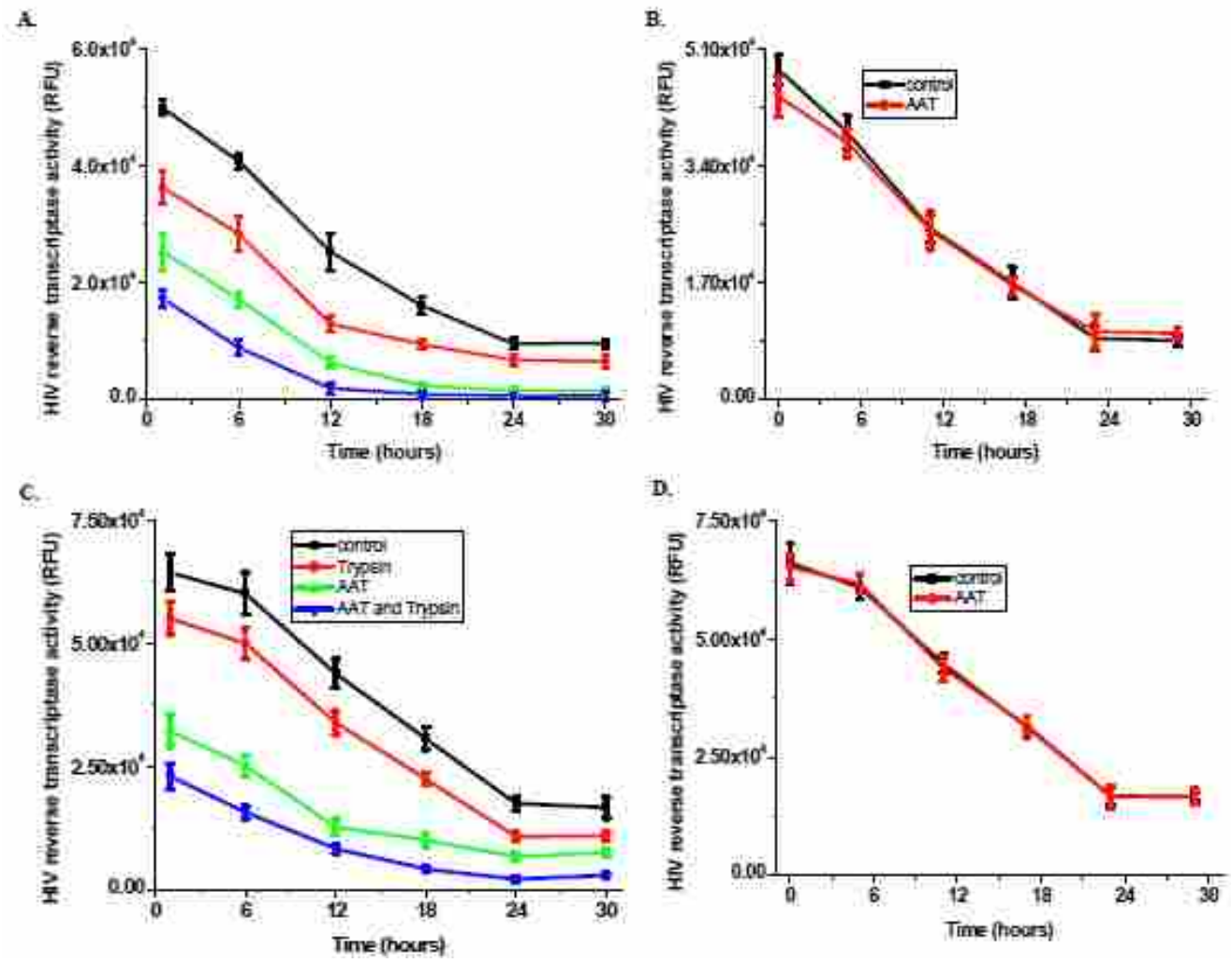

Figure 27. AAT inhibited primary HIV infection of CD4+ T cells without interfering with the activity of HIV reverse transcription. Activated primary CD4+ T cells (10^6 cells/sample in a final volume of 1 mL culture medium) were divided into two aliquots. One aliquot was pretreated with or without 5 mg/mL AAT for 1 hour. After AAT pretreatment, these cells were infected with 500 µL HIV-$1_{91US054}$ (A) or 500 µL HIV-$1_{92US714}$ (C) without removing AAT. Infected CD4+ T cells were treated with or without trypsin for 10 minutes. After trypsin-treatment to remove unbound virus, these cells were washed. Subsequently, the cells were incubated in the presence or absence of AAT (the same condition as before HIV infection) for 1, 6, 12, 18, 24, or 30 hours to isolate whole cell and viral proteins. The activity of HIV reverse transcriptase was detected as in Figure 26. Meanwhile, the other aliquot was infected directly with primary HIV-$1_{91US054}$ (B) or HIV-$1_{92US714}$ (D) without AAT pretreatment and then incubated for 1 more hour. Next, the samples were incubated with or without the presence of AAT. After 0, 5, 11, 17, 23, or 29 hours incubation, the whole cell and viral proteins were extracted and the activity of HIV reverse transcriptase was detected.

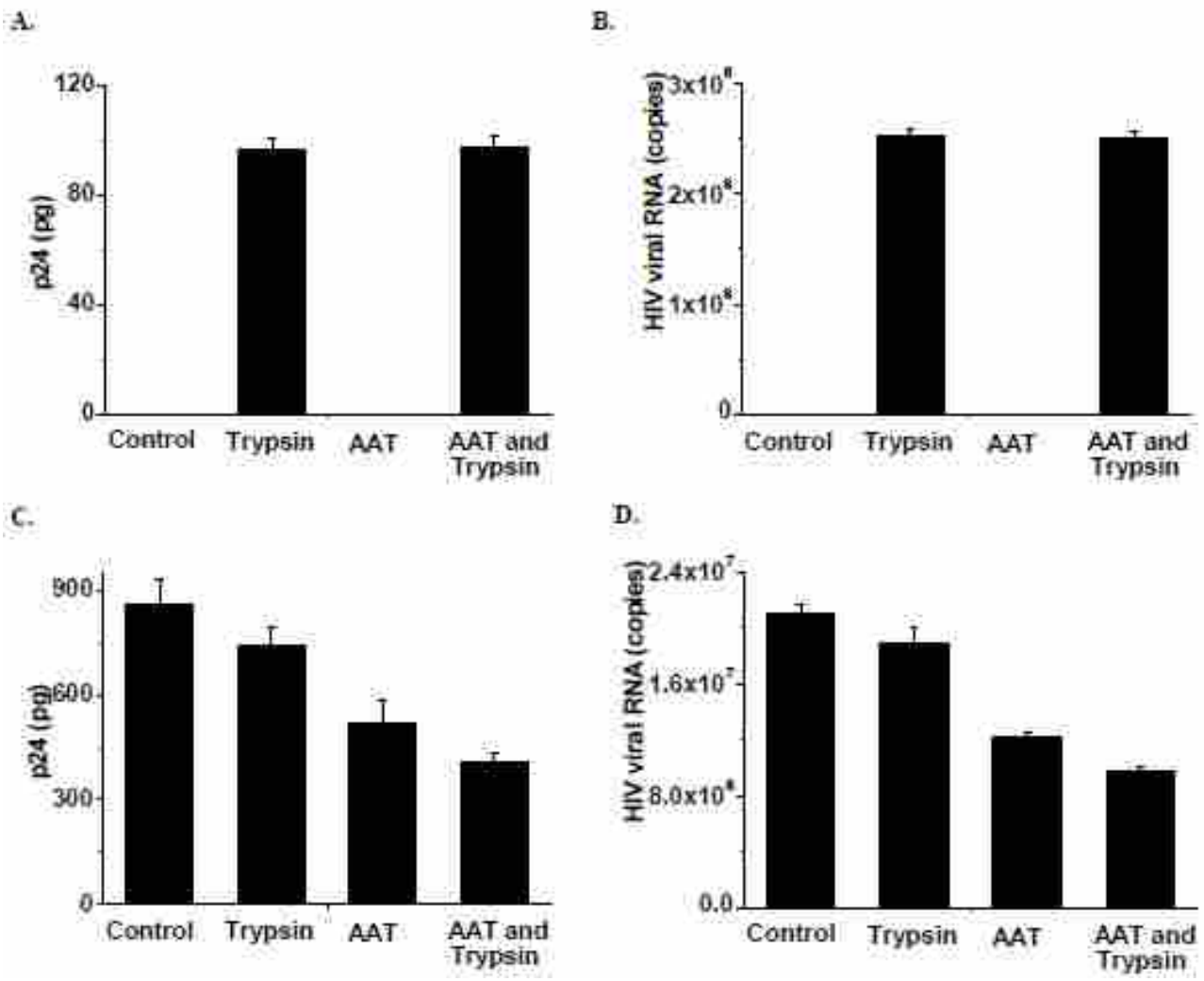

Figure 28. AAT inhibited HIV entry into CD4+ T cells. Activated primary CD4+ T cells (10^6 cells/sample in a final volume of 1 mL culture medium) were pretreated with or without 5 mg/mL AAT for 1 hour. After the pretreatment, these cells were infected by HIV-1_{IIIB} (500 μL) in the presence of AAT. Subsequently, the infected CD4+ T cells were treated with or without trypsin for 10 minutes to remove extracellular attached virus. After trypsin treatment, the supernatant fluid and cells were collected for analysis. The supernatant fluid was washed and concentrated by centrifuging at 60,000 × g for 2 hours at 4 ºC for three times. The amount of HIV particles in the supernatant fluid was determined by HIV p24 (A) and viral RNA (B). The collected cells were incubated for 2 hours and lysed to extract the whole cell proteins (including HIV p24) and RNA. HIV entry into CD4+ T cells was determined by measuring cytosolic HIV p24 (C) and viral RNA (D). GAPDH expression was used as an endogenous control.

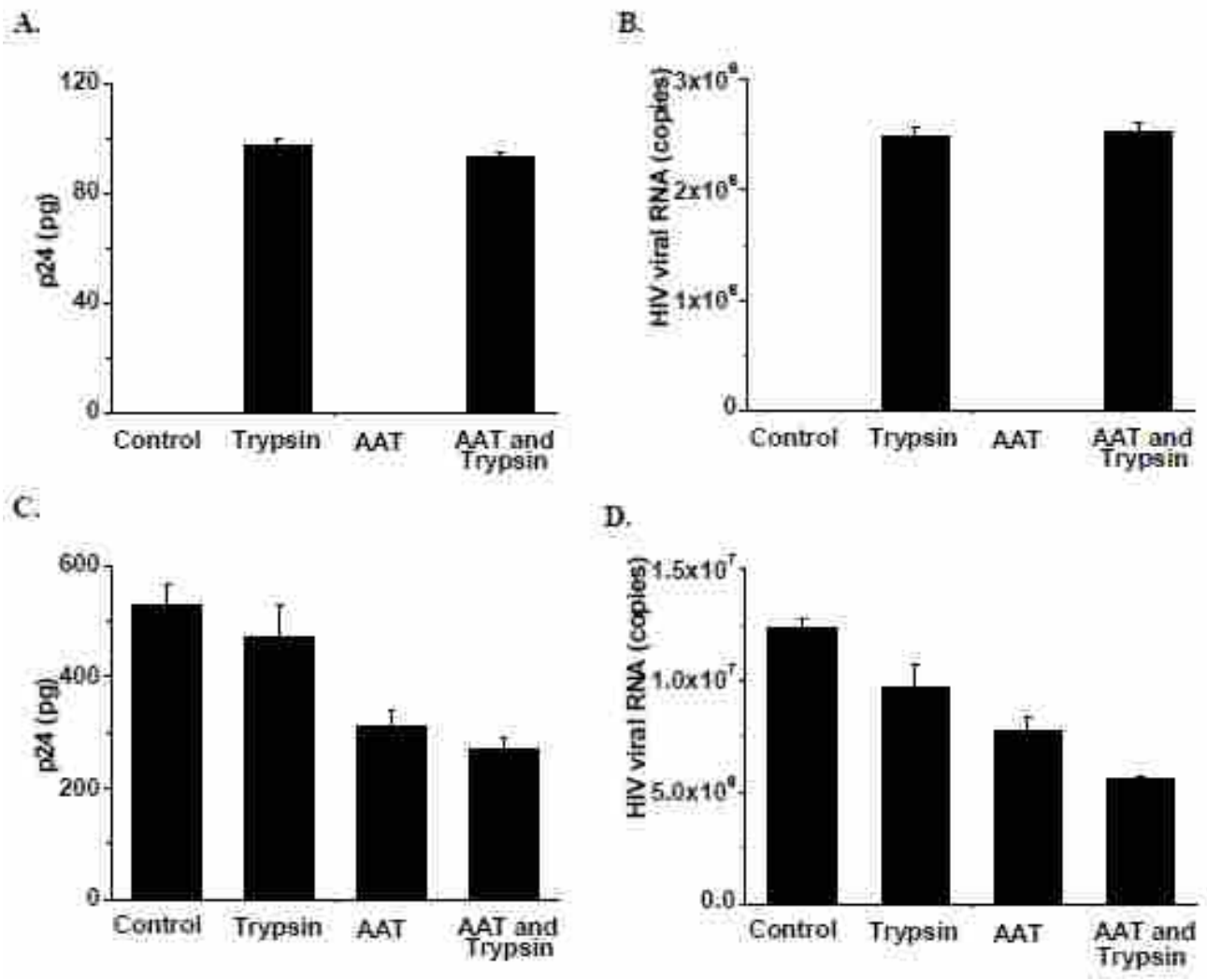

Figure 29. AAT inhibited primary X4 HIV entry into CD4+ T cells. Activated primary CD4+ T cells (10^6 cells/sample in a final volume of 1 mL culture medium) were pretreated with or without 5 mg/mL AAT for 1 hour. After the pretreatment, these cells were infected by 500 μL HIV-$1_{91US054}$ in the presence of AAT. Subsequently, the infected CD4+ T cells were treated with or without trypsin for 10 minutes to remove extracellular attached virus. After trypsin treatment, the supernatant fluid and cells were collected for analysis. The supernatant fluid was washed and concentrated by centrifuging at 60,000 × g for 2 hours at 4 ºC for three times. The amount of HIV particles in the supernatant fluid was determined by HIV p24 (A) and viral RNA (B). The collected cells were incubated for 2 hours and lysed to extract the whole cell proteins (including HIV p24) and RNA. HIV entry into CD4+ T cells was determined by measuring cytosolic HIV p24 (C) and viral RNA (D). GAPDH expression was used as an endogenous control.

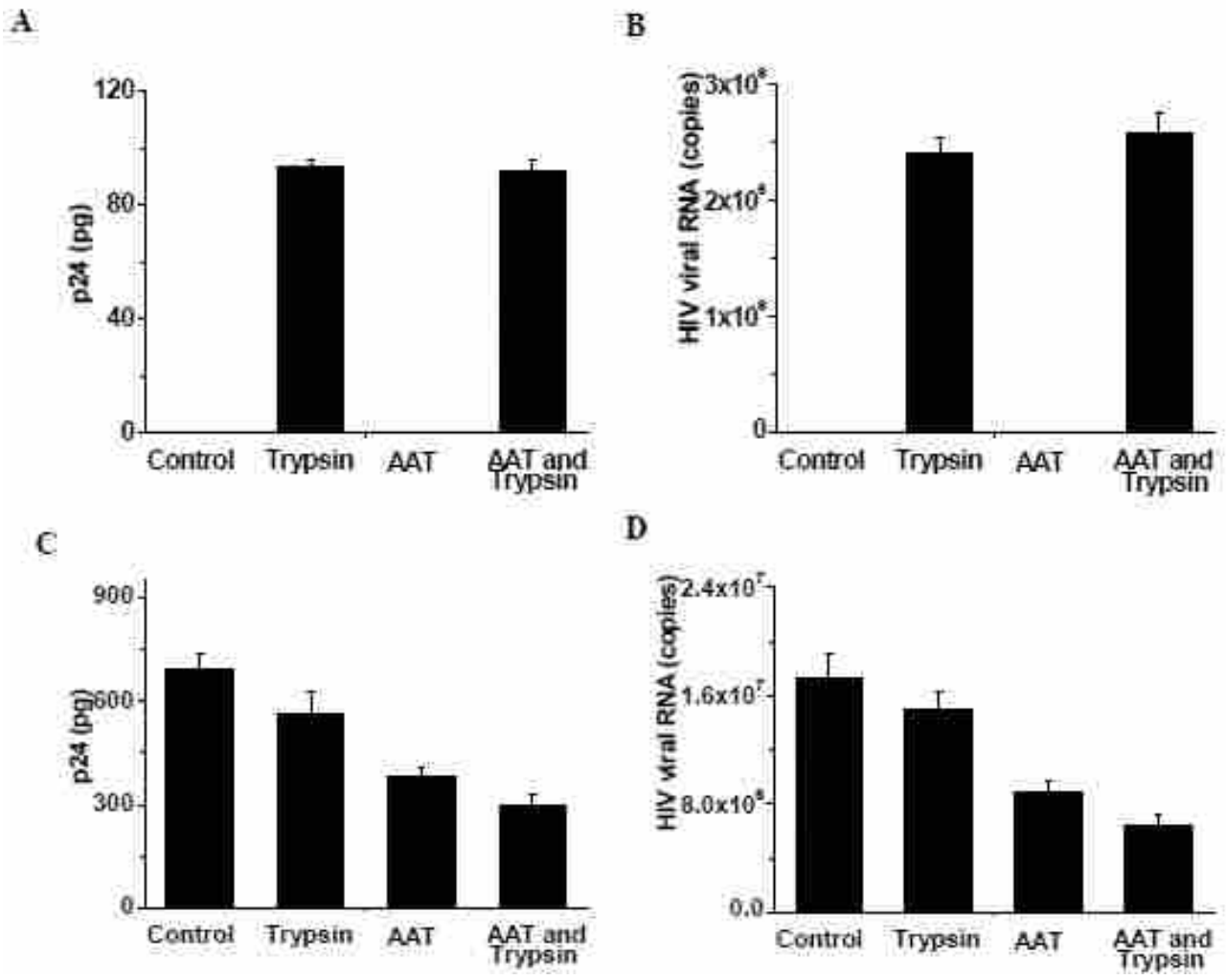

Figure 30. AAT inhibited primary R5 HIV entry into CD4+ T cells. Activated primary CD4+ T cells (10^6 cells/sample in a final volume of 1 mL culture medium) were pretreated with or without 5 mg/mL AAT for 1 hour. After the pretreatment, these cells were infected by 500 μL HIV-$1_{92US714}$ in the presence of AAT. Subsequently, the infected CD4+ T cells were treated with or without trypsin for 10 minutes to remove extracellular attached virus. After trypsin treatment, the supernatant fluid and cells were collected for analysis. The supernatant fluid was washed and concentrated by centrifuging at 60,000 × g for 2 hours at 4 ºC for three times. The amount of HIV particles in the supernatant fluid was determined by HIV p24 (A) and viral RNA (B). The collected cells were incubated for 2 hours and lysed to extract the whole cell proteins (including HIV p24) and RNA. HIV entry into CD4+ T cells was determined by measuring cytosolic HIV p24 (C) and viral RNA (D). GAPDH expression was used as an endogenous control.

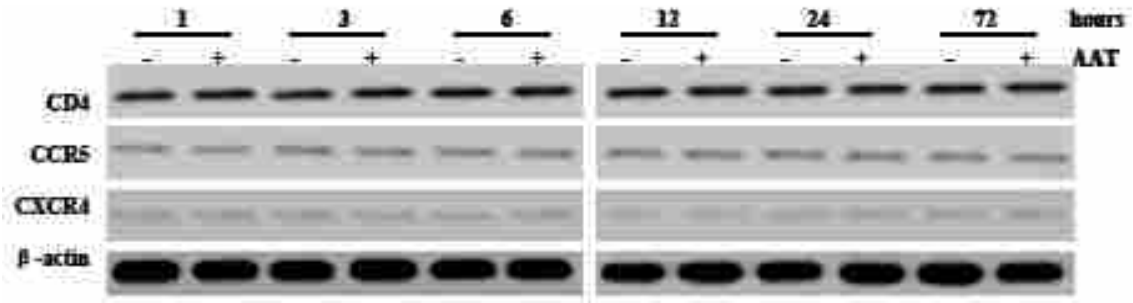

Figure 31. AAT did not alter CD4, CCR5, or CXCR4 expression on CD4+ T cells. Activated primary CD4+ T cells (2×10^6 cells/sample in a final volume of 2 mL culture medium) were incubated with 5 mg/mL AAT for 1, 3, 6, 12, 24, or 72 hours and extracted the whole cell proteins. The expression of CD4, CCR, and CXCR4 was detected by Western blotting. β-actin served as a loading control.

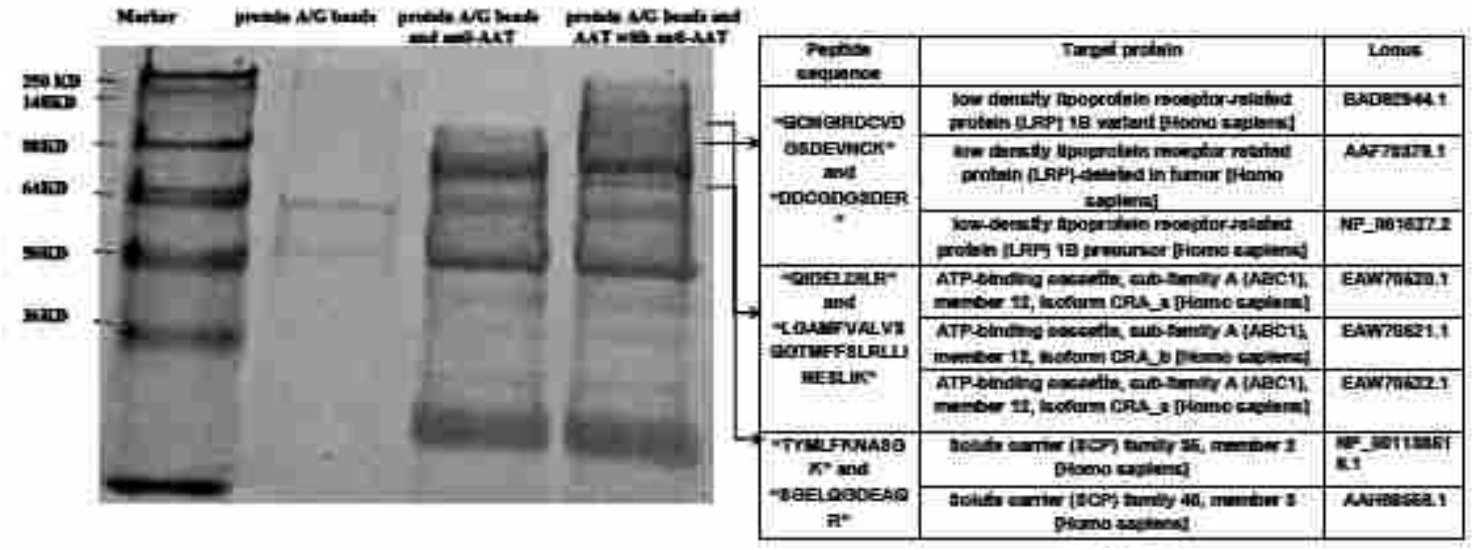

Peptide sequence	Target protein	Locus
SCNGIRDCVD GSDEVNCK and *DDCGDQSDER*	low density lipoprotein receptor-related protein (LRP) 1B variant [Homo sapiens]	BAD92944.1
	low density lipoprotein receptor related protein (LRP)-deleted in tumor [Homo sapiens]	AAF72378.1
	low-density lipoprotein receptor-related protein (LRP) 1B precursor [Homo sapiens]	NP_061877.2
QIDELDRLR and *LQAMFVALVS GGTMFFSLRLLI REELIK*	ATP-binding cassette, sub-family A (ABC1), member 12, isoform CRA_a [Homo sapiens]	EAW78629.1
	ATP-binding cassette, sub-family A (ABC1), member 12, isoform CRA_b [Homo sapiens]	EAW78621.1
	ATP-binding cassette, sub-family A (ABC1), member 12, isoform CRA_a [Homo sapiens]	EAW78622.1
TYMLFRNASG K and *SSELQSDEAS R*	Solute carrier (SCP) family 35, member 2 [Homo sapiens]	NP_001138611.1
	Solute carrier (SCP) family 40, member 3 [Homo sapiens]	AAH88568.1

Figure 32. AAT interacted with LRP, ABC, and SCP on CD4+ T cells. Activated primary CD4+ T cells (10^7 cells/sample in a final volume of 10 mL culture medium) were infected with HIV-1_{IIIB} (2 mL). After infection, these cells were cultured in the presence or absence of 5 mg/mL AAT for 2 hours and unbound AAT was removed by washing after which the cells were collected. The interactions between AAT the the membrane receptors were stabilized using 3 mM DSP. Membrane proteins were then extracted from the cells and AAT-specific antibody was added to precipitate the proteins interacting with AAT. The precipitated proteins were separated by SDS-PAGE and visalized using Coomassie Blue (digital image saved as a balck and gray picture). The specific bands were collected and identified by mass spectrometry.

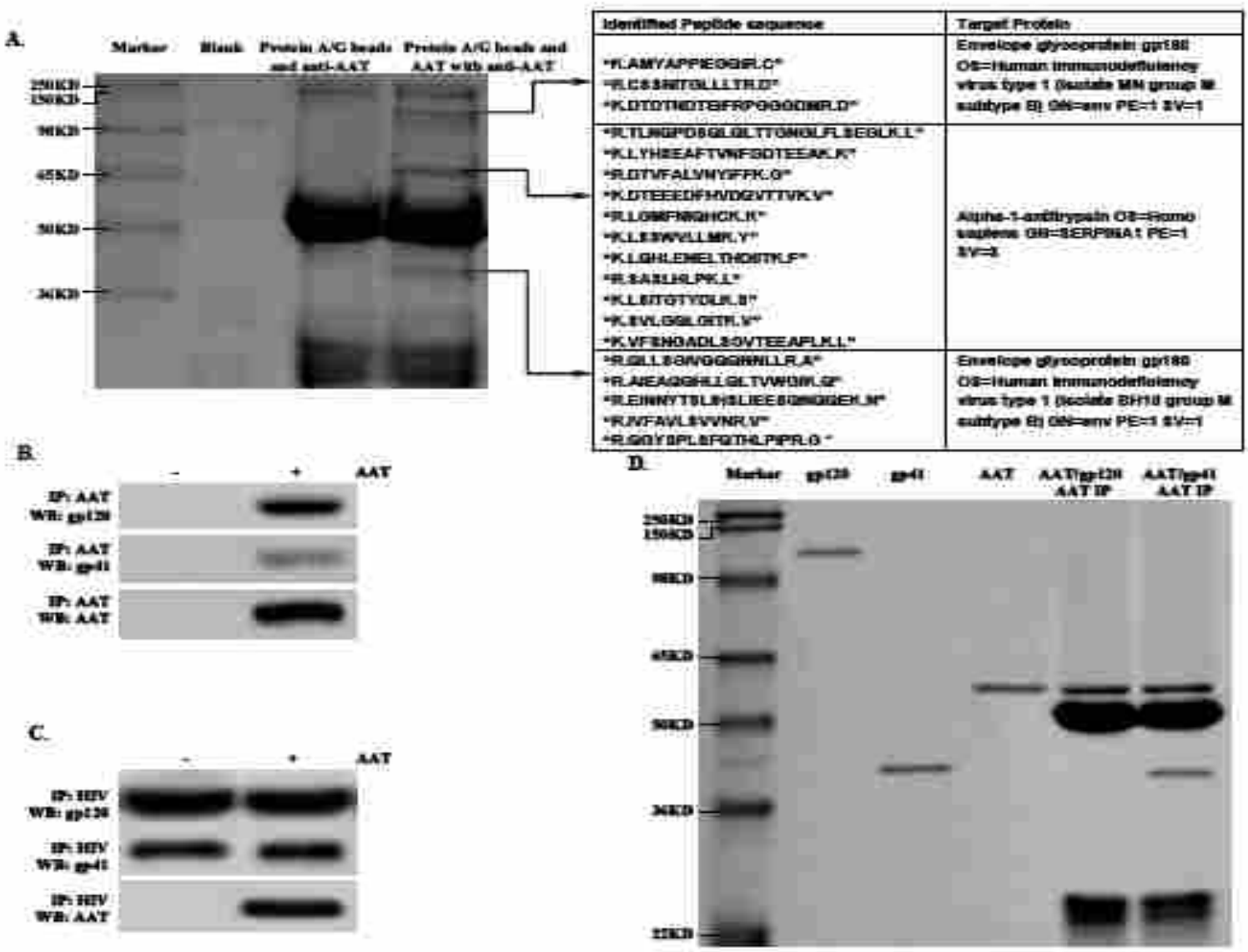

Figure 33. AAT interacted with HIV gp41. Propagated HIV-1_{IIIB} (containing more than 5 μg of HIV p24) was concentrated by ultracentrifuginf at 60,000 × g and incubated with 5 mg/mL AAT for 2 hours after which the virus was fixed with 3 mM DSP to stabilize the interaction between the HIV and AAT. Subsequently, the HIV-AAT complex was divided into two aliquots. (A). One aliquot was lysed to extract the viral proteins which were incubated with AAT-specific antibody followed by immunoprecipitation. The precipitated proteins were separated by SDS-PAGE and visalized with Coomassie Blue (digital image saved as a black and gray picture). The specific bands were cut to identify the proteins using mass spectrometry. (B). The precipitated proteins were also detected by Western blotting with antibody to AAT, gp120, or gp41. (C). The other aliquot was incubated with gp120 antibody to precipitate HIV and the interacting proteins. The precipitated HIV-AAT complex was lysed and immunoprecipitated using protein A/G beads. The precipitated proteins were also detected by Western blotting with antibody to AAT, gp120, or gp41. (D). AAT (1 μg) was also incubated with 1 μg recombinant gp120 or gp41 and precipitated with AAT-specific antibody. The precipitated proteins were separated with SDS-PAGE and visualized using Coomassie blue staining (digital image saved as a black and gray picture) to determine the direct interaction between AAT and gp120 or gp41.

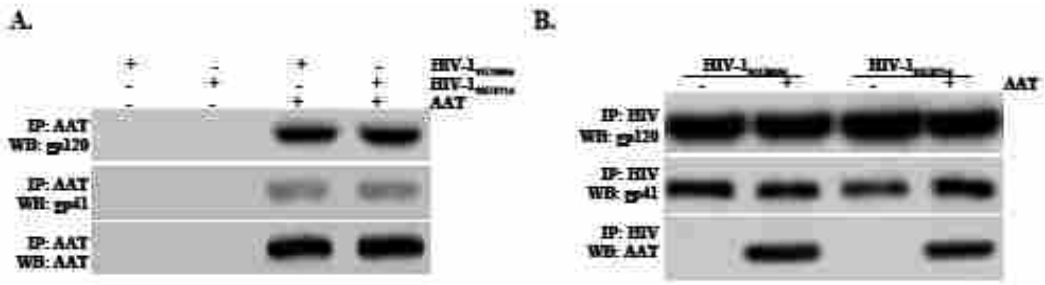

Figure 34. AAT interacted with gp120/gp41. Activated primary CD4+ T cells (5×10^6 cells/sample in a final volume of 5 mL culture medium) were infected by HIV-$1_{91US054}$ or HIV-$1_{92US714}$ and incubated in 50 mL culture medium for 2 weeks to produce HIV. Subsequently, HIV was collected and incubated with 5 mg/mL AAT for 2 hours. After 2 hours incubation, HIV was fixed using 3 mM DSP to stabilize the interaction between the virus and AAT. Next, the HIV-AAT complex was divided into two aliquots. (A). One aliquot was lysed to extract the viral proteins Isolated viral proteins were incubated with AAT-specific antibody for 2 hours to immunoprecipitate AAT and the proteins that interacted with AAT. The proteins on the beads were detected by Western blotting with antibody to AAT, gp120, or gp41. (B). The other aliquot was incubated with gp120 antibody for 2 hours to precipitate HIV and the proteins that interacted with HIV. Next, the precipitated HIV with AAT were lysed and separated by SDS-PAGE and detected by Western blotting with antibody to AAT, gp120, or gp41.

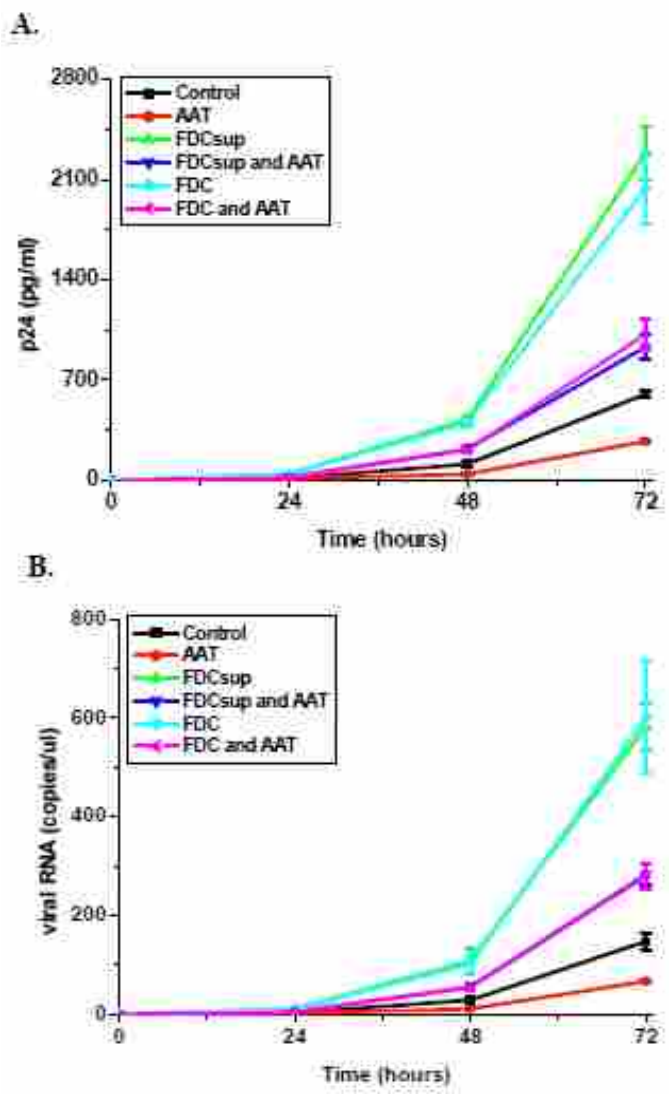

Figure 35. AAT inhibited HIV replication in CD4+ T cells. Activated primary CD4+ T cells were infected with HIV-1_{IIIB} as before. After infection, the T cells (5×10^5 cells/sample in a final volume of 500 µL culture medium) were cultured in the presence or absence of FDC supernatant fluid (FDCsup, 1/10 (V/V)), FDCs (10 CD4+ T cells to 1 FDC), or 5 mg/mL AAT. After 0, 24, 48, or 72 hours incubation, the supernatant fluid was collected to detect HIV p24 (A) and viral RNA (B) production. Part of the figure was published in my previous paper (88).

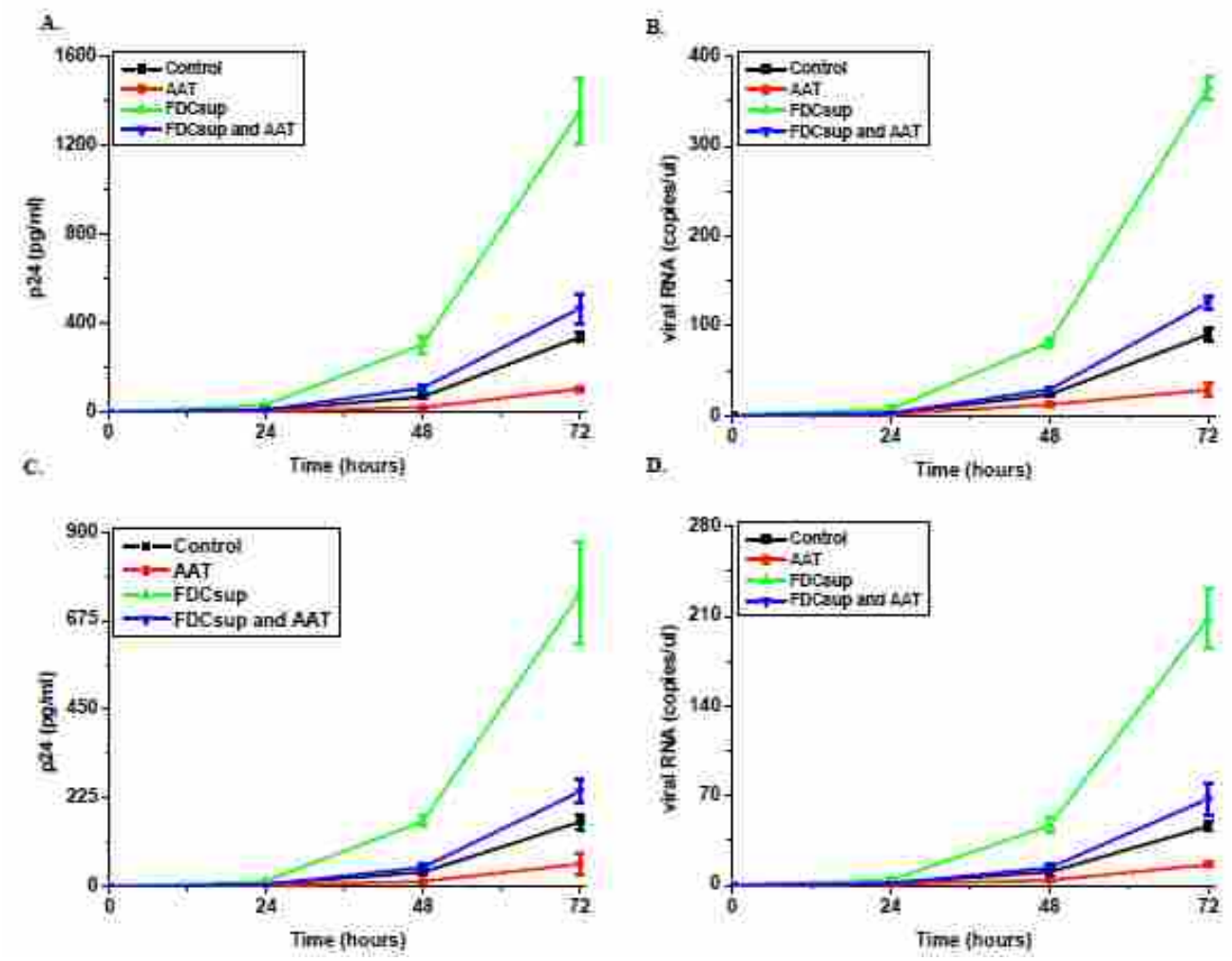

Figure 36. AAT inhibited HIV replication. Activated primary CD4+ T cells were infected with primary HIV isolate, HIV-1_{1714} (A and B) or HIV-1_{2054} (C and D). After infection, these infected cells (5×10^5 cells/sample in a final volume of 500 µL culture medium) were cultured in the presence or absence of FDC supernatant fluid (FDCsup, 1/10 (V/V)) or 5 mg/mL AAT. After 0, 24, 48, or 72 hours incubation, the supernatant fluid was collected to detect p24 (A and C) and viral RNA (B and D) production. The figure was published in my previous paper (88).

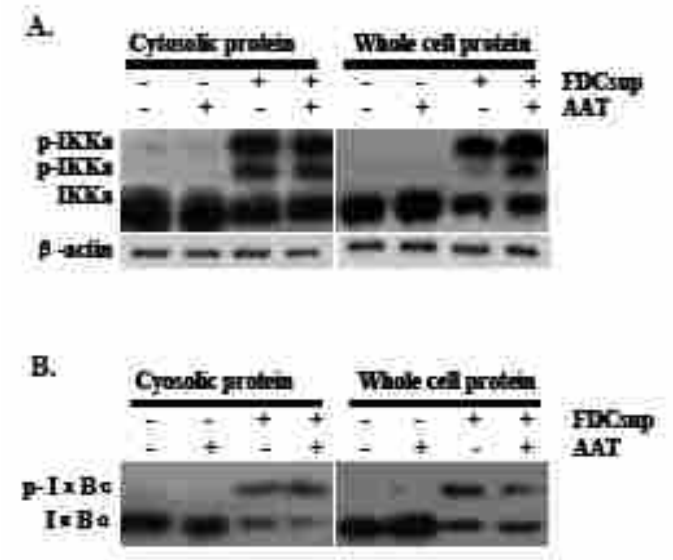

Figure 37. AAT did not interfere with the expression and activation of IKKα. Activated primary CD4+ T cells were infected with HIV-1_{IIIB}. After infection, the T cells (10^7 cells/sample in a final volume of 10 mL culture medium) were cultured in the presence or absence of FDC supernatant fluid (FDCsup, 1/10 (V/V)) or 5 mg/mL AAT. After 24 hours incubation, the cells were collected and lysed to extract the cytosolic or whole cell proteins. (A). IKKα expression was detected by Western blotting. β-actin served as a loading control. (B). The IKK complex was also precipitated with IKKα-specific antibody. The purified IKK complex was incubated with recombinatant IκBα in the presence of ATP to detect the activity of IKK by measuring IκBα phosphorylation. Phosphorylated IκBα was detected by Western blotting. Part of the figure was published in my previous paper (88).

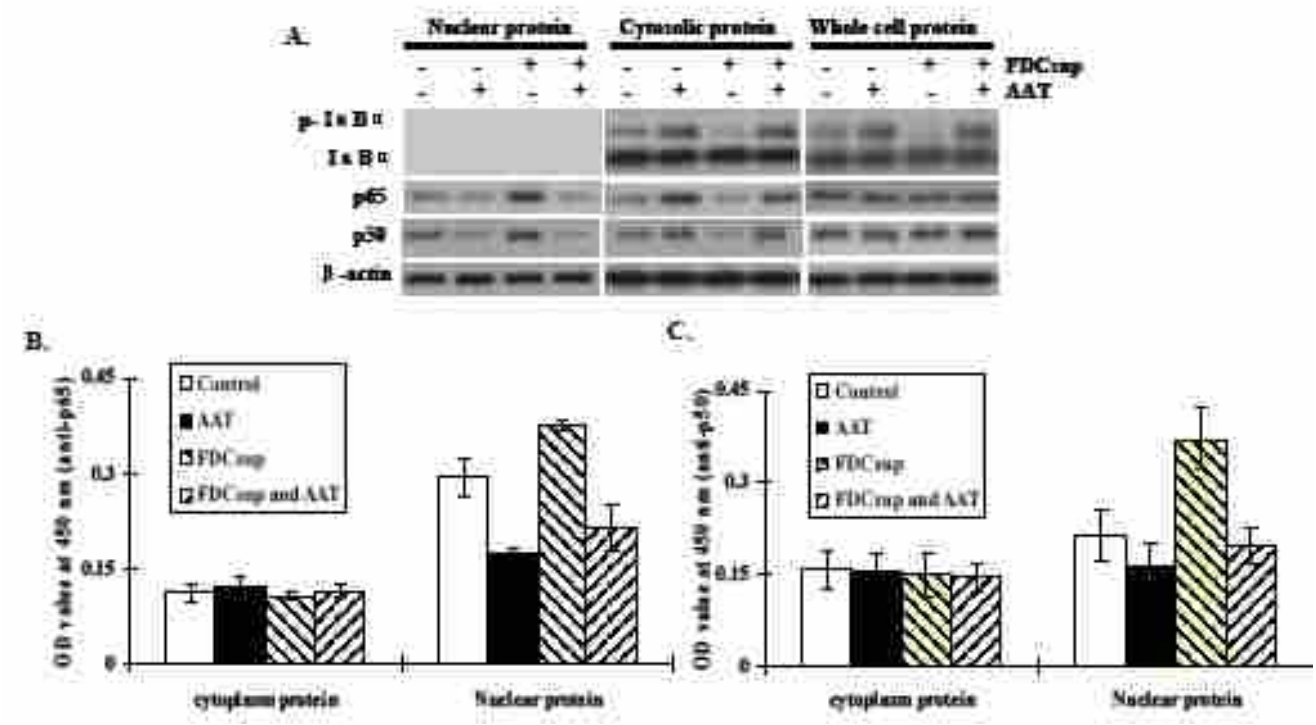

Figure 38. AAT inhibited the nuclear translocation and DNA binding activity of NF-κB and suppressed the degradation of phosphorylated IκBα. Activated primary CD4+ T cells were infected with HIV-1_{IIIB} as before. After infection, the T cells (10^7 cells/sample in a final volume of 10 mL culture medium) were cultured in the presence or absence of FDC supernatant fluid (FDCsup, 1/10 (V/V)) or 5 mg/mL AAT. After a 24-hour incubation, the cells were collected and lysed to extract the cytosolic, nuclear or whole cell proteins. (A). Cellular distribution of p65, p50, IκBα, and phosphorylated IκBα was detected by Western blotting. The expression of β-actin served as a loading control. The DNA binding activity of NF-κB was detected using ELISA with p65-specific antibody (B) and p50-specific antibody (C). Part of the figure was published in my previous paper (88).

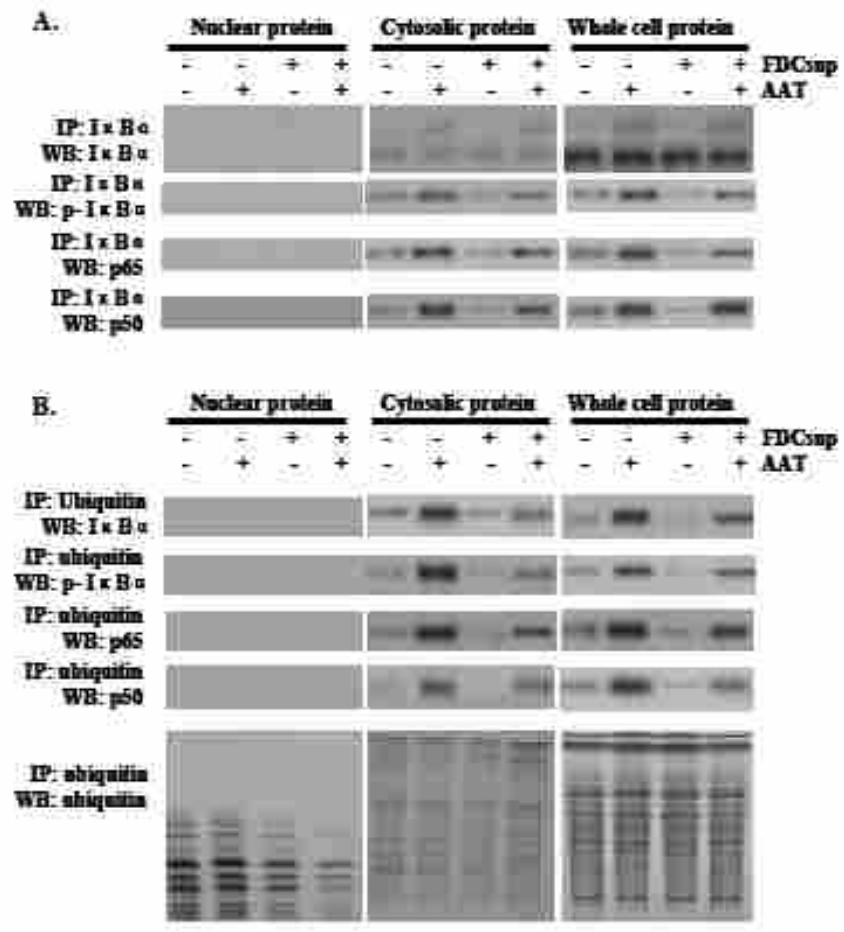

Figure 39. AAT inhibited the degradation and dissociation of phosphorylated and ubiquitinylated IκBα from NF-κB complex. Activated primary CD4+ T cells were infected with HIV-1_{IIIB} as before. After infection, these infected cells (10^7 cells/sample in a final volume of 10 mL culture medium) were cultured in the presence or absence of FDC supernatant fluid (FDCsup, 1/10 (V/V)) or 5 mg/mL AAT. After 24 hours incubation, the cells were collected and lysed to extract cytosolic, nuclear or whole cell proteins. Subsequently, IκBα antibody (A) or ubiquitin antibody (B) was added to the extracted proteins to precipitate the proteins. Precipitated proteins were separated by SDS-PAGE to detect the presence of p65, p50, IκBα, phosphorylated IκBα, and ubiquitinylated IκBα by Western blot. The figure was published in my previous paper (88).

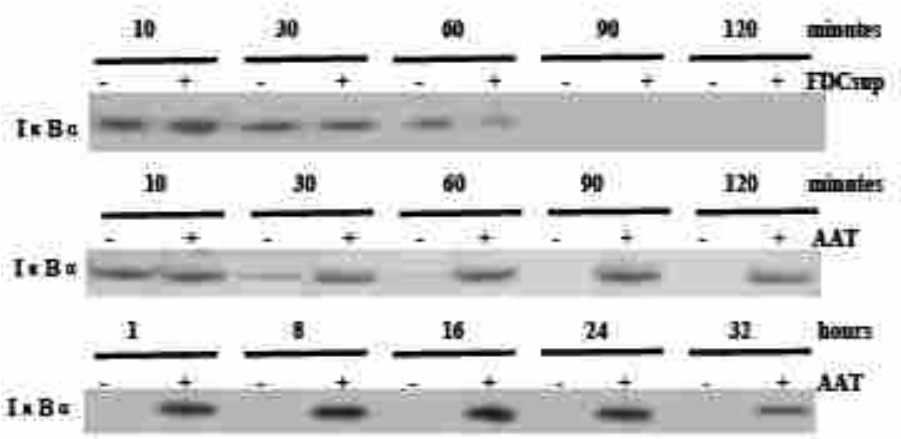

Figure 40. AAT increased the half life of IκBα in infected CD4+ T cells. Activated primary CD4+ T cells were infected by HIV-1_{IIIB} as before. After infection, these cells (5×10^5 cells/sample in a final volume of 500 μL culture medium) were cultured in the presence or absence of FDC supernatant fluid (FDCsup, 1/10 (V/V)) or 5 mg/mL AAT. After 24 hours incubation, the half-life of IκBα was detected by pulse-chase assay. Briefly, the cells were incubated with ^{35}S-labeled methionine to label cellular proteins and then re-incubated in the presence or absence of FDC supernatant fluid or AAT. At different time point, the cells were lysed and IκBα antibody was added to pull down and detect IκBα. The figure was published in my previous paper (88).

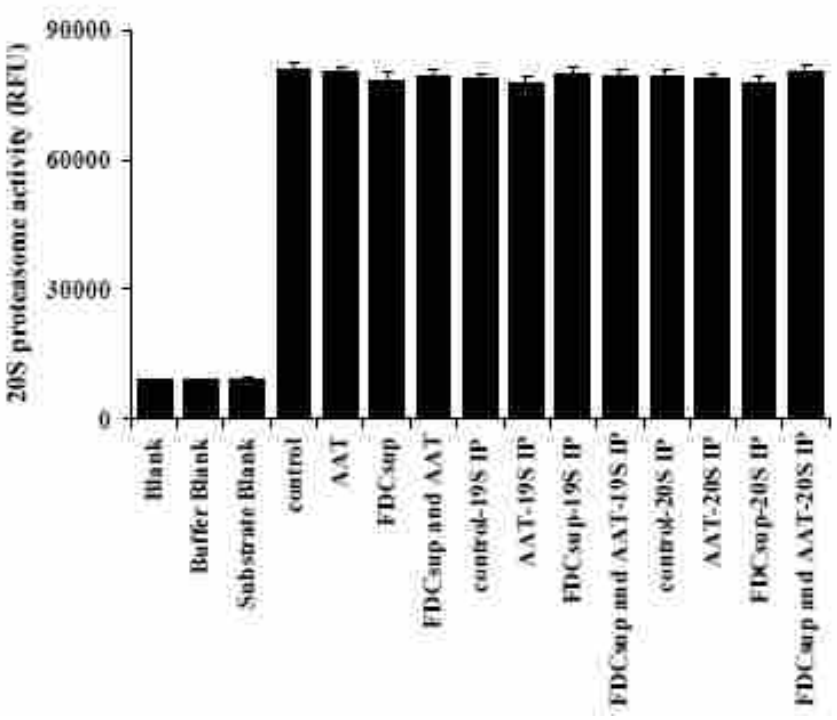

Figure 41. AAT did not interfere with the activity of the 20S proteasome in infected CD4+ T cells. Activated primary CD4+ T cells were infected with HIV-1_{IIIB} as before. After infection, these cells (5×10^6 cells/sample in a final volume of 5 mL culture medium) were cultured in the presence or absence of FDC supernatant fluid (FDCsup, 1/10 (V/V)) or 5 mg/mL AAT. After 24 hours incubation, these cells were collected and lysed to extract the whole cell proteins. The activity of the 20S proteasome was detected following the manufacture's protocol by using cell lysate or purified 26S proteasome (precipitated with 20S- or 19S-specific antibody). Blank: wells without anything; buffer blank: wells with lysis buffer; Substrate blank: wells with lysis buffer and substrate; control: cell lysate from CD4+ T cells; AAT: cell lysate from AAT-treated CD4+ T cells treated; FDCsup: cell lysate from FDC supernatant-treated CD4+ T cells; 19S IP: cell lysate from T cells immunoprecipitated using a 19S-specific antibody; 20S IP: cell lysate obtained by immunopreciptation using a 20S-specific antibody. Part of the figure was published in my previous paper (88).

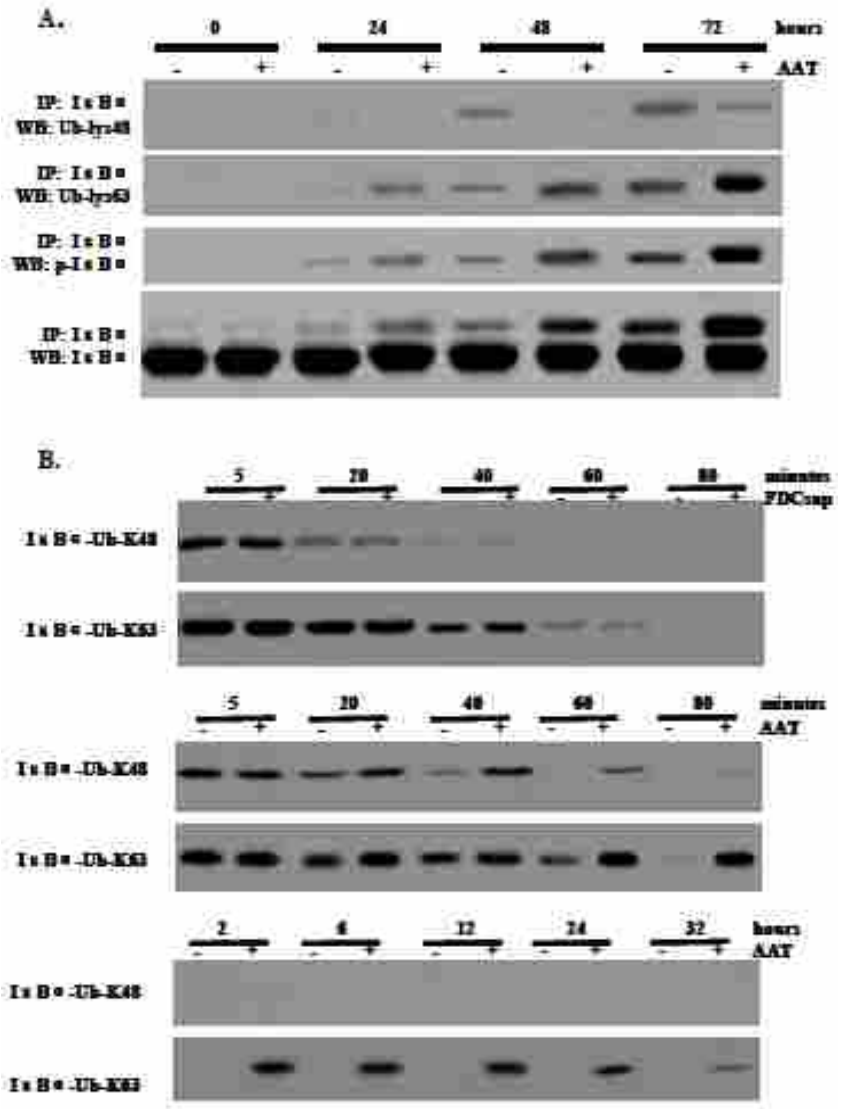

Figure 42. AAT increased the half-life of IκBα ubiquitinylated at K63. Activated primary CD4+ T cells were infected by HIV-1_{IIIB} as before. After infection, these infected cells (5×10^6 cells/sample in a final volume of 5 mL culture medium) were cultured in the presence or absence of FDC supernatant fluid (FDCsup, 1/10 (V/V)) or 5 mg/mL AAT. (A). After 0, 24, 48, or 72 hours incubation, the cells were collected to extract the whole cell proteins. Total IκBα was immuno-precipitated with IκBα-specific antibody. Subsequently, IκBα,, phosphorylated IκBα, IκBα ubiquitinylated at K63 and IκBα ubiquitinylated at K48 were detected by Western blotting. (B). After 24 hours incubation, the half-life of IκBα ubiquitinylated at K48 or K63 was detected using a radiolabeled, pulse-chase assay. Briefly, the cells were incubated with ^{35}S-labeled methionine to label the cellular proteins and then incubated in the presence of FDC supernatant fluid or AAT. At different time points, the cells were lysed and IκBα-specific antibody was added. Immunoprecipitated IκBα was boiled and protein A/G beads were removed. Antibody specific to IκBα ubiquitinylated at K63 or K48 was added to immunoprecipitate IκBα ubiquitinylated at K63 or K48. Subsequently, the immunoprecipitated IκBα ubiquitinylated at K63 or K48 was detected. The figure was published in my previous paper (88).

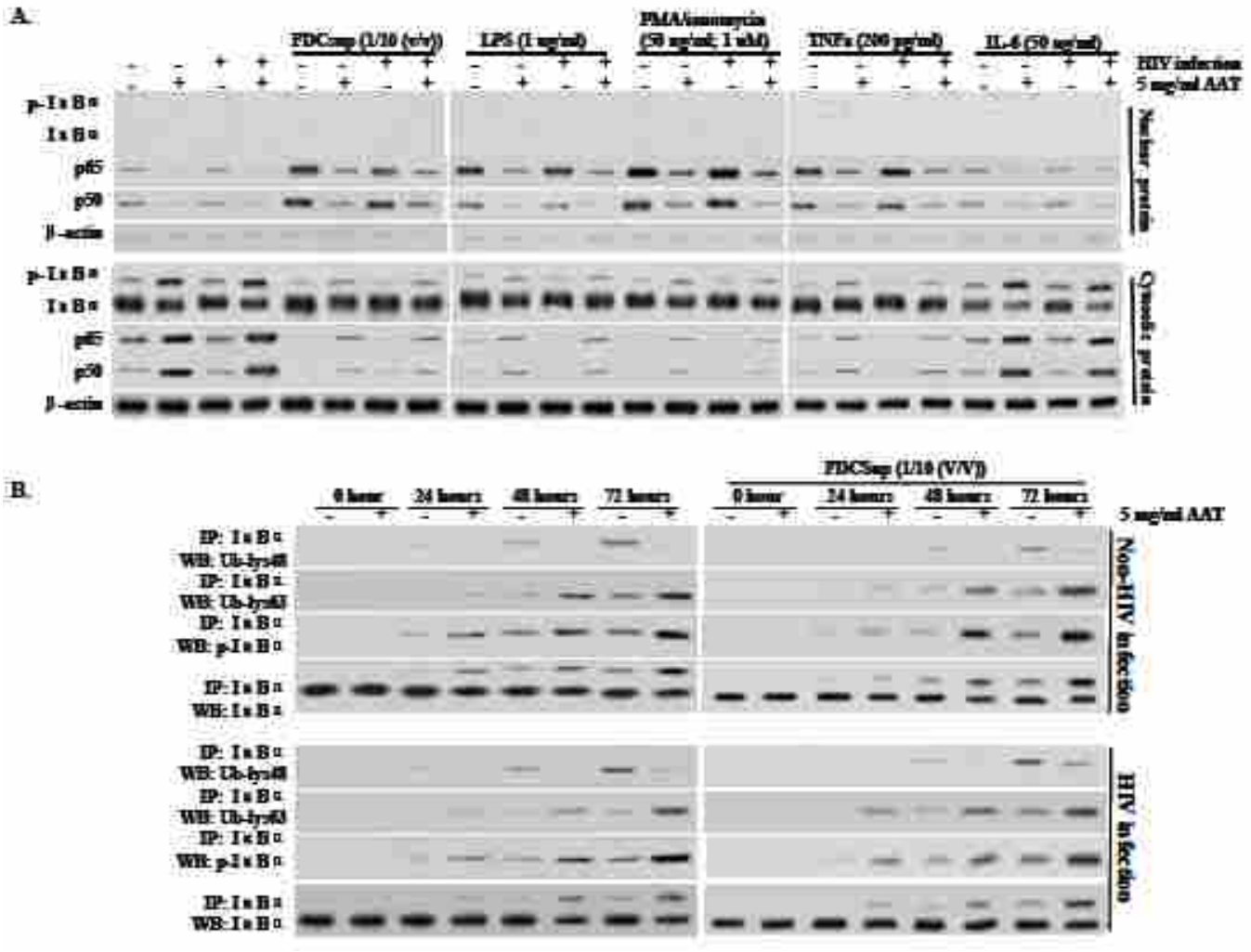

Figure 43. AAT inhibited the nuclear translocation of NF-κB and changed the ubiquitinylation pattern of IκBα in CD4+ T cells. Activated primary CD4+ T cells were infected with HIV-1_{IIIB} as before. Subsequently, the cells (5×10^6 cells/sample in a final volume of 5 mL culture medium) were cultured in the presence or absence of stimuli (FDC supernatant fluid (FDCsup, 1/10 (V/V)); 1 μg/mL LPS; 50 ng/mL PMA/1 μM ionomycin, 50 ng/mL Il-6, or 200 pg/mL TNFα) or 5 mg/mL AAT. (A). After 24 hours incubation, the cells were collected and lysed to extract the cytosolic and nuclear proteins. IκBα, phosphorylated IκBα, p65, and p50 were detected by Western blotting. β-actin served as a l oading control. (B). After 0, 24, 48, or 72 hours of incubation, the cells were collected and lysed to extract proteins. Total IκBα was immuno-precipitated with IκBα-specific antibody. Subsequently, IκBα, phosphorylated IκBα, IκBα ubiquitinylated at K63, and IκBα ubiquitinylated at K48 were detected by Western blotting. The figure was published in my previous paper (88).

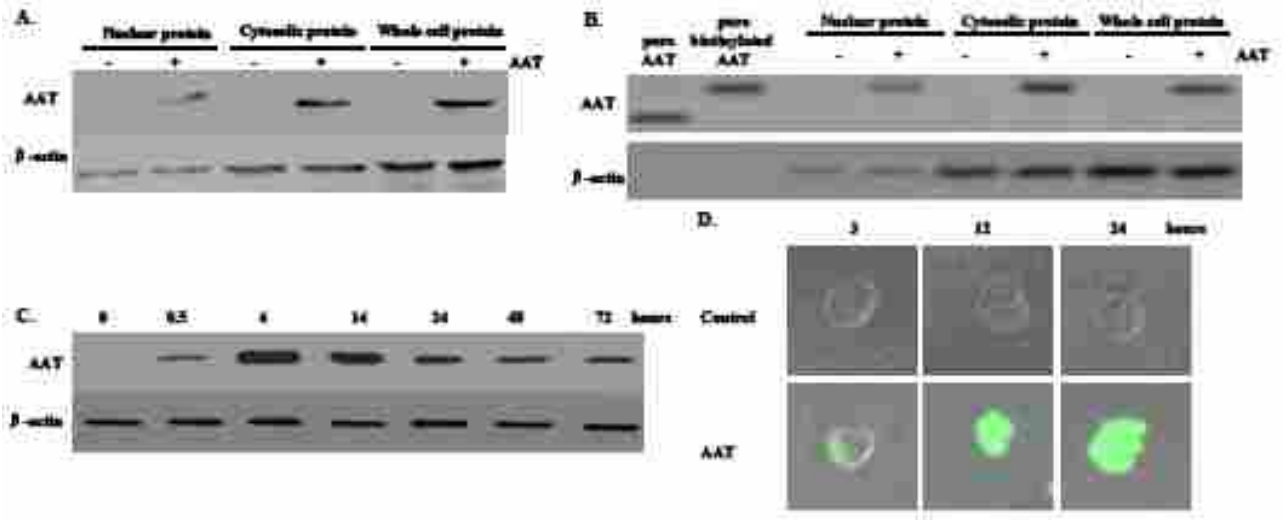

Figure 44. CD4+ T cells internalized AAT. Activated primary CD4+ T cells were infected with HIV-1_{IIIB}. After infection, these infected cells (5×10^6 cells/sample in a final volume of 5 mL culture medium) were cultured in the presence or absence of 5 mg/mL AAT (A) or biotin-labeled AAT (B) and incubated for 24 hours. Subsequently, the cells were collected and lysed to extract the nuclear, cytosolic or whole cell proteins. AAT was detected by Western blotting. AAT and biotinylated AAT were used as a positive control. (C). The infected cells were also cultured with AAT and incubated for 0, 0.5, 5, 14 24, 48, or 72 hours. Next, the cells were collected and lysed to extract the whole cell proteins. AAT was detected by Western blotting. β-actin served as a loading control. (D). Infected cells were cultured in the presence or absence of 5 mg/mL Alexa Fluor® 488-labeled AAT and incubated for 3, 12, or 24 hours. The cells were treated with trypsin to remove non-internalized AAT. Finally, the cells were fixed and imaged on a confocal microscope (600×). Parts of the figures were published in my previous paper (88).

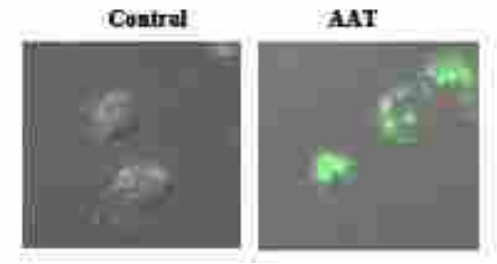

Figure 45. CD4+ T cells internalized AAT. Activated primary CD4+ T cells (2×10^5 cells/sample in a final volume of 200 μL culture medium) were cultured in the presence or absence of 5 mg/mL Alexa Fluor® 488-labeled AAT for 3 hours. At the end of incubation, the cells were treated with trypsin to remove non-internalized AAT. Subsequently, the cells were fixed and imaged with using a confocal microscope (600×).

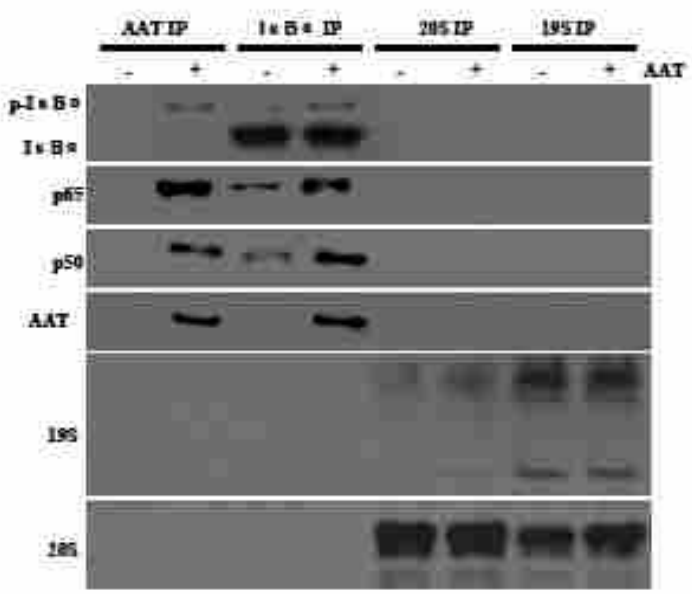

Figure 46. AAT was associated with IκBα/NF-κB complex. Activated primary CD4+ T cells were infected by HIV-1_{IIIB} as before. After infection, these infected cells (5×10^6 cells/sample in a final volume of 5 mL culture medium) were cultured in the presence or absence of 5 mg/mL AAT or FDC supernatant fluid (FDCsup, 1/10 (V/V)) and incubated for 24 hours. Next, the cells were collected and lysed to extract the whole cell proteins. The isolated proteins were incubated with antibodies specific for AAT, IκBα, 19S, or 20S to immunoprecipitate the proteins. Subsequently, AAT, the IκBα/NF-κB complex (IκBα, p65 and p50), and 26S proteasome (19S and 20S) were detected by Western blotting. The figure was published in my previous paper (88).

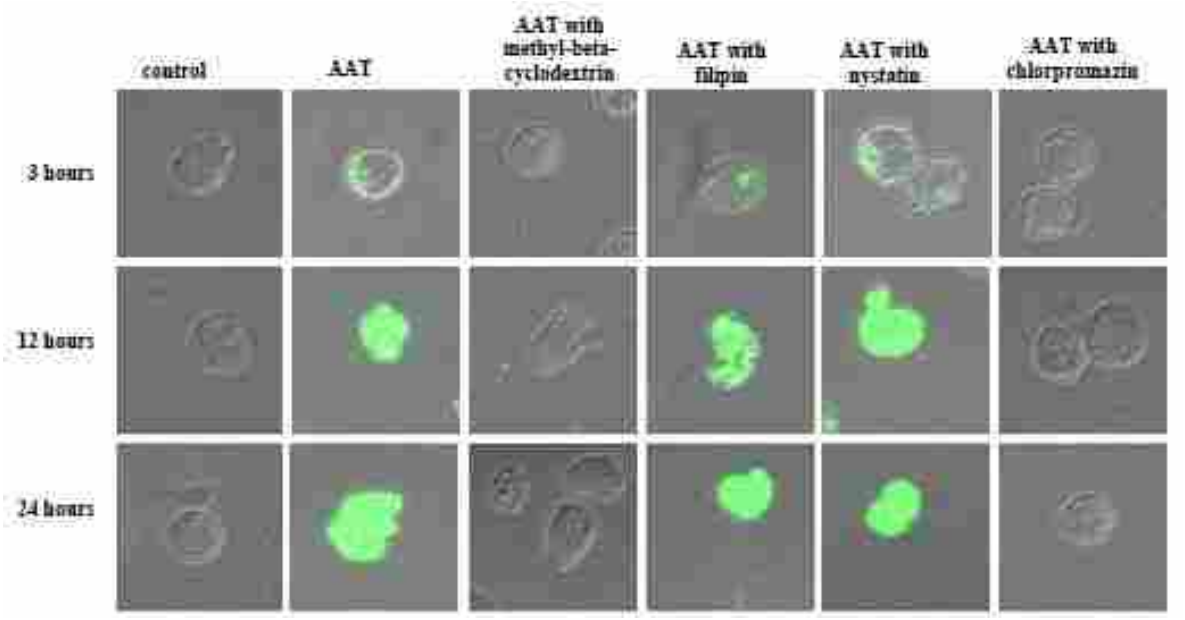

Figure 47. CD4+ T cells internalized AAT through a clathrin-dependent endocytosis process. Activated primary CD4+ T cells (2×10^5 cells/sample in a final volume of 200 μL culture medium) were infected with HIV-1_{IIIB} and then pretreated with 20 μg/mL general endocytosis inhibitor (methyl-β-cyclodextrin), 20 μg/mL caveoli-dependent endocytosis inhibitor (filipin and nystatin), or 20 μg/mL clathrin-dependent endocytosis inhibitor (chlorpromazine) for 1 hour. Subsequently, the cells were cultured in the presence or absence of 5 mg/mL Alexa Fluor® 488-labeled AAT for 3, 12, or 24 hours. At the end of incubation, the cells were collected and treated with trypsin to remove non-internalized AAT. Finally, these cells were fixed and imaged with confocal microscopy (600×) (B).

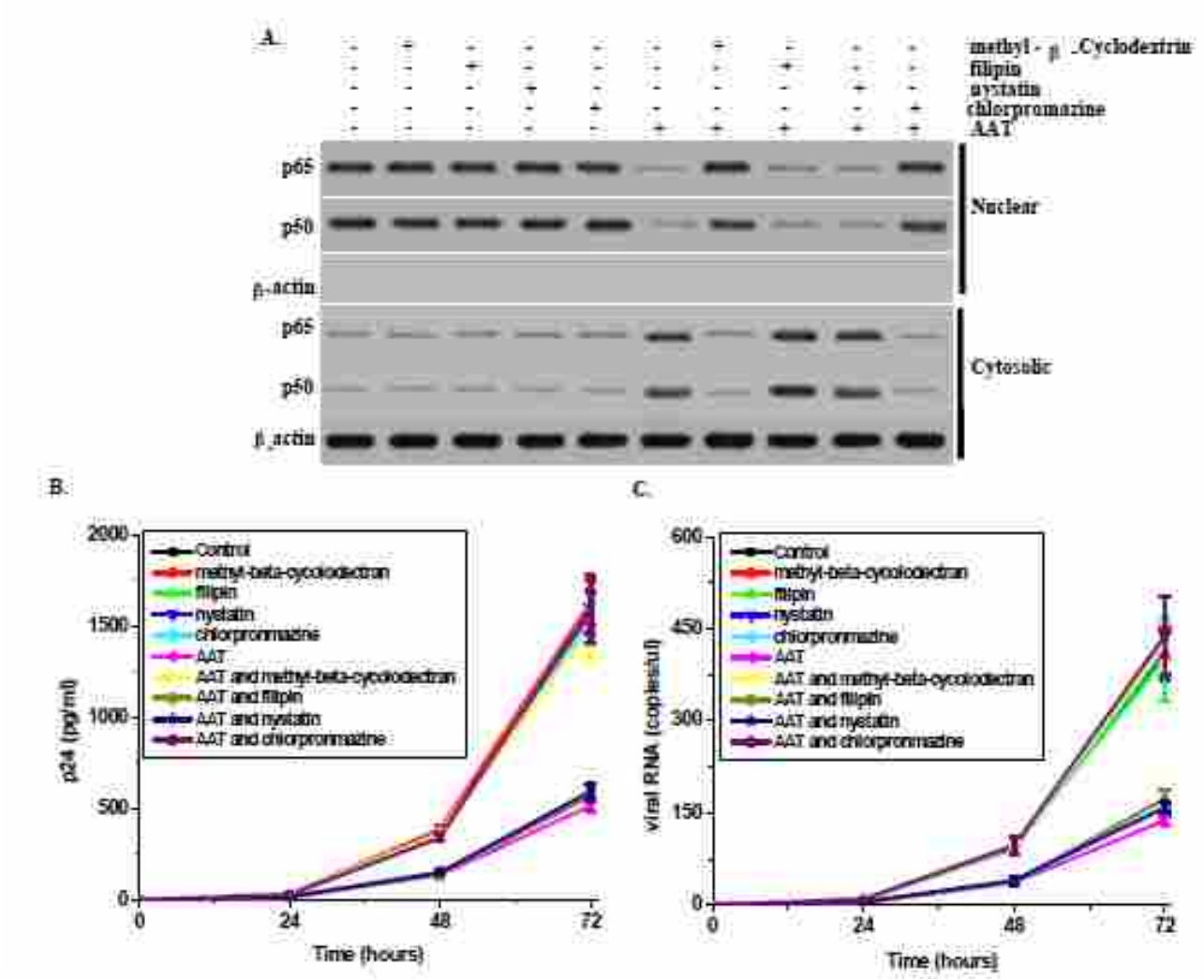

Figure 48. Endocytosis inhibitors blocked the effect of AAT on NF-κB activation and HIV replication. Activated primary CD4+ T cells were infected with HIV-1_{IIIB}. After HIV infection, these cells (10^7 cells/sample in a final volume of 10 mL culture medium) were pre-treated with 20 μg/mL methyl-β-cyclodextrin, 20 μg/mL filipin, 20 μg/mL nystatin, or 20 μg/mL chlorpromazine for 1 hour and then incubated in the presence or absence of 5 mg/mL AAT for 0, 24, 48, or 72 hours. Subsequently, the cells with 24-hour incubation were collected to extract the cytosolic and nuclear proteins. The distribution of p50 and p65 (A) was detected by Western blotting. β-actin served as a loading control. Meanwhile, the supernatant fluid from 0, 24, 48, or 72-hour incubations was collected to detected HIV replication by measuring p24 (B) and viral RNA (C).

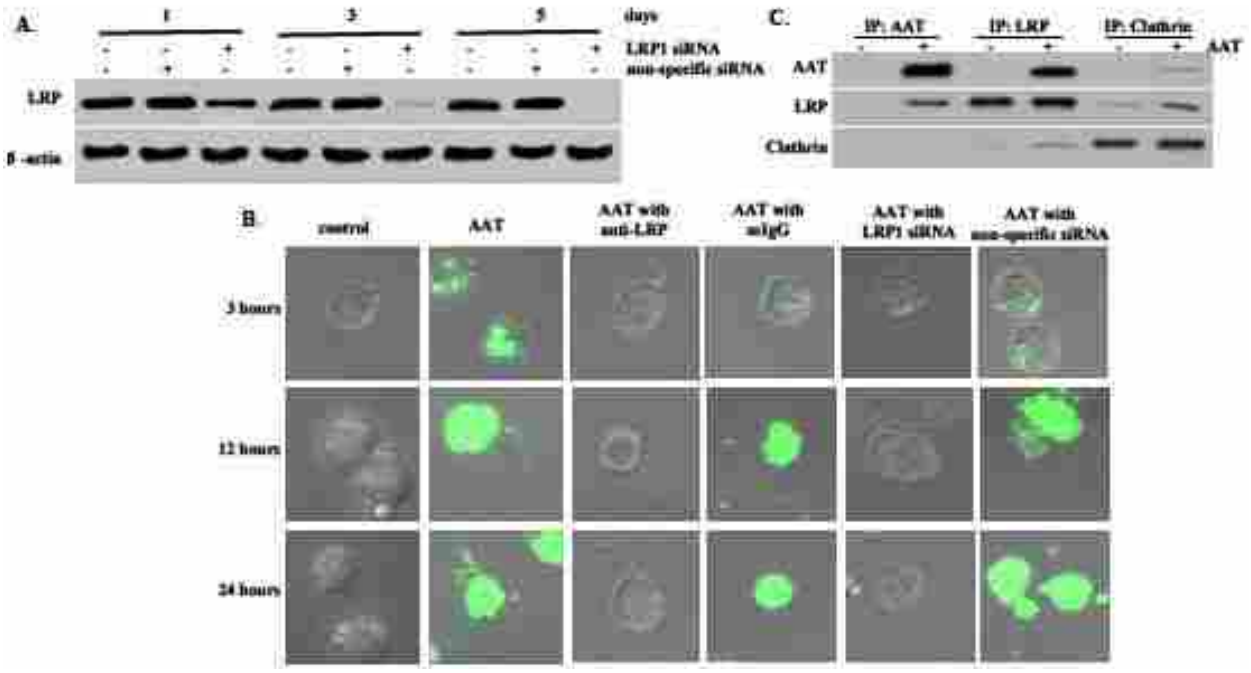

Figure 49. The clathrin-dependent AAT internalization was mediated by LRP1. Activated primary CD4+ T cells (5×10^6 cell/sample in a final volume of 5 mL culture medium) were treated with LRP1 or non-specific siRNA. After 1, 3, or 5 days incubation, the cells were collected and lysed to detect LRP expression by Western blotting (A). β-actin served as a l oading control. 3 days after siRNA treatment, these cells were infected with HIV-1_{IIIB} and unbound viruses were removed. Subsequently, these cells (5×10^5 cell/sample in a final volume of 500 μL culture medium) were incubated in the presence or absence of 5 mg/mL Alexa Fluor® 488-labeled AAT, 5 ug LRP antibody or 5 ug mouse IgG for 3, 12, or 24 hours and the internalization of AAT was detected with confocal microscopy (B) (600×). Additionally, activated primary CD4+ T cells (5×10^6 cell/sample in a final volume of 5 mL culture medium) were infected with HIV-1_{IIIB} and cultured with 5 mg/mL AAT for 3 hours. The cells were then lysed and antibody specific to AAT, LRP or clathrin was added to immunoprecipitate proteins. AAT, LRP and clathrin were detected by Western blotting (C).

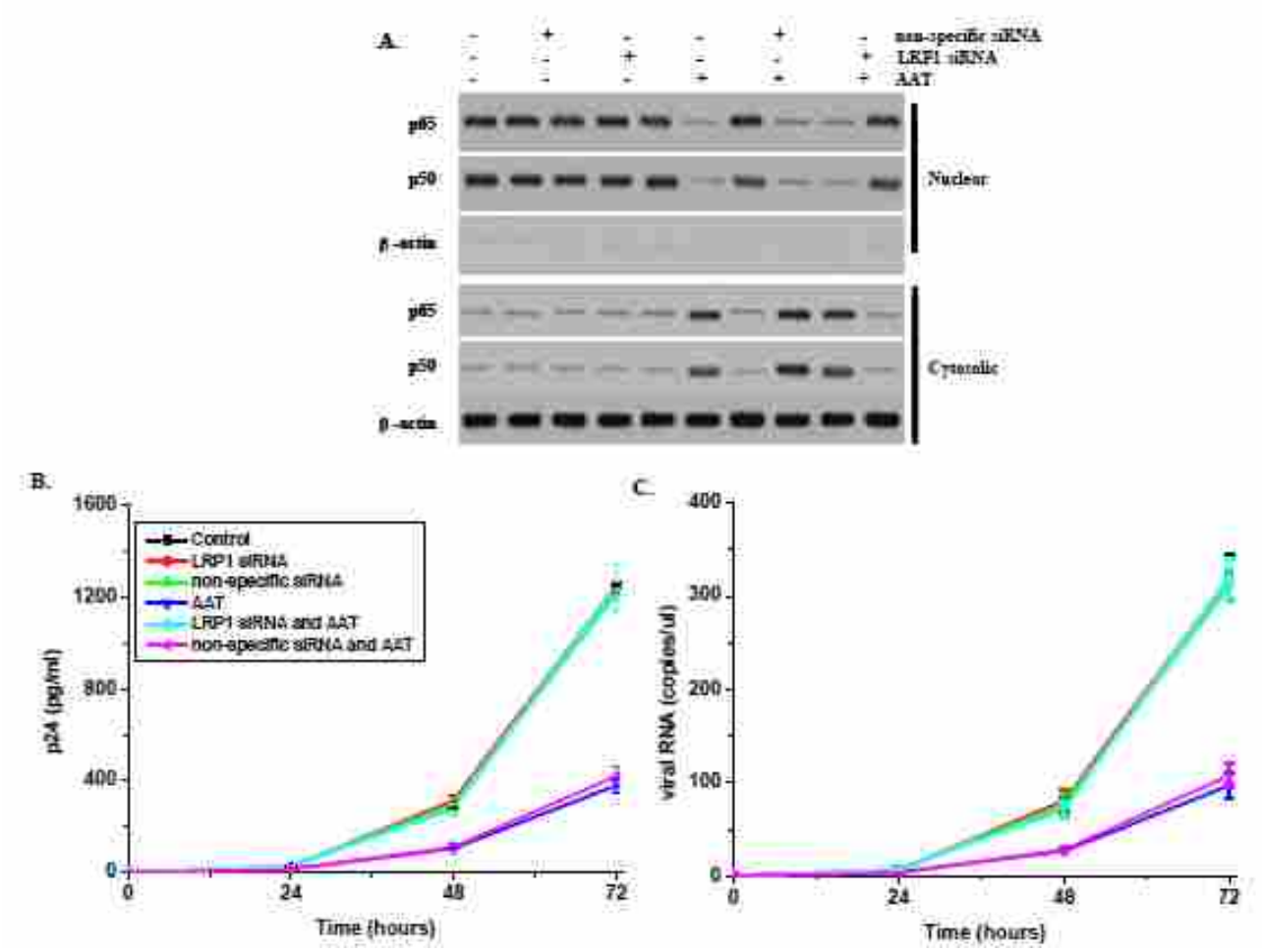

Figure 50. LRP1-specific siRNA blocked the inhibitory effect of AAT on NF-κB activation and HIV replication. Activated primary CD4+ T cells (10^7 cell/sample in a final volume of 10 mL culture medium) were treated with or without LRP1-specific or non-specific siRNA for 3 days. Subsequently, these cells were infected with HIV-1_{IIIB} and incubated in the presence or absence of 5 mg/mL AAT for 0, 24, 48, or 72 hours. At the end of 24 hours incubation, CD4+ T cells were collected to extract the cytosolic and nuclear proteins. The distribution of p50 and p65 (A) were detected by Western blotting. β-actin served as a loading control. Meanwhile, the supernatant fluid from 0, 24, 48, or 72 hours incubation was collected to detected HIV replication by measuring p24 (B) and viral RNA (C).

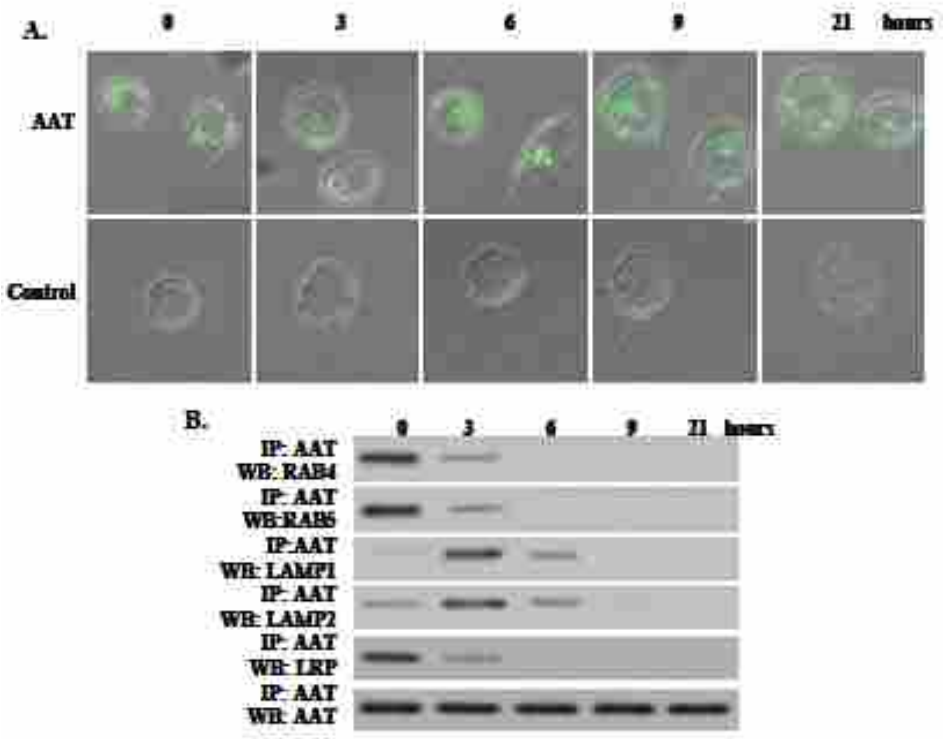

Figure 51. AAT distribution in HIV-infected CD4+ T cells. Activated primary CD4+ T cells were infected with HIV-1_{IIIB} and then incubated with 5 mg/mL AAT or 5 mg/mL Alexa Fluor® 488-labeled AAT for 3 hours. After incubation, non-internalized AAT was removed and the cells (2×10^5 cell/sample in a final volume of 200 µL culture medium) were incubated for 0, 3, 6, 9, or 21 hours. Subsequently, the internalization of AAT was detected with confocal microscopy (600×) (A). After 0, 3, 6, 9 or 21 hours incubation, the cells (5×10^6 cell/sample in a final volume of 5 mL culture medium) were collected and lysed to extract the whole cell proteins. AAT-specific antibody was added to the lysate to permit immunoprecipitation of the proteins that interacted with AAT. LRP, RAB4, RAB5, LAMP1, AAT and LAMP2 were detected by Western blotting (B).

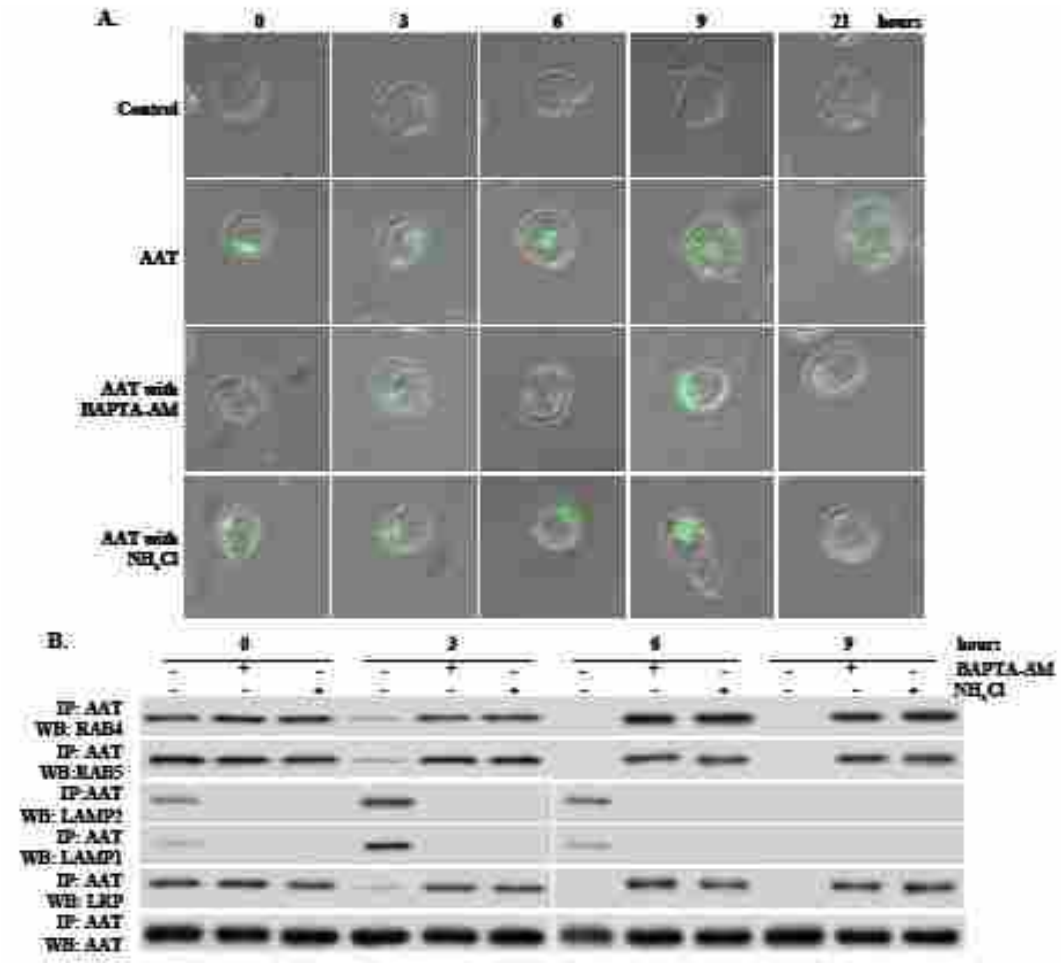

Figure 52. Lysosome inhibitor (NH_4Cl) and endosome-lysosome fusion inhibitor (BAPTA-AM) both suppressed the translocation of AAT from the endosome to the lysosome. Activated primary CD4+ T cells were infected with HIV-1_{IIIB} and incubated with 5 mg/mL Alexa Fluor® 488-labeled AAT for 3 hours. After incubation, unbound AAT was removed and these cells (2×10^5 cell/sample in a final volume of 200 μL culture medium) were incubated in the presence or absence of 10 mM NH_4Cl or 10 μM BAPTA-AM for 0, 3, 6, 9, or 21 hours. AAT internalization was detected with confocal microscopy (600×) (A). Cells (5×10^6 cell/sample in a final volume of 5 mL culture medium) with 0, 3, 6, and 9 hours incubation were collected and lysed to extract the whole cell proteins. AAT-specific antibody was added to the lysate to immunoprecipitate the proteins that interacted with AAT. LRP, RAB4, RAB5, LAMP1, AAT and LAMP2 were detected by Western blotting (B).

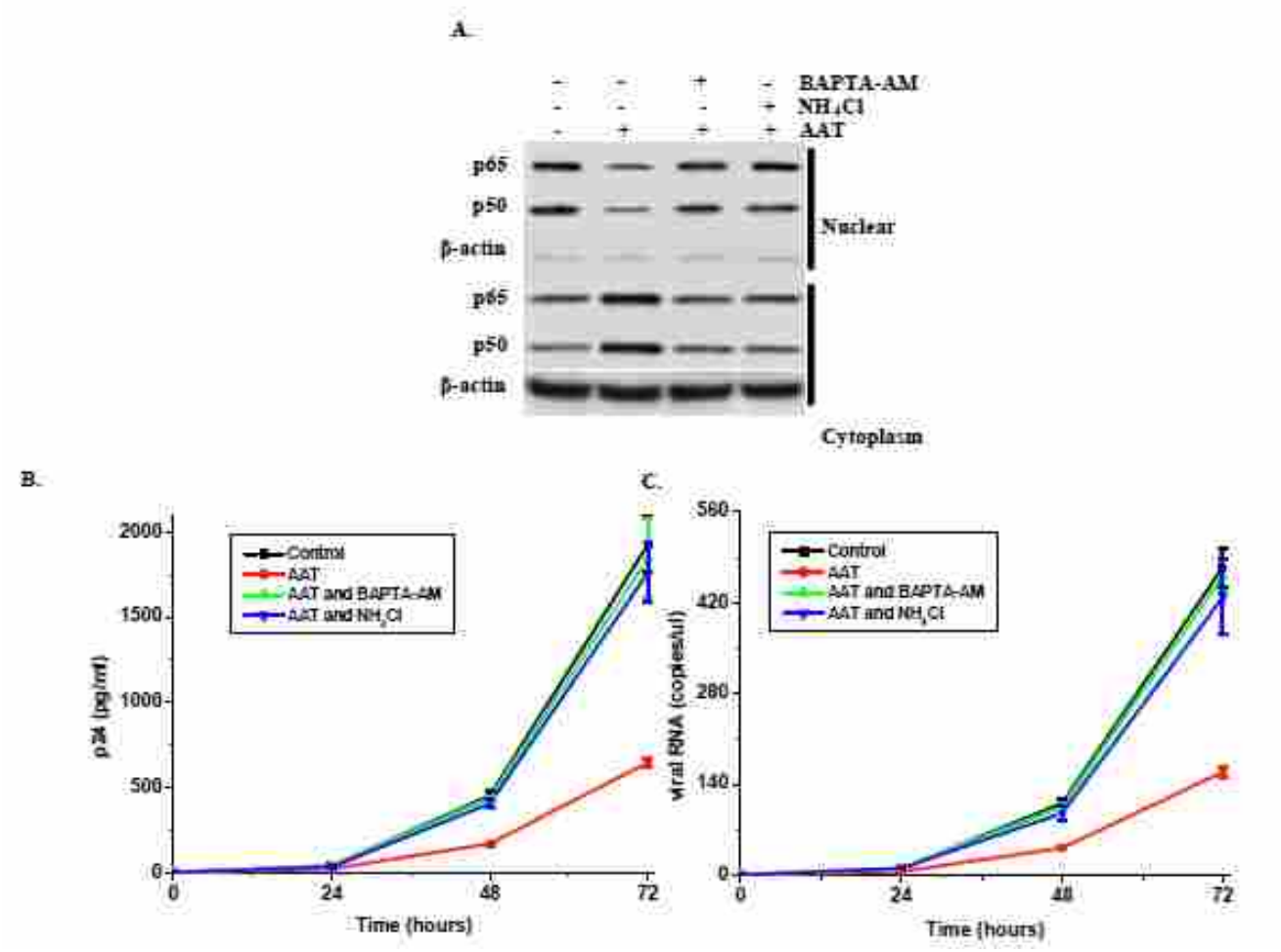

Figure 53. NH_4Cl and BAPTA-AM suppressed the inhibitory effect of AAT on NF-κB activation and HIV replication. Activated primary CD4+ T cells were infected with $HIV\text{-}1_{IIIB}$ and incubated with 10 mM NH_4Cl or 10 μM BAPTA-AM for 30 minutes. Next, 5 mg/mL AAT was added and the cells were incubated. After a 24-hour incubation, the cells (5×10^6 cell/sample in a final volume of 5 mL culture medium) were then collected to extract the cytosolic and nuclear proteins. The distribution of p50 and p65 (A) was detected by Western blotting. β-actin served as a loading control. In addtion, the supernatant fluid (5×10^5 cell/sample in a final volume of 500 μL culture medium) from 0, 24, 48, or 72 hours of incubation was collected to detected HIV replication by measuring p24 (B) and viral RNA (C).

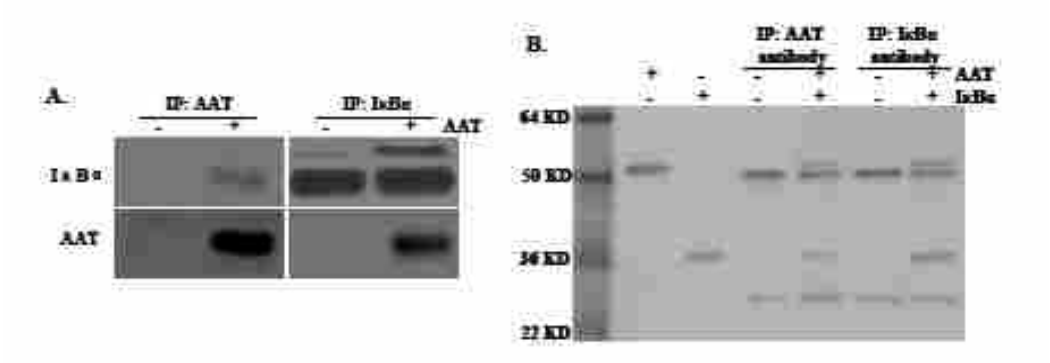

Figure 54. AAT interacted with IκBα. Activated primary CD4+ T cells were infected with HIV-1_{IIIB} and cultured in the presence or absence of 5 mg/mL AAT for 24 hours. At the end of incubation, the cells (5×10^6 cell/sample in a final volume of 5 mL culture medium) were collected and lysed to extract cytosolic proteins. Isolated proteins were incubated with AAT or IκBα-specific antibodies to immunoprecipitate the respective proteins. AAT and IκBα were detected by Western blotting (A). Furthermore, AAT (1 μg) was also incubated with recombinant IκBα (1 μg) for 30 minutes. AAT or IκBα-specific antibody was added to precipitate the proteins. Precipitated proteins were separated by SDS-PAGE and visualized by Coomassie blue staining (digital image saved as black and gray picture) (B).

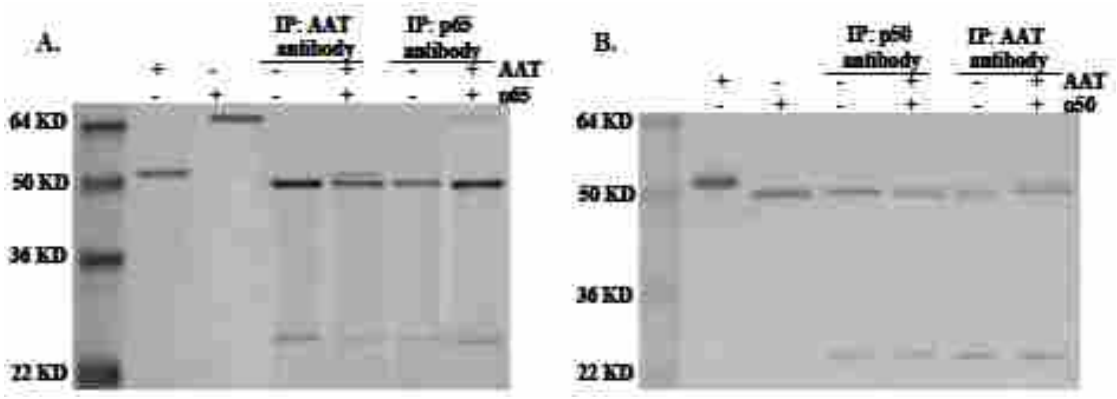

Figure 55. AAT did not interact with p65 and p50. AAT (1 μg) was incubated with recombinant p65 (1 μg) (A) or p50 (1 μg) (B) for 30 minutes. Next, AAT-, p65-, or p50-specific antibodies were added to immunoprecipitate the proteins. The precipitated proteins were separated by SDS-PAGE and visualized by Coomassie blue staining (digital image saved as balck and gray picture).

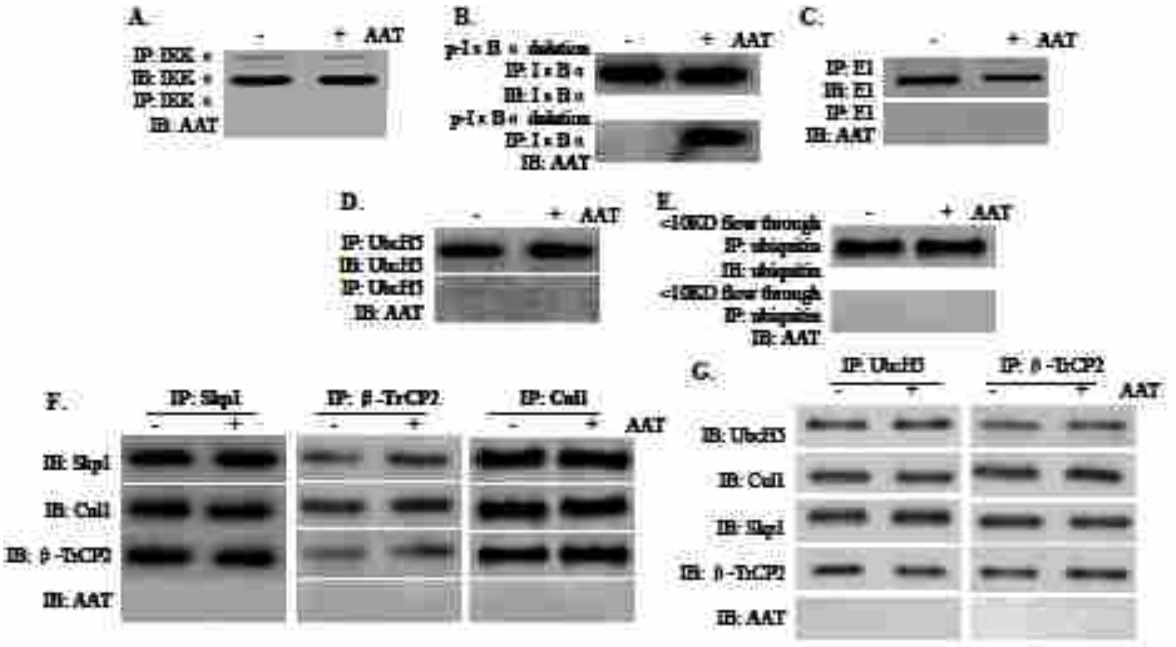

Figure 56. AAT interacted with the IκBα complex. Activated primary CD4+ T cells were infected and then cultured for 24 hours. Next, these cells (10^7 cells/sample in a final volume of 10 mL culture medium) were collected and lysed to extract cellular proteins. The isolated proteins were incubated with antibodies against IKKα, the E1 ubiquitin-activating enzyme, UbcH5, or the SCF E3 ubiquitin ligase complex (Cul1, Skp1 and β-TRCP2) to immunoprecipitate IKK, and the E1, E2 and SCF E3 ligase complex. Whole cell proteins were also treated with phosphorylated IκBα-specific antibody for precipitation and to remove phosphorylated IκBα. Whole cell proteins without phosphorylated IκBα were incubated with IκBα-specific antibody to immunprecipitate the IκBα complex. Furthermore, whole cell proteins were passed through a 10KD-cutoff filter and the flow-through were treated with ubiquitin-specific antibody to immunoprecipitate ubiquitin. Precipitated IKK (A), IκBα (B), E1 (C), E2 (D), ubiquitin (E), or the E3 (F) complex were each incubated with AAT (1 μg) for 1 hour and the interaction between these complexes and AAT was detected by Western blotting. Meanwhile, the E2 and E3 complex (G) was mixed to incubate with AAT (1 μg) and the interaction between the E2/E3 complex and AAT was also detected by Western blotting.

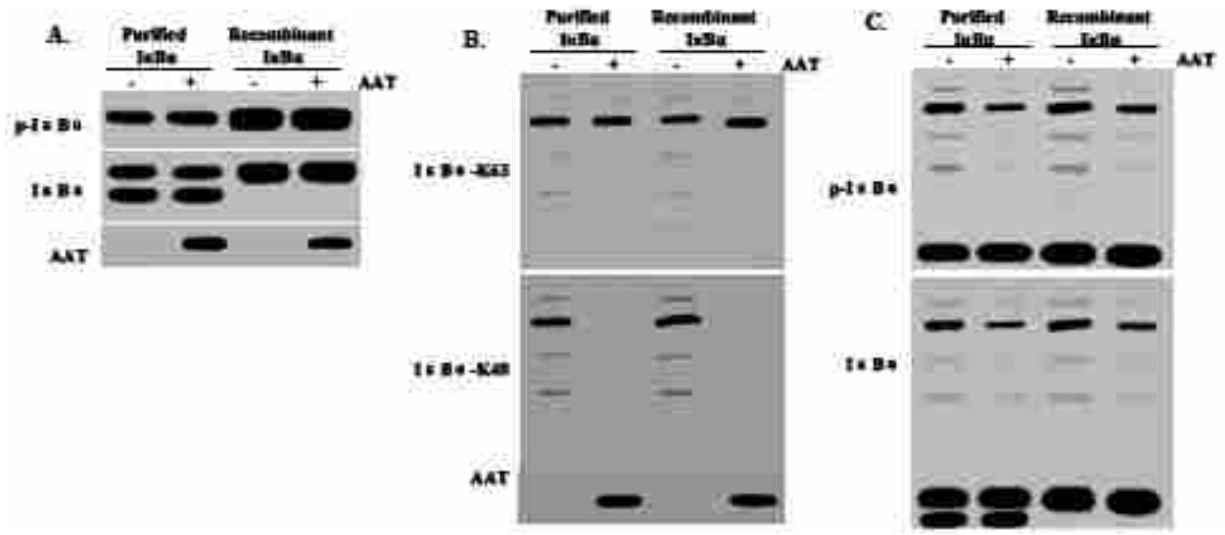

Figure 57. AAT altered the ubiquitinylation pattern of IκBα *in vitro*. IKKα complex, IκBα, E1 ubiquitin-activating enzyme, E2 ubiquitin-conjugating enzymes (UbcH5), E3 ligase complex (Cul1, Skp1 and β-TRCP2), and ubiquitin were isolated from HIV-infected CD4+ T cells (10^7 cells/sample in a final volume of 10 mL culture medium). Next, IKKα complex was incubated with recombinant IκBα (1 μg) or separated IκBα in the presence of ATP for 30 minutes. The phosphorylation of IκBα was detected by Western blot in the presence or absence of AAT (A). Subsequently, E1 ubiquitin-activating enzyme, E2 ubiquitin-conjugating enzyme, E3 ligase complex, and ubiquitin were added and incubated for 2 hours in the presence or absence of AAT (1 μg). After 2 hours incubation, the ubiquitinylation pattern of IκBα was detected by Western blot (B). IκBα and phosphorylated IκBα were also detected by Western blot (C).

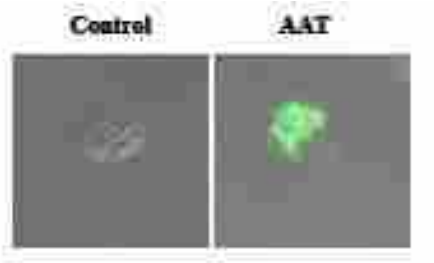

Figure 58. FDCs internalized AAT. Isolated tonsillar FDCs (2×10^5 cells/sample in a final volume of 200 μL culture medium) were incubated with or without 5 mg/mL Alexa Fluor® 488-labelled AAT for 24 hours. At the end of incubation, the FDCs were washed three times to remove non-internalized AAT and then fixed to detect the green fluorescence with confocal microscopy (600 ×).

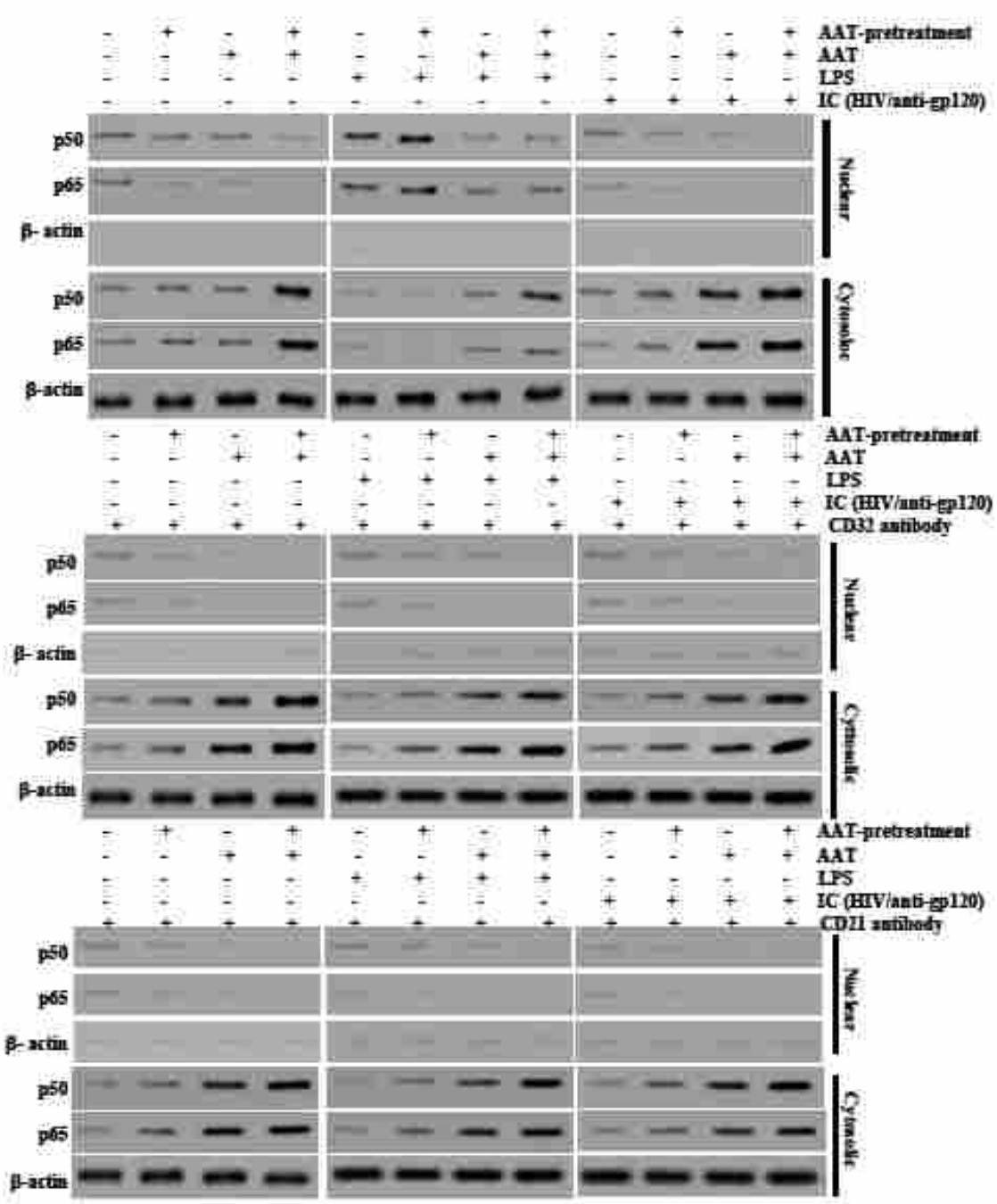

Figure 59. AAT inhibited NF-κB nuclear translocation in FDCs. Isolated tonsillar FDCs (2×10^6 cells/sample in a final volume of 2 mL culture medium) were pre-treated with or without 5 mg/mL AAT for 1 day. AAT was then removed and the cells were incubated with 5 mg/mL AAT, 10 μg/mL LPS, HIV immune complexes (preformed by incubating 50 μL HIV-1_{IIIB} with 10 μg gp120 antibody for 30 minutes), CD32 antibody (10 μg), or CD21 antibody (10 μg) for 1 day. At the end of incubation, the nuclear and cytosolic proteins were extracted. The accumulation of p50 and p65 in the cytosol or nucleus was detected by Western blotting. β-actin served as a loading control.

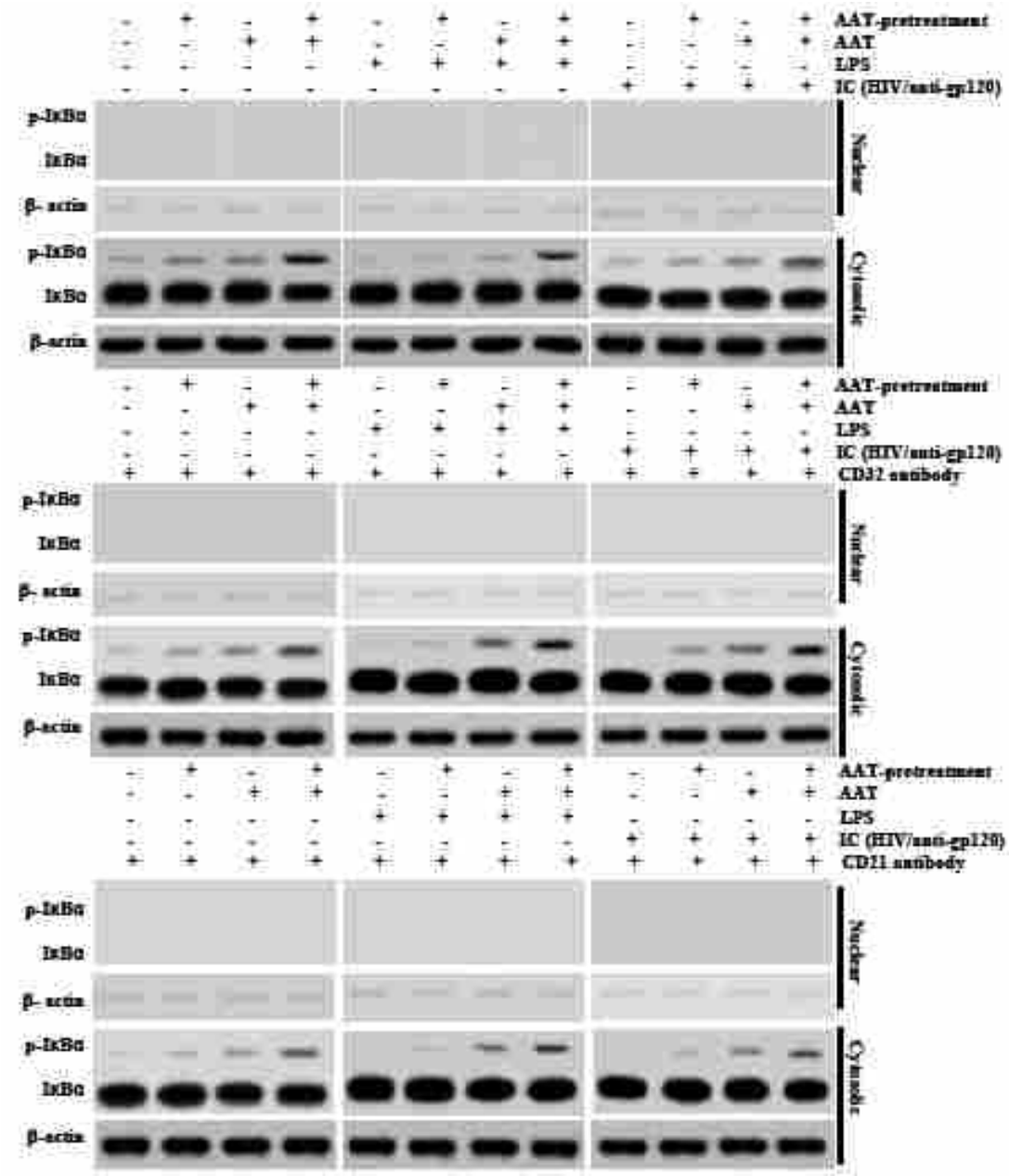

Figure 60. AAT inhibited IκBα degradation in FDCs. Isolated tonsillar FDCs (2×10^6 cells/sample in a final volume of 2 mL culture medium) were pre-treated with or without 5 mg/mL AAT for 1 day. AAT was then removed and the cells were incubated with 5 mg/mL AAT, 10 μg/mL LPS, HIV immune complexes (preformed by incubating 50 μL HIV-1_{IIIB} with 10 μg gp120 antibody for 30 minutes), CD32 antibody (10 μg), or CD21 antibody (10 μg) for 1 day. At the end of incubation, FDC nuclear and cytosolic proteins were extracted. The accumulation of phosphorylated IκBα and IκBα in the cytosol or nucleus was detected by Western blotting. β-actin served as a loading control.

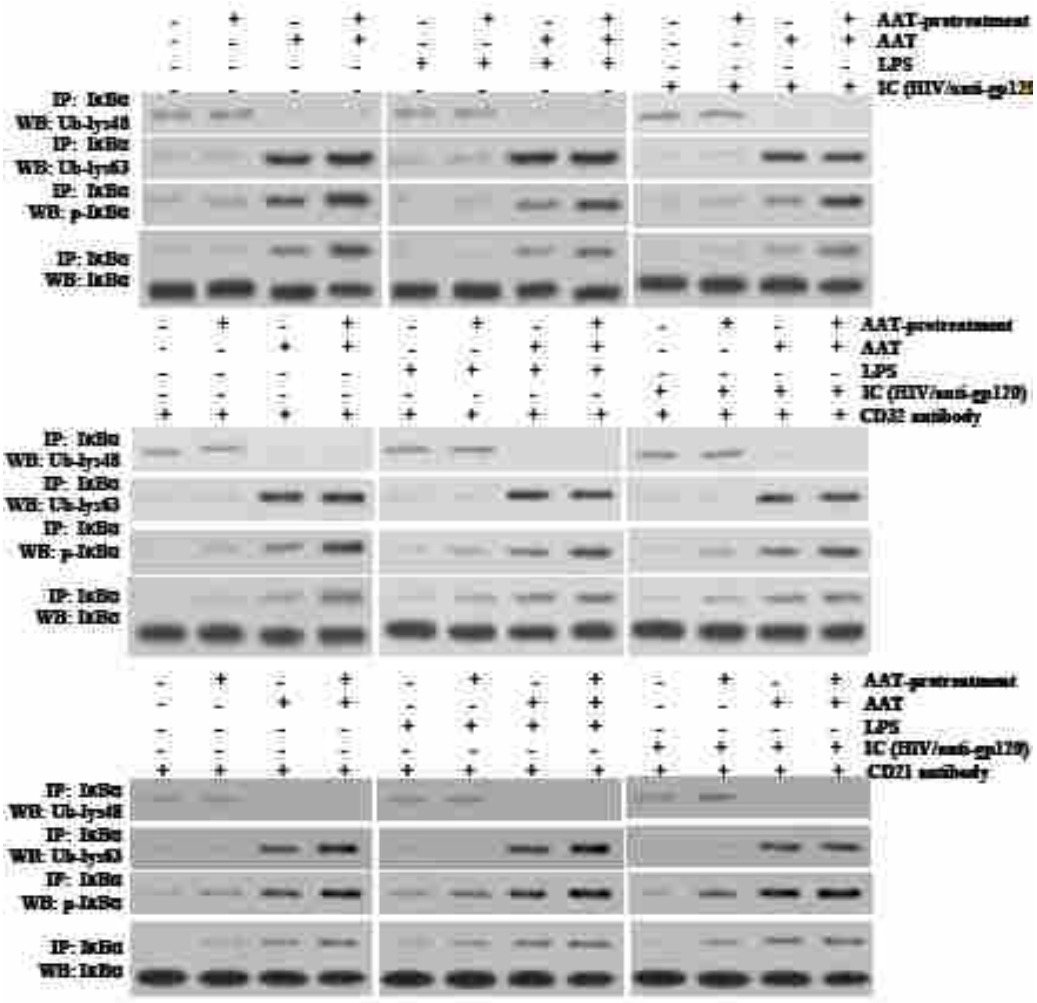

Figure 61. AAT increased the amount of FDC-IκBα polyubiquitinylated at K63 and decreased the amount of IκBα polyubiquitinylated at residue K48. Isolated tonsillar FDCs (2×10^6 cells/sample in a final volume of 2 mL culture medium) were pre-treated with or without 5 mg/mL AAT for 1 day. AAT was then removed and the cells were incubated with 5 mg/mL AAT, 10 μg/mL LPS, HIV immune complexes (preformed by incubating 50 μL HIV-1_{IIIB} with 10 μg gp120 antibody for 30 minutes), CD32 antibody (10 μg), or CD21 antibody (10 μg) for 1 day. At the end of incubation, cellular proteins were extracted. The accumulation of IκBα polyubiquitinylated at K48 or K63 was detected by Immunoprecipitation and Western blotting.

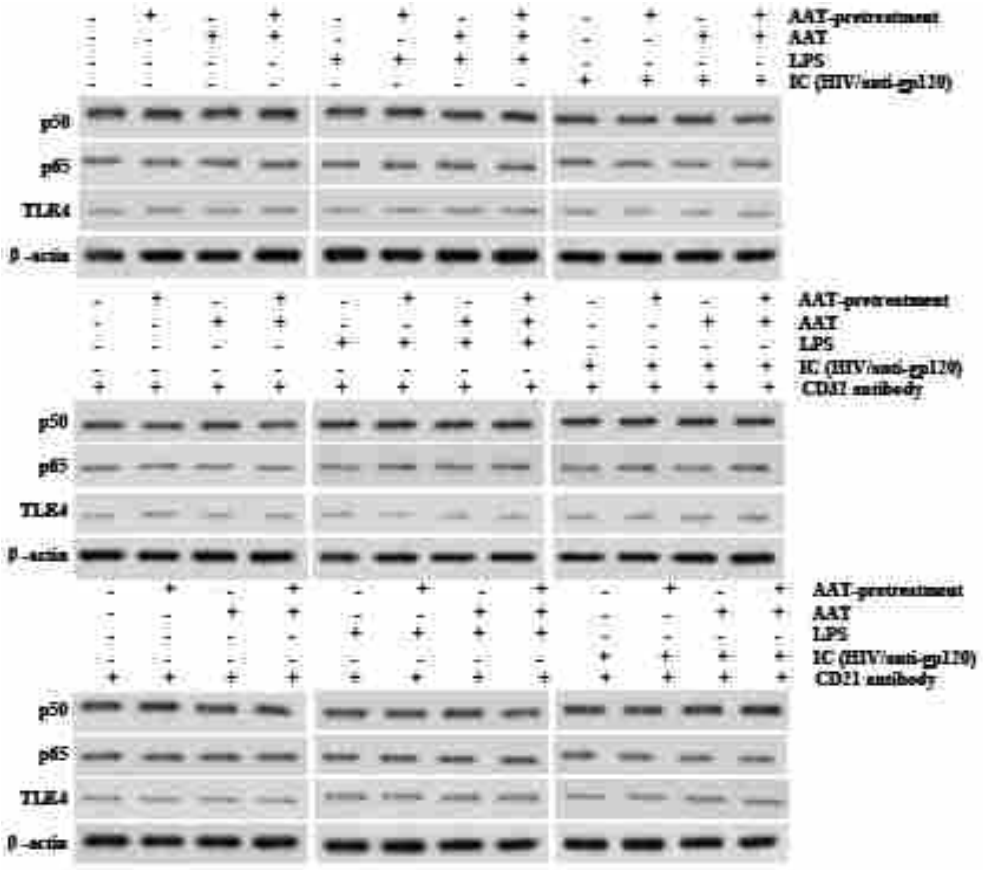

Figure 62. AAT did not alter the expression of p65, p50, and TLR4 on FDCs. Isolated tonsillar FDCs (10^6 cells/sample in a final volume of 1 mL culture medium) were pre-treated with or without 5 mg/mL AAT for 1 day. AAT was then removed and the cells were incubated with 5 mg/mL AAT, 10 μg/mL LPS, HIV immune complexes (preformed by incubating 50 μL HIV-1_{IIIB} with 10 μg gp120 antibody for 30 minutes), CD32 antibody (10 μg), or CD21 antibody (10 μg) for 1 day. At the end of incubation, FDC proteins were extracted and the expression of p50, p65, and TLR4 was detected by Western blotting. β-actin was used as a loading control.

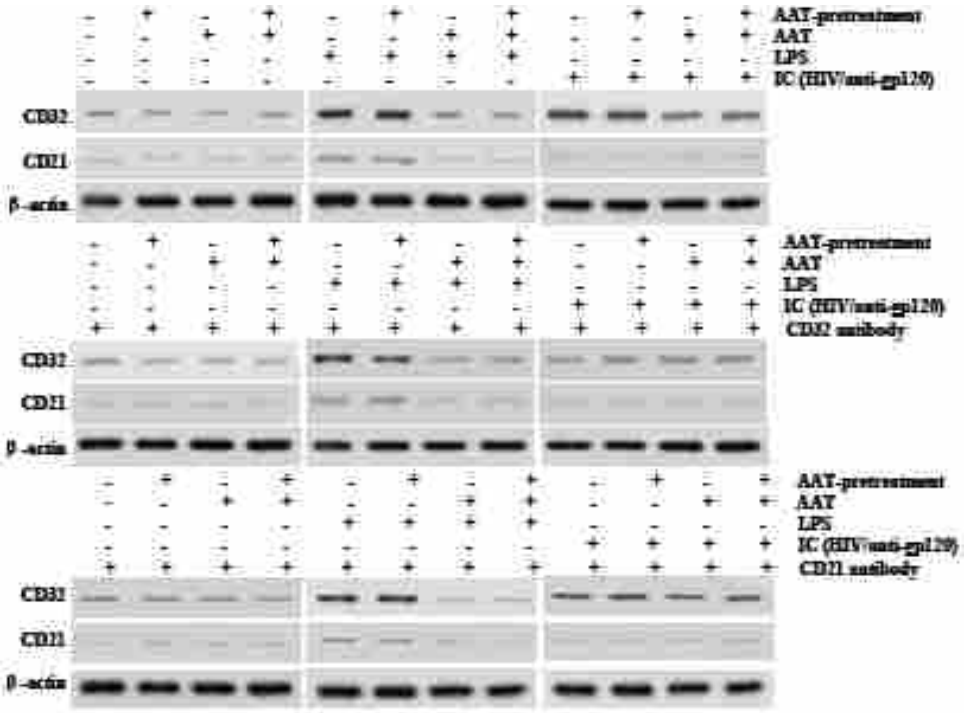

Figure 63. AAT inhibited the expression of CD32 and CD21 on FDCs. Isolated tonsillar FDCs (10^6 cells/sample in a final volume of 1 mL culture medium) were pre-treated with or without 5 mg/mL AAT for 1 day. AAT was then removed and the cells were incubated with 5 mg/mL AAT, 10 μg/mL LPS, HIV immune complexes (preformed by incubating 50 μL HIV-1_{IIIB} with 10 μg gp120 antibody for 30 minutes), CD32 antibody (10 μg), or CD21 antibody (10 μg) for 1 day. At the end of incubation, FDC proteins were extracted. The expression of CD32 and CD21 was detected by Western blotting. β-actin was used as a loading control.

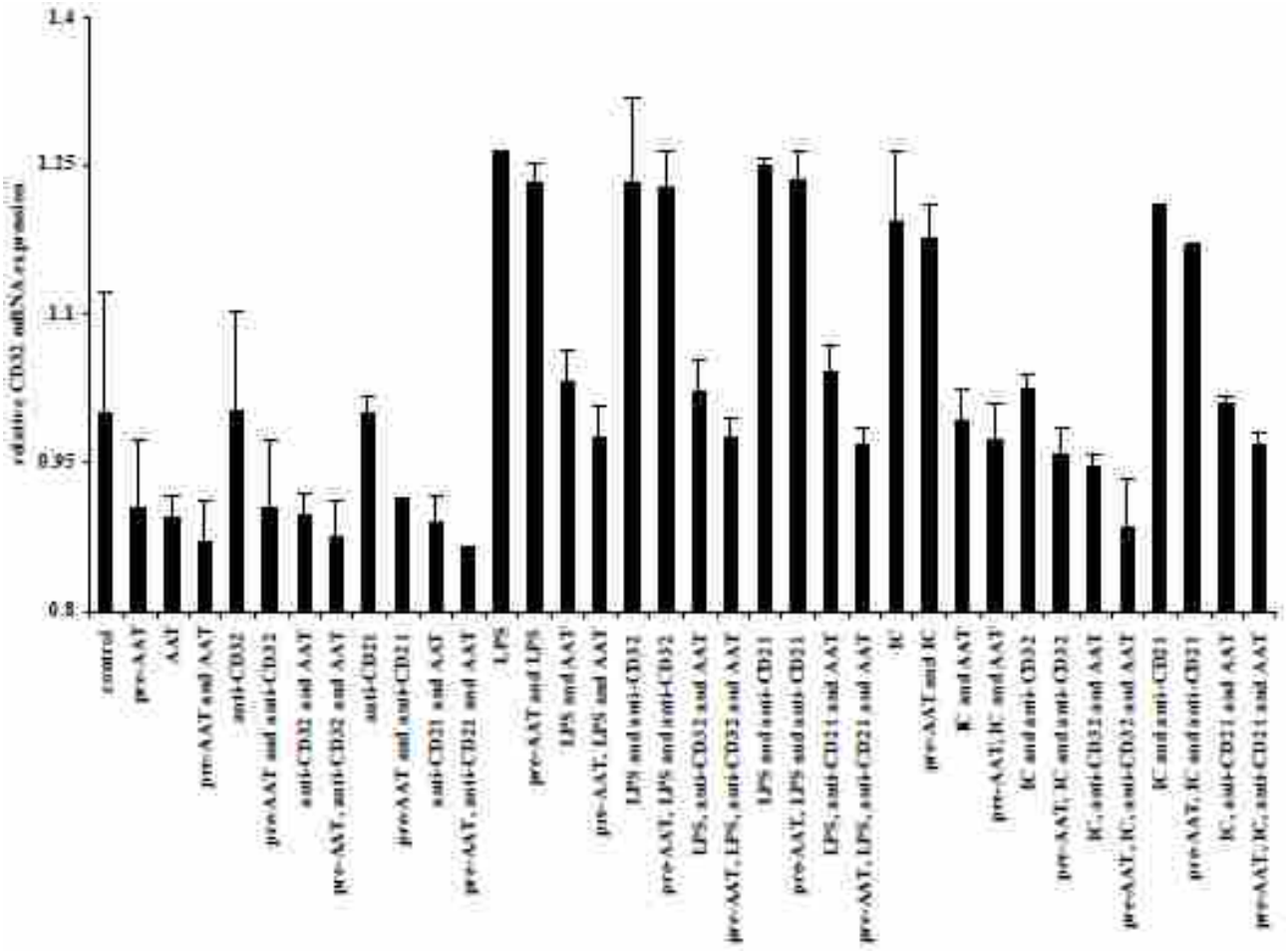

Figure 64. AAT inhibited FDC-CD32 mRNA expression. Isolated tonsillar FDCs (2×10^5 cells/sample in a final volume of 200 µL culture medium) were pre-treated with or without 5 mg/mL AAT for 1 day. AAT was then removed and the cells were incubated with 5 mg/mL AAT, 10 µg/mL LPS, HIV immune complexes (preformed by incubating 50 µL HIV-1_{IIIB} with 10 µg gp120 antibody for 30 minutes), CD32 antibody (10 µg), or CD21 antibody (10 µg) for 1 day. After incubation, FDC total RNA was collected and reverse transcribed. CD32 mRNA was detected by qPCR and normalized to endogenous GAPDH expression.

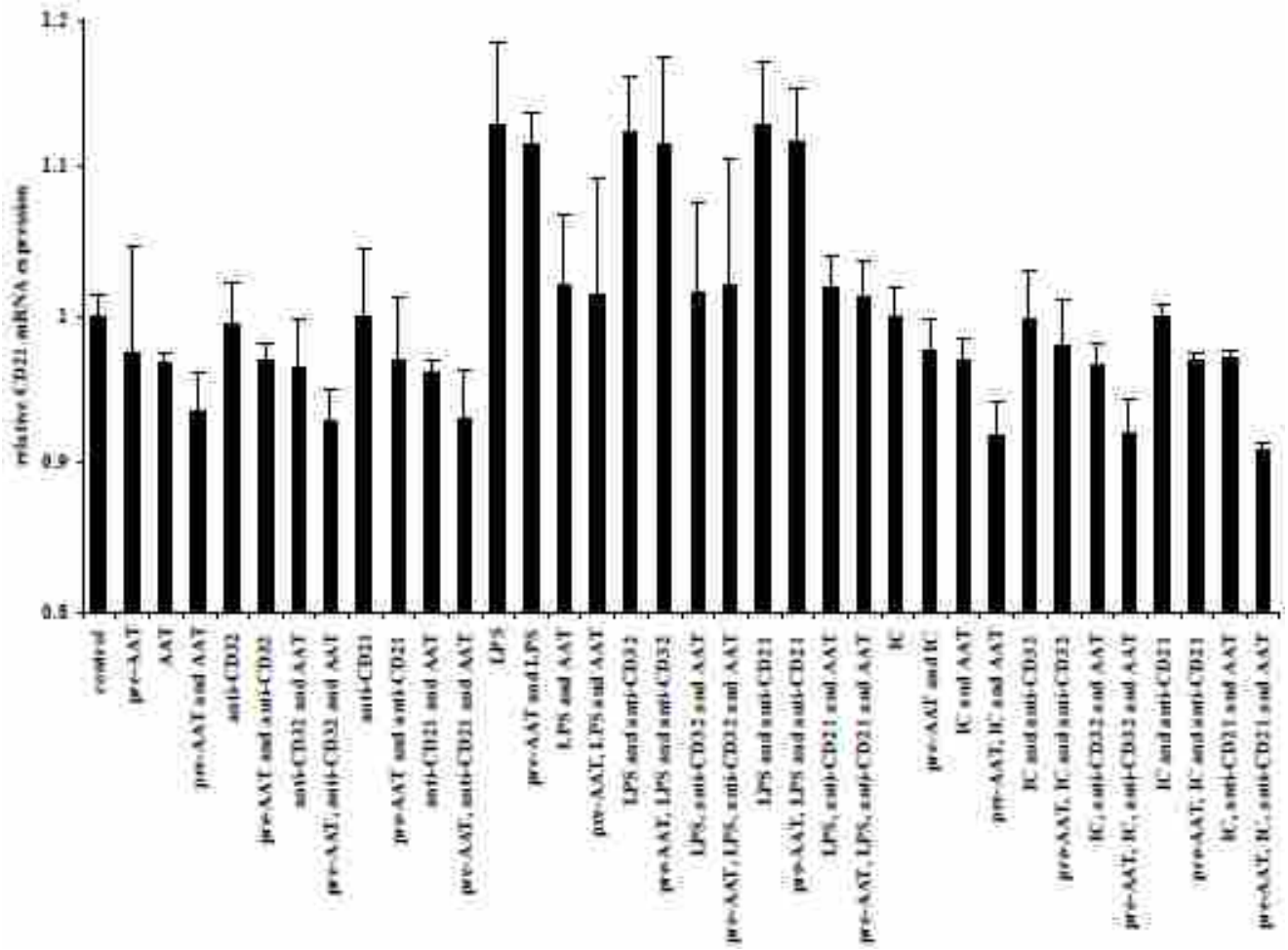

Figure 65. AAT inhibited FDC-CD21 mRNA expression. Isolated tonsillar FDCs (2×10^5 cells/sample in a final volume of 200 µL culture medium) were pre-treated with or without 5 mg/mL AAT for 1 day. AAT was then removed and the cells were incubated with 5 mg/mL AAT, 10 µg/mL LPS, HIV immune complexes (preformed by incubating 50 µL HIV-1_{IIIB} with 10 µg gp120 antibody for 30 minutes), CD32 antibody (10 µg), or CD21 antibody (10 µg) for 1 day. After incubation, FDC total RNA was collected and reverse transcribed. CD21 mRNA was detected by qPCR and normalized to endogenous GAPDH expression.

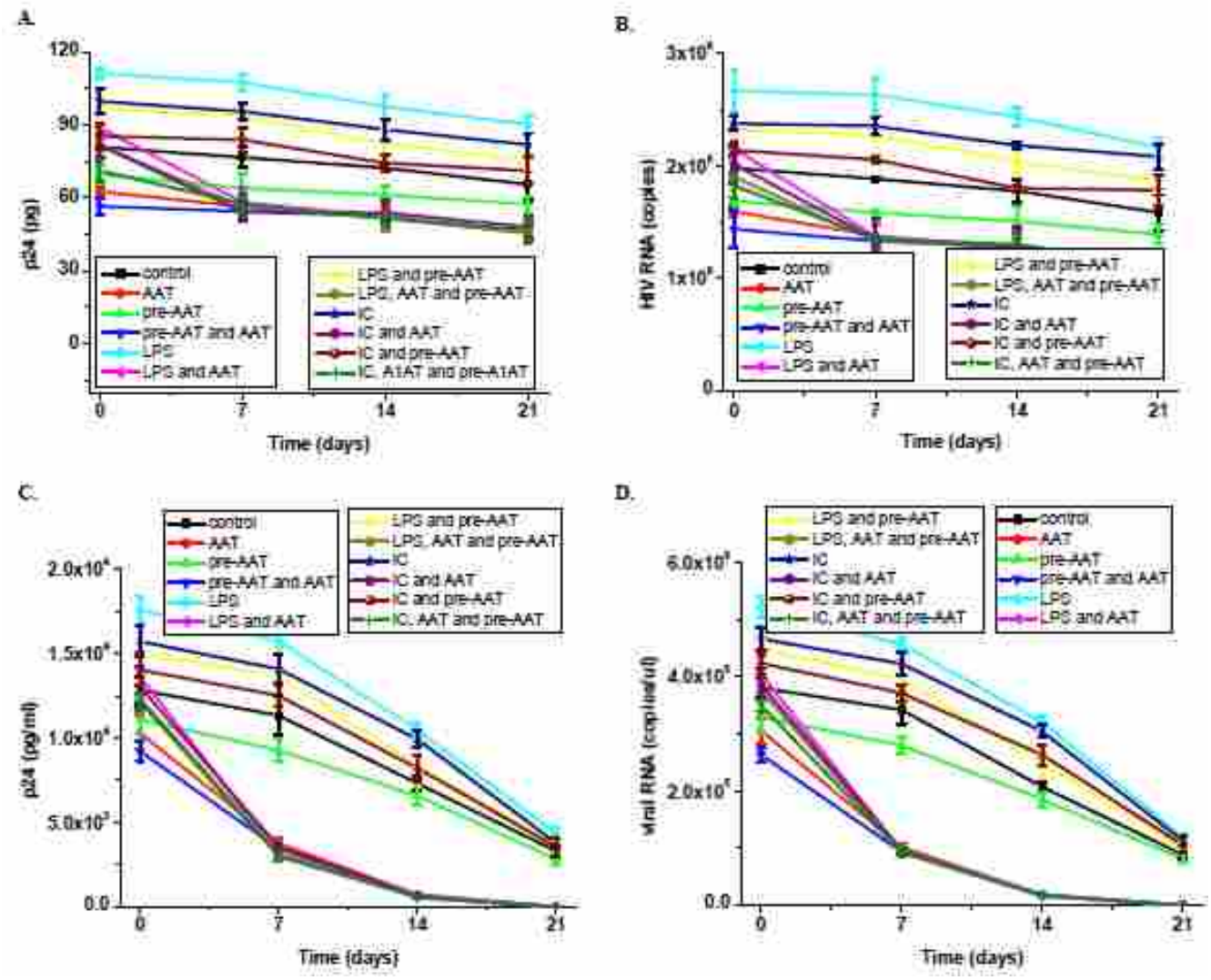

Figure 66. AAT inhibited the trapping and infectivity of HIV-1_{IIIB} on FDCs. Isolated tonsillar FDCs (10^5 cells/sample in a final volume of 100 µL culture medium) were pre-treated with or without 5 mg/mL AAT for 1 day. AAT was then removed and the cells were incubated with 5 mg/mL AAT, 10 µg/mL LPS, or HIV immune complexes (preformed by incubating 50 µL HIV-1_{IIIB} with 10 µg gp120 antibody for 30 minutes) for 1 day. Subsequently, the FDCs were incubated with HIV-1_{IIIB} (50 µL), human serum (5 µL), and gp120 antibody (10 µg) for 2 hours. Unbound viruses were removed by washing and virus-bearing FDCs were incubated for 0, 7, 14, or 21 days in the presence or absence of 5 mg/mL AAT, 10 µg/mL LPS or HIV immune complexes (preformed by incubating 50 µL HIV-1_{IIIB} with 10 µg gp120 antibody for 30 minutes) as determined by the initial incubation conditions. FDCs were then divided into two aliquots. One aliquot was lysed to detect cytosolic p24 (A) and viral RNA (B). The other aliquot was washed to remove AAT, LPS, and HIV immune complex and then incubated with CD4+ T cells (10 CD4+ T cells : 1 FDC) for 7 days to allow infection after which the virus bearing supernatant was collected and used to determine p24 production (C) and viral RNA production (D).

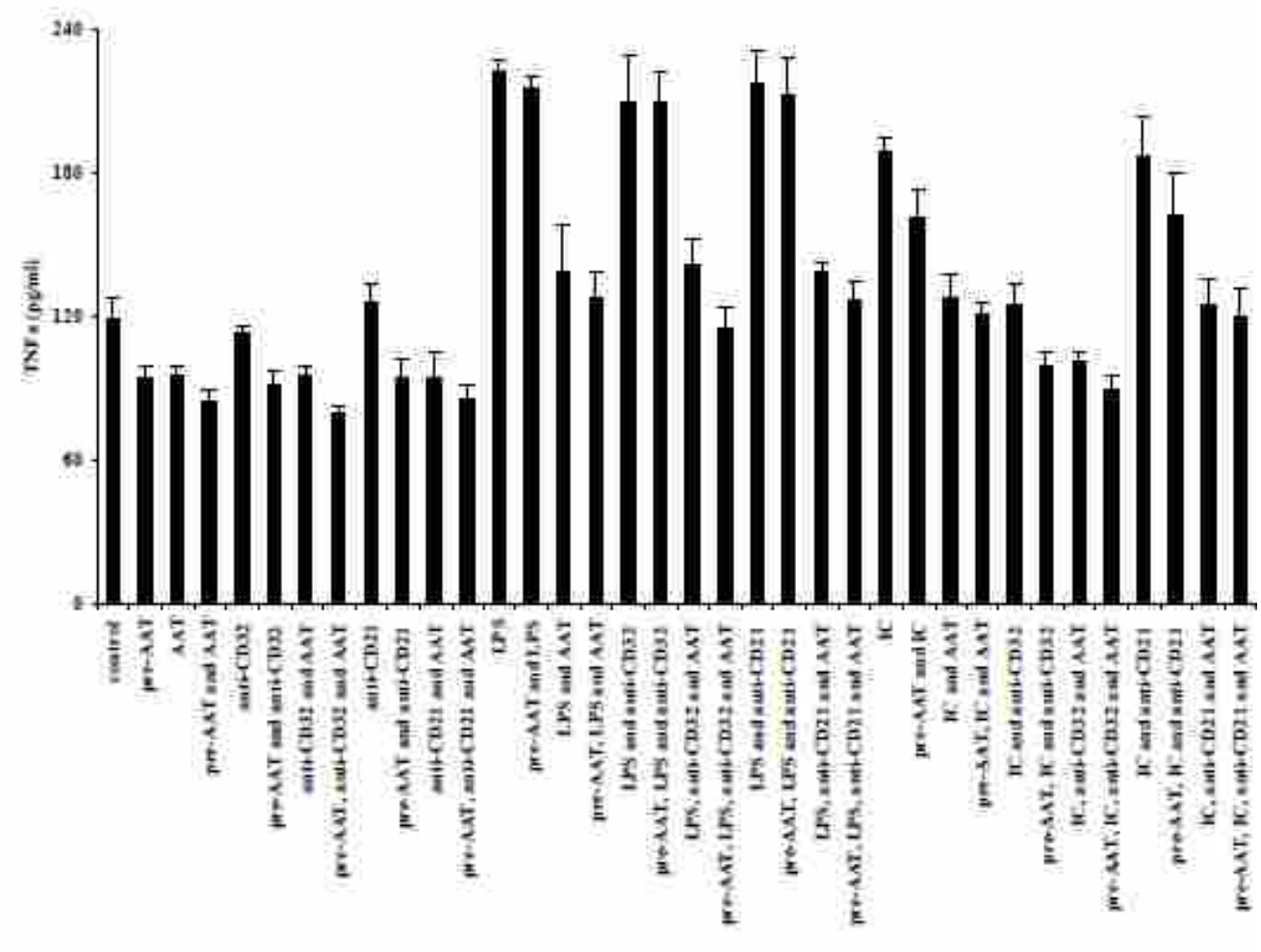

Figure 67. AAT inhibited the production of TNFα by FDCs. Isolated tonsillar FDCs (2×10^5 cells/sample in a final volume of 200 μL culture medium) were pre-treated with or without 5 mg/mL AAT for 1 day. AAT was then removed and the cells were incubated with 5 mg/mL AAT, 10 μg/mL LPS, HIV immune complexes (preformed by incubating 50 μL HIV-1_{IIIB} with 10 μg gp120 antibody for 30 minutes), CD32 antibody (10 μg), or CD21 antibody (10 μg) for 1 day. After incubation, the supernatant fluid was collected to detect the production of TNFα by ELISA.

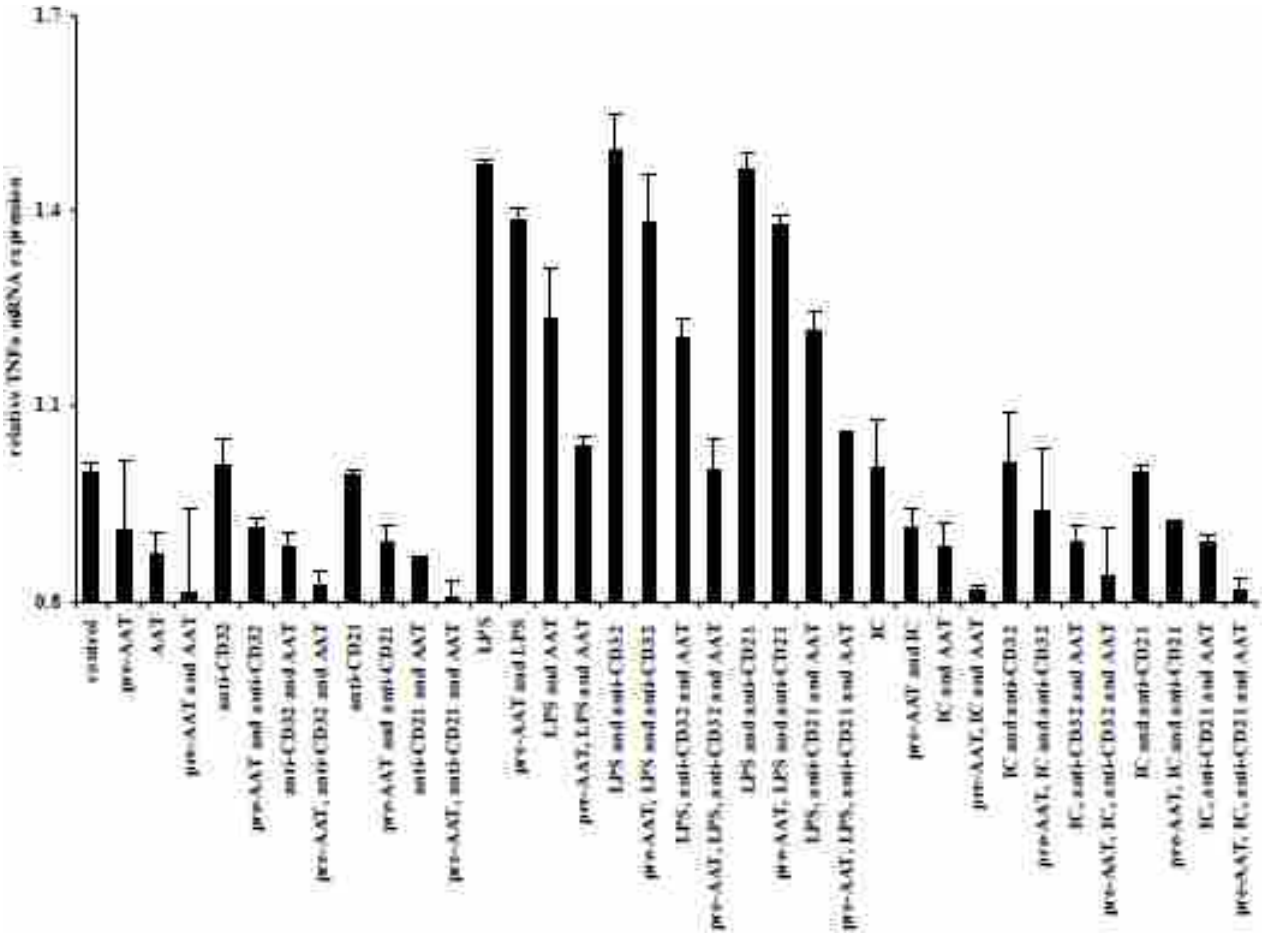

Figure 68. AAT inhibited FDC-TNFα mRNA expression. Isolated tonsillar FDCs (2×10^5 cells/sample in a final volume of 200 µL culture medium) were pre-treated with or without 5 mg/mL AAT for 1 day. AAT was then removed and the cells were incubated with 5 mg/mL AAT, 10 µg/mL LPS, HIV immune complexes (preformed by incubating 50 µL HIV-1_{IIIB} with 10 µg gp120 antibody for 30 minutes), CD32 antibody (10 µg), or CD21 antibody (10 µg) for 1 day. At the end of incubation, FDC total RNA was obtained and reverse transcribed to detect the mRNA expression of CXCL13 with values normalized to the expression of endogenous GAPDH.

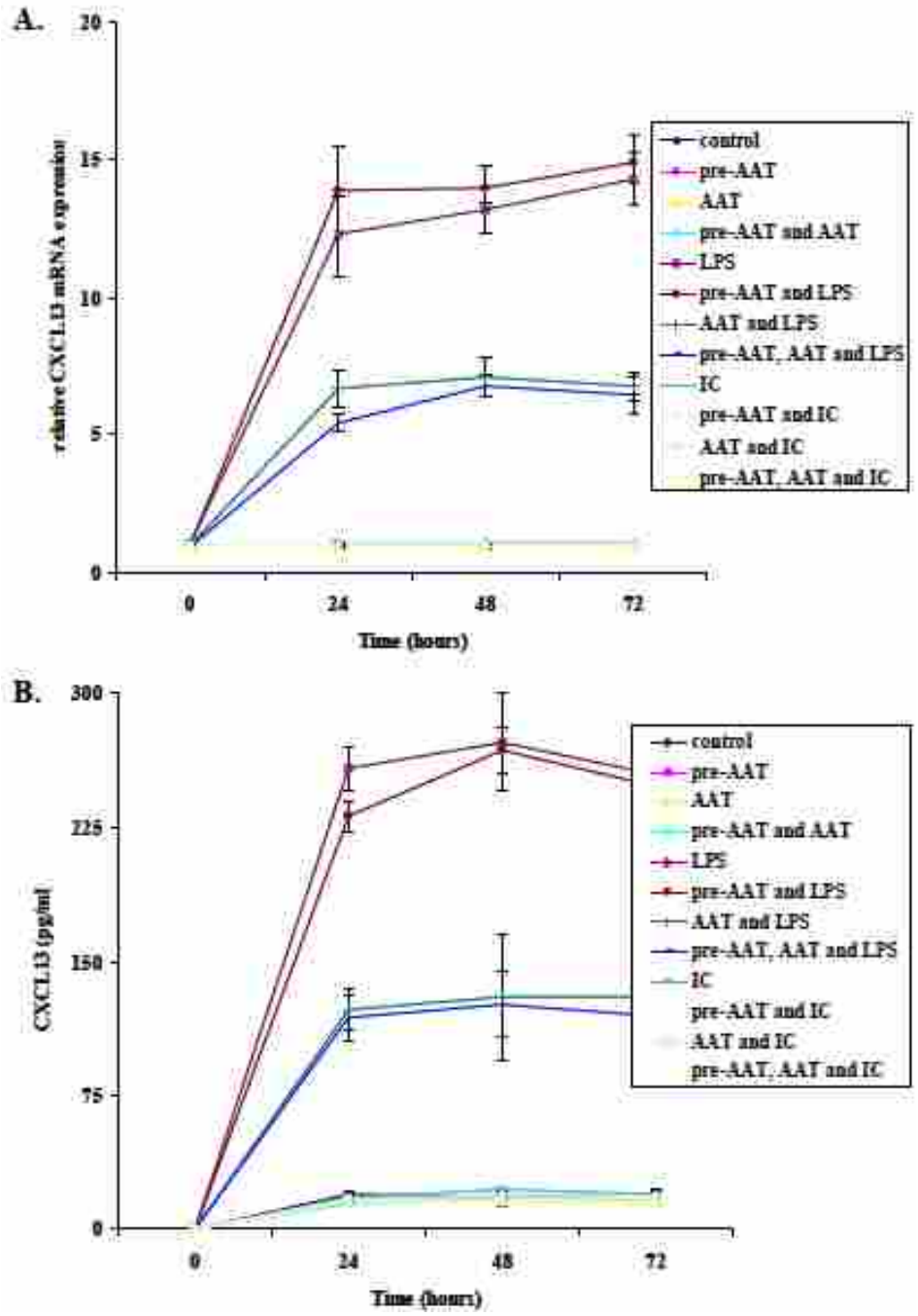

Figure 69. AAT inhibited the expression and production of CXCL13 by FDCs. Isolated tonsillar FDCs (2×10^5 cells/sample in a final volume of 200 µL culture medium) were pre-treated with or without 5 mg/mL AAT for 1 day. AAT was then removed and the cells were incubated with 5 mg/mL AAT, 10 µg/mL LPS, or HIV immune complexes (preformed by incubating 50 µL HIV-1_{IIIB} with 10 µg gp120 antibody for 30 minutes) for 1 day. At the end of incubation, the supernatant fluid was collected to detect the production of CXCL13 by ELISA (A). FDC total RNA was obtained and reverse transcribed to detect the mRNA expression of CXCL13 with values normalized to the expression of endogenous GAPDH (B).

REFERENCE

1. Wain-Hobson, S., J. P. Vartanian, M. Henry, N. Chenciner, R. Cheynier, S. Delassus, L. P. Martins, M. Sala, M. T. Nugeyre, and D. Guetard. 1991. LAV revisited: origins of the early HIV-1 isolates from Institut Pasteur. *Science* **252**: 961-965.

2. Barre-Sinoussi, F., J. C. Chermann, F. Rey, M. T. Nugeyre, S. Chamaret, J. Gruest, C. Dauguet, C. Axler-Blin, F. Vezinet-Brun, C. Rouzioux, W. Rozenbaum, and L. Montagnier. 1983. Isolation of a T-lymphotropic retrovirus from a patient at risk for acquired immune deficiency syndrome (AIDS). *Science* **220**: 868-871.

3. Gallo, R. C., P. S. Sarin, E. P. Gelmann, M. Robert-Guroff, E. Richardson, V. S. Kalyanaraman, D. Mann, G. D. Sidhu, R. E. Stahl, S. Zolla-Pazner, J. Leibowitch, and M. Popovic. 1983. Isolation of human T-cell leukemia virus in acquired immune deficiency syndrome (AIDS). *Science* **220**: 865-867.

4. Kallings, L. O. 2008. The first postmodern pandemic: 25 years of HIV/AIDS. *J Intern Med* **263**: 218-243.

5. Heath, S. L., J. G. Tew, J. G. Tew, A. K. Szakal, and G. F. Burton. 1995. Follicular dendritic cells and human immunodeficiency virus infectivity. *Nature* **377**: 740-744.

6. Burton, G. F., B. F. Keele, J. D. Estes, T. C. Thacker, and S. Gartner. 2002. Follicular dendritic cell contributions to HIV pathogenesis. *Semin Immunol* **14**: 275-284.

7. Keele, B. F., L. Tazi, S. Gartner, Y. Liu, T. B. Burgon, J. D. Estes, T. C. Thacker, K. A. Crandall, J. C. McArthur, and G. F. Burton 2008. Characterization of the follicular dendritic cell reservoir of human immunodeficiency virus type 1. *J Virol* **82**: 5548-5561.

8. Congote, L. F. 2006. The C-terminal 26-residue peptide of serpin A1 is an inhibitor of HIV-1. *Biochem Biophys Res Commun* **343**: 617-622.

9. Münch, J., L. Ständker, K. Adermann, A. Schulz, M. Schindler, R. Chinnadurai, S. Pöhlmann, C. Chaipan, T. Biet, T. Peters, B. Meyer, D. Wilhelm, H. Lu, W. Jing, S. Jiang, W. G. Forssmann, and F. Kirchhoff. 2007. Discovery and optimization of a natural HIV-1 entry inhibitor targeting the gp41 fusion peptide. *Cell* **129**: 263-275.

10. Potthoff, A. V., J. Münch, F. Kirchhoff, and N. H. Brockmeyer. 2007. HIV infection in a patient with alpha-1 antitrypsin deficiency: a detrimental combination? *AIDS* **21**: 2115-2116.

11. Shapiro, L., G. B. Pott, and A. H. Ralston. 2001. Alpha-1-antitrypsin inhibits human immunodeficiency virus type 1. *FASEB J* **15**: 115-122.

12. Hughes, A. and M. Nelson. 2009. HIV entry: new insights and implications for patient management. *Current Opinion in Infectious Diseases* **22**: 35-42.

13. Klatzmann, D., E. Champagne, S. Chamaret, J. Gruest, D. Guetard, T. Hercend, J. Gluckman, and L. Montagnier. 1984. T-lymphocyte T4 molecule behaves as the receptor for human retrovirus LAV. *Nature* **312**: 767-768.

14. Dalgleish, A. G., P. C. Beverley, P. R. Clapham, D. H. Crawford, M. F. Greaves, and R. A. Weiss. 1984. The CD4 (T4) antigen is an essential component of the receptor for the AIDS retrovirus. *Nature* **312**: 763-767.

15. Feng, Y., C. C. Broder, P. E. Kennedy, and E. A. Berger. 1996. HIV-1 entry cofactor: functional cDNA cloning of a seven-transmembrane, G protein-coupled receptor. *Science* **272**: 872-877.

16. Oberlin, E., A. Amara, F. Bachelerie, C. Bessia, J. L. Virelizier, F. Arenzana-Seisdedos, O. Schwartz, J. M. Heard, I. Clark-Lewis, D. F. Legler, M. Loetscher, M. Baggiolini, and B. Moser 1996. The CXC chemokine SDF-1 is the ligand for LESTR/fusin and prevents infection by T-cell-line-adapted HIV-1. *Nature* **382**: 833-835.

17. Combadiere, C., S. K. Ahuja, H. L. Tiffany, and P. M. Murphy. 1996. Cloning and functional expression of CC CKR5, a human monocyte CC chemokine receptor selective for MIP-1(alpha), MIP-1(beta), and RANTES. *J Leukoc Biol* **60**: 147-152.

18. Alkhatib, G., C. Combadiere, C. C. Broder, Y. Feng, P. E. Kennedy, P. M. Murphy, and E. A. Berger. 1996. CC CKR5: a RANTES, MIP-1alpha, MIP-1beta receptor as a fusion cofactor for macrophage-tropic HIV-1. *Science* **272**: 1955-1958.

19. Choe, H., M. Farzan, Y. Sun, N. Sullivan, B. Rollins, P. D. Ponath, L. Wu, C. R. Mackay, G. LaRosa, W. Newman, N. Gerard, C. Gerard, and J. Sodroski. 1996. The beta-chemokine receptors CCR3 and CCR5 facilitate infection by primary HIV-1 isolates. *Cell* **85**: 1135-1148.

20. Deng, H., R. Liu, W. Ellmeier, S. Choe, D. Unutmaz, M. Burkhart, P. D. Marzio, S. Marmon, R. E. Sutton, C. M. Hill, C. B. Davis, S. C. Peiper, T. J. Schall, D. R. Littman, and N. R. Landau. 1996. Identification of a major co-receptor for primary isolates of HIV-1. *Nature* **381**: 661-666.

21. Doranz, B. J., J. Rucker, Y. Yi, R. J. Smyth, M. Samson, S. C. Peiper, M. Parmentier, R. G. Collman, and R. W. Doms. 1996. A dual-tropic primary HIV-1 isolate that uses fusin and the beta-chemokine receptors CKR-5, CKR-3, and CKR-2b as fusion cofactors. *Cell* **85**: 1149-1158.

22. Dragic, T., V. Litwin, G. P. Allaway, S. R. Martin, Y. Huang, K. A. Nagashima, C. Cayanan, P. J. Maddon, R. A. Koup, J. P. Moore, and W. A. Paxton. 1996. HIV-1 entry into CD4+ cells is mediated by the chemokine receptor CC-CKR-5. *Nature* **381**: 667-673.

23. Chan D. C. and P. S. Kim. 1998. HIV Entry and Its Inhibition. *Cell* **93**: 681-684.

24. Wyatt, R. and J. Sodroski. 1998. The HIV-1 Envelope Glycoproteins: Fusogens, Antigens, and Immunogens. *Science* **280**: 1884-1888.

25. Wyatt, R., P. D. Kwong, E. Desjardins, R. W. Sweet, J. Robinson, W. A. Hendrickson, and J. G. Sodroski. 1998. The antigenic structure of the HIV gp120 e nvelope glycoprotein. *Nature* **393**: 705-711.

26. Kowalski, M., J. Potz, L. Basiripour, T. Dorfman, W. G. Goh, E. Terwilliger, A. Dayton, C. Rosen, W. Haseltine, and J. Sodroski. 1987. Functional regions of the human immunodeficiency virus envelope glycoproteins. *Science* **237**: 1351-1355.

27. Stein, B., S. Gouda, J. Lifson, R. Penhallow, K. Bensch, and E. Engleman. 1987. pH-independent HIV entry into CD4-positive T cells via virus envelope fusion to the plasma membrane. *Cell* **49**: 659-668.

28. Helseth, E., M. Kowalski, D. Gabuzda, U. Olshevsky, W. Haseltine, and J. Sodroski. 1990. Rapid complementation assays measuring replicative potential of HIV-1 envelope glycoprotein mutants. *J. Virol.* **64**: 2416-2420.

29. Imamichi, T. 2004. A ction of anti-HIV drugs and resistance: reverse transcriptase inhibitors and protease inhibitors. *Curr Pharm Des.* **10**: 4039-4053.

30. Tarrago-Litvak, L., M. L. Andreola, M. Fournier, G. A. Nevinsky, V. Parissi, V. R. de Soultrait, and S. Litvak. 2002. Inhibitors of HIV-1 reverse transcriptase and integrase: classical and emerging therapeutical approaches. *Curr Pharm Des.* **8**: 595-614.

31. Zheng, Y. H., N. Lovsin, and B. M. Peterlin. 2005. Newly identified host factors modulate HIV replication. *Immunol. Lett.* **97**: 225-234.

32. Miller, M. D., C. M. Farnet, and F. D. Bushman. 1997. Human immunodeficiency virus type 1 preintegration complexes: studies of organization and composition. *J. Virol.* **71**: 5382-5390.

33. Mikovits, J., N. Lohrey, R. Schulof, J. Courtless, and F. Ruscetti. 1992. Activation of infectious virus from latent human-immunodeficiency-virus infection of monocytes in vivo. *J. Clin. Invest.* **90**: 1486-1491.

34. Pereira, L. A., K. Bentley, A. Peeters, M. J. Churchill, and N. J. Deacon. 2000. A compilation of cellular transcription factor interactions with the HIV-1 LTR promoter. *Nucleic. Acids. Res.* **28**: 663-668.

35. Leggett, R. W., S. A. Armstrong, D. Barry, and C. R. Mueller. 1995. Sp1 is phosphorylated and its DNA binding activity down-regulated upon terminal differentiation of the liver. *J. Biol. Chem.* **270**: 25879-25884.

36. Vinals, F., C. Fandos, T. Santalucia, J. Ferre, X. Testar, M. Palacin, and A. Zorzano. 1997. Myogenesis and MyoD down-regulate Sp1. A mechanism for the repression of GLUT1 during muscle cell differentiation. *J. Biol. Chem.* **272**: 12913-12921.

37. Black, A. R., D. Jensen, S. Y. Lin, and J. C. Azizkhan. 1999. Growth/cell cycle regulation of Sp1 phosphorylation. *J. Biol .Chem.* **274**: 1207-1215.

38. Mandel, T. E., R. P. Phipps, A. Abbot, and J. G. Tew. 1980. The follicular dendritic cell: long term antigen retention during immunity. *Immunol.Rev.* **53**: 29-59.

39. Szakal, A. K., K. L. Holmes, and J. G. Tew. 1983. Transport of immune complexes from the subcapsular sinus to lymph node follicles on the surface of nonphagocytic cells, including cells with dendritic morphology. *J Immunol* **131**: 1714-1727.

40. Szakal, A. K., M. H. Kosco, and J. G. Tew. 1989. Microanatomy of lymphoid tissue during the induction and maintenance of humoral immune responses: structure function relationships. *Annu Rev Immunol* **7**: 91-109.

41. Szakal, A. K., Z. F. Kapasi, A. Masuda, and J. G. Tew. 1992. Follicular dendritic cells in the alternative antigen transport pathway: microenvironment, cellular events, age and retrovirus related alterations. *Sem in Immunol* **4**: 257-265.

42. El Shikh, M. E., R. M El Sayed, J. G Tew, and G. F Burton. 2009. Follicular Dendritic Cells (B Lymphocyte Stimulating). *In Encylopedia of Life Sciences*. J. A. Wiley, ed. Wiley, J.A.

43. El Shikh, M. E., R. El Sayed, A. K. Szakal, and J. G. Tew. 2006. Follicular dendritic cell (FDC)-FcgammaRIIB engagement via immune complexes induces the activated FDC phenotype associated with secondary follicle development. *Eur J Immunol* **36**: 2715-2724.

44. El Shikh, M. E., R. M. El Sayed, Y. Wu, A. K. Szakal, and J. G. Tew. 2007. TLR4 on follicular dendritic cells: an activation pathway that promotes accessory activity. *J Immunol* **179**: 4444 -4450.

45. Pantaleo, G., C. Graziosi, J. F. Demarest, L. Butini, M. Montroni, C. H. Fox, J. M. Orenstein, D. P. Kotler, and A. S. Fauci. 1993. HIV infection is active and progressive in lymphoid tissue during the clinically latent stage of disease. *Nature* **362**: 355-358.

46. Embretson, J., M. Zupancic, J. L. Ribas, A. Burke, P. Racz, K. Tenner-Racz, and A. T. Haase. 1993. Massive covert infection of helper T lymphocytes and macrophages by HIV during the incubation period of AIDS. *Nature* **362**: 359-362.

47. Thacker, T. C., X. Zhou, J. D. Estes, Y. Jiang, B. F. Keele, T. S. Elton, and G. F. Burton. 2009. Follicular Dendritic Cells and Human Immunodeficiency Virus Type 1 Transcription in CD4+ T Cells. *J. Virol.* **83**: 150-158.

48. Brenchley, J. M., D. A. Price, T. W. Schacker, T. E. Asher, G. Silvestri, S. Rao, Z. Kazzaz, E. Bornstein, O. Lambotte, D. Altmann, B. R. Blazar, B. Rodriguez, L. Teixeira-Johnson, A. Landay, J. N. Martin, F. M. Hecht, L. J. Picker, M. M. Lederman, S. G. Deeks, and D. C. Douek. 2006. Microbial translocation is a cause of systemic immune activation in chronic HIV infection. *Nat Med* **12**: 1365-1371.

49. Brenchley J. M. and D. C. Douek. 2008. The mucosal barrier and immune activation in HIV pathogenesis. *Curr Opin HIV AIDS* **3**: 356-361.

50. Douek, D. C., M. Roederer, and R. A. Koup. 2009. Emerging concepts in the immunopathogenesis of AIDS. *Annu Rev Med* **60**: 471-484.

51. Cavert, W., D. W. Notermans, K. Staskus, S. W. Wietgrefe, M. Zupancic, K. Gebhard, K. Henry, Z. Q. Zhang, R. Mills, H. McDade, C. M. Schuwirth, J. Goudsmit, S. A. Danner, and A. T. Haase. 1997. Kinetics of response in lymphoid tissues to antiretroviral therapy of HIV-1 infection. *Science* **276**: 960-964.

52. Pantaleo, G., C. Graziosi, L. Butini, P. A. Pizzo, S. M. Schnittman, D. P. Kotler, and A. S. Fauci. 1991. Lymphoid organs function as major reservoirs for human immunodeficiency virus. *Proc.Natl.Acad.Sci.USA* **88**: 9838-9842.

53. Pope, M. and A. T. Haase. 2003. Transmission, acute HIV-1 infection and the quest for strategies to prevent infection. *Nat. Med.* **9**: 847-852.

54. Haase, A. T. 1999. Population biology of HIV-1 infection: viral and CD4+ T cell demographics and dynamics in lymphatic tissues. *Annu Rev Immunol* **17**: 625-656.

55. Smith, B. A., S. Gartner, Y. Liu, A. S. Perelson, N. I. Stilianakis, B. F. Keele, T. M. Kerkering, A. Ferreira-Gonzalez, A. K. Szakal, J. G. Tew, and G. F. Burton. 2001. Persistence of infectious HIV on follicular dendritic cells. *J Immunol* **166**:690-696

56. Kacani, L., W. M. Prodinger, G. M. Sprinzl, M. G. Schwendinger, M. Spruth, H. Stoiber, S. Döpper, S. Steinhuber, F. Steindl, and M. P. Dierich. 2000. Detachment of human immunodeficiency virus type 1 from germinal centers by blocking complement receptor type 2. *J Virol* **74**: 7997-8002.

57. Estes, J. D., B. F. Keele, K. Tenner-Racz, P. Racz, M. A. Redd, T. C. Thacker, Y. Jiang, M. J. Lloyd, S. Gartner, and G. F. Burton. 2002. Follicular dendritic cell-mediated up-regulation of CXCR4 expression on CD4 T cells and HIV pathogenesis. *J. Immunol.* **169**: 2313-2322.

58. Estes, J. D., T. C. Thacker, D. L. Hampton, S. A. Kell, B. F. Keele, E. A. Palenske, K. M. Druey, and G. F. Burton. 2004. Follicular dendritic cell regulation of CXCR4-mediated germinal center CD4 T cell migration. *J. Immunol.* **173**: 6169-6178.

59. Bristow, C. L., H. Patel, and R. R. Arnold. 2001. Self antigen prognostic for human immunodeficiency virus disease progression. *Clin Diagn Lab Immunol* **8**: 937-942.

60. Burton, G. F., A. Masuda, S. L. Heath, B. A. Smith, J. G. Tew, and A. K. Szakal. 1997. Follicular dendritic cells (FDC) in retroviral infection: host/pathogen perspectives. *Immunol. Rev.* **156**: 185-197.

61. Smith-Franklin, B. A., B. F. Keele, J. G. Tew, S. Gartner, A. K. Szakal, J. D. Estes, T. C. Thacker, and G. F. Burton. 2002. Follicular Dendritic Cells and the Persistence of HIV Infectivity: The Role of Antibodies and Fcγ Receptors. *J. Immunol.* **168**: 2408-2414

62. Qin, D., J. Wu, K. A. Vora, J. V. Ravetch, A. K. Szakal, T. Manser, and J. G. Tew. 2000. Fcγ receptor IIB on follicular dendritic cells regulates the B cell recall response. *J Immunol* **164**: 6268-6275.

63. Phipps, R. P., G. F. Mitchell, T. E. Mandel, and J. G. Tew. 1980. Antibody isotypes mediating antigen retention in passively immunized mice. *Immunology* **40**: 459-466.

64. Tew, J. G. and T. E. Mandel. 1979. Prolonged antigen half-life in the lymphoid follicles of specifically immunized mice. *Immunology* **37**: 69-76.

65. Fujiwara, M., R. Tsunoda, S. Shigeta, T. Yokota, and M. Baba. 1999. Human follicular dendritic cells remain uninfected and capture human immunodeficiency virus type 1 through CD54-CD11a interaction. *J Virol* **73**: 3603-3607.

66. Joling, P., L. J. Bakker, J. A. G. Van Strijp, T. Meerloo, L. de Graaf, M. E. M. Dekker, J. Goudsmit, J. Verhoef, and H. J. Schuurman. 1993. Binding of human immunodeficiency virus type-1 to follicular dendritic cells in vitro is complement dependent. *J Immunol* **150**: 1065-1073.

67. Ho, J., S. Moir, L. Kulik, A. Malaspina, E. T. Donoghue, N. J. Miller, W. Wang, T. W. Chun, A. S. Fauci, and V. M. Holer. 2007. Role for CD21 in the Establishment of an Extracellular HIV Reservoir in Lymphoid Tissues. *J Immunol* **178**: 6968-6974.

68. Voulgari, F., P. Cummins, T. I. Gardecki, N. J. Beeching, P. C. Stone, and J. Stuart. 1982. Serum levels of acute phase and cardiac proteins after myocardial infarction, surgery, and infection. *Br Heart J* **48**: 352-356.

69. Kushner, I. and A. Mackiewicz. 1993. The acute phase response: an overview. In Acute Phase Proteins:Molecular Biology, Biochemistry and Clinical Applications. *CRC Press*. 3-20.

70. Stoller, J. K. and L. S. Aboussouan. 2005. α1-Antitrypsin deficiency. *Lancet* **365**: 2225-2236.

71. Koulmanda, M., M. Bhasin, L. Hoffman, Z. Fan, A. Qipo, H. Shi, S. Bonner-Weir, P. Putheti, N. Degauque, T. A. Libermann, H. Auchincloss, J. S. Flier, and T. B. Strom. 2008. Curative and beta cell regenerative effects of alpha1-antitrypsin treatment in autoimmune diabetic NOD mice. *Proc Natl Acad Sci U S A* **105**: 16242-16247.

72. Lewis, E. C., M. Mizrahi, M. Toledano, N. Defelice, J. L. Wright, A. Churg, L. Shapiro, and C. A. Dinarello. 2008. alpha1-Antitrypsin monotherapy induces immune tolerance during islet allograft transplantation in mice. *Proc Natl Acad Sci U S A* **105**: 16236-16241.

73. Pott, G. B., E. D. Chan, C. A. Dinarello, and L. Shapiro. 2009. a -1-antitrypsin is an endogenousinhibitor of proinflammatory cytokine production in whole blood. *J Leukoc Biol* **85**: 886-895.

74. Fiore, J. R., G. Angarano, C. Fico, L. Monno, S. Carbonara, G. F. Salamina, C. Fracasso, and G. Pastore. 1990. HIV isolation from whole blood: a new approach to HIV detection. *Microbiologica* **13**: 311-315.

75. Mayer, K. H. and V. DeGruttola. 1987. Human immunodeficiency virus and oral intercourse. *Ann. Int. Med.* **107**: 428-429.

76. Lyman, D., M. Ascher, and J. A. Levy. 1986. Minimal risk of transmission of AIDS-associated retrovirus infection by oralgenital contact. *J. Am. Med. Assoc.* **255**: 1703-1704.

77. Fox, P. C., A. Wolff, C. K. Yeh, J. C. Atkinson, and B. J. Baum. 1988. Saliva inhibits HIV-1 infectivity. *J. Am. Dental Assoc.* **116**: 635-637.

78. McNeely, T. B., M. Dealey, D. J. Dripps, J. M. Orenstein, S. P. Eisenberg, and S. M. Wahl. 1995. Secretory leukocyte protease inhibitor: a human saliva protein exhibiting antihuman immunodeficiency virus type 1 activity in vitro. *J. Clin. Invest.* **96**: 456-464.

79. McNeely, T. B., D. C. Shugars, M. Rosendahl, C. Tucker, S. P. Eisenberg, and S. M. Wahl. 1997. Inhibition of human immunodeficiency virus type 1 infectivity by secretory leukocyte protease inhibitor occurs prior to viral reverse transcription. *Blood* **90**: 1141-1149.

80. Cordelier, P. and D. S. Strayer. 2003. Conditional expression of alpha1-antitrypsin delivered by recombinant SV40 vectors protects lymphocytes against HIV. *Gene Ther.* **10**: 2153-2156.

81. Cordelier, P. and D. S. Strayer. 2003. Mechanisms of alpha1-antitrypsin inhibition of cellular serine proteases and HIV-1 protease that are essential for HIV-1 morphogenesis. *Biochim. Biophys. Acta.* **1638**: 197-207.

82. Cordelier, P., M. A. Zern, and D. S. Strayer. 2003. HIV-1 proprotein processing as a target for gene therapy. *Gene Ther.* **10**: 467-477.

83. Hayes, V. M. and M. Gardiner-Garden. 2003. Are polymorphic markers within the alpha-1-antitrypsin gene associated with risk of human immunodeficiency virus disease? *J Infect. Dis.* **188**: 1205-1208.

84. Bahbouhi, B., M. Bendjennat, D. Guétard, N. G. Seidah, and E. Bahraoui. 2000. Effect of alpha-1 antitrypsin Portland variant (alpha 1-PDX) on HIV-1 replication. *Biochem J.* **352**: 91-98.

85. Bahbouhi, B., N. G. Seidah, and E. Bahraoui. 2001. Replication of HIV-1 viruses in the presence of the Portland alpha1-antitrypsin variant (alpha1-PDX) inhibitor. *Biochem J.* **360**: 127-134.

86. Anderson, E. D., L. Thomas, J. S. Hayflick, and G. Thomas. 1993. Inhibition of HIV-1 gp160-dependent membrane fusion by a furin-directed alpha 1-antitrypsin variant. *J Biol. Chem.* **268**: 24887-24891.

87. Mehtali, M., M. Munschy, D. Ali-Hadji, and M. P. Kieny. 1992. A novel transgenic mouse model for the in vivo evaluation of anti-human immunodeficiency virus type 1 drugs. *AIDS Res. Hum. Retroviruses.* **8**: 1959-1965.

88. Zhou, X., L. Shapiro, G. Fellingham, B. M. Willardson, and G. F. Burton. 2011. HIV Replication in CD4+ T Lymphocytes in the Presence and Absence of Follicular Dendritic Cells: Inhibition of Replication Mediated by α-1-Antitrypsin through Altered IκBα Ubiquitination. *J Immunol* **168**: 3148-3155.

89. Burton, G. F., D. H. Conrad, A. K. Szakal, and J. G. Tew. 1993. Follicular dendritic cells and B cell costimulation. *J Immunol.* **150**: 31-38.

90. Kosco, M. H., E. Pflugfelder, and D. Gray. 1992. Follicular dendritic cell-dependent adhesion and proliferation of B cells in vitro. *J. Immunol.* **148**:2331-2339.

91. Reinhart, T. A., M. J. Rogan, G. A. Viglianti, D. M. Rausch, L. E. Eiden, and A. T. Haase. 1997. A new approach to investigating the relationship between productive infection and cytopathicity in vivo. *Nat. Med.* **3**: 218-221.

92. Schmitz, J., J. van Lunzen, K. Tenner-Racz, G. Grossschupff, P. Racz, H. Schmitz, M. Dietrich, and F. T. Hufert. 1994. Follicular dendritic cells retain HIV-1 particles on their plasma membrane, but are not productively infected in asymptomatic patients with follicular hyperplasia. *J. Immunol.* **153**: 1352-1359.

93. Duh, E. J., W. J. Maury, T. M. Folks, A. S. Fauci, and A. B. Rabson. 1989. Tumor necrosis factor alpha activates human immunodeficiency virus type 1 through induction of nuclear factor binding to the NF-kappa B sites in the long terminal repeat. *Proc. Natl. Acad. Sci. USA* **86**: 5974-5978.

94. Emilie, D., R. Fior, B. Jarrousse, A. Marfaing-Koka, D. Merrien, O. Devergne, M. C. Crevon, M. C. Maillot, and P. Galanaud. 1994. Cytokines in HIV infection. *Int. J. Immunopharmacol.* **16**: 391-396.

95. Fu, Y. X. and D. D. Chaplin. 1999. Development and maturation of secondary lymphoid tissues. *Annu. Rev. Immunol.* **17**: 399-433.

96. Korner, H., M. Cook, D. S. Riminton, F. A. Lemckert, R. M. Hoek, B. Ledermann, F. Kontgen, B. Fazekas de St. Groth, and J. D. Sedgwick. 1997. Distinct roles for lymphotoxin-alpha and tumor necrosis factor in organogenesis and spatial organization of lymphoid tissue. *Eur. J. Immunol.* **27**: 2600-2609.

97. Pasparakis, M., L. Alexopoulou, V. Episkopou, and G. Kollias. 1996. Immune and inflammatory responses in TNF alpha-deficient mice: a critical requirement for TNF alpha in the formation of primary B cell follicles, follicular dendritic cell networks and

germinal centers, and in the maturation of the humoral immune response. *J. Exp. Med*. **184**: 1397-1411.

98. Jones, K. A. and B. M. Peterlin. 1994. Control of RNA initiation and elongation at the HIV-1 promoter. *Annu. Rev. Biochem.* **63**:717-743.

99. Luciw, P. A. 1996. Human immunodeficiency viruses and their replication, p. 845–916. In B. *N. Fields, D. M. Knipe, and P. M. Howley (ed.), Fundamental virology, 3rd ed. Lippincott-Raven*, Philadelphia, PA.

100. Zhou, X., W. Yang, and J. Li. 2006. Ca2+- and Protein Kinase C-dependent Signaling Pathway for Nuclear Factor-κB Activation, Inducible Nitric-oxide Synthase Expression, and Tumor Necrosis Factor-α Production in Lipopolysaccharide-stimulated Rat Peritoneal Macrophages. *J Biol Chem* **281**: 31337-31347.

101. Vallabhapurapu, S. and M. Karin. 2009. Regulation and function of NF-kappaB transcription factors in the immune system. *Annu. Rev. Immunol.* **27**: 693-733.

102. Yoshida, K., T. K. van den Berg, and C. D. Dijkstra. 1993. Two functionally different follicular dendritic cells in secondary lymphoid follicles of mouse spleen, as revealed by CR1/2 and FcR gamma II-mediated immune-complex trapping. *Immunology* **80**: 34-39.

103. Layne, S. P., M. J. Merges, M. Dembo, J. L. Spouge, S. R. Conley, J. P. Moore, J. L. Raina, H. Renz, H. R. Gelderblom, and P. L. Narat. 1992. Factors underlying spontaneous inactivation and susceptibility to neutralization of human immunodeficiency virus. *Virology* **189**: 695-714.

104. Murakami, T. and E. O. Freed. 2000. The long cytoplasmic tail of gp41 is required in a cell type-dependent manner for HIV-1 envelope glycoprotein incorporation into virions. *PNAS* **97**: 343-348.

105. Congote, L. F. 2007. Serpin A1 and CD91 as host instruments against HIV-1 infection: are extracellular antiviral peptides acting as intracellular messengers? *Virus Res* **125**: 119-134.

106. Wang, J. and M. A. Maldonado. 2006. The Ubiquitin-Proteasome System and Its Role in Inflammatory and Autoimmune Diseases. *Cell Mol Immunol* **3**: 255-261.

107. Deshaies, R. J. and C. A. Joazeiro. 2009. RING domain E3 ubiquitin ligases. *Annu. Rev. Biochem.* **78**: 399-434.

108. Newton, K., M. L. Matsumoto, I. E. Wertz, D. S. Kirkpatrick, J. R. Lill, J. Tan, D. Dugger, N. Gordon, S. S. Sidhu, F. A. Fellouse, L. Komuves, D. M. French, R. E. Ferrando, C. Lam, D. Compaan, C. Yu, I. Bosanac, S. G. Hymowitz, R. F. Kelley, and V. M. Dixit. 2008. Ubiquitin chain editing revealed by polyubiquitin linkage-specific antibodies. *Cell* **134**: 668-678.

109. Wu, C. J., D. B. Conze, T. Li, S. M. Srinivasula, and J. D. Ashwell. 2006. Sensing of Lys 63-linked polyubiquitination by NEMO is a key event in NFkappaB activation. *Nat. Cell Biol.* **8**: 398-406.

110. Marsh, M. and A. Helenius. 2006. Virus entry: open sesame. *Cell* **124**: 729-740.

111. Mukherjee, S. A., R. N. Ghosh, and F. R. Maxfield. 1997. Endocytosis. *Physiological Reviews* **77**: 759-803.

112. Poller, W., T. E. Willnow, J. Hilpert, and J. Herz. 1995. Differential Recognition of α-1-Antitrypsin-Elastase and α-1-Antichymotrypsin-Cathepsin G Complexes by the Low Density Lipoprotein Receptor-related Protein. *J Biol Chem.* **270**: 2841-2845.

113. Kounnas, M. Z., F. C. Church, W. S. Argraves, and D. K. Strickland. 1996. Cellular Internalization and Degradation of Antithrombin III-Thrombin, Heparin Cofactor II-Thrombin, and α-1-Antitrypsin-Trypsin Complexes Is Mediated by the Low Density Lipoprotein Receptor-related Protein. *J Biol Chem.* **271**: 6523-6529.

114. Cuervo, A. M. and J. F. Dice. 1998. Lysosomes, a meeting point of proteins, chaperones, and proteases. *J. Mol. Med.* **76**: 6-12.

115. Turk, B., V. Stoka, J. Rozman-Pungercar, T. Cirman, G. Droga-Mazovec, K. Oresic, and V. Turk. 2002. Apoptotic pathways: involvement of lysosomal proteases. *Biol. Chem.* **383**: 1035-1044.

116. Turk, B. and V. Turk. 2009. Lysosomes as "Suicide Bags" in Cell Death: Myth or Reality? J. *Biol. Chem.* **284**: 21783-21787.

117. Spencer, E., J. Jiang, and Z. J. Chen. 1999. Signal-induced ubiquitination of IκBα by the F-box protein Slimb/β-TrCP. *Genes & Dev.* **13**: 284-294.

118. Suzuki, H., T. Chiba, M. Kobayashi, M. Takeuchi, T. Suzuki, A. Ichiyama, T. Ikenoue, M. Omata, K. Furuichi, and K. Tanaka. 1999. IkappaBalpha ubiquitination is catalyzed by an SCF-like complex containing Skp1, cullin-1, and two F-box/WD40-repeat proteins, betaTrCP1 and betaTrCP2. *Biochem. Biophys. Res. Commun.* **256**: 127-132.

119. Williams, T. and R. Tjian. 1991. Characterization of a dimerization motif in AP-2 and its function in heterologous DNA-binding proteins. *Science* **251**: 1067-1071.

120. Hilger-Eversheim, K., M. Moser, H. Schorle, and R. Buettner. 2000. Regulatory roles of AP-2 transcription factors in vertebrate development, apoptosis and cell-cycle control. *Gene* **260**: 1-12.

121. Lin, S. Y., A. R. Black, D. Kostic, S. Pajovic, C. N. Hoover, and J. C. Azizkhan. 1996. Cell cycle-regulated association of E2F1 and Sp1 is related to their functional interaction. *Mol. Cell. Biol.* **16**: 1668-1675.

122. Rotheneder, H., S. Geymayer, and E. Haidweger. 1999. Transcription factors of the Sp1 family: interaction with E2F and regulation of the murine thymidine kinase promoter. *J. Mol. Biol.* **293**: 1005-1015.

123. Hayden, M. S., A. P. West, and S. Ghosh. 2006. NF-kB and the immune response. *Oncogene* **25**: 6758-6780.

124. Takada, N., T. Sanda, H. Okamoto, J. P. Yang, K. Asamitsu, L. Sarol, G. Kimura, H. Uranishi, T. Tetsuka, and T. Okamoto. 2002. RelA-associated inhibitor blocks transcription of human immunodeficiency virus type 1 by inhibiting NF-kappaB and Sp1 actions. *J. Virol.* **76**: 8019-8030.

125. Pace, M. J., L. Agosto, E. H. Graf, and U. O'Doherty. 2011. HIV reservoirs and latency models. *Virology*. **411**: 344-354.

126. Haase, A. T., K. Henry, M. Zupancic, G. Sedgewick, R. A. Faust, H. Melroe, W. Cavert, K. Gebhard, K. Staskus, Z.-Q. Zhang, P. Dailey, H. H. Balfour, Jr., A. Erice, and A. S. Perelson. 1996. Quantitative image analysis of HIV-1 infection in lymphoid tissue. *Science* **274**: 985-989.

127. Hufert, F. T., J. van Lunzen, G. Janossy, S. Bertram, J. Schmitz, O. Haller, P. Racz, and D. von Laer. 1997. Germinal centre CD4+ T cells are an important site of HIV replication in vivo. *AIDS* **11**: 849-857.

128. Folkvord, J. M., C. Armon, and E. Connick. 2005. Lymphoid follicles are sites of heightened human immunodeficiency virus type 1 (HIV-1) replication and reduced antiretroviral effector mechanisms. *AIDS Res. Hum. Retrovir.* **21**: 363-370.

129. Butch, A. W., G. H. Chung, J. W. Hoffmann, and M. H. Nahm. 1993. C ytokine expression by germinal center cells. *J. Immunol.* **150**: 39-47.

130. Kutsch, O., E. N. Benveniste, G. M. Shaw, and D. N. Levy. 2002. Direct and quantitative single-cell analysis of human immunodeficiency virus type 1 r eactivation from latency. *J. Virol.* **76**: 8776-8786.

131. Aydar, Y., J. Wu, J. Song, A. K. Szakal, and J. G. Tew. 2004. F cgammaRII expression on f ollicular dendritic cells and immunoreceptor tyrosine-based inhibition motif signaling in B cells. *Eur. J. Immunol.* **34**: 98-107.

132. Balogh, P., Y. Aydar, J. G. Tew, and A. K. Szakal. 2001. O ntogeny of the follicular dendritic cell phenotype and function in the postnatal murine spleen. *Cell. Immunol.* **214**: 45-53.

133. Balogh, P., Y. Aydar, J. G. Tew, and A. K. Szakal. 2002. Appearance and phenotype of murine follicular dendritic cells expressing VCAM-1. *Anat. Rec.* **268**: 160-168.

134. Kosco-Vilbois, M. H. 2003. Are follicular dendritic cells really good for nothing. *Nat Rev Immunol* **3**: 764-769.

135. Quigley, M. F., V. D. Gonzalez, A. Granath, J. Andersson, and J. K. Sandberg. 2007. CXCR5+ CCR7- CD8 T cells are early effector memory cells that infiltrate tonsil B cell follicles. *Eur J Immunol* 37: 3352-3362.

136. Bolland, S. and J. V. Ravetch. 1999. Inhibitory pathways triggered by ITIM-containing receptors. *Adv. Immunol.* **72**: 149-177.

137. Sinclair, N. R. 2000. I mmunoreceptor tyrosine-based inhibitory motifs on activating molecules. *Crit. Rev. Immunol.* **20**: 89-102.

138. Victoratos, P., J. Lagnel, S. Tzima, M. B. Alimzhanov, K. Rajewsky, M. Pasparakis, and G. Kollias. 2006. FDC-specific functions of p55TNFR and IKK2 in the development of FDC networks and of antibody responses. *Immunity* **24**: 65-77.

139. Bryan, C. L., K. S. Beard, G. B. Pott, J. Rahkola, E. M. Gardner, E. N. Janoff, and L. Shapiro. 2010. HIV infection is associated with reduced serum alpha-1-antitrypsin concentrations. *Clin Invest Med.* **33**: E384 - E389.

140. Kramer, H. B., K. J. Lavender, L. Qin, A. R. Stacey, M. K Liu. , K. di Gleria, A. Simmons, N. Gasper-Smith, B. F. Haynes, A. J. McMichael, P. Borrow, and B. M. Kessler. 2010. Elevation of intact and proteolytic fragments of acute phase proteins constitutes the earliest systemic antiviral response in HIV-1 infection. *PLoS Pathog* **6**: e1000893.

141. Sohrab, S., D. N. Petrusca, A. D. Lockett, K. S. Schweitzer, N. I. Rush, Y. Gu, K. Kamocki, J. Garrison, and I. Petrache. 2009. Mechanism of α-1 antitrypsin endocytosis by lung endothelium. *FASEB J* **23**: 3149-3158.

142. Hinrichsen, L., J. Harborth, L. Andrees, K. Weber, and E. J. Ungewickell. 2003. Effect of clathrin heavy chain- and alpha-adaptin-specific small inhibitory RNAs on

endocytic accessory proteins and receptor trafficking in HeLa cells. *J. Biol. Chem.* **278:** 45160-45170.

143. Aldonyte, R., E. T. Hutchinson, B. Jin, M. Brantly, E. Block, J. Patel, and J. Zhang. 2008. E ndothelial alpha-1-antitrypsin attenuates cigarette smoke induced apoptosis in vitro. *COPD* **5**: 153-162.

144. Brodsky, F. M., C. Y. Chen, C. Knuehl, M. C. Towler, and D. E. Wakeham. 2001. Biological basket weaving: formation and function of clathrin-coated vesicles. *Annu. Rev. Cell Dev. Biol.***17:** 517-568.

145. Schmid, S. L. 1997. C lathrin-coated vesicle formation and protein sorting: an integrated process. *Annu. Rev. Biochem.* **66:** 511-548.

146. Joslin, G., R. J. Fallon, J. Bullock, S. P. Adams, and D. H. Perlmutter. 1991. The SEC Receptor Recognizes a P entapeptide Neodomain of al-Antitrypsin-Protease Complexes. *J. Biol. Chem.* **266**: 11282-11288.

147. Joslin, G., A. Wittwer, S. Adams, D. M. Tollefsen, A. August, and D. H. Perlmutter. 1993. Cross-competition for Binding of a-l-Antitrypsin *(a1* AT)-Elastase Complexes to the Serpin-Enzyme Complex Receptor by Other Serpin-Enzyme Complexes and by Proteolytically Modified a1 AT. *J. Biol. Chem.* **268**: 1886-1693.

148. Maxfield, F. R. and T. E. McGraw. 2004. ENDOCYTIC RECYCLING. *Nat. Rev. Mol. Cell Biol.* **5**: 121-132.

149. Grant, B. D. and J. G. Donaldson. 2009. Pathways and mechanisms of endocytic recycling. *Nat. Rev. Mol. Cell Biol.* **10**: 597-608.

150. Eskelinen, E. L., Y. Tanaka, and P. Saftig. 2003. At the acidic edge: emerging functions for lysosomal membrane proteins. *Trends Cell Biol.* **13**: 137-145.

151. Luzio, J. P., P. R. Pryor, and N. A. Bright. 2007. Lysosomes: fusion and function. *Nat. Rev. Mol. Cell Biol.* **8**: 622-632.

152. Feldstein, A. E., N. W. Werneburg, A. Canbay, M. E. Guicciardi, S. F. Bronk, R. Rydzewski, L. J. Burgart, and G. J. Gores. 2004. Free fatty acids promote hepatic lipotoxicity by stimulating TNF-alpha expression via a lysosomal pathway. *Hepatology* **40**: 185-194.

153. Guicciardi, M. E., J. Deussing, H. Miyoshi, S. F. Bronk, P. A. Svingen, C. Peters, S. H. Kaufmann, and G. J. Gores. 2000. Cathepsin B contributes to TNF-α-mediated hepatocyte apoptosis by promoting mitochondrial release of cytochrome c. *J. Clin. Invest.* **106**: 1127-1137.

154. Werneburg, N. W., M. E. Guicciardi, S. F. Bronk, and G. J. Gores. 2002. Tumor necrosis factor-alpha-associated lysosomal permeabilization is cathepsin B dependent. *Am. J. Physiol.- Gastroint. Liver Physiol.* **283**: G947-956.

155. Werneburg, N. W., M. E. Guicciardi, S. F. Bronk, S. H. Kaufmann, and G. J. Gores. 2007. Tumor necrosis factor-related apoptosis inducing ligand activates a lysosomal pathway of apoptosis that is regulated by Bcl-2 proteins. *J. Biol. Chem.* **282**: 28960-28970.

156. Werneburg, N. W., M. E. Guicciardi, X. M. Yin, and G. J. Gores. 2004. TNF-alpha-mediated lysosomal permeabilization is FAN and caspase 8/Bid dependent. *Am. J. Physiol.-Gastroint. Liver Physiol.* **287**: G436-443.

157. Qin, J., H. Konno, D. Ohshima, H. Yanai, H. Motegi, Y. Shimo, F. Hirota, M. Matsumoto, S. Takaki, J. Inoue, and T. Akiyama. 2007. Developmental stage-dependent

collaboration between the TNF receptor-associated factor 6 and lymphotoxin pathways for B cell follicle organization in secondary lymphoid organs. *J Immunol*. **179**: 6799-807.